

Concepts for the implementation of  
physiologic conditions for the cultivation of  
human mesenchymal stem cells

Von der Naturwissenschaftlichen Fakultät der Gottfried  
Wilhelm Leibniz Universität Hannover

zur Erlangung des Grades  
Doktor der Naturwissenschaften (Dr. rer. nat.)

genehmigte Dissertation  
von

Dominik Egger, M. Sc.

2017

**Referent:** Prof. Dr. rer. nat. Thomas Scheper

**Korreferentin:** Prof. Dr. rer. nat. Cornelia Kasper

**Korreferent:** Prof. DI. Dr. techn. Christoph Herwig

**Tag der Promotion:** 11.09.2017

# Kurzfassung

Mesenchymale Stammzellen (MSCs) werden als vielversprechendster Kandidat für zellbasierte Therapien und Tissue Engineering Produkte angesehen. Sie stellen eine unkomplizierte und ethisch unbedenkliche Quelle multipotenter Stammzellen mit großer Proliferations- und Differenzierungskapazität dar. Für die Anwendung in zellbasierten Therapien müssen MSCs isoliert und *in vitro* expandiert oder in Tissue Engineering Prozessen auf dreidimensionale (3D) Matrizes angesiedelt und differenziert werden. Anschließend können solche 3D Strukturen als Implantat oder *in vitro* Modell in der Forschung dienen. Generell wird die *in vitro* Kultivierung auf zweidimensionalen Kunststoffoberflächen unter statischen Bedingungen durchgeführt, welches nicht die natürliche Umgebung der Stammzellen repräsentiert. Tatsächlich wurde gezeigt, dass sich das Verhalten von Zellen signifikant ändert, wenn physiologische Bedingungen wie 3D Strukturen, mechanische Belastung oder geeignete Sauerstoffkonzentrationen eingeführt werden. Um die Vorhersagbarkeit von Forschung für die Anwendung in klinischen Versuchen zu verbessern, scheint es daher wünschenswert physiologische Bedingungen zu implementieren.

Diese Arbeit präsentiert deshalb Ansätze für die Implementierung von physiologischen Bedingungen während der Isolation, Expansion und Differenzierung von MSCs. Die Isolation aus dem Fettgewebe durch Explantkultivierung wurde verglichen mit der Isolation durch enzymatischen Aufschluss und die resultierenden Zellen hinsichtlich ihrer Stammzeleigenschaften überprüft. Darüber hinaus zeigt ein neu entwickelter Ansatz die Expansion von MSCs als Aggregate ohne Trägerstrukturen in einem Rührkesselreaktor. Abschließend wird ein Konzept für die Charakterisierung und die Erzeugung einer mechanischen Umgebung für die osteogene Differenzierung von MSCs in einem Perfusionsreaktor vorgestellt. Dafür wurden die genutzten 3D Matrizes und die Fluidik des Reaktors charakterisiert. Anschließend wurde ein neuer Inkubator mit integrierten, nicht-invasiven Drucksensoren genutzt, um mechanische Parameter zu optimieren. In allen Schritten der Kultivierung wurden zusätzlich reduzierte Sauerstoffbedingungen getestet.

Die vorliegenden Ergebnisse zeigen einerseits, dass physiologische Bedingungen nützliche Effekte auslösen, andererseits betonen sie die Wichtigkeit gewissenhafter und umfassender Charakterisierung relevanter Kultivierungsparameter, um physiologische Bedingungen zu definieren, erzeugen und zu kontrollieren. Die vorgestellten Konzepte für die Implementierung von physiologischen Bedingungen während des gesamten Kultivierungsprozesses zeigen Relevanz im Kontext translationaler Forschung.

**Schlagerwörter:** Mesenchymale Stammzellen, 3D, dynamische Kultivierung, physiologische Bedingungen, Hypoxie.

# Abstract

Mesenchymal stem cells (MSCs) are still considered as the primary candidate for cell-based therapies and tissue engineering products in Regenerative Medicine (RM). They are easily accessible and ethically unobjectionable multipotent stem cells with remarkable properties such as high proliferation and differentiation capacity or the secretion of trophic factors involved in wound healing. For cell-based therapies MSCs are isolated from various tissues and expanded *in vitro* before they are applied to a patient. For tissue engineered products cells are seeded on three-dimensional (3D) matrices after expansion and then differentiated into a specific lineage. Those cell-seeded constructs are then used for transplantation or as *in vitro* models. In general, all steps of *in vitro* cell culture are traditionally carried out on two-dimensional (2D) plastic surfaces in a static conditions which does not represent the physiologic environment that cells are exposed to *in vivo*. In fact, the implementation of physiologic conditions, such as 3D scaffolds, mechanical forces or suitable oxygen concentrations were shown to influence cellular behavior significantly. Thus, in order to improve the predictability of basic research for clinical trials, the implementation of physiologic conditions seems desirable.

Therefore, this work presents approaches and considerations for the implementation of physiologic conditions in the isolation, expansion and differentiation of mesenchymal stem cells (MSCs). The isolation of adipose derived MSCs by explant culture is compared to the traditional isolation by enzymatic digestion and the resulting cells were characterized towards their stem cell properties. Also, a novel approach for the expansion of MSCs was developed. For this, cells were cultivated as scaffold-free 3D aggregates in a continuously stirred tank reactor. Finally, a concept for the characterization and control of the mechanical environment in a perfused bioreactor for osteogenic differentiation of MSCs is presented. For this, the 3D matrices and the behavior of fluid elements in the bioreactor were characterized. Subsequently, a novel incubator system with integrated non-invasive pressure sensors was harnessed to screen and optimize mechanical conditions. Additionally, reduced oxygen concentrations were implemented in all phases of cultivation.

On the one side, the presented results point out beneficial effects of physiologic conditions, on the other side it underlines the importance of diligent and comprehensive characterization of relevant cultivation parameters in order to define, generate and control physiologic conditions. These concepts for the implementation of physiologic conditions throughout the entire *in vitro* cultivation of MSC are highly fundamental to improve translational research.

**Keywords:** Mesenchymal stem cells, 3D, dynamic cultivation, physiologic conditions, hypoxia.

# Acknowledgements

I would like to express my sincere thanks Prof. Cornelia Kasper for the opportunity to work on this interesting research topic and for the great supervision and support.

I want to thank Prof. Thomas Scheper for being co-supervisor of this work. I also want to thank Prof. Monica Egerbacher, Dr. Martin Glösmann and Stephan Handschuh from the University of Veterinary Medicine and Dr. Jan Hansmann, Thomas Schwarz and Ivo Schwedhelm from the University Hospital of Würzburg for exciting collaboration and great scientific support.

Special thanks goes to Dr. Verena Charwat for being a great colleague and friend; for helpful scientific advise and support at all times. I also want to thank my colleagues Anne Lauermann, Dolly Mushahary, Andreas Clementi, Sarah Spitz and Christine Strauß for being a cheerful, motivational and supportive team (I hope we will have another BBQ on the roof top).

I want to thank all students I had the possibility to work with and supervise, Kathrina Radl, Sabrina Nebel, Stefan Stoiber, Lukas Baumgartner, Sarah Spitz, Haris Babic and Monica Fischer. It was a pleasure to accompany you on your scientific way.

Most importantly, I want to thank my wife Maria for her daily love and never ending support and encouragement.

Finally, I want to thank my family for endless support, always being encouraging and believing in me.

# Contents

<b>Acknowledgements</b>	<b>iv</b>
<b>List of abbreviations</b>	<b>vii</b>
<b>1 Introduction</b>	<b>1</b>
1.1 Motivation . . . . .	1
1.2 Aims . . . . .	2
<b>2 Theoretical Background</b>	<b>4</b>
2.1 Regenerative Medicine - Where Are We? . . . . .	4
2.1.1 Europe's regulatory framework . . . . .	5
2.1.2 Translational research . . . . .	7
2.2 Adipose Mesenchymal Stem Cells in Regenerative Medicine . . . . .	10
2.3 Physiologic Conditions in MSC Cultivation . . . . .	11
2.3.1 The Third Dimension . . . . .	12
2.3.2 Mechanical Forces: a Necessary Burden . . . . .	16
2.3.3 Medium composition - the endless endeavor . . . . .	20
2.3.4 Oxygen: Keeping the Finger On the Switch . . . . .	21
2.3.5 The physiologic toolbox . . . . .	22
2.4 Dynamic Cultivation of MSCs . . . . .	22
2.4.1 Commercially available bioreactors . . . . .	22
2.4.2 Development and Characterization of Bioreactors . . . . .	24
<b>3 Mesenchymal Stem Cell Isolation</b>	<b>29</b>
3.1 Isolation of adipose derived MSCs by explant culture . . . . .	32
3.2 Characterization of adipose derived MSCs isolated by explant culture . . . . .	35
3.3 From 3D to 3D - Isolation by explant culture in a 3D environment . . . . .	43
3.4 Conclusion . . . . .	44
<b>4 Scaffold-free Stem Cell Cultivation</b>	<b>46</b>
4.1 Aggregates in Stem Cell Cultivation . . . . .	46
4.2 Aggregate Cultivation in Microtiter Plates . . . . .	48
4.3 Approaches for Upscale of Aggregate Cultivation . . . . .	49
4.4 Aggregate Cultivation in a Stirred Tank Reactor . . . . .	52
4.5 Conclusion . . . . .	57
<b>5 Physiologic Differentiation Towards Osteogenic Lineage</b>	<b>58</b>
5.1 Setting a physiologic environment for osteogenic differentiation . . . . .	58
5.2 Biaxial Bioreactor . . . . .	60
5.3 Mini Perfusion Bioreactor . . . . .	63
5.3.1 Incubator System . . . . .	64
5.3.2 Characterization . . . . .	65
5.3.3 Application . . . . .	76

5.4 Conclusion . . . . .	84
<b>6 Conclusion and prospects</b>	<b>85</b>
<b>References</b>	<b>88</b>
<b>List of Figures</b>	<b>110</b>
<b>List of Tables</b>	<b>112</b>
<b>A Material</b>	<b>113</b>
A.1 Instruments and laboratory equipment . . . . .	113
A.2 Disposables . . . . .	114
A.3 Chemicals . . . . .	114
A.4 Buffers and solutions . . . . .	116
A.5 Kits . . . . .	116
A.6 Media . . . . .	117
A.7 Bioreactor components . . . . .	117
A.8 Software . . . . .	118
<b>B Methods</b>	<b>119</b>
B.1 Cell culture . . . . .	119
B.2 Three dimensional cell culture . . . . .	121
B.3 Bioreactor cultivation . . . . .	121
B.4 Biomaterial characterization . . . . .	123
B.5 Bioreactor characterization . . . . .	124
B.6 Assays . . . . .	126
B.7 Histology . . . . .	128
B.8 Staining procedures . . . . .	128
B.9 Scanning electron microscopy . . . . .	130
B.10 X-ray microtomography . . . . .	130
B.11 Image processing . . . . .	130
B.12 Aggregate size analysis with ImageJ . . . . .	131
<b>Curriculum Vitae</b>	<b>132</b>

# List of abbreviations

<b>2D</b>	two-dimensional
<b>3D</b>	three-dimensional
<b>ADM</b>	adipogenic differentiation medium
<b>AM</b>	acetoxy-methylester
<b>ALP</b>	alkaline phosphatase
<b>ATMP</b>	advanced therapy medicinal product
<b>ASC</b>	adipose derived mesenchymal stem cell
<b>CAD</b>	computer aided design
<b>CAGR</b>	compounded annual growth rate
<b>CAT</b>	Committee for Advanced Therapies
<b>CCM</b>	cell culture medium
<b>CDM</b>	chondrogenic differentiation medium
<b>CFD</b>	computational fluid dynamics
<b>CI</b>	confidence interval
<b>microCT</b>	x-ray computed microtomography
<b>CSTR</b>	continuous stirred tank reactor
<b>DO</b>	dissolved oxygen
<b>ECM</b>	extracellular matrix
<b>EMA</b>	European Medicines Agency
<b>ESC</b>	embryonic stem cell
<b>EUTCD</b>	European Union Tissue and Cells Directives
<b>FBS</b>	fetal bovine serum
<b>FSS</b>	fluid shear stress
<b>GvHD</b>	graft-versus-host disease
<b>HE</b>	hematoxylin and eosin
<b>HP</b>	hydrostatic pressure
<b>HPL</b>	human platelet lysate



<b>HS</b>	human serum
<b>iPSC</b>	induced pluripotent stem cell
<b>MDU</b>	medium distribution units
<b>MOA</b>	mode of action
<b>MSC</b>	mesenchymal stem cell
<b>OCN</b>	osteocalcin
<b>ODM</b>	osteogenic differentiation medium
<b>OPN</b>	osteopontin
<b>PDL</b>	population doubling level
<b>PI</b>	propidium iodide
<b>PFA</b>	paraformaldehyde
<b>PFR</b>	plug flow reactor
<b>POM</b>	polyoxymethylene
<b>RM</b>	Regenerative Medicine
<b>RPM</b>	revolutions per minute
<b>RTD</b>	residence time distribution
<b>RWV</b>	rotating wall vessel
<b>SEM</b>	scanning electron microscope
<b>STR</b>	stirred tank reactor
<b>SVF</b>	stromal vascular fraction
<b>TIS</b>	tanks-in-series
<b>UTS</b>	ultimate tensile strength
<b>VK</b>	Von Kossa

## List of Symbols

$\rho$	Density
$\mu$	Dynamic viscosity
$Q$	Volumetric flow rate
$k$	Permeability
$\varepsilon$	Porosity
$\psi$	Sphericity
$Re_i$	Interstitial Reynolds number
$\tau_w$	Wall shear stress
$\tau_{wavg}$	Average wall shear stress
$\tau_{wmax}$	Maximum wall shear stress
$V_R$	Reactor volume
$T$	Hydrodynamic residence time
$T_m$	Mean residence time
$N$	Number of tanks in series
$Bo$	Bodenstein number
$k_{La}$	kla
$t_{PD}$	Population doubling time

# 1 Introduction

## 1.1 Motivation

The market for regenerative medicine is rapidly growing worldwide with a stunning estimated compounded annual growth rate of up to 70 % for stem cell-based therapies [1]. Furthermore, within the field of regenerative medicine the vast amount of companies is related to cell-based therapies and tissue engineering. Although it stated that embryonic stem cells (ESCs) and induced pluripotent stem cells (iPSCs) have great potential in the field of regenerative medicine they are still far away from clinical application due to ethical and safety concerns. Therefore, mesenchymal stem cells (MSCs) are still considered as the primary candidate for stem cell-based therapies and tissue engineering products. Nevertheless, regulatory frameworks in the US or Europe are demanding and product development requires careful considerations on the later manufacturing and approval process from the beginning of basic research throughout clinical trials. Although the number of clinical trials where MSCs are involved is increasing with approximately 250 ongoing trials (*clinicaltrials.gov*, May '17) most of the tested therapies fail to show therapeutic benefits. Thus, translational research needs to be improved to increase success in clinical trials. For this, researchers, clinicians and manufacturer need to be closely connected and work hand in hand on the one side. On the other side, results from basic research need to be more predictable for *in vivo* human trials which requires in depth knowledge on relevant biological parameters and how to mimic them *in vitro*. However, in the case of MSCs, traditional two-dimensional (2D) static cell culture on plastic surfaces do not represent the *in vivo* situation.

To generate a physiologic environment that represents the natural conditions of human MSCs numerous parameters need to be considered. Three dimensional (3D) biomaterials made of ceramics, synthetic polymers or natural polymers mimic the natural environment and thus have detrimental influence on cellular behavior like tissue generation or differentiation [2]. Cell-seeded scaffolds are then used for *in vitro* models or to replace damaged tissue *in vivo*. Moreover, mechanical forces such as compression, tension, fluid shear and hydrostatic pressure can be harnessed to exert mechanical loading on cells and induce mechanotransductive effects such as differentiation into a specific lineage or enhanced matrix mineralization [3]. Other parameters such as medium composition, xeno-free serum supplements and oxygen concentration can also contribute to generate more *in vivo*-like culture conditions. Implementation of these parameters was shown to trigger *in vivo* behavior of MSCs comprising many effects such as increased proliferation, induction of or enhanced differentiation into specific lineages, elevated secretion of anti-inflammatory factors but also increased survival rate of cells *in vivo* [2–4].

Bioreactors were traditionally developed to carry out reproducible, automated bioprocesses and to ensure proper control over relevant cultivation parameters during cultivation. However,

for the generation of tissue engineered products the implementation of physiologic conditions with regards to the mechanical environment became crucial. Therefore, numerous bioreactors for the exertion of the above mentioned mechanical forces have been developed within the last two decades [5, 6]. Still, quantitative methods for the online measurement of forces in bioreactors as well as for the automated control and application remain to be developed. Besides the application of mechanical forces, agitation, stirring or perfusion in bioreactors enhanced mass transfer which is critical for nutrient and oxygen supply into 3D scaffolds. Mass transfer, fluid dynamics and scaffold properties are closely related and therefore extensive characterization of the bioreactor and the 3D scaffold are required to gain knowledge and control over the bioprocess. X-ray computed microtomography and other novel imaging techniques are used to determine porosity, pore size, interconnectivity and the macroscopic structure of a scaffold [2, 7]. Together with computational fluid dynamics (CFDs) this data can be used to predict the fluid characteristics, such as flow velocity profile and streamlines of fluid elements in the bioreactor but also to simulate the mechanical environment, such as shear rates, wall shear stress and hydrostatic pressure that cells on the scaffold are exposed to.

A typical tissue engineering process comprises the isolation, expansion and differentiation of MSCs towards a specific lineage in order to generate a functional tissue construct for transplantation or for use in an *in vitro* model. Furthermore, for cell-based therapies rapid expansion of MSCs while maintaining their stem cell properties is required. Therefore, the implementation of physiologic conditions in all steps of stem cell cultivation seems desirable.

## 1.2 Aims

The present work focuses on the implementation of physiologic conditions for the *in vitro* cultivation of human MSCs with regards to isolation procedures, expansion and osteogenic differentiation (Figure 1.1).

First, the isolation of MSCs from adipose tissue by explant culture is presented and compared with the traditional isolation by enzymatic digestion.

Second, the cultivation of scaffold-free 3D MSC aggregates is characterized and approaches for the upscale of this method are presented.

Third, a concept on how to define and generate a physiologic mechanical environment for osteogenic differentiation is presented.

In all steps of cultivation a reduced oxygen concentration of 5% O<sub>2</sub> was implemented and compared with ambient oxygen concentration of 21% O<sub>2</sub>. Furthermore, the three dimensional cultivation in dynamic bioreactor systems is emphasized.

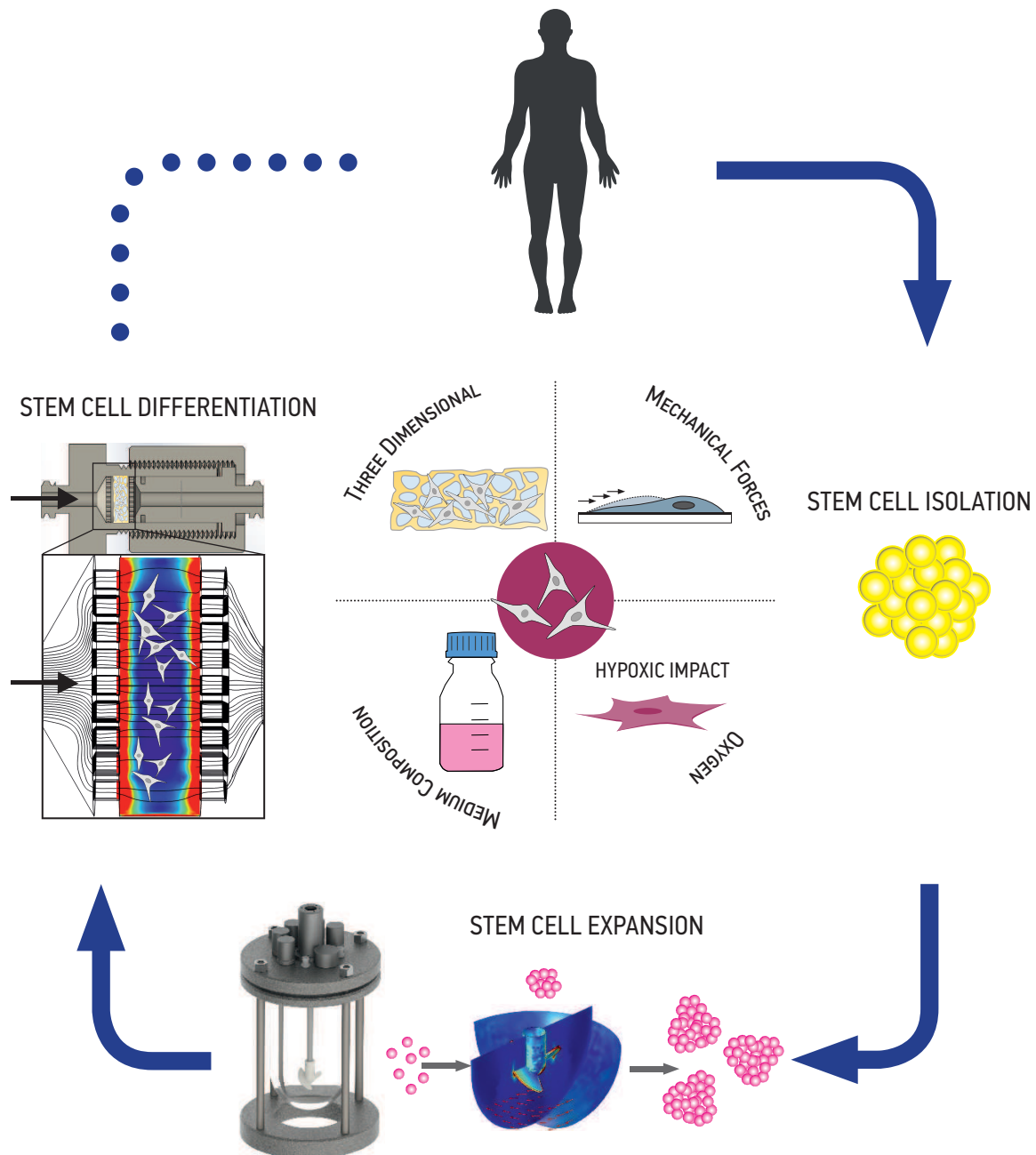


**Figure 1.1:** The graphical abstract depicts concepts for the implementation of physiologic conditions during major steps of *in vitro* human mesenchymal stem cells (MSCs). For the therapeutic application of MSCs in cell-based therapies the three major steps of stem cell isolation, *in vitro* expansion and differentiation (in tissue engineering approaches) need to be conducted. The inner circle depicts crucial factors that contribute to the generation of a physiologic environment *in vitro*. For the experimental work of this thesis these factors were considered and implemented for the isolation, expansion and differentiation of human MSCs.

## 2 Theoretical Background

### 2.1 Regenerative Medicine - Where Are We?

The beginnings of Regenerative Medicine (RM) can be pinpointed back to the late 70's where first discoveries on artificial skin paved the way to far more advanced research and commercialization of RM products. Since then, hopes were risen and promises given and after an enormous development it is time to evaluate the current status and future prospects of RM.

Today the field of RM comprises cell-based therapies, gene therapies, biologics and small molecules, tissue engineering approaches and utilization of stem cells for drug discovery, toxicity testing and disease modeling with the aim of replacing damaged tissue, activating the body's own healing response or delivering molecular and gene therapies to targets. Cell and tissue banks as well as service companies are making more than half of the involved enterprises. Regarding therapeutic related companies the largest group provides cell-based therapies followed by tissue engineering products.

By 2017 the global market of RM products is estimated to reach a US\$24.7 billion while the orthopedic branch alone will reach US\$10.3 billion with a compounded annual growth rate (CAGR) of 12.2 % between 2013 – 2019 [8]. The Asia-Pacific market is assumed to display the highest CAGR with 18.1%. The annual data report 2016 from the "Alliance for Regenerative Medicine" counts more than 770 RM related companies worldwide with North America representing about 50 % of it and Europe and Israel 27 % (see). Likewise, the number clinical trials increases drastically. In 2016 worldwide 804 clinical trials were reported of which 238 were reported from Europe, which displays an increase of 21 % compared to 2015 with 631 reported trials [9].

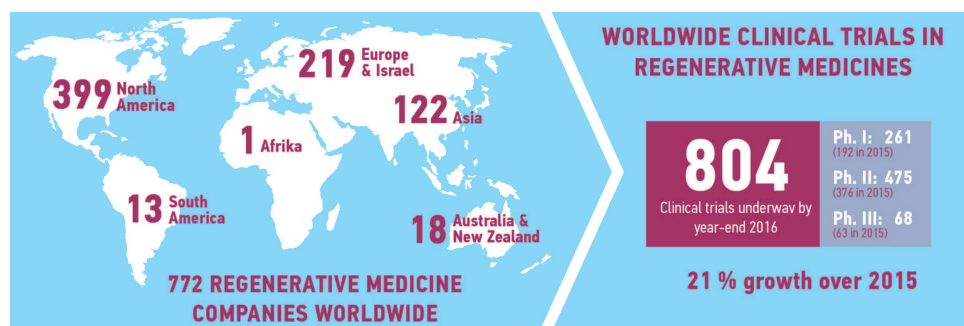


**Figure 2.1:** Worldwide companies and clinical trials in the field of Regenerative Medicine from 2016. Data obtained from [9].

Three stages of living cell product development have been observed in the field of RM: (a) vaccines, blood transfusions and stem cell transplantations, (b) bioengineered skin and chondrocyte-based therapies, (c) chimeric antigen receptor (CAR) T cells for cancer therapy and other diseases [10]. The CAGR of stem cell-based therapies is estimated 70 % from US\$5 million in 2012 to US\$9 billion in 2025 [1]. Indeed, many products are currently in Phase III trials such as MSC-100-IV, mesenchymal stem cell preparation developed for acute pediatric graft-versus-host disease (GvHD), MPC-150-IM, a mesenchymal precursor cell preparation to treat chronic heart failure or MPC-06-ID (also mesenchymal precursor) for treatment of lower back pain due to degeneration of spinal discs. After stunning success in cancer therapy of CAR T cells in clinical trials [11] (i.e. the treatment of lymphoblastic leukemia [12]) it is likely that the market for RM will grow even more.

Still, considering the paradigm "*from bench to bedside*", people from all fields of RM notice a serious gap between *bench* and *bedside*. Indeed, to improve and foster product development and clinical outcome, translational research was recently covered in several expert reviews [10, 13–16] and discussed on international conferences (i.e. "ATMP 2015 - Issues and challenges from bench to bedside" Tutzingen, Germany or TERMIS World Congress 2015, Boston, USA). As a result, Fernandez-Moure proposes the current paradigm "*from bench to bedside*" needs to change to "*from the bedside to bench and back*" [13].

Ronfard et al. defined five drivers for research in RM: manufacturing, reimbursement, multicompentence collaborations, regulatory compliance and clinical trials [10]. Although manufacturing and reimbursement issues are important they are more relevant in later stages of product development and not of primary concern for researchers. Multicompentence collaborations are valuable but need to be elaborated and strengthened before research is conducted. However, the later two, regulatory compliance and clinical trials, are issues that researchers should take into account from the very beginning. Many ideas, approaches and promising results are or cannot be pursued further since they are conceptually incompatible with the approval for clinical trials. Also Gardner et al. come to the conclusion that regulation and clinical trials are very specific challenges of RM and therefore people on all levels need more clarification and information on these topics.

To avoid those so called "valleys of death" where the development of a product comes to halt, prior considerations regarding the national regulations on the "research-level" are crucial. In the following section the regulatory framework of Europe will be outlined and considerations on how basic research can be conducted to increase the translation to clinical trials are discussed.

### 2.1.1 Europe's regulatory framework

In Europe medicinal products are regulated by the European Medicines Agency (EMA). Before a product enters the approval process it must be assigned to one of the following categories: medicinal product, advanced therapy medicinal product (ATMP), medical device or combined ATMP. Their definitions and related EU directives are depicted in Table 2.1. Most products that are developed in the field of RM fall into the category of (combined) ATMPs which are subdivided into somatic cell therapies, gene therapies or tissue engineered products. Since late 2008, the approval and market authorization process is regulated by Regulation (EC) 1394/2007.

Since then the evaluation, authorization and follow-up is supervised by the Committee for Advanced Therapies (CAT). The classification which is defined by the mode of action (MOA) of the product finally determines which path of approval a product needs to take [17, 18]. For example, if a product consisting of human tissue or cells (viable or non-viable) is only minimally manipulated and intended for homologous use (as defined by the EMA in their recent reflection paper on ATMPs [19]) it is not regulated by the ATMP regulation but only by the European Union Tissue and Cells Directives (EUTCD). In contrast, expansion of cells or enzymatic digestion during cell isolation, is already considered as substantial manipulation and is thus regulated by (EC) 1394/2007. Furthermore, other directives may also apply. ATMPs must be manufactured according to good manufacturing process (GMP) guidelines (directive 2003/94/EC). Also, if human tissue and cells are involved the EUTCD which regulate the donation, procurement, testing, processing, preservation, storage and distribution of tissue and cells across Europe applies (directive 2004/23/EC, 2006/17/EC and 2006/86/EC). Clinical trials must be planned and performed according to good clinical practice (GCP) guidelines (2001/20/EC). The interplay and overlap of applicable directives is depicted in Figure 2.2.

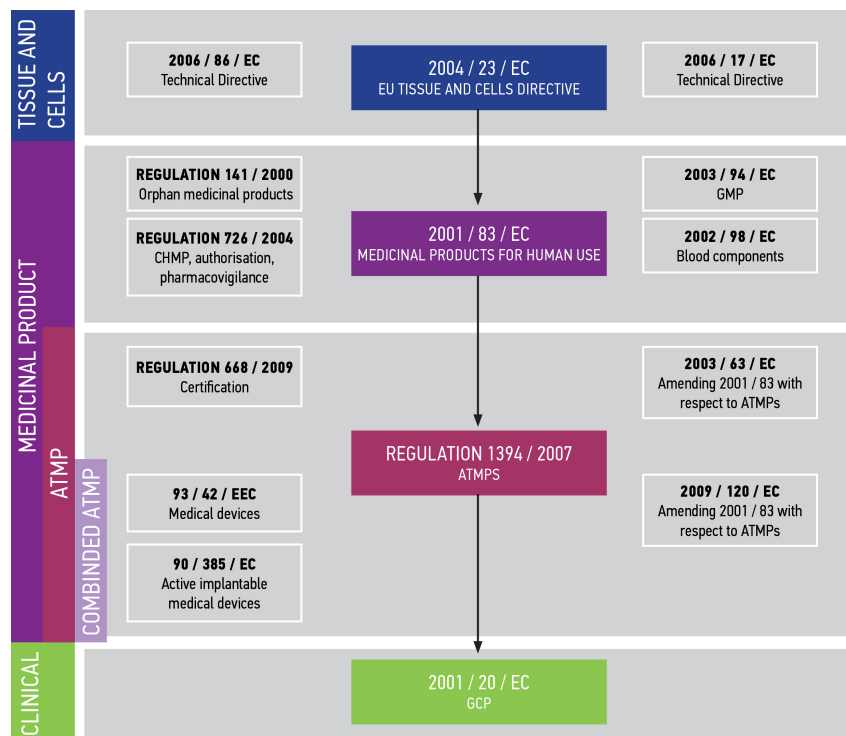


**Figure 2.2:** Overlap and interplay of EU directives that apply for the approval of ATMPs. The directives comprise handling with tissues and cells, the regulatory framework for medicinal products and ATMPs and handling in the clinic. Modified from [21].

Together, these guidelines and regulations ensure safety and traceability of RM products that want to enter the European market. However, since December 2008, when the ATMP regulation came into force, only 8 products have been approved by the EMA with Zalmoxis, an *ex vivo* genetically engineered cell therapy for the treatment of GvHD after hematopoietic stem cell transplantation, from MolMed being the most recent (see Table 2.2).

To overcome the challenges of successful approval and market authorization early decisions



**Table 2.1:** Definitions of the different classifications of medicinal products as defined by the EMA (modified from [20]).

Classification	Definition
Medicinal product	(i) Any substance or combination of substances presented as having properties for treating or preventing disease in human beings or (ii) any substance or combination of substances which may be used in or administered to human beings either with a view to restoring, correcting or modifying physiological functions by exerting a pharmacological, immunological or metabolic action, or to making a medical diagnosis. (Directive 2001/83/EC, Article 1.2)
ATMP	Consists of either: (i) a gene therapy medicinal product as defined in Part IV of Annex I to Directive 2001/83/EC or (ii) a somatic cell therapy medicinal product as defined in Part IV of Annex I to Directive 2001/83/EC or (iii) a tissue engineered product as defined in (1[d] [EC] No. 1394/2007)
Combined ATMP	Must incorporate, (i) as an integral part of the product, one or more medical devices within the meaning of Article 1(2)(a) of Directive 93/42/EEC or (ii) one or more active implantable medical devices within the meaning of Article 1(2)(c) of Directive 90/385/EEC <b>and</b> (i) its cellular or tissue part must contain viable cells or tissues, or (ii) its cellular or tissue part containing nonviable cells or tissues must be liable to act upon the human body with action that can be considered as primary to that of the devices referred to (2001/83/EC) or tissue engineered product (1[d] [EC] No. 1394/2007)
Medical device	Any instrument or other article to be used in human beings for the purpose of (i) diagnosis, prevention, monitoring, treatment or alleviation of disease or compensation for an injury or handicap or (ii) investigation, replacement or modification of the anatomy or of a physiological process or (iii) control of conception, and which does not achieve its principal intended action in or on the human body by pharmacological, immunological or metabolic means, but which may be assisted in its function by such means (Directive 93/42/EEC, article 1.2[a]) 90/385/EEC

on important issues will be of tremendous benefit. Researchers and investors need to clarify in advance whether there is a true "clinical pull" to conduct the following steps in research and translation and early classification of the product will help to make considerations on the requirements of the later approval and manufacturing process. Still, the pre-clinical data must be robust and promising in order to apply for approval for clinical trials. Therefore, considerations on the very basic research level may improve the later translation process.

### 2.1.2 Translational research

The translation of results from basic research to clinical application has always been difficult. In general, about 85 % of therapies fail in phase I or II clinical trials and only half of products that enter phase III trials are then approved [23]. Besides the fact that some products are just not effective in a statistical significant number of human beings, possible sources of failure during clinical trial but also basic research exist. Translational research comprises at least five phases

**Table 2.2:** Approved ATMPs since 2009. CT = cell therapy, GT = gene therapy, TEP = tissue engineered product. Marketing authorization \* withdrawn or ★ suspended. Data obtained from [22].

Product, Type	year	Treatment	Company
ChondroCelect, TEP	2009	Autologous Chondrocytes for repair of single symptomatic cartilage defects of the femoral condyle of the knee	TiGenix *
Glybera, GT	2012	Human lipoprotein lipase in a vector for treatment of lipoprotein lipase deficiency ind adults	UniQUre
Maci, TEP	2013	Autologous cultured chondrocytes for repair of symptomatic cartilage defects of the knee.	Vericel Corp. ★
Provenge, CT	2013	Autologous CD54+ cells for treatment of prostate cancer	Dendreon Corp. *
Holoclar, TEP	2015	Autologous corneal epithelial cells for repair of damaged corneal surface in patients with limbal stem cell deficiency	Chiesi
Imlygic, GT	2015	Genetically modified oncolytic herpes virus for the local treatment of unresectable lesions in patients with melanoma	Amgen
Strimvelis, GT	2016	Autologous CD34+ cells to treat severe combined immunodeficiency due to adenosine deaminase deficiency	GSK
Zalmoxis, GT	2016	Genetically modified allogeneic T cells for the treatment of GvHD after hematopoietic stem cell transplantation	MolMed

which means four "translations" in between and all of them need to be successful to ensure proper outcome (Figure 2.3). Researches, clinicians, health care and industry need to work hand in hand but do not speak the same language. Especially in the area of ATMPs, several uncertainties are present. Tissues or cells are fragile and thus require a complex, yet suitable and safe infrastructure. Furthermore, the production of the demanded quantities for phase III trials often require a more advanced manufacturing process already. Additionally, therapeutically beneficial effects observed in the lab are often not present in first human trials and thus projects come to a halt very early. To overcome the hurdles of early translational research, pre-clinical science might take into account regulatory standards and the later manufacturing process.

The GLP standards for example require to record lot numbers, store all raw data, choose significant controls and the development and use of standard operating procedures (SOPs) is mandatory. These standards ensure reliable data that would also pass later safety or risk assessments. Also, approaching the regulatory authorities might be beneficial in an early stage of development since authorities' advice will help align routine work to the required standards.

Research in the field of ATMPs relies on basic products or raw materials which should be considered carefully keeping in mind later approval procedures. For example the use of xenogeneic

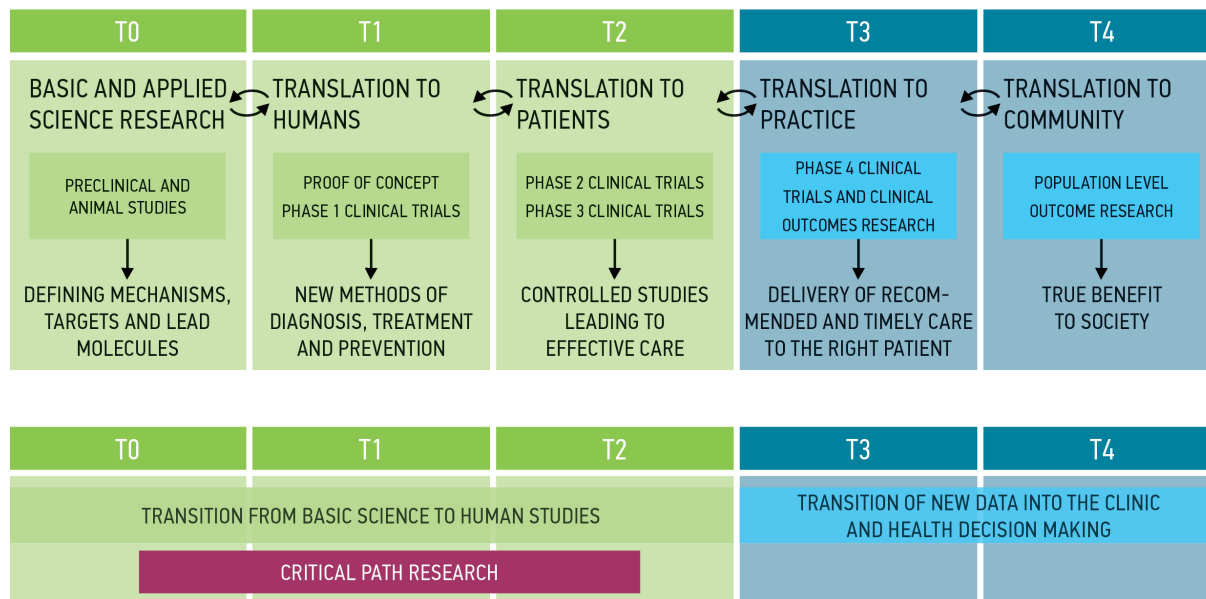


**Figure 2.3:** Translational research comprises five different phases depicted as T0 – T4 where T0 – T2 comprises translation from basic research to clinical trials and T3/T4 comprise follow up studies. Each phase is defined by distinct challenges and moreover need to communicate with the prior and advancing phase; modified from [13].

compounds such as fetal bovine serum (FBS) might complicate the later approval process. Furthermore, xenogeneic compounds might cause non-physiologic reactions that are not predictable for later *in vivo* testing. The approval status of every single component that comes into contact with the product needs to be assessed.

To increase the predictability of pre-clinical studies proper models for *in vitro* testing are of tremendous importance. These models must be relevant from a regulatory perspective and robust with regards to safety, efficacy, purity and dose response. Owing to advances in three dimensional cell cultivation and dynamic cultivation systems *in vitro* models are getting better and thus more predictable for clinical outcome [24–26].

In contrast, to the production of traditional (bio)pharmaceuticals, ATMPs are always based on the use of cells or tissue. Therefore, maintaining the quality from the isolation through the manufacturing process to delivery of the product is different and challenging. The determination and characterization of crucial process parameters is fundamental to gain understanding and comprehensive control. There are peripheral subprocesses such as reagent preparation, cryopreservation, cell sources or starting materials and the core process that is again subdivided, i.e. in expansion, differentiation, product formulation and logistics of a tissue engineering process. It is tremendously important to determine and characterize relevant process parameters to understand each process step so that the extent of variations remains within required limits [27]. New technologies for process characterization or online monitoring, such as novel imaging techniques or process-modeling algorithms, are emerging and will enable for complicated processes. However, the process is also dependent on the understanding of cellular response to a specific environment. The extracellular conditions that build the artificial environment of cells during a manufacturing process affects potency and safety of cells [28]. During isolation or expansion of cells the culture conditions might select for specific subtypes resulting in altered potency of

these cells. Also keeping cells undifferentiated or guide their differentiation into only one specific cell type depends on the macro- and microenvironment. Therefore, novel bioreactor systems for expansion and differentiation of cells that provide comprehensive control on process parameters and thus the cell properties are required [29].

## 2.2 Adipose Mesenchymal Stem Cells in Regenerative Medicine

Although human embryonic stem cells (ESCs) offer great promise to the field of RM they are not approved for clinical application due to ethical concerns and safety issues [30]. Also, iPSCs raised hopes since the simple yet effective process of reprogramming adult cells from almost every source gave rise to a seemingly endless source of pluripotent cells [31]. However, iPSCs are not genetically stable and therefore are still not considered for clinical application [32]. Therefore, the primary and most promising candidate for therapeutic stem cell therapies are currently human mesenchymal stem cells (MSCs).

MSCs comprise a heterogeneous cell population that is derived from the mesenchyme (embryonic connective tissue). They are mostly isolated from bone marrow [33], adipose tissue [34], umbilical chord [35, 36], dental tissue [37] and the amniotic membrane [38] but are also present in a variety of other tissues such as tendon [39], ligaments [40] or skin [41]. Minimal criteria for the characterization of MSCs were defined in a position paper from 2009 by the International Society for Cellular Therapy and since then they are defined by plastic adherence, trilineage differentiation (adipogenic, chondrogenic, osteogenic) and a specific surface marker expression profile (positive for CD105, CD73, and CD90 and negative for CD14, CD19, CD34, CD45, and HLA-DR) [42]. The regenerative potential of MSCs is not limited to their high *in vitro* proliferation potential and their ability to differentiate into adipocytes, chondrocytes, osteoblasts. Research from the last decade reported also *in vitro* differentiation to neurons [43], cardiomyocytes [44] and corneal epithelial cells [45] as well as effects strongly related to injury repair. These are migration to injury sites [46], immunomodulatory and anti-inflammatory properties mediated by cellular cross talk or secretion of trophic factors [47], angiogenesis [48] and anti-scarring effects [49]. However, the regenerative potential of MSCs seems to be dependent on donor age, sex and tissue origin [50]. For example bone marrow derived MSCs display a higher osteogenic differentiation potential than umbilical chord derived MSCs [51]. These findings confirm the heterogeneous character of MSCs and indicate that specific subpopulations are more prominent in specific tissues than others. Also differing cultivation conditions might select for, and thus enrich or diminish, specific subpopulations in isolated MSCs.

The experimental work in this thesis was exclusively conducted with human adipose derived mesenchymal stem cells (ASCs). They are easily isolated by mechanical dissociation or enzymatic digestion of resected adipose tissue or lipoaspirates, as discussed later in chapter 3, and display similar properties as bone marrow derived MSCs which are still considered as the gold standard for clinical application. However, characterization of these cells still lacks accuracy and uniformity which probably contributes to heterogeneity of terms used for this population such as preadipocytes, pericytes, stromal vascular fraction (SVF) cells, adipose derived adult

stem cells/stromal cells, adipose mesenchymal stem cells or processed lipoaspirate cells. In this work the term adipose derived mesenchymal stem cell (ASC) is used interchangeably for this population as proposed by the international Fat Applied Technology Society [52].

Directly after isolation of ASCs the population is not only characterized by mesenchymal markers but also endothelial markers CD31 and C144 and hematopoietic markers CD11, CD14, CD45, CD86 and HLA-DR were reported in small percentages [53, 54]. However, the population is enriched by cells expressing mesenchymal markers over passages. Detailed definition and functional characterization of subpopulations that express different sets of non-typical MSC markers besides the typical MSC markers is a fast advancing field. Effects of distinct subpopulations were studied *in vitro* and *in vivo* [55]. For example ASC populations selected for CD34<sup>+</sup>, commonly referred to as a hematopoietic marker, displayed increased proliferation compared to CD34<sup>-</sup> cells. Furthermore, CD34<sup>-</sup> cells display increased adipogenic and osteogenic differentiation compared to CD34<sup>+</sup> cells [56]. CD34<sup>+</sup>/CD90<sup>+</sup> cells displayed endothelial differentiation and formation of capillary structures with high VEGF formation [57]. A population selected for CD271, a nerve growth factor receptor, was reported to differentiate not only into adipocytes, chondrocytes and osteocytes but also into neuronal cells compared to CD271<sup>-</sup> cells [58]. Also, populations enriched for CD105<sup>+</sup> cells display an increased chondrogenic differentiation potential [59]. In fact, selection for distinct subpopulations with distinct properties might enable for more advanced therapeutic approaches in RM as current *in vivo* studies (mostly carried out in mice) report beneficial effects on fat graft retention [60], osteogenic differentiation [61] or liver function [62]. However, authors also conclude that effects may not be predictable for application in human and moreover, since subpopulations display only small percentages of the total ASC population, the observed effects might not justify the effort for isolation and selection procedures [61, 63].

Regarding the clinical applications of ASC, by the time of writing a search for "adipose mesenchymal stem cells" at *clinicaltrials.gov* resulted in 109 worldwide ongoing studies related to musculoskeletal, metabolic, cardiac, neurological and other diseases. Completed studies report the application of ASCs in reconstructive surgery where they are thought to increase retention and integration of fat grafts [64, 65] but also orthopedic applications have been reported where ASCs were used to treat osteoarthritis, meniscus tear, osteonecrosis or tendon injuries [66] and authors report great clinical potential.

### 2.3 Physiologic Conditions in MSC Cultivation

Traditional cultivation conditions like the cultivation of MSCs on 2D plastic surfaces in a static environment, such as given with a standard T-flask, well-plate or petri dish are far away from representing the natural, physiologic environment of these cells. Research from the last decade proved without any doubt that when biological, chemical, physical and mechanical cues are adjusted to mimic the physiologic environment, cellular behavior changes dramatically. The biological context comprises cell-cell contacts, cell-extracellular matrix (ECM) contacts as well as the ECM itself. Chemical cues embrace growth factors, cytokines, nutrients, salts and toxic compounds. Physical cues are temperature, partial gas pressures or viscosity and mechanical cues describe the environment generated by physical forces, such as shear, pressure or tension.

To mimic the physiologic environment myriads of three-dimensional (3D) matrices from different materials and of different shape and geometry have been developed together with various bioreactor systems for the application of mechanical forces. The implementation of physiologic conditions is thought to increase the predictability of *in vitro* testing for *in vivo* trials and therefore to reduce animal testing. In the following section the most relevant parameters for the experimental work of this thesis, their effects on cellular behavior and engineered solutions are described.

### 2.3.1 The Third Dimension

Expanding the cellular *in vitro* environment by a third dimension adds immensely to the generation of a physiologic environment. To extend cellular growth to the third dimension supportive structures, also called scaffolds or matrices, have been engineered from numerous materials. However the vast amount consist of ceramics (like tri-calcium phosphate or hydroxyapatite), synthetic polymers (like polystyrene, poly-L-lactic acid or polyglycolic acid) or natural polymers (such as collagen, alginate or silk), each having different physicochemical properties, architecture and biodegradability [67]. Inherent material characteristics such as porosity, pore size and distribution, surface-to-volume ratio, mechanical characteristics and surface chemistry have an influence on cellular behavior. Cell attachment, migration, proliferation and differentiation were shown to be impacted by material characteristics. In return, 3D cultivation has a remarkable impact on the outcome of drug screening, cell shape, cell-cell and cell-ECM interactions [68, 69]. Obviously, every material has its own advantages and disadvantages and must be therefore chosen to fit the respective biological requirements. Ceramics are porous structures with high stiffness and thus suitable for bone tissue engineering approaches whereas softer, fibrous or gel-like matrices are more suitable for mimicking a skin, cartilage or tendon environment. To combine the best of different materials, composites containing two or more materials are gaining interest. Exemplary, the effects of the architecture and mechanical cues of porous materials on the biological response will be covered in the following.

**Porous materials** In a recent review article Gariboldi and Best propose four hierarchically scaled levels of abstraction for porous materials to allow for "*independent variation of parameters that give rise to all possible architectures*" [2] (see Figure 2.4). These levels comprise the surface topography, the pore size and shape, the interconnectivity of pores and the macroscopic arrangement of them. The surface topography comprises *roughness* and *microporosity*, that is the presence of pores with diameters  $< 10 \mu\text{m}$ . Surface topography has been reported to have impact on cell attachment, ingrowth, proliferation, protein synthesis and alkaline phosphatase (ALP) activity, however with conflicting results [70–72]. In fact, it is challenging to evaluate the isolated effects of surface topography on cellular behavior. Still, more thorough characterization in terms of geometry and topography might help conduct more reproducible studies.

The pore size and shape define the curvature which cells on the surface sense. Rumpler et al. demonstrated that radii much larger than the cells have an impact on cellular behavior. For example tissue generation was found to be proportional to the surface curvature [73]. A following study conducted with MSCs confirmed and found narrower pores to increase tissue generation

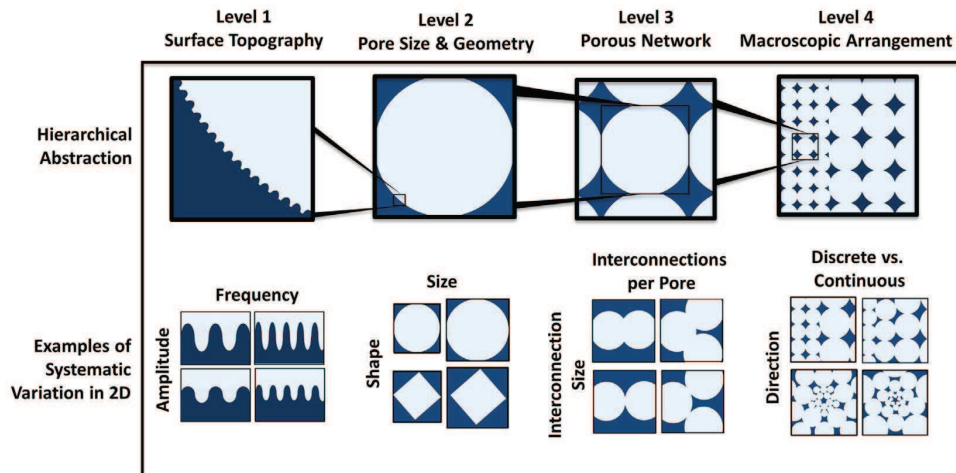


**Figure 2.4:** Hierarchical structure of 3D matrices for cell culture as proposed by Gariboldi and Best. Each level is defined by distinct features that cause various effects on the cellular behavior (adapted from [2]).

[74]. Also, cell attachment, migration speed and morphology are affected by the curvature [75]. Furthermore, the pore shape itself influences the cellular behavior. For example M3T3 cells on scaffolds with a parallelogram pore shape displayed higher ALP activity than scaffold with other shapes [76]. Again, it is challenging to determine the isolated effect of pore size, porosity and interconnectivity since they are to some extent dependent on each other. Also, altering the pore size while keeping porosity might result in altered mechanical characteristics of the scaffold which again affect cellular behavior. A curvature driven mathematical model by Bidan et al. successfully described and predicted tissue growth in a porous scaffold [77, 78]. It was further improved to describe the growth on convex vs. concave surfaces and thus incorporate effects of surface stress and tensile forces exerted by actin and myosin [79]. Computational models might help to choose in advance specific geometric properties to generate a physiologic environment. The effect of pore size on *in vitro* cartilage or bone generation is discussed in detail by Perez and Mestres [7]. They demonstrate that pore size of scaffolds have effects on proliferation and differentiation of progenitor cells and that the optimal pore size needs to be figured out for each individual cultivation process. For this, they propose gradient scaffolds to be effective for screening the optimal pore size. For example, ASCs displayed enhanced chondrogenic differentiation but lower proliferation at the highest pore size (400  $\mu\text{m}$ ) [80].

The interconnection of pores together with the pore size and shape determines the permeability of the matrix and thus is a crucial factor for cellular ingrowth but also nutrient supply and waste removal. It is defined by the pore size, interconnection size and shape (also referred to as tortuosity). Pores might be open, closed (disconnected) or blind-ended and thus contribute differently to the biological response. The size of interconnection was shown to influence cellular ingrowth of osteoblasts and chondrocytes [81, 82] but also the chondrogenic differentiation of MSCs [83]. Still, giving values of parameters like pore size and porosity is not sufficient to describe the interconnectivity of a scaffold and thus recent studies aim to better characterize and quantify this aspect of a scaffold. Ashworth, Best, and Cameron adapted the concept of percolation from geological research and introduce the *percolation diameter* which describes the

largest sphere that can travel through an infinitely large porous structure [84] (see Figure 2.5). In a following study they demonstrated the independence of interconnectivity and pore size and the relevance of a scaffold's percolation diameter for the extent of human fibroblast invasion into the scaffold [85].

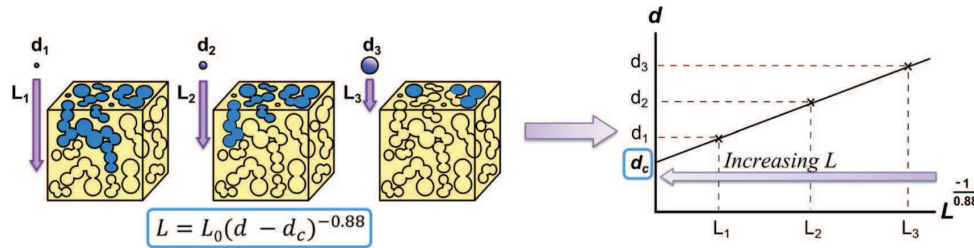


**Figure 2.5:** The percolation diameter as a quantitative parameter for the characterization of the interconnectivity of scaffolds. The maximum distance traveled in the z-direction ( $L$ ) for spheres with different diameters ( $d$ ) is plotted, allowing to infer the percolation diameter,  $d_c$ , the diameter of the largest sphere that can percolate through an infinitely long scaffold (adapted from [85]).

The macroscopic arrangement of the porous network of a scaffold can be used to direct biologic activity to specific parts of a scaffold. In this context, the pore network orientation, architectural gradients or patterns play a major role. For example, bone anisotropy, as caused by trabecula and osteonal orientation, is necessary for its biomechanical function and thus the scaffolds for bone regeneration should also resemble anisotropic properties which is caused by the macroscopic arrangement of pores. Tissues formed in isotropic scaffolds lack structural and functional relationships with the native tissues [86]. MSCs were found to proliferate and differentiate into osteoblasts on isotropic scaffolds [87]. However, studies that compare the isolated effect of isotropic against anisotropic matrices remain to be carried out. Since different material properties recruit different cell types, macroscopic gradation can be used to variate mechanical cues or interconnectivity and other properties to create tissue transitions or interfaces [88]. However, gradiated scaffolds were rather developed and tested for *in vivo* bone regeneration than for 3D cell culture [89, 90].

Stem cells reside in a broad range of tissues with highly differing mechanical properties such as stiffness and elasticity which were shown to have an impact on differentiation of MSCs [91, 92]. In a 3D environment MSCs were shown to display increased adipogenic differentiation in soft gels and in contrast increased osteogenic differentiation in stiffer gels [93]. Furthermore, matrix stiffness regulates the cell shape [94] which was previously shown to be linked to lineage commitment [95]. In general, cells seem to migrate to stiffer regions while still being influenced by the stiffness of the former region. Therefore, Justin and Engler propose that stiffness variation and not stiffness alone might be an important regulator for MSC fate. Although it is known that an interplay of cell shape, substrate stiffness and cytoskeletal tension owe to these mechanotransductive effects, the exact mechanisms remain to be evaluated [94].

In conclusion, it is obvious that all parameters together comprise the scaffold's effect on cellular behavior and thus for each cultivation process the scaffold needs to be chosen individually.



However natural derived scaffolds may represent the most physiologic environment. Decellularized native ECM holds the promise of matching the biophysical requirements of host cells in the case of transplantation [97] but were already used for tissue engineering approaches [98]. Numerous methods for decellularization exist [99] but the harsh conditions that are required to reduce disease transmission also impair preservation of bioactive molecules in the ECM. Also, these kind of materials are limited in availability and may not be as standardizable as synthetic materials.

**Scaffold-free 3D cultivation** Although biomaterials are necessary in most 3D cultivation setups also scaffold-free approaches exist. The cultivation of cellular aggregates, often referred to as spheroids, is used since decades in the field of embryonic stem cell research where it is also referred to as organoid culture [100]. However, this approach gained more interest also in the field of tumor research and tissue engineering where predictable 3D models that consist of cellular aggregates were developed. Cultivation of MSC aggregates was formerly conducted in the context of chondrogenic differentiation but is now used to study cellular behavior of MSCs. Spontaneous formation of cellular aggregates from a single cell suspension can be achieved by hanging drop culture or cultivation in cell-repellent cavities. Investigation of MSC aggregates revealed dramatic changes in cellular behavior including changes in morphology, mechanophysical properties and gene expression. Furthermore, enhanced anti-inflammatory [101], angiogenic and tissue regenerative effects [102] were observed as well as enhanced differentiation [103], maintenance of stem cell properties and delayed replicative senescence [102, 104]. Therefore, MSC aggregates are considered to represent a more physiologic environment and are thus of increasing clinical significance. In fact, in a recent review from 2017 Chimenti et al. state "*We need to consider the possibility that scaffold-free in vivo applications may represent a more physiological approach for tissue regeneration*" [105].

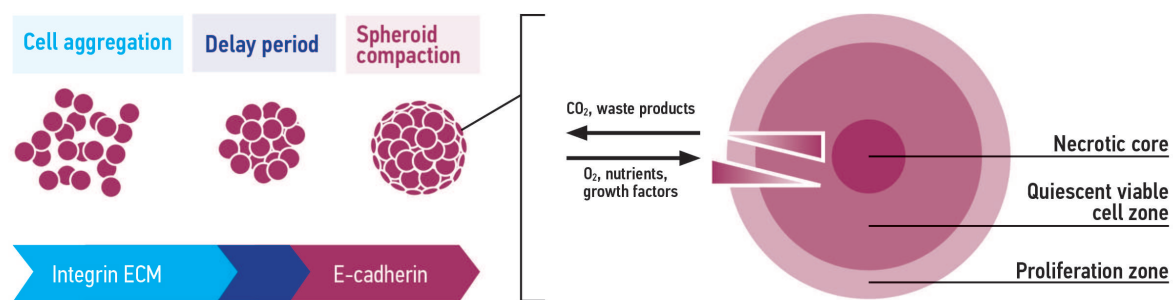


**Figure 2.6:** The formation of cellular aggregates is thought to be a three-step process: in the first phase integrin-ECM contacts cause loose aggregate formation. After a delay phase in which E-cadherin is accumulated the aggregate experiences compaction. Since oxygen, nutrient and waste gradients from the core to the aggregate surface exist, aggregates are composed of a necrotic core, a layer of quiescent cells and a layer of proliferative cells on the surface. However, necrotic cores only appear in aggregates with a diameter  $>500 \mu\text{m}$  in static cultivation conditions. Illustrations adapted from [106].

Aggregate formation by spontaneous self-assembly of single cells is proposed to be a three-step process [106] (see Figure 2.6). Loose aggregate formation through integrin-ECM binding is, after a delay phase, followed by compaction of the spheroid through enhanced cell-cell contacts via cadherin binding. However, cellular aggregates are limited in their size since mass transfer is

impaired and thus oxygen, nutrient and waste product gradients build up over time. Therefore, aggregates with a diameter  $>500\ \mu\text{m}$  generally display a necrotic core region surrounded by a layer of quiescent cells and an upper layer of proliferating cells [107]. MSC are usually cultivated in static cultivation systems (hanging drop, microtiter plates) but recent studies also report cultivation in dynamic systems such as spinner flasks or horizontal and orbital shaking platforms [103, 108–110]. Notably, in these studies no necrotic areas have been observed indicating sufficient mass transfer.

### 2.3.2 Mechanical Forces: a Necessary Burden

Research from the last decades revealed that MSCs are sensitive to mechanical forces. In fact, the exertion of mechanical forces (mechanical loading) on cells causes a biological response which is described by the term *mechanotransduction*. Mechanical forces are known to affect cellular behavior in manifold ways and thus are a crucial factor in MSC cultivation. For example, differentiation into specific lineages, proliferation and apoptosis are directly influenced by mechanical loading [3]. The physiologic relevance of mechanical forces seems obvious since every tissue is subject to motion and therefore to mechanical forces throughout all stages of development. Although none of these forces can occur independently they are subdivided into three main categories: compression, strain and shear forces while other forces like torsion, bending or hydrostatic pressure are derived from these. However, it is challenging to define which magnitude of the respective force represents the *in vivo* situation since *in vivo* measurements are difficult to carry out. Still, some data on *in vivo* forces exist and are summarized in Table 2.3. The following section describes occurrence of compression, tension, shear and hydrostatic pressure in the human body and their effects on MSC behavior.

**Compression** Compression is the application of an uniaxial force on two opposing points of a certain material resulting in size reduction in at least one direction and is thus the opposite of tension. Both are expressed in Pascal ( $\text{Pa} = \text{kg} \cdot \text{m}^{-1} \cdot \text{s}^{-2} \equiv \text{N} \cdot \text{m}^{-2}$ ) but are also expressed as strain  $\varepsilon$  which is a dimensionless factor that describes the fractional change in length. In the human body compression occurs mainly in bone and cartilage tissue of joints. Hodge et al. estimate compression in the human hip joint to occur in the range of 10 – 20 MPa during normal daily motion [111]. Compressive loading was mainly investigated with regards to chondrogenic differentiation in the field of MSC research where it was overall found to promote differentiation.

First works on compression were carried out by Huang et al. who found that cyclic compressive loading induced TGF- $\beta$ 1 synthesis and promoted chondrogenesis of rabbit MSCs. Further studies confirmed that compression increased chondrogenic gene expression in the absence of exogenous stimulation by other factors indicating that compression alone might be able to induce chondrogenic differentiation [113–115]. Again, recent studies indicate that effects of compression are in close relationship with properties of the surrounding matrix. For example, MSCs seeded in fibrin hydrogels underwent myogenic differentiation in long-term culture but chondrogenic differentiation when exposed to compressive loading [116]. Studies on the effect of compression on osteogenic differentiation of MSCs are scarce. However, Horner et al. cultivated MSCs on

electrospun 3D matrices and subjected them to 5, 10, 15 or 20 % strain ( $\varepsilon = 0.05, 0.1, 0.15, 0.2$ ) at 1 Hz for 2 h daily for 28 days in osteogenic medium. They found chondrogenic gene expression upregulated in a magnitude dependent manner with increasing strain whereas, in contrast, osteogenic gene expression was downregulated with increasing strain. They conclude that differentiation can be controlled by variations of the applied compression regime [117].

**Tension** As mentioned above tension is the opposing force to compression and therefore describes an axial pulling force on an object resulting in an increase of size. Thus, it is expressed by the same unit (Pa or  $\varepsilon$ ). Tensile forces mainly occur in muscles, tendons and bones. Tendons are thought to be subjected to one quarter of the ultimate tensile strength (UTS), the magnitude of tension where a tendon is disrupted, which is equal to approximately 25 MPa [118]. Studies on human tendon determined an UTS of 65 MPa for patellar tendon [119] and 100 MPa for the tendon of the extensor digitorum longus (muscle of the lower extremity) [118]. Thus, the physiologic range of tensile forces of human tendon may lie between 15 – 25 MPa for standard daily movements. However, explosive and dynamic movements might exert loading near the UTS. For bone the ultimate strength of femur bone was found to be approximately 55 MPa [120].

Mechanical strain has been shown to affect ligamentous [121], osteogenic [122] and chondrogenic differentiation [123]. Cyclic tensile strain caused increased BMP-2 expression [124], osteogenic gene expression [125] and matrix mineralization [126]. For example, Kearney et al. report a fivefold increase in BMP-2 expression in MSCs after 14 days of stimulation (2.5 % uniaxial strain at a rate of 0.17 Hz). Also, the induction of osteogenic differentiation without additional osteogenic supplements was observed [128]. In a direct comparison of compressive and tensile loading, compression activated chondrogenic gene expression whereas tension activated osteogenic gene expression [129]. As for compression, the magnitude, frequency, duration, application mode (continuous or intermittent) and total time span offer a multitude of variations that might cause different mechanotransductive effects.

**Fluid shear stress** When a fluid flows over a solid surface fluid shear forces are exerted on this surface. In a Newtonian fluid like water the shear stress is proportional to the shear rate which describes the gradient of flow velocity that is perpendicular to the flow direction. Consequently, fluid shear stress describes the deformation of a solid body where a force acts anti-parallel to its surface. As with compression and tension a force is exerted on a surface and therefore fluid shear stress (FSS) is also expressed by Pa. Another common unit to express FSS is  $\text{dyne}\cdot\text{cm}^{-2}$  which equals  $10^{-5}$  Pa. In the human body FSS is present in every tissue since about 20 % of the body's mass consists of interstitial fluids which is constantly in motion with a speed of approximately  $0.1 - 2 \mu\text{m}\cdot\text{s}^{-1}$  mostly due to osmotic and hydrostatic pressure differences [130]. In cartilage or bone tissue it is driven by compressive forces that for example are exerted by walking or exercising.

Since shear forces cannot be measured directly the physiologic range is difficult to estimate and calculations are often based on models. Therefore, only few data that describes physiologic *in vivo* FSS conditions exist. The most relevant model for excitation of osteocytes which was

developed by Weinbaum, Cowin, and Zeng estimates shear forces in the range of 0.8 – 3 Pa [131]. However, it is known that MSCs are also affected by significantly lower shear forces. Many studies report increased cell viability, matrix deposition and upregulation of differentiation genes when stem cells were exposed to fluid shear stress. As much as the effect of compression and hydrostatic pressure on chondrogenesis is investigated, the effect of fluid shear stress on the osteogenic differentiation of stem cells is subject of current research. In 3D cultivation FSS was observed to upregulate osteogenic genes like ALP [132, 133], different BMPs [134] or osteopontin [135] and improve matrix deposition [136, 137]. Though, in 2D experiments other genes are upregulated than in 3D. Also, in 3D experiments shear forces one order of magnitude lower than predicted by Weinbaum et al. displayed higher viability and in contrast, higher shear stress often resulted in cell detachment or apoptosis. Probably, geometric specifications and the arrangement of cells on the respective structure (pores, fibrils, meshes) have a substantial impact on the actual shear forces that are exerted on the cells as described in a detailed review by McCoy and O'Brien [138].

Since the body is not always in motion and therefore it is unlikely that steady-state flow and shear forces are always present the evaluation of intermittent and oscillatory flow has also been investigated. In general, intermittent flow seems to enhance osteogenic differentiation but results are not consistent. Increased expression of osteopontin [139], bone sialo protein [140] and PGE2 [141] were observed in osteoblasts while collagen I [141], ALP [139] and COX-2 [142] were not affected by intermittent low (or no) flow conditions. Unfortunately, the majority of studies only give information on flow velocity or the volumetric flow rate which does not allow for a quantitative comparison of studies. However, CFD analysis together with x-ray computed microtomography (microCT) data are getting more common and thus estimations on the exerted FSS are made more frequently [137]. Besides osteogenic differentiation, FSS also seems to promote cardiomyogenic differentiation of MSCs [143, 144].

**Hydrostatic pressure** hydrostatic pressure (HP) is a compressive force that is exerted by a stationary fluid in a closed system. It depends on the density of the fluid, the gravitational acceleration and height of the liquid column above a given point. Thus, for incompressible fluids HP can be written as  $p = \rho \cdot g \cdot h$  with  $p$  as the hydrostatic pressure,  $\rho$  the fluid density,  $g$  the gravitational acceleration and  $h$  the height of the liquid column. Notably, HP is an isotropic force acting uniformly with equal magnitude in all directions. Therefore, in contrast to compression, tension and shear, HP is a non-deforming force. Since the entire human body is based on the interplay of different fluids almost all cells experience hydrostatic pressure to some extent. However, pressure varies significantly depending on tissue and location in the human body. The interstitial fluid (0.27 kPa) and cerebrospinal fluid (1.2 kPa) exert pressure at the lower end of the physiologic range [145, 146]. Blood pressure which is mainly experienced by endothelial cells lies between 8 – 24 kPa [147]. Osteocytes in the lacunar–canalicular pores of load-bearing cortical bone experience a HP of  $\sim 270$  kPa [148]. The upper end of the physiologic range is for example found at the femoral head during exercise ( $\sim 18$  MPa) and is more than five orders of magnitude higher than in the interstitial fluid [149]. Furthermore, due to compressive loading and unloading during movement HP increases and decreases frequently with varying magnitude.

**Table 2.3:** Characteristics of mechanical forces in the human body.

Mechanical force	Induction of	Physiologic range	Reference
Compression	Chondrogenic differentiation	10 – 20 MPa	[111]
Tension	Osteogenic, chondrogenic, ligament differentiation	15 – 25 MPa	[118, 119, 154]
Hydrostatic pressure	Chondrogenic differentiation	5 — 6 MPa average, up to 18 MPa peak loading	[111]
Fluid shear stress	Osteogenic differentiation	0.8 – 3 Pa	[131]

For example the human walking frequency is approximately one stride per second (1 Hz) whereas it can easily increase up to three strides per second ( $>3$  Hz) or more during running. Therefore, the physiologic pressure of a specific cell type depends substantially on the location in the body.

The effect of hydrostatic pressure on the differentiation of stem cells was and still is under investigation, though more studies deal with the effect of chondrogenic rather than osteogenic differentiation. Bone marrow stem cells constantly are subject to medullary pressure during bone loading. Since they give rise to osteoblasts which are key players of the bone remodeling process it seems reasonable that HP plays also an important role in the differentiation process. HP has been found to increase osteogenic [150, 151] and chondrogenic [152, 153] differentiation in terms of mineralization and gene expression although some studies did not observe any effect on stem cell differentiation [94].

However, controversial results might be caused by the different experimental setups and loading regimes. Since HP is not constant in the human body most studies apply not constant but intermittent or cyclic pressure of different frequency and magnitude. Depending on the research question some studies applied a pressure regime over the entire cultivation period while other studies chose to apply pressure only once, i.e. at the beginning or end of the experiment. Therefore, it remains unclear what pressure conditions result in either osteogenic or chondrogenic differentiation of stem cells. Nevertheless, HP up to 10 MPa was found to increase chondrogenic gene expression whereas high pressure of 20 — 50 MPa causes cell apoptosis, tissue disruption and often a decrease in chondrogenic gene expression [94].

In general, three parameters can be altered when hydrostatic pressure is applied in cell culture. First, the operation mode: it can be either constant, intermittent (pauses alternating with periods of a specific pressure regime; not necessarily uniform) or cyclic (constant uniform pattern). It is also possible to apply a cyclic pattern in an intermittent pressure regime. Second, the frequency: this is the rate of pressure increase per second. Usually this parameter is given in the unit Hz, though other units may be used if longer intervals are applied. Third, the magnitude: it defines the maximum pressure and thus the height of amplitude. If pressure is increased and decreased steadily it constitutes a sinusoidal wave. Theoretically, it is also possible to alter the rate of increase/decrease and thus the shape of the wave itself. Nevertheless, the majority of studies were carried out at 0.5 – 1 Hz, for 1 – 4 h per day, with a magnitude of 0.1 - 10 MPa for a time-span of 14 – 21 days.

### 2.3.3 Medium composition - the endless endeavor

To generate a physiologic environment also physicochemical parameters of the cultivation medium as well as soluble factors need to be considered. Growth factors have great impact on proliferation, differentiation or senescence of cells. However, a multitude of growth factors exist and finding the optimal composition is challenging. The most prominent growth factor families that trigger cell proliferation (and therefore are used in standard cell culture media) are transforming growth factors beta (TGF- $\beta$ ), fibroblast growth factors (FGFs), platelet-derived growth factors (PDGFs) and epithelium growth factor (EGF). These and a variety of other factors are usually supplemented by addition of blood products, such as serum, platelet-rich plasma (PRP) and platelet lysate. Traditionally, fetal bovine serum (FBS) has been used in cell culture. However, due to the risk of immunogenic reactions and zoonotic infections FBS should not be used in the context of cell-based therapies. Moreover, FBS was shown to underly lot-to-lot inconsistency and its preparation has ever raised ethical concerns [155]. Consequently, the use of human serum (HS) was established for the cultivation of MSCs [156]. Since basal media have to be supplemented with a comparably high amount of 10 % HS the use of human platelet lysate (HPL) as an alternative was investigated. HPL has been proposed to be a more physiologic alternative than other blood derived products [155, 157]. In general, platelets are irregular shaped, non-nucleated bodies and are found in the blood at a concentration of  $1.5 - 4 \cdot 10^5$  / ml. They are involved in the formation of blood clots, blood vessels and wound healing by secretion of growth factors [158]. In fact, a wide array of growth factors was identified in HPL and their concentration is significantly higher than in FBS or PRP [155, 159, 160] (see Table 2.4). Therefore, HPL is usually applied at a concentration of 2.5 – 5 % which results in comparable proliferation observed at 10 % HS or even 20 % FBS [161]. GMP-grade HPL was shown to increase chromosomal stability of MSCs compared to FBS and to exhibit a high lot-to-lot consistency.

**Table 2.4:** Content of growth factors in different blood derived sera. All values are approximations and given in ng/ml [159, 160, 162].

Growth factor	Function	FBS	PRP	HPL
PDGF-AB	proliferation, wound healing	n.n.	160	50 – 300
PDGF-BB	proliferation, wound healing	n.n.	0.6	10 – 30
PDGF-AA	proliferation, wound healing	n.n.	0.6	1 – 10
TGF- $\beta$ 1	tissue differentiation, homeostasis, repair	12	70	50 – 300
VEGF	cell recruitment for neovascularization	n.n.	-	5 – 20
EGF	growth and tissue repair	n.n.	0.3	0.5 – 20
IGF1	proliferation	110	0.06	50 – 200

Also, the concentration of glucose as the source of energy impacts cellular proliferation and replicative senescence. Several studies demonstrated increased proliferation and reduced replicative senescence of MSCs at low glucose conditions (usually 1 g/l) compared to high glucose conditions (4 – 6 g/l) [163–165]. The addition of glutamine in a stable form was also found to increase proliferation.

Although these data indicate trends for optimizing media towards physiologic conditions, other factors like the concentration of amino acids, salts or minerals are crucial as well. Further research on the physiologic level on these could contribute to the development of physiologic, chemically defined cell culture media.

### 2.3.4 Oxygen: Keeping the Finger On the Switch

Conventional in vitro cell culture is usually performed under ambient or so called “normoxic” oxygen concentrations (21 % O<sub>2</sub>). Since the average oxygen concentration in human tissues varies between 2 and 15 % depending on the vascularization of the tissue or organ and its metabolic activity, conventional cell culture techniques do not reflect the physiological environment of MSC [166–168]. High concentrations of oxygen can lead to oxidative stress via the production of reactive oxygen species (ROS) that can damage lipids, proteins and DNA [169]. Thus, lowering the oxygen concentration is thought to reduce stress caused by ROS. The effect of hypoxia

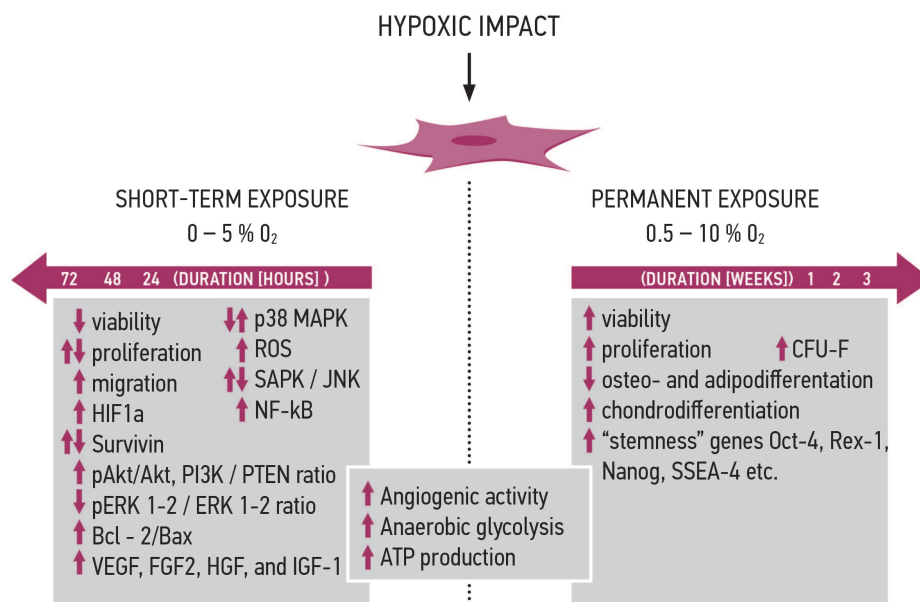


**Figure 2.7:** Effects of short- and long-term hypoxia on MSC behavior (adapted from [170]).

on MSC is certainly dependent on several parameters, including the degree of experimental hypoxia, the source of MSC and the presence or absence of cell culture media supplements [170]. Nevertheless, increased proliferation [171–173], delayed replicative senescence [174], prolonged genetic stability [175], altered differentiation capacity [176] and altered glucose metabolism [177] are the most prominent effects observed in MSCs under hypoxic conditions.

However, different effects were observed in short-term (< 72 h) compared to long-term (> 4 days) exposure to reduced oxygen concentrations (see Figure 2.7). Short-term exposure seems to provoke cell damage and apoptosis, while under long-term exposure cells adapt to hypoxia by switching their metabolism to anaerobic glycolysis which in turn contributes to maintenance of an undifferentiated multipotent state [170]. Also, adipogenic and osteogenic differentiation seems to be impaired by hypoxic conditions whereas chondrogenic differentiation is promoted.

Obviously, implementation of reduced oxygen conditions seems favorable in the context of stem cell expansion or to guide differentiation into specific lineages.

### 2.3.5 The physiologic toolbox

Table 2.5 gives a conclusive overview of the above mentioned factors that need to be considered for the generation of a physiologic environment. Since every cultivation process demands different prerequisites the choice of the matrix, mechanical loading or medium composition is always different. However, research from the last two decades elucidated many aspects and nowadays prior considerations may help to start with suitable initial conditions.

**Table 2.5:** Crucial factors for the implementation of physiologic conditions in the cultivation of MSCs.

Factor	Effects	References
<b>3D cultivation</b>		
Microtopography	Microporosity: cellular ingrowth $\uparrow$ ; proliferation $\downarrow$ , protein synthesis $\downarrow$ , ALP activity $\downarrow$ . Roughness: cell adhesion $\uparrow$ , proliferation $\uparrow$	[70–72]
Curvature & pore size	increasing curvature: tissue generation $\uparrow$ ; pore size influences proliferation and differentiation	[73, 74, 80]
Interconnectivity	impacts cellular ingrowth and differentiation	[83, 85]
Macroscopic arrangement	isotropy: theoretically lacks structural and functional relationships with the native tissues and thus should be avoided; studies on isotropy vs. anisotropy are required	[86]
Stiffness & elasticity	low stiffness: adipogenesis $\uparrow$ ; high stiffness: osteogenesis $\uparrow$ ; influences cell shape and lineage commitment	[93, 94]
Scaffold-free (aggregate)	affects morphology, mechanophysical properties and gene expression; anti-inflammatory factors $\uparrow$ , angiogenesis $\uparrow$ , replicative senescence $\downarrow$ ,	[101, 102, 104]
<b>Mechanical forces</b>		
Compression	chondrogenic differentiation $\uparrow$	[113–115]
Tension	ligamentous, osteogenic and chondrogenic differentiation $\uparrow$	[121–123]
Fluid shear stress	osteogenic differentiation $\uparrow$ , including ALP $\uparrow$ , BMPs $\uparrow$ , osteopontin $\uparrow$ , matrix deposition $\uparrow$	[132–137]
Hydrostatic pressure	osteogenic and chondrogenic differentiation $\uparrow$	[150–153]
<b>Medium composition</b>		
Humans serum	increased proliferation compared to FBS, supplementation with 10 % sufficient to replace 20 % FBS	[178]
Human platelet lysate	increased proliferation compared to FBS and human serum, supplementation with 2.5 – 5 % sufficient to replace 10 % human serum	[179]
<b>Oxygen tension</b>		
Short-term	proliferation, cell damage $\uparrow$ , apoptosis $\uparrow$	[170]
Long-term	stemness $\uparrow$ , proliferation $\uparrow$ , replicative senescence $\downarrow$ , altered glycolytic metabolism, altered differentiation compared to normoxic	[170]

## 2.4 Dynamic Cultivation of MSCs

### 2.4.1 Commercially available bioreactors

During the last decade the importance of 3D cultivation of stem cells in dynamic bioreactor systems for tissue engineering processes, expansion of cells or *in vitro* models became very important



(Figure 2.8). Conventional 2D static cultivation systems are used in many studies although they do not represent the *in vivo* situation. Moreover, static systems have disadvantages in mass transport of nutrients and oxygen into 3D constructs [180]. To overcome these drawbacks different bioreactors have been developed ranging from spinner flasks [132, 181, 182], stirred systems [183, 184], rotating wall [185] and rotating bed [186, 187] to perfusion bioreactors [188–190]. Obviously, every bioreactor has its advantages and drawbacks and thus must be carefully chosen according to the cultivation process.

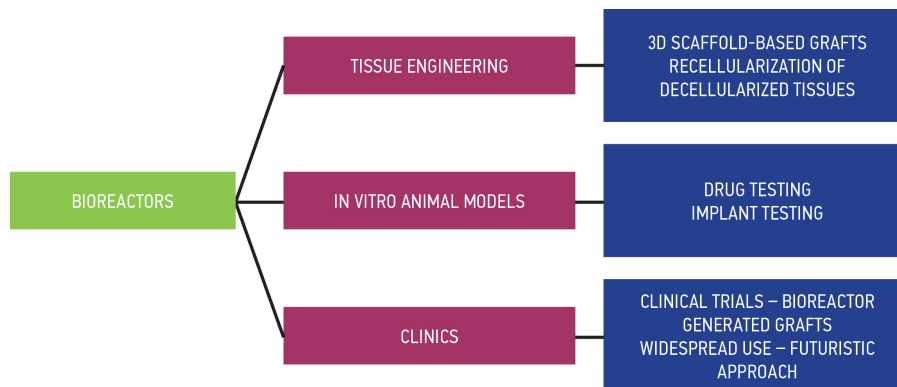


**Figure 2.8:** Bioreactors in the field of RM are either used for tissue engineering of cell-matrix constructs, *in vitro* models or in clinical setup, for example for the expansion of stem cells (adapted from [191]).

Bioreactors for tissue engineering were mainly developed to enhance cell seeding uniformity and efficiency on 3D scaffolds, mass transport into thicker constructs and to exert defined mechanical forces to enhance differentiation processes. For example, compared to static conditions higher viability was reported in the core region of 3D constructs after cultivation in a biaxial bioreactor system [192]. Even large-size engineered grafts (up to 200 cm<sup>3</sup>) were sufficiently supplied with nutrients and oxygen in dynamic bioreactor systems and thus displayed high viability and differentiation markers [137, 193]. As described in subsection 2.3.1, mechanical forces are crucial to generate a physiologic environment and induce or enhance differentiation processes. Therefore, different bioreactor for the exertion of compression, tension, shear, hydrostatic pressure or combinations have been developed [6]. Although a multitude of studies harnessed bioreactors for the application of mechanical forces only few bioreactors are commercially available today. Most of them are restricted to the application of only one force or a distinct shape and size of the scaffold. However, the TC-3 by EBERS Medical is highly versatile system that enables for the application of compression/tension, flow and hydrostatic pressure on scaffolds of different shape and size [194]. Still, different chambers with various modifications are required to exert the respective force or combinations of them. So far it was used in to generate cardiac patches [195], to investigate effects of *in vitro* mechanical stimulation on morphogenesis of developing limb explants [196] and to engineer cell seeded constructs for stress urinary incontinence [197]. Other commercially available systems are listed in Table 2.6.

Bioreactors for expansion of adherent cells like MSCs mainly focus on a high surface-to-volume ratio in order to reduce footprint and required medium and thus save resources. Usually these kind of bioreactors are either based on cell-factory like fixed-beds, hollow-fibers or microcarrier. The

GMP compliant Z<sup>®</sup>RP system by Zellwerk is based on a rotating cell-factory like unit consisting of multiple layers of polycarbonate cell carrier slides offering a surface of up to 8000 cm<sup>2</sup>. It allows for the automated control of oxygen concentration, pH and medium feed and a 8-fold expansion of MSCs has been successfully carried out in it with a final cell number of 25·10<sup>6</sup> cells after 5 days of cultivation[187]. The Quantum Cell Expansion System (Terumo BCT) is probably the most advanced system for the automated expansion of cells. It is based on hollow fiber modules that offer a surface of 2.1 m<sup>2</sup> and requires only 180 ml medium to prime the fluid system. A total of up to 1.5 – 3·10<sup>8</sup> MSCs were harvested equal to a ~ 7 – 15 fold expansion of cells. The third approach, the cultivation of MSCs on microcarrier is mainly carried out in spinner flasks or stirred tank reactors. Expansion up to 30-fold have been reported in different systems [203, 204]. Suspension culture is in general easier to handle and more reproducible but the final detachment of cells from microcarrier has been reported to be insufficient. Several systems like the Mobius 3L by Merck Millipore are commercially available and can be used for expansion on microcarrier.

### 2.4.2 Development and Characterization of Bioreactors

The development of bioreactors requires the consideration of numerous factors in advance (see Table 2.7). Thus, prior to design or development the main purpose of the bioreactor needs to be determined. This comprises decisions on whether the bioreactor is used for tissue engineering, expansion of cells or as an *in vitro* model system and if it is intended to be used in a research environment or in a clinical setting (where it would need to comply to GMP guidelines). Also, theoretical predictions for the effectiveness of a bioreactor to fulfill its specific role can help to understand the influence of crucial process parameters such as oxygen tension and mechanical forces. Based on the inherent properties of a 3D scaffold predictions of the flow profile or mechanical forces are possible. Also, based on known biological behavior of the cells and the physicochemical properties of the bioreactor predictions on mass transport, proliferation or other cellular processes can help saving resources, costs and time. Computational modelling and fluid dynamic analysis were harnessed in the past to gain knowledge on the microenvironment of bioreactors [192, 205–207]. After deciding on the structural design other aspects like material, shape and size need to be clarified. The material should be inert, autoclavable in a research setting and disposable in a clinical setting. Furthermore, the implementation of multiple independent small-scale bioreactor chambers might be interesting since it would allow to screen several conditions at once and thus optimize culture conditions faster. Furthermore, the integration of relevant sensors and imaging facilities to monitor physicochemical, mechanical and biological parameters is crucial in order to gain comprehensive control and to set up feedback loops for automated cultivation. However, regarding cultivation of 3D constructs, this is one of the main challenges researchers are currently facing. Non-invasive sensor and imaging techniques are often not versatile, costly and very complicated in handling. Advanced, non-invasive sensors are available for measurement of oxygen and the most common nutrients but online monitoring of i.e. differentiation markers like ALP activity in the culture medium still need to be developed. Also, monitoring of proliferation is challenging on 3D constructs. Optical systems like (fluorescence) confocal or raman microscopes or ultrasound systems are limited in their ability to visualize deeper areas of the construct. X-ray-based techniques (micro or nano CT) can visualize

ECM deposition but not soft tissue (only with the use of contrast agents). Moreover, all of these techniques are challenging to implement into a bioreactor system for online monitoring.

Besides traditional cultivation parameters, mechanical cues are of increasing interest as described in subsection 2.3.2. Since mechanical forces can not be measured with the same principles that apply for glucose or oxygen but are rather measured in a destructive way there are only a few approaches on how to gain control on them. Although systems like the TC-3 from EBERS medical allow to apply defined compression or tension on the scaffold it is difficult to estimate as to which extent cells inside the scaffold experience these forces. Also, fluid shear stress can only be estimated or modeled via CFD simulations but not online. Pressure sensors like the MEMSCAP which are currently used in the hospital to non-invasively measure blood pressure might enable for determination of hydrostatic pressure or shear forces. Still, extensive knowledge of the inherent scaffold characteristics are required to convert data from the sensors and estimate mechanical forces.

Despite all challenges, information on the current state of the process is crucial to develop feedback controlled, automated systems to ensure reproducible outcome. To gain comprehensive control over the process a bioreactor requires to be extensively characterized. Therefore, the following section describes which characteristics are relevant and how they can be determined.

**Characterization** Physicochemical parameters like gas levels, dissolved gass, pH and temperature influence the biological response of culture cells (proliferation, differentiation, changes of metabolism). This again has an influence on the physicochemical parameters. Therefore, not only the biological characteristics must be known but also bioreactor characteristics like mass and heat transfer or gas transmission rates. Also, material characteristics of a 3D matrix are crucial to determine the mass transfer inside the scaffold. In general, mass transfer is dependent on diffusion and convection which is often increased in bioreactors by agitation (shaker), stirring (stirred tanks, spinner flasks) or steady laminar flow (perfusion reactors). In bioreactor technology mass transfer coefficients are used to quantify mass transfer and are often expressed by dimensionless numbers that describe the proportion of diffusive to convective effects. Important characteristic numbers are for example the Péclet number  $Pe$ , Bodenstein number  $Bo$  and Reynolds number  $Re$  [208]. They are often part of theoretical models for the calculation of mass transfer and can be derived from the residence time distribution (RTD). The RTD is a probability distribution function that describes the time span a fluid element spends in the bioreactor and can be determined by simple wash-out experiments. Yet, it is a powerful method to characterize mixing and mass transfer of a bioreactor at a specific operational mode (e.g. flow rate, flow pattern, stirrer speed). Although characteristic numbers derived from RTD experiments can describe the overall mass transfer process they do not describe the spatial behavior of fluid elements in detail. Thus, the presence of dead spaces or recirculation areas, although sometimes indicated by the RTD, can not be narrowed down to a specific location in the reactor.

However, computational fluid dynamics (CFD) can be harnessed to simulate the behavior of fluid elements in the bioreactor. Moreover, combined with a 3D model of the matrix, parameters like shear rate, wall shear stress or pressure can be derived from the simulation data and give detailed insight about mechanical loading. In fact, CFD simulations have been used in the past

to predict mechanical loading for tissue engineering bioreactors [192, 207, 209]. Besides mass transfer, dissolved oxygen (DO) is crucial parameter for the control of a bioprocess. As described before reduced oxygen concentrations can alter cellular behavior and also increase proliferation (subsection 2.3.4). Therefore, it is not only a "consumable" but a signal molecule of special interest in the context of stem cell expansion. During proliferation, especially under reduced oxygen conditions, the risk of anoxic regions or phases is increased. Therefore, the oxygen transfer rate (OTR) of a bioreactor at a specific operational mode is an important characteristic. The OTR describes the oxygen transfer from the gas to the liquid phase and can be used to determine if the oxygen supply is sufficient. It is given as

$$OTR = k_L a \cdot (c_{O_2}^* - c_{O_2}) \quad (2.1)$$

where  $k_L a$  is the volumetric mass-transfer coefficient,  $c_{O_2}^*$  the oxygen concentration in equilibrium (or maximum oxygen concentration) and  $c_{O_2}$  the oxygen concentration at the gas/liquid interface. If the OTR is known it is possible to control the DO via the composition of the gaseous atmosphere. Furthermore, if the oxygen uptake rate and growth kinetics of the cultivated cells are known the process can be simulated by coupling of CFD analysis and chemical reaction models [210]. The  $k_L a$  is dependent on several parameters such as medium composition, viscosity, temperature or convection (shaking, stirring, perfusion) and thus might be adjusted by alteration of these parameters or active aeration to increase the gas/liquid interface area.

Conclusively, in order to develop a bioreactor from the scratch a multitude of parameters has to be taken into account. Modern computational technologies can help to develop a reasonable bioreactor design. However, bioreactor prototypes need to be characterized extensively to increase knowledge and therefore control on the conducted process. For tissue engineering and cell expansion processes characterization of mass transfer, fluid flow velocity profiles of the bioreactor and scaffold, shear rate, wall shear stress and shear stress distribution as well as oxygen transfer are the most important parameter. Still, other parameters might be of interest in a specific set up or process.

**Table 2.6:** Commercially available bioreactors for tissue engineering and cell expansion.

Mode of operation	Application	System, Manufacturer	Scale	Key features	Ref.
Orbital shaking	Expansion	Micro-24 microreactor system (Pall)	3 – 7 ml	24-well cassettes with individual heating, gas injection, pH and oxygen sensors	pall.com
Wave-mixed	Expansion	WAVE Bioreactor (GE Healthcare)	0.3 – 500 l	disposable bags, GMP compliant available	[198]
Stirred tank	Expansion	Mobius® bioreactors	– 2000 l	Scale-up and automation	emdmillipore.com
Stirred tank	Expansion	Spinner-flask (various manufacturer)	0.1 – 36 l	inexpensive, simple design	[199]
Rotating bed	Expansion, osteogenic differentiation	Z®RP cell cultivation system (Zellwerk)	2000 – 8000 cm <sup>2</sup> cell culture surface or up to 12 scaffolds	High degree of automation, GMP compliant	[186, 187]
Compression	Chondrogenic differentiation	CartiGen (BISS)	single-sample (d = 30 mm), multi-sample (d = 10 mm)	multiple samples possible, simultaneous perfusion possible	tissuegrowth.com
Tension	Osteogenic differentiation	FX-5000™ Tension (Flexcell)	24 well and 6 well	flexible membrane, monolayer cell cultivation	flexcellint.com
Tension	Osteogenic differentiation	TC-3 (Ebers Medical)	Up to 3 independent samples	Stretching of scaffolds	ebersmedical.com
Hydrostatic pressure	Chondrogenic differentiation	TC-3 (Ebers Medical)	Up to 3 independent samples, pressure up to 0.4 MPa	Compatible with a variety of scaffold	ebersmedical.com
Perfusion	Expansion, co-cultivation, differentiation	Quantum® Cell Expansion System (Terumo)	2.1 m <sup>2</sup> cell culture surface	High degree of automation, GMP compliant	terumobct.com, [200]
Perfusion	Expansion / differentiation	U-Cup bioreactor (Cellec Biotek)	Up to 10 independent samples (d = 6 – 10 mm)	[201, 202]	

**Table 2.7:** Factors for design and development of bioreactors.

Factor	Elements	Purpose
System set up	Chamber material	inert, non-corrosive
	Versatile design	Enables for scaffolds of different shape and size
	Multiple independent chambers	Enables for parallel cultivation of independent chambers, e.g. for screening / optimization of cultivation parameters
System size	Autoclavable vs. single use tubing, connectors,...	autoclavable = reduces pricing, increases effort; single use = increases pricing, decreases effort and risk of contamination
	Small scale Bench top	Reduces required resources Easy handling and transportation
Mechanical stimulation	Compression	induction of chondrogenesis
	Tension	induction of osteogenic, ligamentous, chondrogenic differentiation
	Fluid shear	induction of osteogenesis
	Hydrostatic pressure	induction of chondrogenesis
Control of physical parameters	Composition of gaseous atmosphere, dissolved oxygen, temperature, flow rate, mechanical stimulation	Maintenance of desired cultivation conditions
Sensors	Composition of gaseous atmosphere, dissolved oxygen, temperature	Determination of physical cultivation parameter
	Mechanical cues	Determination mechanical stimulation
	Sampling of medium	Determination of biological cultivation parameter (nutrients, soluble factors,...)
Non-invasive imaging	Optical imaging	enables for superficial observations of viability, proliferation, differentiation, ECM deposition; limitation: scaffold thickness
	Ultrasound	enables for assessment of ECM deposition, tissue generation; limitation: penetration depth
	X-ray based	enables for assessment of ECM deposition, generation of soft tissue (requires contrast agents); limitation: long-data acquisition, exposition to radiation
	Nuclear imaging	Cell viability, metabolic activity, tracking; limitation: poor spatial resolution,
Feedback	Sensor & imaging based	Enables for automated control of physical, biological and mechanical conditions.

### 3 Mesenchymal Stem Cell Isolation

The most widely approach used for the isolation of human MSCs from adipose tissue is performed via enzymatic treatment with collagenase. It was formerly developed for isolation of rat MSCs [211] and has further been modified for isolation of human MSCs [212]. Briefly, adipose tissue is either obtained from liposuction or tissue resection (i.e. from abdominoplasty surgeries), hematopoietic cells are removed by washing and the tissue is then digested by collagenase treatment. Several washing and centrifugation steps remove unwanted cell types and yield the SVF. MSCs in the SVF are then selected by plastic adherence. This procedure is well established and frequently used. However, this process holds several disadvantages which most of all are regarded to economic and safety concerns. First, isolation by enzymatic treatment is a time-consuming procedure. Comprising the time from arrival of tissue to final freezing of cells in passage 0 (P0) it takes approximately 6 person-hours per  $1 \cdot 10^6$  cells. Also, a comparably high demand of disposables (caused by centrifugation and washing steps) and the use of collagenase make it a costly process. The cost of  $1 \cdot 10^6$  cells at P0 was calculated to be approximately € 95 (time and cost calculations were determined from 8 isolation procedures performed in association with the experimental work of this thesis). However, the use of collagen is rather problematic, most of all in the context of regulatory issues. Commercially available collagenase products were shown to contain endotoxins [213, 214] and may also contain other impurities or unwanted proteases since they are rarely purified products. Batch to batch variations or manufacturer dependent variations of the overall composition cause inhomogeneity of the protease composition and thus their enzymatic activity [215–217].

Cell populations that fulfill the minimal criteria for MSCs are known to comprise not a single cell type but several subpopulations. Also adipose derived MSCs are composed of different subpopulations that are different in their surface marker expression profile and differentiation capacity [218–220]. Variations in collagenase products may therefore select for different subpopulations. In fact, several studies report differing surface marker profiles of adipose derived populations [54, 212, 221]. Finally, cells that undergo enzymatic digestion were demonstrated to show decreased viability due to lytic activity of the enzyme [222]. To overcome the need of an enzymatic treatment other isolation procedures have been developed. ASC isolation by mechanical dissociation of lipoaspirates was demonstrated by Baptista et al. [223]. However, MSCs are known to be sensitive to physical forces such as ultrasonic [224], pressure [225], strain [226] or shear stress [227] which can result in decreased proliferation [228] or spontaneous differentiation [94]. The Puregraft<sup>®</sup> System by Cytori was developed to prepare fat grafts with higher retention rates. In this system the lipoaspirate is filtered and washed several times in a closed bag during surgery in order to enrich the cell population for bone-marrow-derived mononuclear cells [229]. Since neither the lipoaspirate nor the patient leaves the operating room it is not

considered as an ATMP. However, quality of the resulting cell population can not be evaluated by functionality tests before transplantation. Also washing-out of ASCs from the crude lipoaspirate has been proposed by Shah et al. [230]. Cells derived from this procedure displayed an altered immunophenotype while the differentiation capacity was comparable to enzymatic isolated cells. Also, they reported a 19-fold lower yield with this method. Isolation of human ASCs from tissue resection and lipoaspirates by explant culture was described by Priya et al. [231]. They reported a significantly higher yield of cells with comparable immunophenotypic and functional properties compared to enzymatic isolated cells. A second study where a modified protocol was implemented confirmed findings on immunophenotype and functionality but did not make a statement on cell yield.

In general, isolation by explant cultivation may have several advantages. First, the ECM of the explanted tissue is still intact and not dissociated by proteolytic enzymes. The complex composition and interplay of ECM components triggers biochemical and biomechanical signals of cells and therefore may contribute to morphogenesis, differentiation and homeostasis of the tissue [232]. During explant procedure the tissue is injured resulting in a wound-healing response which activates also the release of growth factors and cytokines and triggers migration of stem cells to the injured site. This is also thought to be the mechanism by which stem cell outgrowth is triggered during explant isolation.

Second, the ECM is known to work as a reservoir of growth factors. In adipose tissue FGF-2 (also known as  $\beta$ -FGF) and vascular endothelial growth factor (VEGF) are prominent but also FGF-1, FGF-7, FGF-9 and FGF-10 were found in human adipocytes and the SVF [233, 234]. Mesenchymal stem cell media are often supplemented with FGF-2 since it is known to be involved in the key pathways of differentiation and proliferation [235]. Stem cell properties of MSCs from umbilical chord were shown to be better maintained when cells were cultivated together with the initial tissue explants [236] indicating that the natural environment of intact tissue is essential to keep stem cell properties. Therefore, it is thought that the intact ECM and tissue explants support outgrowth and proliferation of cells during explant culture.

In conclusion, the isolation of ASCs via explant culture seems to be the most promising procedure at the moment. However, implementation of physiologic conditions, such as the use of human derived platelet lysate or reduction of the oxygen concentration, might improve this procedure. Therefore, in this chapter isolation procedures via enzymatic treatment and explant culture are compared towards cell yield and the resulting population evaluated towards their immunophenotype and differentiation and proliferation capacity (Figure 3.1).



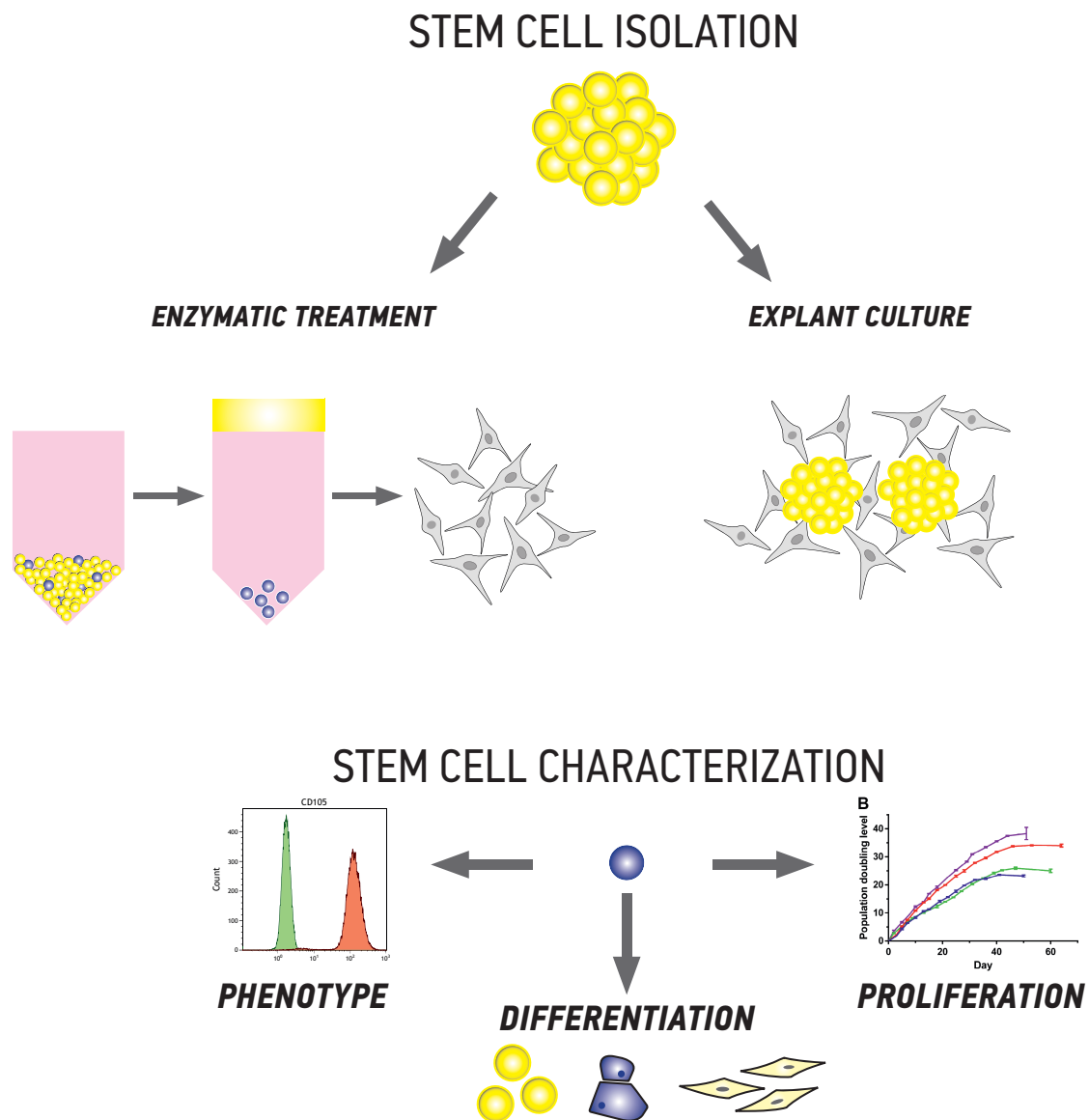


**Figure 3.1:** Graphical abstract describing the experimental work of chapter 3: the isolation of human MSCs by explant culture is compared with the isolation by traditional enzymatic treatment. The resulting cells are characterized towards their proliferation and differentiation capacity and surface marker expression.

### 3.1 Isolation of adipose derived MSCs by explant culture

Human MSCs were isolated from adipose tissue either by enzymatic treatment or explant culture as described in section B.1. The protocol for isolation via enzymatic treatment comprises manual mincing of the tissue, collagenase treatment and several washing and centrifugation steps. Subsequently, the resulting SVF is released into tissue culture flasks and ASCs selected by plastic adherence (several steps of the procedure are depicted in Figure 3.2 A – H). However, for the isolation via explant culture, the tissue is washed several times with PBS to eliminate erythrocytes. Further, the tissue is cut into small pieces of approximately  $5 \text{ mm}^3$  which were placed on cell culture dishes (100 mm diameter) and carefully covered with cell culture medium (CCM) as depicted in Figure 3.2 I – L. T-flasks and petri dishes from both procedures were equally split in two groups and incubated in either 21 %  $\text{O}_2$  or 5 %  $\text{O}_2$ . All dishes and flasks were examined daily towards cell outgrowth and confluence. When outgrowing cells were observed in the majority of tissue pieces, the pieces were removed from the petri dish. Subsequently, the dish was carefully washed with PBS, fresh medium was added and cells allowed to grow to 80 – 90 % confluency. Since the initial weight of adipose tissue processed for each T-flask or petri dish was determined before processing the yield of cells derived per initial gram adipose tissue  $Y_{\text{cells/g}}$  was determined. Also the yield per gram and day  $Y_{\text{cells/g-d}}$  was calculated since time may be a crucial parameter for stem cell isolation in a therapeutic process.

**Table 3.1:** Comparison of cellular outgrowth and harvest of different isolation conditions. Data represented as mean  $\pm$  SD (from at least  $n = 3$  donors).

Condition	Days until first outgrowth	Days until harvest	Homogeneity
Enzymatic 21 % $\text{O}_2$	$3.0 \pm 1.4$	$8.0 \pm 2.8$	high
Enzymatic 5 % $\text{O}_2$	$3.0 \pm 1.4$	$7.2 \pm 2.9$	high
Explant 21 % $\text{O}_2$	$4.8 \pm 0.4$	$13.3 \pm 1.3$	low
Explant 5 % $\text{O}_2$	$5.3 \pm 0.5$	$12.7 \pm 0.9$	low

Plastic adherent cells were found to grow out from the tissue between 1 – 6 days after isolation dependent on isolation procedure and were 80 – 90 % confluent (and thus harvested) after 6 – 15 days (see Table 3.1). Figure 3.3 depicts typical outgrowth of cells from SVF and crude adipose tissue. The time until harvest was significantly lower when cells were isolated by enzymatic digestion ( $\alpha = 0.05$ ,  $p < 0.01$ ).

Comprising all conditions,  $Y_{\text{cells/g}}$  was found to be approximately  $3 \cdot 10^5$  cells per gram of initial adipose tissue whereas the isolation procedure did not have a significant effect on  $Y_{\text{cells/g}}$ . Regarding the time dependent yield, for enzymatic isolation  $Y_{\text{cells/g-d}}$  was  $51826 \pm 13406$  at 21 %  $\text{O}_2$  and  $49257 \pm 8397$  at 5 %  $\text{O}_2$ . For explant culture the yield was  $25299 \pm 5241$  at 21 %  $\text{O}_2$  and  $27343 \pm 21647$  at 5 %  $\text{O}_2$  (see Figure 3.4). In fact,  $Y_{\text{cells/g-d}}$  was found to be significantly higher for the enzymatic isolation in normoxic and hypoxic conditions ( $\alpha = 0.05$ ,  $p < 0.001$ ).

**Discussion** In this section the isolation of MSCs was evaluated towards the yield of cells per gram and cells per gram and day. Both values are important benchmarks to estimate the feasibility of an isolation procedure in the context of a therapeutic process. When very large amounts

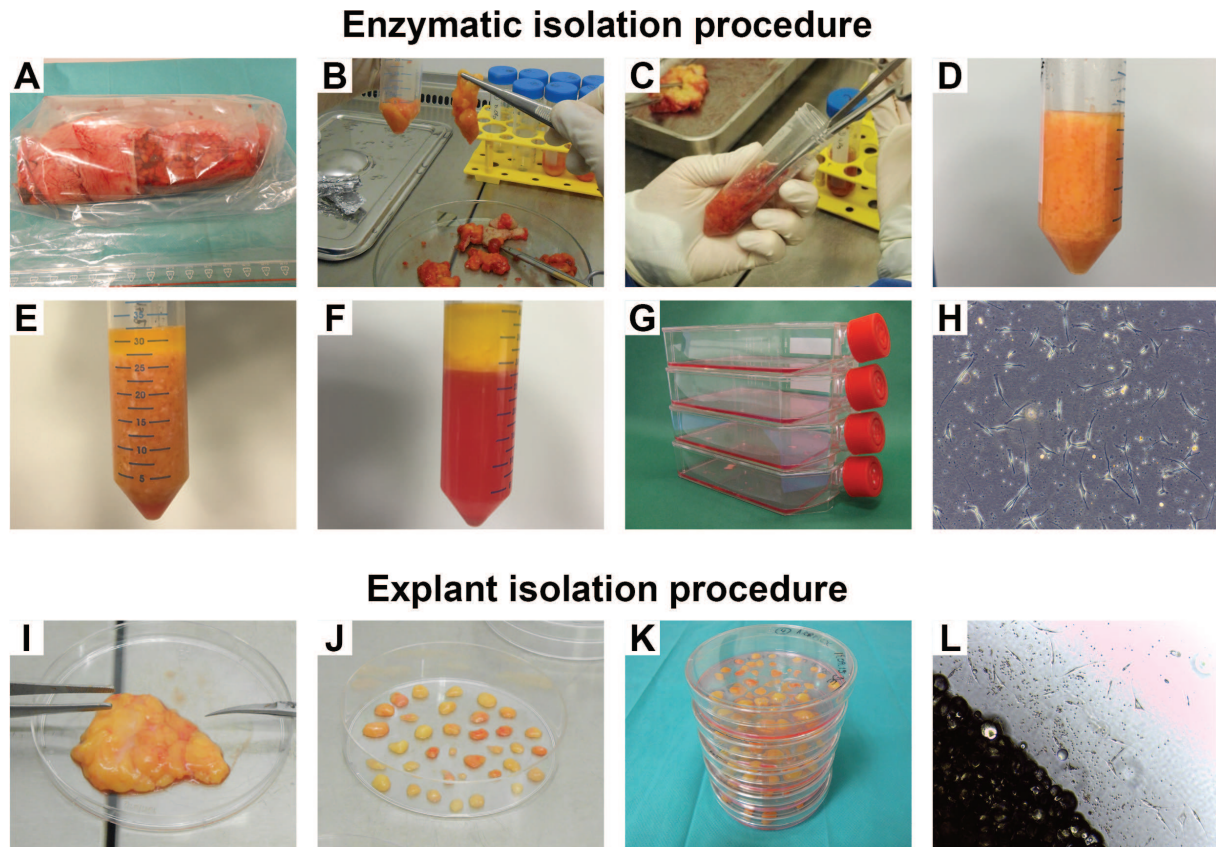


**Figure 3.2:** Working steps from isolation via enzymatic treatment (A – H) and explant cultivation (I – L). Enzymatic isolation: A) crude adipose tissue after surgery, B) connective tissue and blood vessels are eliminated and only pieces of pure fat tissue kept, C) thorough mincing of tissue, D) minced tissue before collagenase treatment, E) after collagenase treatment, F) after centrifugation, G) release of the SVF into T-flasks, H) outgrowth of cells on day 2 after isolation. Isolation by explant culture: I) crude adipose tissue, J) cutting into small pieces of  $\sim 5 \text{ mm}^3$ , K) pieces covered with medium, L) outgrowth of cells after 5 days.

of initial tissue or a comparably long time span is required the isolation procedure becomes less attractive. The major differences to the work of Priya et al. was the implementation of HPL, the use of a low glucose basal medium and a reduced oxygen concentration in order to mimic the physiologic environment and thus reduce stress and improve the yield and quality of isolated cells. Priya et al. reported  $Y_{\text{cells/g}\cdot\text{d}}$  to be in the range of  $5 - 8 \cdot 10^5$  cells/g for explant culture and  $1.4 \cdot 10^5$  cells/g for enzymatic isolation under normoxic conditions. In contrast, no significant differences between enzymatic or explant were found in the present work. Also, the average  $Y_{\text{cells/g}\cdot\text{d}}$  was approximately half of what was reported by Priya et al. for the explant culture but 2-fold higher for enzymatic isolation [231]. Therefore, implementation of more physiologic conditions resulted in a higher yield for cells from enzymatic isolation but at the same time in a lower yield of cells from explant culture. Delayed outgrowth (and thus a reduced time dependent yield) was observed in explant culture. Probably it takes longer for cells to migrate through an intact ECM and out of an intact piece of tissue. Also, direct contact between tissue and cell culture plastic surface is a crucial requirement. However, lipid droplets were observed on the cell culture plastic surface and in the medium and cells were observed to not grow on plastic surface covered by droplets (data not shown). Therefore the presence of a thin lipid layer between tissue

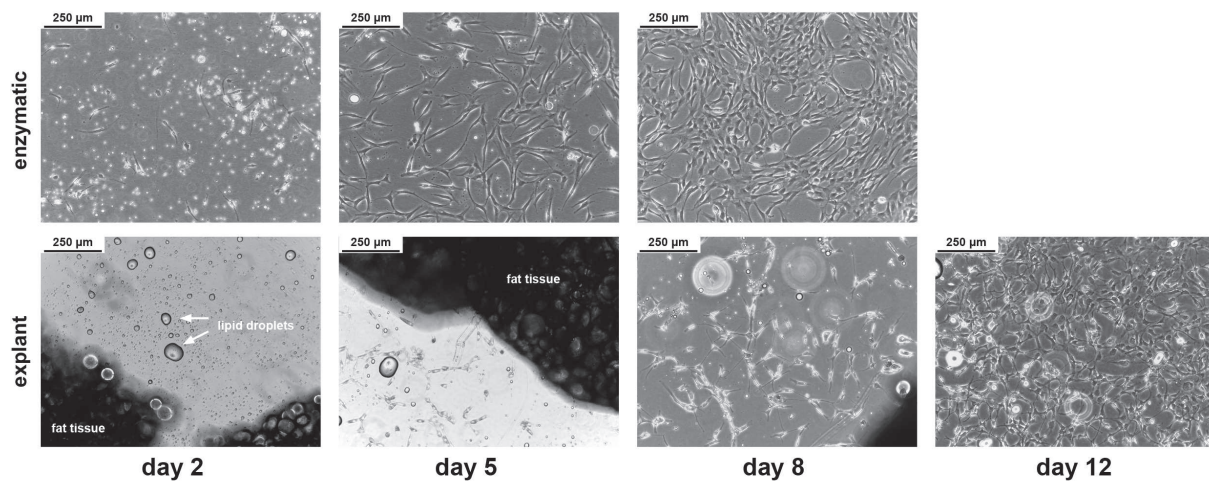


**Figure 3.3:** Microscopic pictures of cells derived via isolation by enzymatic treatment or explant culture of MSCs on day 2, 5, 8 and 12 (enzymatic isolated cells already were harvested before day 12).

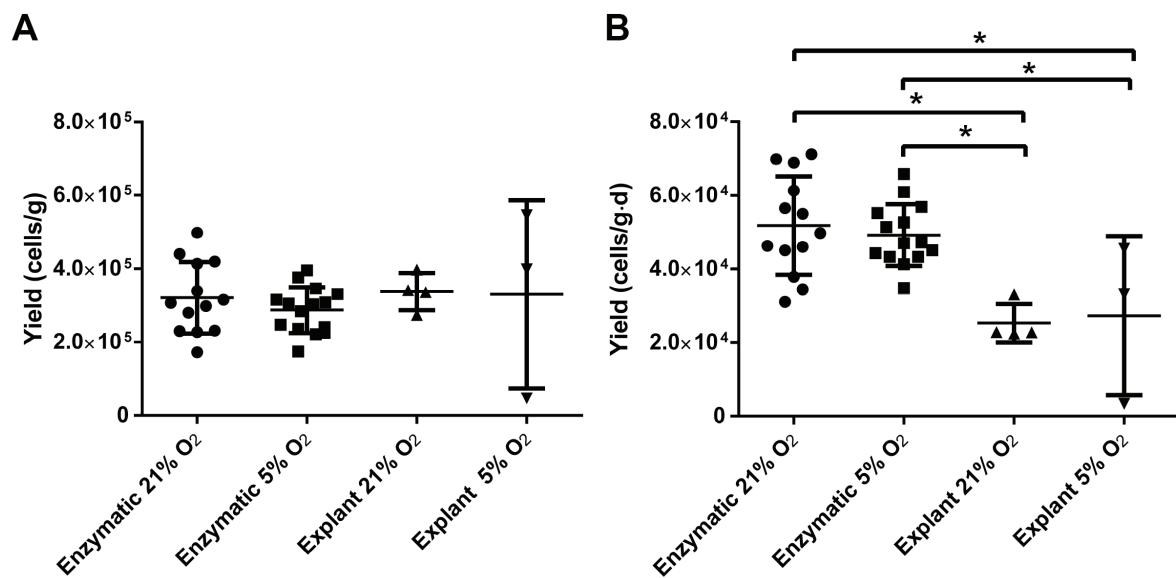


**Figure 3.4:** A)  $Y_{cells/g}$  and B)  $Y_{cells/g·d}$  of isolation by enzymatic treatment or explant culture of MSCs at 21 and 5%  $O_2$ . Each data point represents the harvest from one T-flask (enzymatic) or all petri dishes of one conditions (explant) from at least  $n = 3$  donors. Data represents mean  $\pm$  SD; \* indicates significant difference ( $\alpha = 0.05$ ,  $p < 0.01$ ).

and plastic surface, forming a natural barrier for cell migration, is likely and might impair rapid cellular outgrowth. Also, during explant culture of tissue pieces (and not lipoaspirates) cells did not grow out homogeneously from all tissue pieces and were not allowed to cover the entire plastic surface due to the presence of lipid droplets. Thus, cells on petri dishes grew not as homogeneously confluent as cells from isolation by enzymatic treatment in the T-flasks which might be a reason for lower yield observed for isolation by explant culture. Also, the implementation of a hypoxic environment did not result in significantly faster outgrowth or higher cell yield. In the current work previously reported benefits of the isolation by explant culture were not confirmed. Instead the widely used isolation by enzymatic treatment resulted in a better time dependent yield and is from an economic point of view considered as the more efficient procedure. Although the current study is not completely comparable with the study of Priya et al. it indicates that the use of HPL and low glucose basal medium might be beneficial for the isolation by enzymatic treatment.

In general, not only yield but also maintaining stem cell properties is strikingly important during isolation of stem cells. Therefore, in the next section the characterization of stem cells derived from isolation by explant culture and enzymatic treatment was evaluated.

## 3.2 Characterization of adipose derived MSCs isolated by explant culture

To confirm that isolated cells fulfill minimal criteria for MSCs (see section 2.1) their immunophenotype and differentiation capacity were analyzed as described in section B.6. Furthermore, the growth kinetics and proliferation capacity of MSCs isolated by enzymatic treatment and explant culture were evaluated at 21 and 5 % O<sub>2</sub> (also described in section B.6).

**Surface marker expression profile** The surface marker profile of the isolated cells was found to be according to the minimal criteria for MSCs. Thus, cells were found to be positive for CD73, CD90, CD105 and negative for CD14, CD20, CD35, CD45 and HLA-DR. The expression profile was found to be similar throughout cells from all isolation procedures (see Figure 3.5).

**Proliferation capacity** To determine the proliferation capacity isolated cells were expanded in CCM and subsequently passaged until cellular senescence occurred and thus cell growth plateaued (see Figure 3.6). Throughout all donors cells displayed more rapid and prolonged growth when cultivated at 5 % O<sub>2</sub>. Comprising the results from all donors cells from enzymatic and explant culture isolation did not display significant differences in their growth kinetics. However, the highest PDL observed in all donors was found in cells from explant culture at 5 % O<sub>2</sub>. The population doubling time  $t_{PD}$  was found to be rather consistent up to approximately passage 6 for normoxia and approximately passage 10 for hypoxia. After P6,  $t_{PD}$  of cells at 21 % O<sub>2</sub> increased dramatically whereas  $t_{PD}$  of cells at 5 % O<sub>2</sub> increased rather steadily until cells became senescent. For therapeutic use, early-passage MSCs are preferable. Therefore PDL and  $t_{PD}$  until P10 of all donors and conditions are compared in Figure 3.8. PDLs of the different conditions at passage 10 were in the range of 17 – 24 with explant normoxic displaying the lowest ( $16.8 \pm 5.1$ )

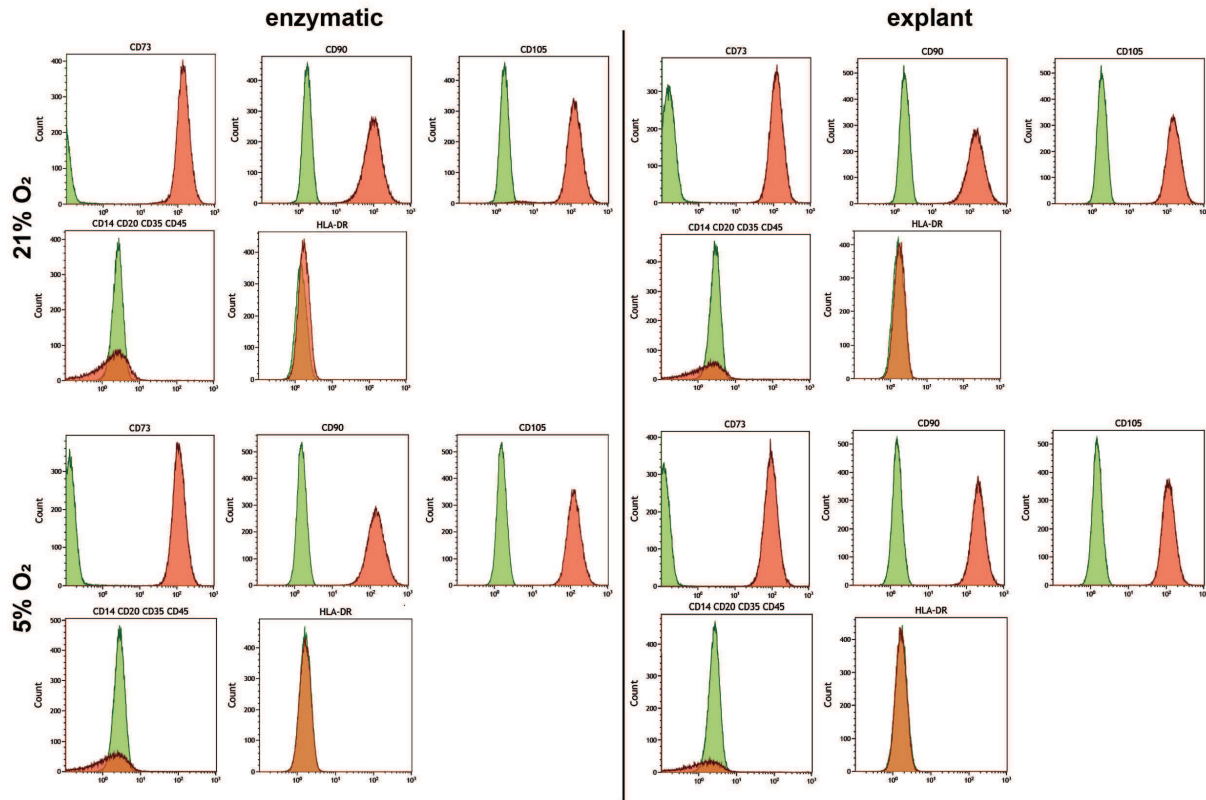


**Figure 3.5:** Representative phenotype analysis of cells from isolation by enzymatic treatment and explant culture at 21 and 5%  $O_2$  from female, 48 years old donor. Red areas represent phenotype, green areas represent isotype control. Data represents at least 50.000 recorded events.

and explant hypoxic displaying the highest PDL ( $23.8 \pm 2.3$ ). In general, PDL was significantly higher in hypoxic conditions. Also, PDL of cells isolated by explant cultivation and under hypoxic conditions was significantly higher compared to explant and enzymatic normoxic but not higher than enzymatic hypoxic. Furthermore, mean  $t_{PD}$  determined during all passaging events until passage 10 were in the range of 30 – 47h with explant normoxic displaying the highest ( $46.8 \pm 28.5$ ) and enzymatic hypoxic displaying the lowest  $t_{PD}$  ( $30.2 \pm 9.1$ ). Explant normoxic displayed a significantly higher  $t_{PD}$  than enzymatic or explant hypoxic.

As stated above cells were passaged until growth plateaued. Subsequently a senescence assay was performed as described in section B.6. Throughout all conditions and all donors enlarged cells, quiescence and  $\beta$ -galactosidase activity was observed indicating senescent cells (see Figure 3.9).

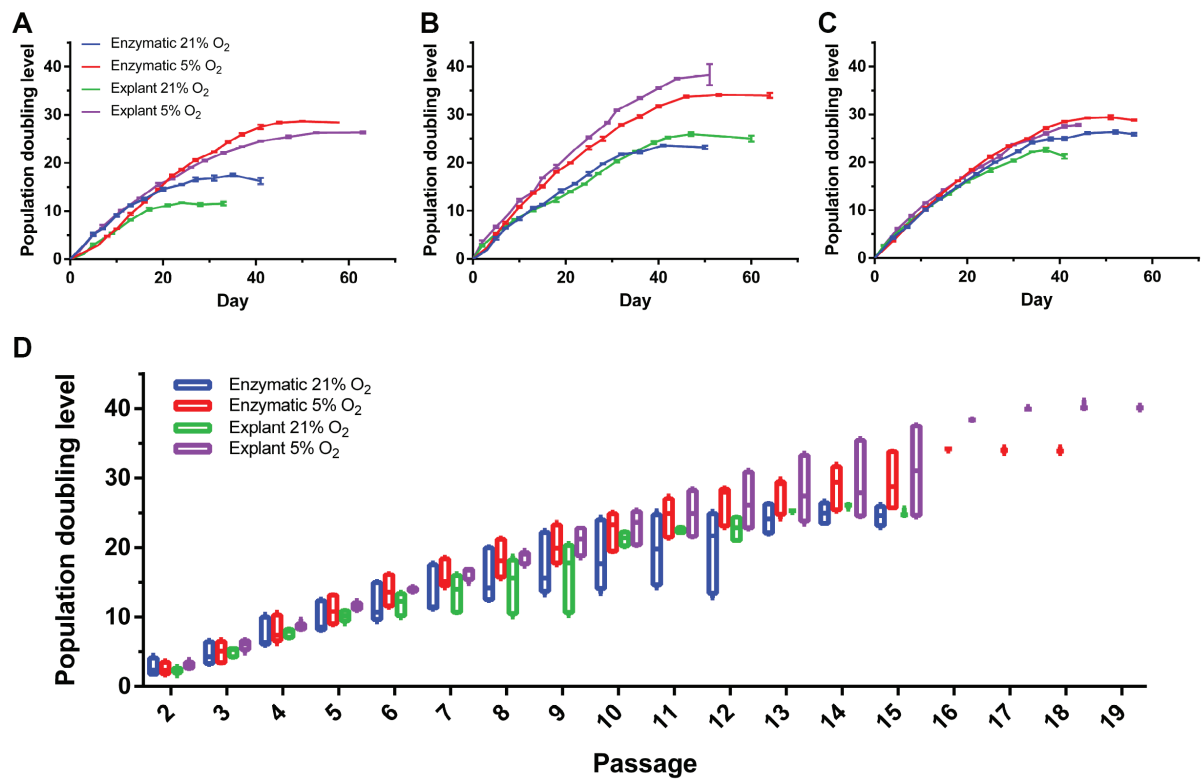


**Figure 3.6:** Time dependent population doubling level (PDL) of MSCs isolated by enzymatic treatment or explant culture from 3 different donors. A) female, 42 years old, B) female, 52 years old, C) female, 48 years old; data represents mean  $\pm$  SD (all n=3). D) Passage dependent PDL comprising data from all donors; boxes represent min to max and mean  $\pm$  SD.

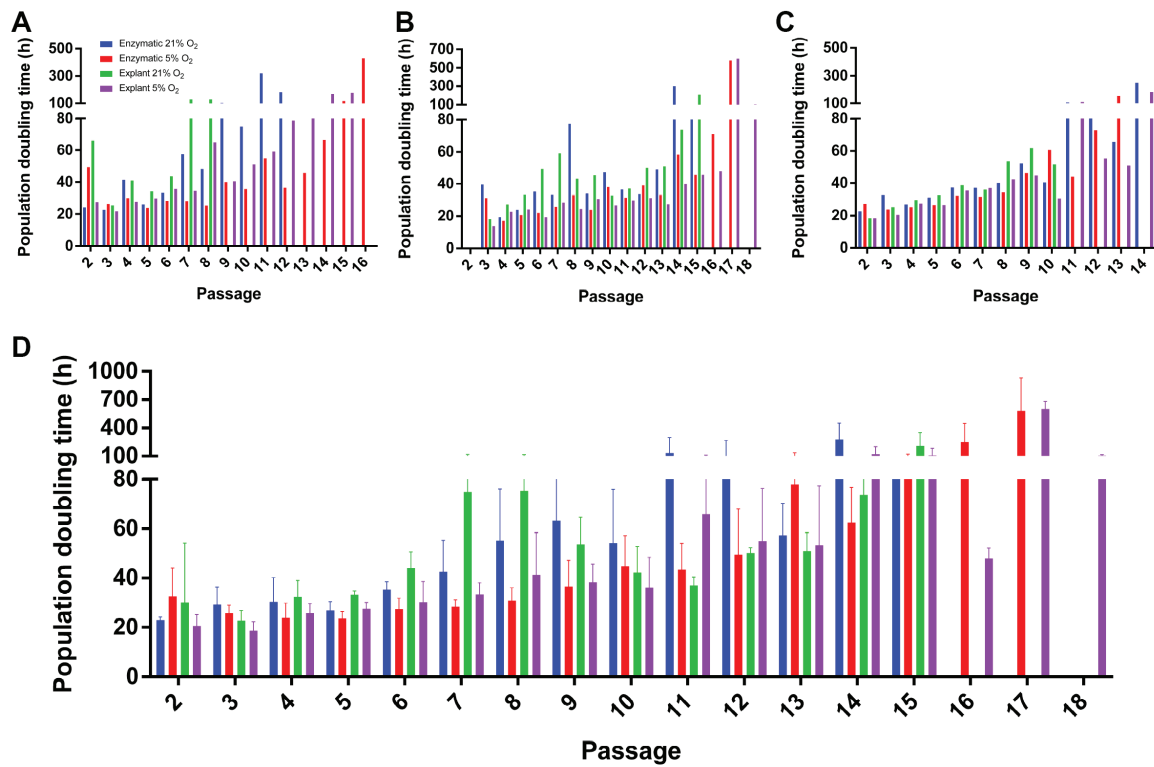


**Figure 3.7:** Passage dependent population doubling time of MSCs isolated by enzymatic treatment or explant culture from 3 different donors. A) female, 42 years old, B) female, 52 years old, C) female, 48 years old ( $n=3$ ) and D) passage dependent populations doubling time comprising data from all donors ( $n=9$ ); data represents mean  $\pm$  SD.

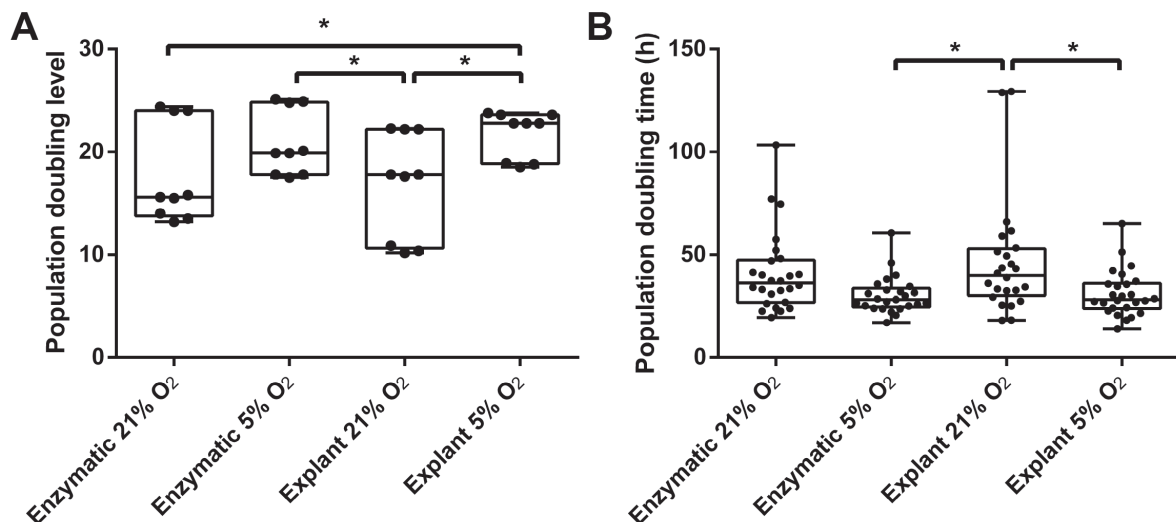


**Figure 3.8:** A) Average population doubling level at passage 10 and B) all population doubling times until passage 10 of MSCs isolated by enzymatic treatment or explant culture at 21 and 5%  $O_2$ . Data represented as median with boxes (25th – 75th percentile) showing all data points from 3 donors (each  $n=3$ ); \* indicates significant difference ( $\alpha = 0.05$ ,  $p < 0.04$ ).



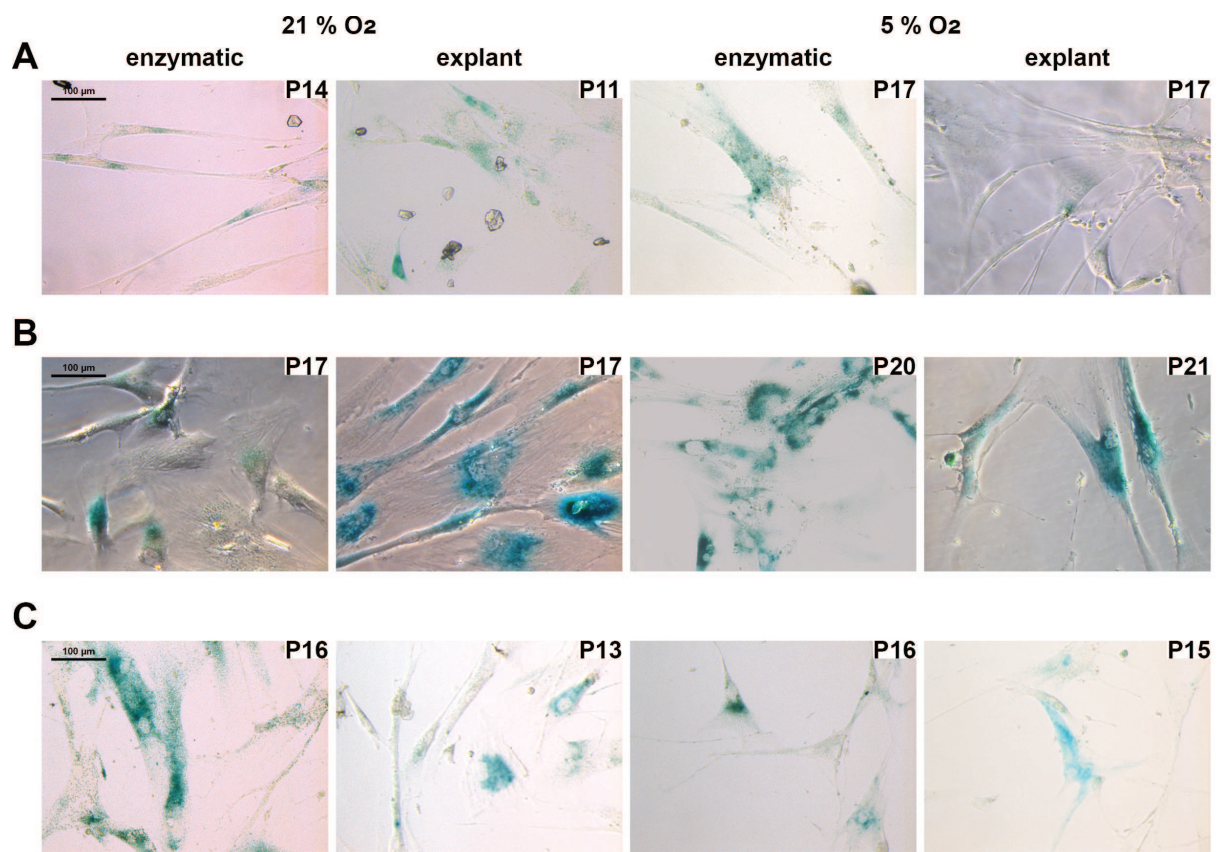


**Figure 3.9:**  $\beta$ -galactosidase assay of cells from MSCs isolated by enzymatic treatment of explant culture cultivated at 21 and 5 % O<sub>2</sub>. A) female, 42 years old, B) female, 52 years old, C) female, 48 years old.

**Differentiation capacity** The differentiation capacity of cells isolated by enzymatic treatment or explant culture was investigated as described in section B.6. Briefly, MSCs were seeded in fibronectin coated cell culture plates and after cells grew confluent differentiation was induced by changing the medium to either adipogenic (ADM), chondrogenic (CDM) or adipogenic differentiation (ADM) medium. Cells cultivated in CCM served as control.

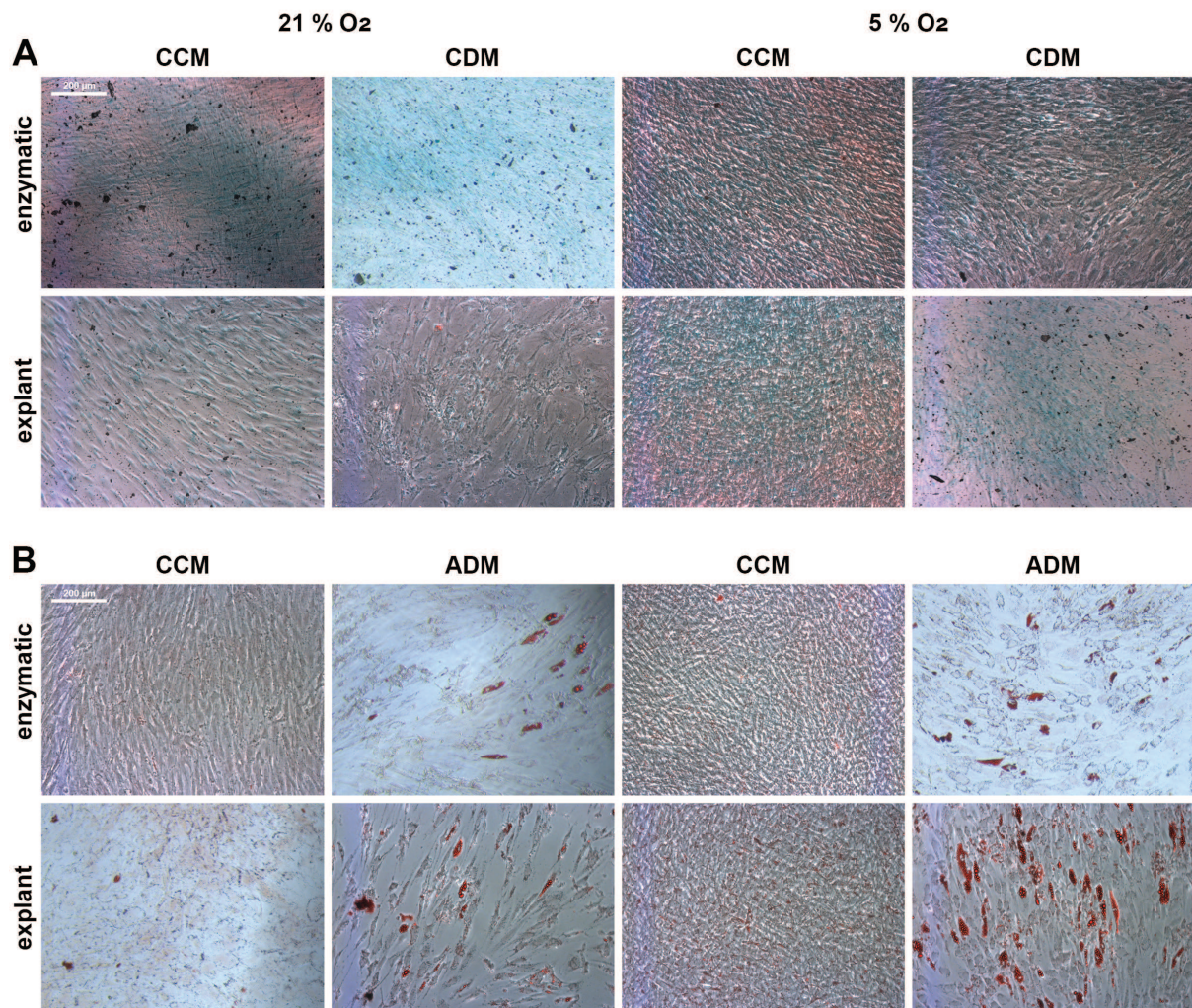


**Figure 3.10:** Differentiation of enzymatically or explant isolated MSCs cultivated at 21 and 5 % O<sub>2</sub>. A) Alcian blue staining of chondrogenic differentiation and control, B) Oil Red O staining of adipogenic differentiation and control. CCM = standard cell culture medium, CDM = chondrogenic differentiation medium, ADM = adipogenic differentiation medium. Scale bar = 200  $\mu$ m.

A clear alcian blue staining of cells cultivated in chondrogenic differentiation medium (CDM) was only observed in 21 % enzymatic. Weaker staining which was comparable to control samples was observed in the other conditions. However, staining of the lipid vacuoles as indicated by Oil Red O staining was observed in all cells cultivated in adipogenic differentiation medium (ADM) but not in control samples. Cells isolated via explant culture at 5 % O<sub>2</sub> displayed the clearest staining with the most lipid vacuoles (see Figure 3.10).

Extracellular matrix (ECM) from osteogenic differentiation was investigated with DAPI/calcein double stain and alicarin red for extracellular calcium and Von Kossa (VK) stain for phosphates (see Figure 3.11). Cells from both isolation procedures were stained positive for calcein, alicarin

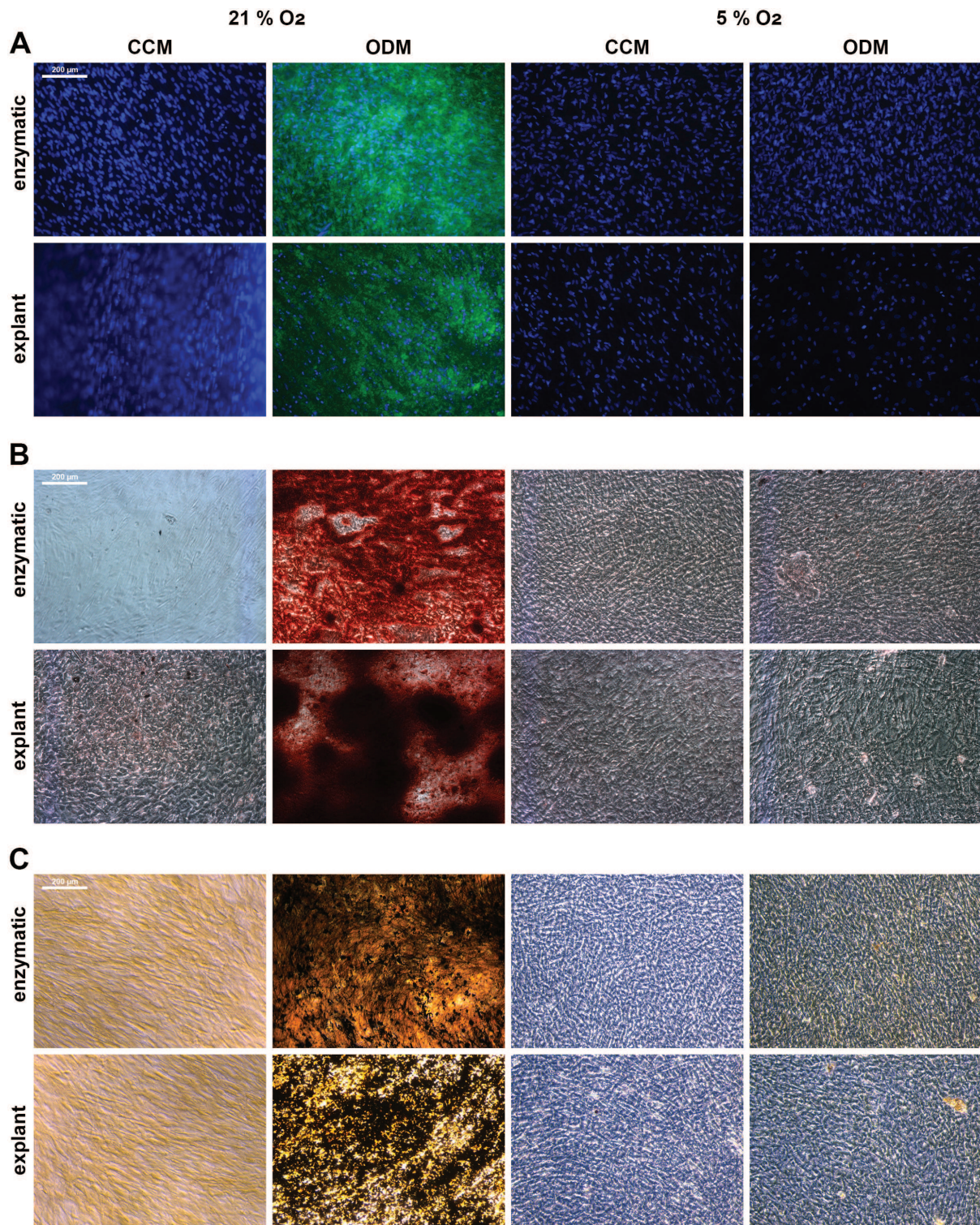


**Figure 3.11:** Differentiation of enzymatically or explant isolated MSCs cultivated at 21 and 5% O<sub>2</sub>. A) DAPI calcein double stain, B) alicarin red stain and C) von Kossa stain of osteogenic differentiation. CCM = standard cell culture medium, ODM = osteogenic differentiation medium.

red and VK at 21% but not at 5% O<sub>2</sub>. Also, no staining was observed in the control samples. Notably, at 5% O<sub>2</sub> considerably less cells were observed in "explant" samples (both CCM and osteogenic differentiation medium (ODM)) compared to all other conditions as indicated by

DAPI staining. However, images from brightfield microscopy display dense cell layers in all other stainings.

**Discussion** In this section cells from isolation via enzymatic treatment and explant culture were compared towards their immunophenotype, growth kinetics and differentiation capacity. The immunophenotype of cells derived from different conditions was similar and fulfilled minimal criteria for MSCs. The treatment with collagenase for the isolation of stem cells from adipose tissue has been discussed to eventually select for distinct subpopulations of MSCs [231]. However, in this study the surface marker expression of CD73, CD90, CD105, CD14, CD20, CD35, CD45 and HLA-DR did not reveal any differences of isolated cell populations. However, other surface marker that were not stained might differ.

No significant differences were found in the overall growth kinetics with regards to the isolation procedure but with regards to the oxygen concentration during cultivation. Cells cultivated under hypoxic conditions displayed a higher PDL after 10 passages and thus a higher growth rate. Although not significant, cells from isolation by explant culture entered earlier into senescence than cells isolated by enzymatic treatment (see Table 3.2). Since passage number and the corresponding PDL is dependent on seeding density, the PDL at a certain passage is not comparable to studies by other researchers. However, the  $t_{PD}$  over 10 passages is a more suitable marker for the comparison of growth kinetics. In the study of Priya et al. the mean doubling time over 10 passages was  $\sim 50$  h regardless of isolation procedure. Differing from that, the mean  $t_{PD}$  was comparably lower (30 – 45 h) in the present work which might be contributed to donor variability but also the use xeno-free, low glucose conditions (see subsection 2.3.3). In the present work *in vitro* behavior of MSCs from different donors was considerably different although all donors were female and differed in age. Growth kinetics as well as the response to the different isolation procedures and oxygen conditions were found to be different. Furthermore, cells from the youngest donor displayed increased  $t_{PD}$ , decreased PDL and entered senescence earlier compared to older donors.

The differentiation capacity of the isolated cells was also not found to be dependent on the isolation procedure but more on the oxygen concentration during cultivation. Chondrogenesis was only observed under normoxic conditions in cells from enzymatic isolation. Adipogenic differentiation was observed in all conditions and was more pronounced in explant 5%  $O_2$ . In contrast, osteogenic differentiation was only present in normoxic cultivated cells but from both isolation procedures. Indeed the differentiation potential of MSCs isolated from explant culture was found to be comparable to cells from enzymatic isolation before [231, 237]. The effect of oxygen on differentiation of MSCs has been extensively studied [170] and a common tendency emerged from these studies. Briefly, hypoxia is thought to enhance chondrogenic differentiation [175] but to attenuate adipogenic and osteogenic differentiation [176, 177]. However, other studies reported conflicting results [238]. In the present work, chondrogenic differentiation seemed not be promoted by hypoxic conditions and adipogenic differentiation only slightly enhanced in cells from explant culture in hypoxic conditions. Again, discrepancies may arise from donor variability, medium composition or different levels and duration of hypoxia in other studies.

**Table 3.2:** Comparative overview of isolation procedures.

	enzymatic		explant	
	21 % O <sub>2</sub>	5 % O <sub>2</sub>	21 % O <sub>2</sub>	5 % O <sub>2</sub>
EFFECTIVENESS				
Procedure	complicated & time consuming		simple & time consuming	
Consumables	very high		low	
Yield (cells/g)·10 <sup>5</sup>	3.2 ± 0.9	2.9 ± 0.6	3.4 ± 0.5	3.3 ± 2.5
Yield (cells/g·d)·10 <sup>4</sup>	5.2 ± 1.3	4.9 ± 0.8	2.5 ± 0.5	2.7 ± 2.1
CHARACTERIZATION				
Immunophenotype	✓	✓	✓	✓
Senescence at passage	15.7 ± 1.2	18 ± 1.6	13.7 ± 2.5	17.7 ± 2.5
PDL at P10	17.8 ± 4.9	20.9 ± 3.2	16.8 ± 5.1	21.7 ± 2.2
<i>t</i> <sub>PD</sub> at P10	40.7 ± 19.4	30.2 ± 9.1	46.8 ± 28.5	31 ± 11.3
Chondrogenic differentiation	⇕	~	~	↑
Adipogenic differentiation	⇕	⇕	⇕	⇕
Osteogenic differentiation	⇕	~	⇕	~

~ = similar to control, ↑ = slightly increased compared to control, ⇕ = considerably increased compared to control.

### 3.3 From 3D to 3D - Isolation by explant culture in a 3D environment

Another approach for the isolation of MSCs from fat tissue is the isolation by explant culture in a 3D environment which might represent more physiologic conditions. In the absence of anticoagulants such as heparin HPL forms a firm gel. Hemeda, Giebel, and Wagner demonstrated that HPL gel can serve as biomaterial and medium for MSCs at the same time [179]. However, the isolation of MSCs from tissue pieces in HPL gel has not been demonstrated yet and therefore initial experiments were carried out. For this HPL gel was formed from a lyophilized HPL formulation (PL<sub>MATRIX</sub>) after reconstitution with 1 ml ddH<sub>2</sub>O and further 1:10 dilution with basal medium. To effectively embed tissue pieces the cultivation vessel was first coated with agarose to avoid cell adhesion. Subsequently, 350 μl HPL gel were added to the well of a 12 well plate and the plate was incubated 60 min at 37 °C for gel formation. Afterwards, a piece of adipose tissue was added on top of the bottom layer and a another 350 μl HPL gel were added to cover the tissue (see Figure 3.12 A). After 2 – 3 days cells started to grow out from the tissue and after 8 days cells seemed to have penetrated the entire gel (see Figure 3.12 B). Harvesting of cells was performed by mechanical dissociation of the gel (pipetting up an down), dilution in medium and centrifugation at 350 x g for 5 min. However, only very few single cells could be recovered from the gel while the vast amount of cells remained in fibrous structures, probably in extracellular matrix. Thus, reproducible harvesting and further passaging of cells from the gel was not possible. However, flow cytometry analysis of cells isolated in HPL gel revealed an MSC phenotype.

Further analysis of the proliferation and differentiation capacity as well as a detailed analysis

of the surface marker expression profile need to be carried out to characterize MSCs from explant isolation in HPL gel. Since expansion and differentiation can be carried out in a 3D environment by now, the isolation procedure remains the only stage of *in vitro* cultivation that currently must be carried out in 2D due to a lack of 3D approaches. However, the conditions during isolation of stem cells determine the subpopulation for the following cultivation steps and thus it seems desirable to gain knowledge and control in this field. A continuous cultivation in 3D during isolation, expansion and differentiation might support a more physiologic behavior of cells *in vitro*.

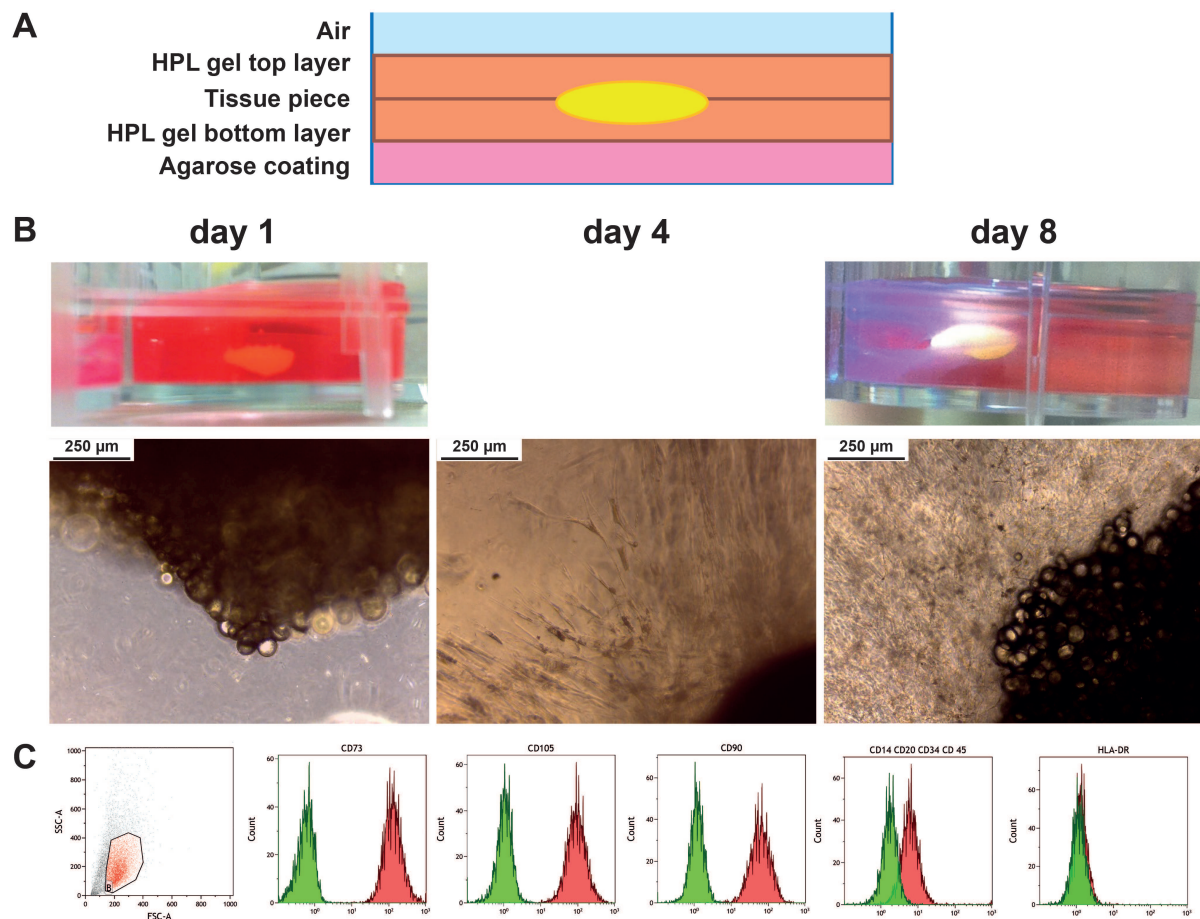


**Figure 3.12:** Isolation of adipose MSCs by explant cultivation in a 3D environment. A) Schematic depiction of the cultivation vessel for isolation of MSCs in HPL gel. The bottom is coated with agarose to avoid cellular adhesion on cell culture plastic while the tissue itself is placed between two layers of a 10 % HPL gel. B) Picture of a well for isolation of MSCs in HPL gel at day 1 and day 8 of isolation. C) Flow cytometry analysis of MSCs from isolation by explant cultivation in HPL gel. Green indicates the isotype control while red indicates the phenotype. Data represent 10.000 events.

### 3.4 Conclusion

In conclusion, the isolation of MSCs via explant culture was found to result in comparable yield of cells with comparable properties compared to cells from enzymatic isolation. However, the

time dependent yield was significantly reduced by isolation via explant culture. Reduced oxygen concentration (5 % O<sub>2</sub>) resulted in increased yield and proliferation capacity with decreased senescence and altered differentiation capacity. A comparative overview of both isolation procedures is given in Table 3.2.

Improvement of stem cell isolation procedures becomes more and more important since therapeutic application of MSCs is increasing. The isolation of stem cells via explant culture provides an suitable and economic way to harvest adipose tissue derived stem cells from patients. Since MSCs derived by explant culture display stem cell properties further improvements should focus on simplification of the isolation procedure, reduction of time until harvest and enhancement of yield. Since migration of cells from explant tissue is currently also interpreted as a wound-healing response further introduction of lesions by cutting or grinding of the tissue might be beneficial. In this context, processing of lipoaspirates might be superior to processing of resected tissue. Also, a fast method for isolation from lipoaspirates in less than 30 min has already been developed [239] and several devices for liposuction were found to not impair later stem cell isolation [240]. Initial cell sorting of cells from the SVF might improve purity of cell populations which might be important for later differentiation of cells [241]. Furthermore, a recent study reports the isolation of MSCs with the help of matrix metalloproteases (MMPs) to result in a purer cell population than received by collagenase and Liberase treatment [242]. Still, it is not clearly evaluated if enzymatic treatment or isolation by explant culture selects for distinct cell populations with different properties, still fulfilling the MSC minimal criteria. For example, differentiation of MSCs derived from explant isolation displayed increased differentiation potential towards retinal photoreceptors compared to cells from enzymatic isolation, which indicates selection of subpopulations with increased differentiation potential [243]. Since conditions during isolation have great impact on the resulting subpopulations this initial step of *in vitro* cultivation deserves more attention. In this context the isolation of MSCs from explant tissue in a 3D environment should be further optimized and cells from this approach need to be further characterized.

## 4 Scaffold-free Stem Cell Cultivation

### 4.1 Aggregates in Stem Cell Cultivation

In general, the term *aggregate* describes a multicellular construct of condensed cells (either forced by centrifugation or spontaneously induced by high density cell suspension) whereas the frequently used term *spheroids* can be considered as a subcategory of *aggregates* and describes exclusively spherical-shaped cellular aggregates. Cultivation of cellular aggregates has mainly been used in cancer research and studies on embryonic development. In the context of cultivation it was utilized to induce chondrogenic differentiation where it was mainly referred to as pellet or micromass cultivation. However, in the last 5 – 10 years self-assembly of MSCs has been studied in a wider spectrum beyond chondrogenesis. In fact, cultivation of MSC aggregates is currently accepted to represent a more *in vivo* like environment since MSCs display improved differentiation [244] and anti-inflammatory properties [101]. Even after short-term aggregate cultivation the regenerative capacity was shown to be improved [102]. Viable research is currently carried out on the molecular mechanisms that cause self-assembly and cellular behavior in aggregates. However, cell-cell contacts (i.e. cadherins) and interactions with ECM proteins (i.e. collagen type I) that are intact (compared to enzymatically treated 2D monolayer culture) are thought to play a major role [106]. Furthermore, regarding cell transplantation, increased retention of cells at transplantation sites has been reported when cells were introduced in the form of aggregates [245]. Understandably, MSC aggregates gain more and more attention for therapeutic use in cell-based therapies and tissue engineering approaches.

The cultivation of aggregates in small scale systems like microtiter plates or hanging drops is well established [246]. However, aggregates display nutrient and oxygen gradients from surface to core which was demonstrated to result in a necrotic core for aggregates  $> 500 \mu\text{m}$  [107]. Therefore, dynamic cultivation systems that enable for enhanced mass transfer seem preferable for aggregate cultivation. Indeed, cultivation of MSC aggregates in rotating wall vessel bioreactors, shake flasks, spinner flasks or on orbital shakers did not result in necrotic tissue [103, 108–110].

In this chapter, the upscale of MSC aggregate formation and cultivation from microtiter plates to a stirred tank reactor (STR) is described. First, formation and cultivation of MSC aggregates in microtiter plates under static and dynamic conditions is characterized and advantages and drawbacks of cultivation in small scale systems are discussed. Second, aggregate formation and cultivation is carried out in volumes between 1 – 10 ml at different initial seeding densities. Since several aspects remained challenging at this scale the cultivation was finally transferred to a small stirred tank reactor (130 ml) and hypoxic conditions were implemented to optimize the process (Figure 4.1)[247].



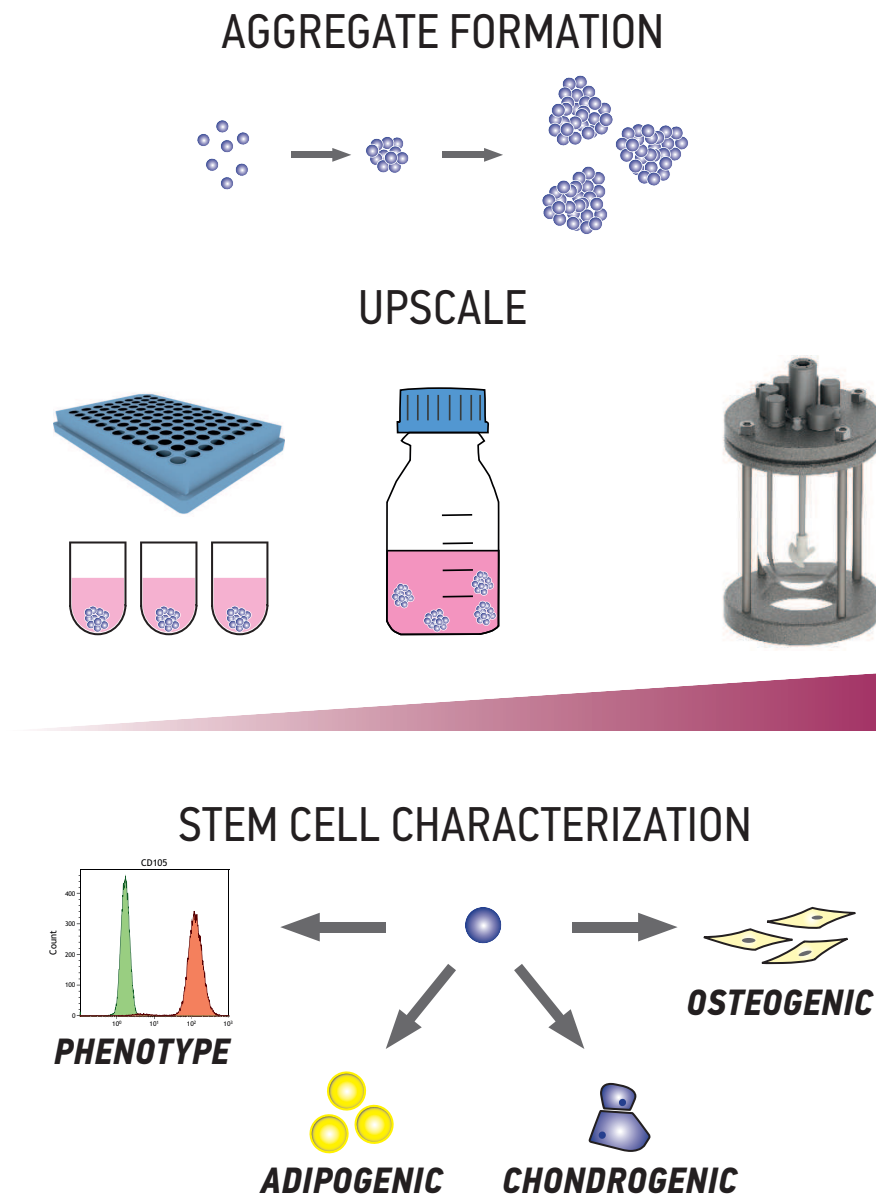


**Figure 4.1:** Graphical abstract describing the experimental work of chapter 4: the scaffold-free 3D aggregate cultivation of MSCs is characterized under static and dynamic conditions. Furthermore, approaches for the upscale of aggregate cultivation from a single cell suspension are described. Finally, expansion of MSC aggregates in a stirred tank bioreactor is demonstrated under normoxic and hypoxic conditions.

## 4.2 Aggregate Cultivation in Microtiter Plates

Cultivation of 3D MSC aggregates was carried out in cell-repellent, round-bottom 96 well plates. Cells were seeded at two different densities and cultivated either under static or dynamic (horizontal shaker at 100 RPM) conditions as described in section B.2. The aggregate size was determined via analysis of microscopic pictures with ImageJ as described in section B.12. To assess viability a TOX8 viability assay was performed and aggregates were stained with Calcein-AM and PI.

Spheroid-shaped aggregates were observed after 1 day cultivation in all conditions. While samples with lower density displayed an increase in aggregate area on day 2, samples that were seeded with a higher density remained the same size (Figure 4.2 A and B). After 2 days area size decreased in all conditions until end of cultivation. Compaction of aggregates on day 4 was found to be 18 – 40 % compared to day 1 and significantly higher for 2500 cells in dynamic conditions compared to static (Figure 4.2 C). However, higher seeding density did not generally result in elevated compaction of aggregates. Further, aggregate area of the respective seeding density was significantly increased in dynamic conditions ( $\alpha = 0.001$ ,  $p < 0.0001$ ).

A similar trend was displayed by the viability assay (Figure 4.2 C). The viability was found to be highest on day 2 and then decreased in all conditions. Still, viability of the respective seeding density was significantly increased until day 2 in dynamic conditions ( $\alpha = 0.01$ ,  $p < 0.0001$ ). Calcein-AM and PI staining on day 4 depicts spheroid shaped aggregates in static conditions and oval shaped aggregates under dynamic conditions. Throughout all conditions no dead cells were visible on the aggregate surface.

**Discussion** Initial cultivation of 3D MSC aggregates under static and dynamic conditions indicate agitation in form of horizontal shaking to be beneficial for aggregate cultivation. First of all aggregate size and viability were found to be increased in dynamic conditions indicating increased cellular growth. MSC aggregates have already been cultivated in shaker flasks, spinner flasks and rotating wall vessel (RWV) bioreactors. Proliferation was found to be comparable to 2D monolayer cultivation and improved osteogenesis and adipogenesis was observed when compared aggregates were cultivated in spinner flasks or RWVs [103]. However, Frith, Thomson, and Genger did not compare dynamic to static aggregate cultivation. Yet, one study reports increased proliferation and differentiation capacity when cells were cultivated in serum-free medium in a shaker flask compared to 3D static conditions [109]. These results suggest dynamic conditions in form of horizontal agitation to improve cellular growth in spheroids which is probably caused by enhanced mass transfer.

Compaction of aggregates occurred rather under dynamic than under static conditions. Interestingly, it was not correlated to the initial seeding density. Considerable compaction of MSC aggregates was reported before [101, 110, 246, 248, 249] and has been proposed to be a three-step process [4, 106, 250]. Direct cell-cell contacts and binding to ECM proteins enables for formation of aggregates (as described in subsection 2.3.1). However, MSC aggregates display a time dependent spatial heterogeneity that is closely linked to intrinsic characteristics such as integrin and cadherin expression and the cortical tension which are again altered by the mechanical microenvironment [4]. Higher compaction observed in dynamic conditions might be caused by changes

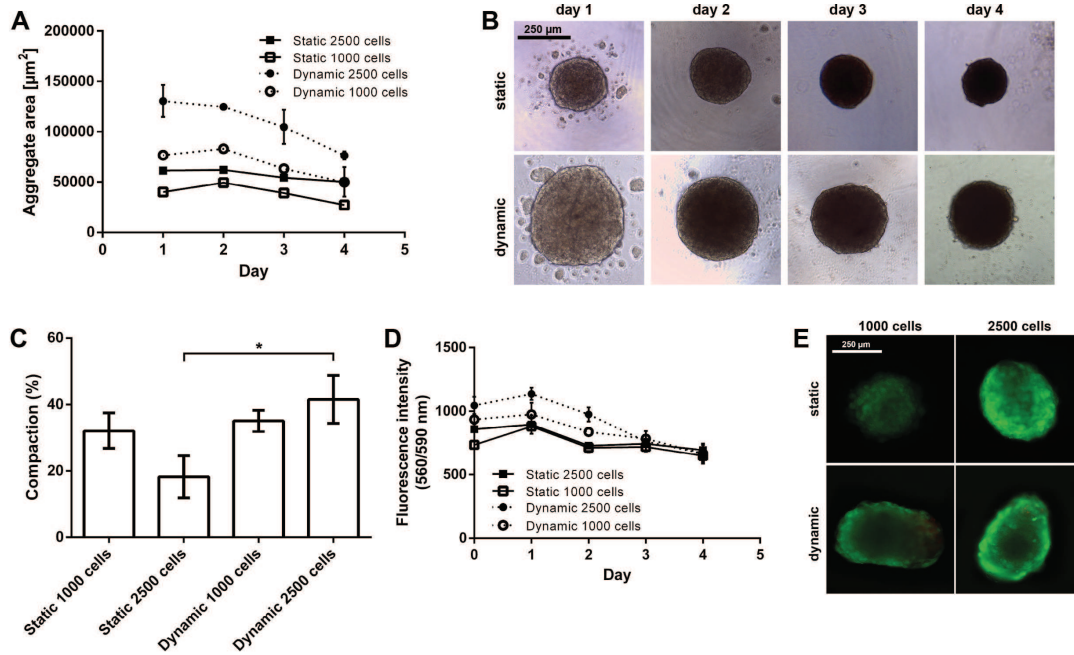


**Figure 4.2:** A) aggregate size, B) microscopic pictures of aggregates seeded with 2500 cells, C) compaction compared to day 1, D) viability and E) Calcein-AM and PI staining on day 4 of MSCs cultivated in cell repellent 96 well plates under static or dynamic conditions (horizontal shaker at 100 RPM) ( $n=6$ ). Data represented as mean  $\pm$  SD; \* indicates significant difference ( $\alpha = 0.01$ ,  $p < 0.0001$ )

in the mechanical environment which again cause mechanotransductive effects and alterations in cytoskeleton [251].

Although aggregate size and viability were elevated until day 2 in dynamic conditions they decreased until end of cultivation. Medium evaporation was found problematic since outer wells on a microtiter plate display higher evaporation than inner wells. Evaporation causes an increase of nutrient concentration and thus reduces control on the cultivation process. It is likely that proliferation and viability decreased because of inconsistencies in nutrient concentration. Therefore, long-term cultivation for expansion or differentiation of MSC aggregates was not considered to be feasible using this setup. In order to perform defined and reliable medium changes and to minimize evaporation effects, several approaches for the upscale of aggregate cultivation were taken into account and tested.

### 4.3 Approaches for Upscale of Aggregate Cultivation

In order to upscale cultivation of 3D MSC aggregates in microtiter plates, the cultivation vessel was changed to a 100 ml Schott flask equipped with a sterile air filter. For initial testing of this approach MSCs were seeded at 500.000 cells/ml (10 ml) and cultivated at 100 RPM on a horizontal shaker for 7 days. The cell number was assessed via DNA quantification of a 500  $\mu\text{l}$  sample and viability was determined via TOX8 assay of 3 x 100  $\mu\text{l}$  sample and Calcein-AM and PI stain randomly picked aggregates (all  $n=2$ ). The cell concentration was found to be approximately one fifth of the initial concentration and decreased further until end of cultivation. Again, compaction

of aggregates was observed. Similarly, viability was 5 – 15% compared to day 0 (measured directly after seeding). Still, aggregates stained with Calcein-AM and PI were viable and no dead cells were spotted on the aggregate surface (Figure 4.3). However, determination of DNA and viability was maybe biased because aggregates were not perfectly distributed like in a single cell suspension, and thus sample volumes might not have been representable for the entire cultivation volume. After the initial drop in cell number and viability both were seemingly stable until day 5. Therefore, further cultivations were carried out until day 5.

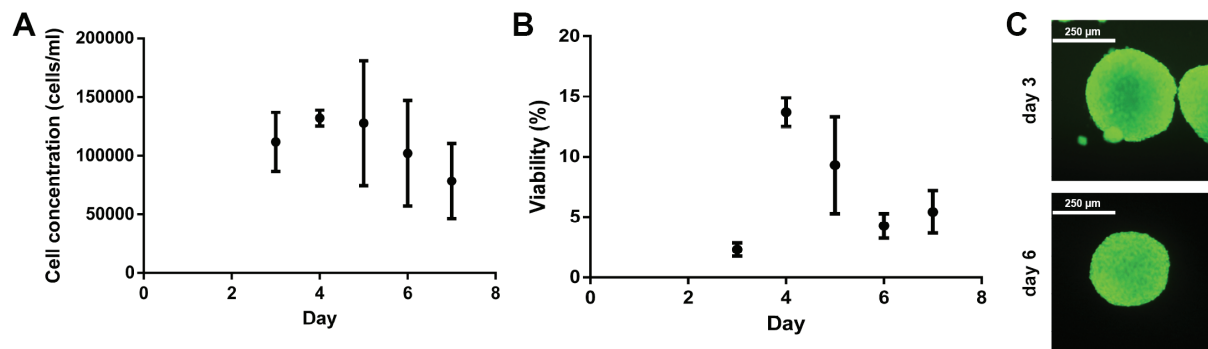


**Figure 4.3:** A) Cell concentration, B) viability and Calcein-AM and PI staining of aggregates cultivated in a Schott flask at 100 RPM (horizontal shaker,  $n=2$ ). Data is represented as mean  $\pm$  SD.

Following, in order to enhance reproducibility and reduce sampling errors cultivation of aggregates was carried out in glass vials of different geometries (17x27 mm, 14x45 mm, and 19x37 mm) which were seeded with 1 ml of either a 500.000 cells/ml single cell suspension (CS) or 50 pre-formed aggregates (PF) each 10.000 cells (see Figure 4.4 A). Cultivation was performed on a horizontal shaker at 100 RPM for 5 days ( $n=2$ ). For the generation of PFs 200  $\mu$ l of a 50.000 cells/ml cell suspension were seeded in a 96 well plate 3 days before (shaker 100 RPM). This time, cell number was determined by lysis of aggregates from the entire cultivation volume to avoid errors caused by sampling. PF aggregates agglomerated to several larger aggregates during cultivation whereas one large aggregate formed in CS. Cell number was again found to be decreased compared to the initial cell number. Further, significantly lower cell numbers were observed in PF compared to CS aggregates ( $\alpha = 0.01, p < 0.0001$ ). Geometries of the vials did not have any effect on aggregate formation or cell proliferation (see Figure 4.4).

Although pH (indicated by phenol red) did not change dramatically the initial seeding density was reduced and a daily medium change was introduced in the next cultivation to assure proper medium supply. Glass vials were seeded with either 1 ml CS (100.000 cell/ml) or 10 PF aggregates (each 10.000 cells) and cultivated for 5 days on a horizontal shaker (100 RPM). 500  $\mu$ l medium was changed on day 2, 3 and 4. To prevent cell loss due to medium change the shaker was stopped 20 min prior to medium change to allow cells and aggregates to sediment. Again, DNA of the entire biomass was quantified after cultivation. After cultivation PF aggregates were not visible by eye whereas 2 – 3 large aggregate formed in CS as depicted in Figure 4.5. Again, CS aggregates displayed a higher cell number compared to PF. Proliferation of cells was observed in CS vial with dimensions of 17x27 mm. However, in all other conditions cell number was lower compared to the initial cell number.

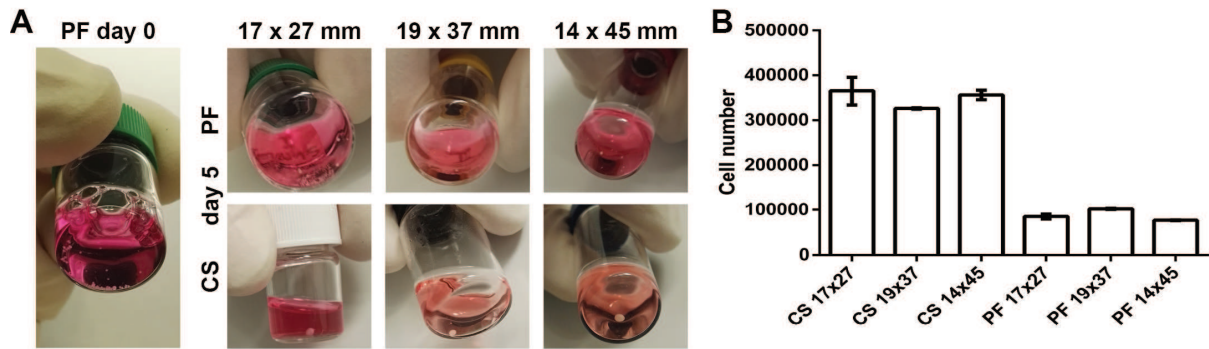


**Figure 4.4:** A) images and B) cell number of of CS (cell suspension) and PF (pre-formed) cultivated aggregates in different glass vials at 100RPM (horizontal shaker, n=2). Data is represented as mean  $\pm$  SD.

Finally, comparing all upscale approaches, the pre-formation of more defined aggregates (PF aggregates) does not improve the cultivation process with regards to proliferation. Spontaneous formation of aggregates from a single cell suspension (CS aggregates) was observed and yielded a higher cell number than found in PF aggregates (see Table 4.1). Cultivation of CS resulted in 70 – 80 % of the initial cell number whereas cultivation of PF resulted in 18 % of the initial cell number only.

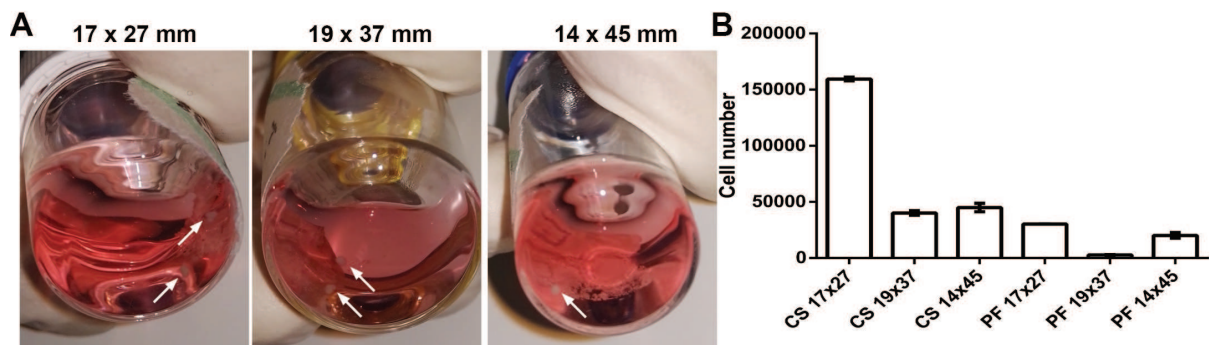


**Figure 4.5:** A) images and B) cell number of of CS (cell suspension) and PF (pre-formed) cultivated aggregates in different glass vials at 100RPM (horizontal shaker, n=2). Data is represented as mean  $\pm$  SD.

**Discussion** In order to upscale the cultivation of 3D MSC aggregates different approaches were tested. When cultivation vessels were seeded with a single cell suspension, large but few aggregates formed and in one condition proliferation was observed. In contrast, aggregates that were pre-formed in 96 well plates and after formation cultivated together displayed significantly lower cell numbers. Considering the effort of pre-formation (seeding of a vast amount of wells and subsequent unification of aggregates in a larger cultivation vessel) and the lower cell number, cultivation of an agitated single cell suspension followed by spontaneous aggregate formation was considered to be more feasible. Also, a lower seeding density did not result in reduced aggregate formation or proliferation but instead in more smaller aggregates with a higher cell number than in PF aggregates. In the context of the production of therapeutically relevant cell numbers a

**Table 4.1:** Comparison of upscaled approaches. Total cell number on day 5 of cultivation. CS = cultivation of single cell suspension, PF = cultivation of pre-formed aggregates.

Approach	Seeding density $\left[\frac{\text{cells} \cdot 10^4}{\text{ml}}\right]$	Volume [ml]	Total cell number $[\text{cells} \cdot 10^4]$	Fraction of initial cell number [%]
Schott flask, CS	50	10	$127.5 \pm 53.3$	$25 \pm 11$
Glass vial, CS	50	1	$34.9 \pm 1.7$	$70 \pm 3$
Glass vial, PF	50	1	$8.9 \pm 1$	$18 \pm 2$
Glass vial, CS	10	1	$8.1 \pm 5.5$	$82 \pm 55$
Glass vial, PF	10	1	$1.7 \pm 1.1$	$18 \pm 11$

lower initial seeding density is also beneficial since less initial material (donor tissue) is needed prior to expansion of MSCs.

In summary, none of the approaches for the upscale of 3D MSC aggregates resulted in satisfactory expansion of MSCs. Nevertheless, cultivation of CS aggregates was found to be superior to PF cultivation and a lower cell density also seemed to be beneficial. Since aggregate formation occurs spontaneously in a single cell suspension further studies concentrated on improving the mode by which dynamic movement was implemented in the process.

#### 4.4 Aggregate Cultivation in a Stirred Tank Reactor

Although cultivation of 3D MSC aggregates was improved by dynamic conditions (horizontal agitation) compared to static, the results were not satisfactory with regards to viability and proliferation. Spinner flasks and orbital shaker have already been used to cultivate MSC aggregates [103, 108, 110], still until now no study reported the cultivation in a stirred tank reactor (STR). Advantages of STRs include simplicity and very good mixing conditions which result in a homogeneous and controllable cultivation system. STRs are easily standardizable and thus allow for a rapid development of cultivation protocols and upscale. Therefore, a STR was employed to cultivate 3D aggregates (see Figure 4.6). CFD analysis was performed in order to estimate shear stress that cells are exposed to (cooperation with the University Hospital Wuerzburg, Germany)[247]. Since under reduced oxygen concentrations MSCs exhibit increased proliferation [171–173], delayed replicative senescence [174] and prolonged genetic stability [175], cultivation was carried out under hypoxic conditions as well.

MSCs were seeded at 100.000 cells/ml and cultivated for 6 days at 21 % or 5 % O<sub>2</sub> in the STR as described in section B.3. Since initial experiments revealed cell adhesion on the glass vessel and impeller, the impeller speed was set to 600 RPM. DO, glucose and lactate were monitored during cultivation and aggregates were dissociated with a modified cell dissociation protocol after cultivation to determine the total cell number (section B.3). In the context of therapeutic use it is crucial that stem cells maintain their functionality. Thus, after cultivation stem cell properties were evaluated according to the current minimal criteria proposed by Dominici et al. [42]. For this, cells were antibody stained for the surface markers CD73, CD90, CD105, CD14, CD20,

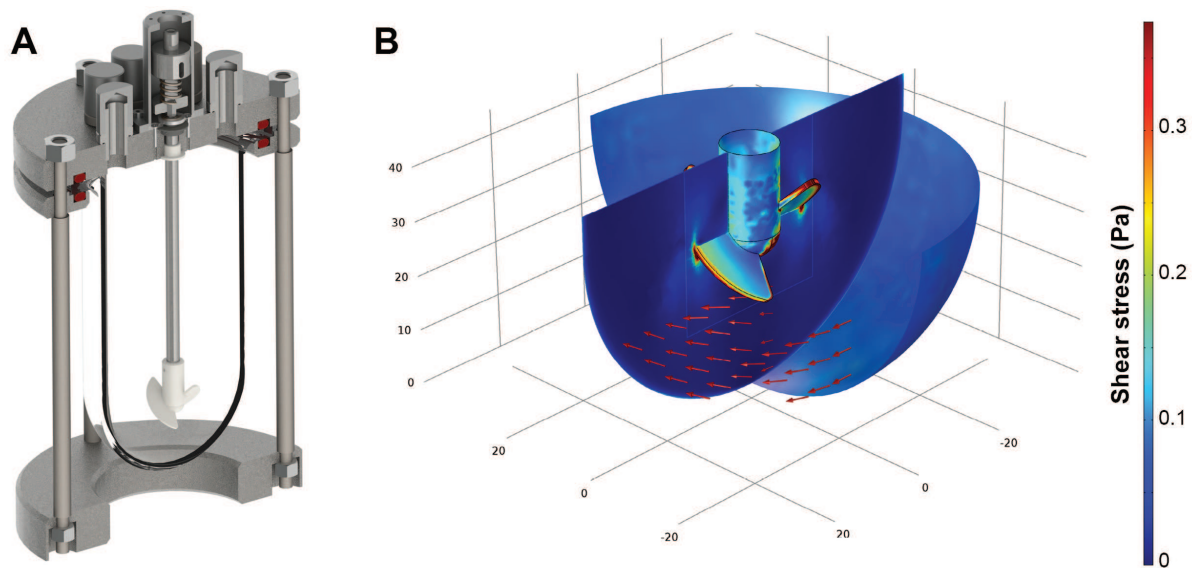


**Figure 4.6:** A) Three-dimensional model of the stirred tank reactor used for aggregate cultivation; B) Flow field direction (red arrows) and shear stress distribution (color legend) at a rotational speed of 600 RPM as estimated by computational fluid dynamics (CFD). The bioreactor was designed and CFD analysis were performed by Ivo Schwedhelm, University Hospital Wuerzburg, Germany (figure adapted from [247]).

CD35, CD45 and HLA-DR and analyzed via flow cytometry. Furthermore, cells were tested towards their adipogenic, chondrogenic and osteogenic differentiation capacity (see section B.6).

**Bioreactor cultivation** Visible aggregates formed spontaneously after approximately 3 days. Although the impeller speed was set to 600 RPM cells and aggregates were still found to adhere and grow on the glass surface of the bioreactor vessel and partially on the impeller. DO decreased slowly under normoxic conditions to approximately 85 % until day 6 whereas under hypoxic conditions it decreased to 0 % after 5 days (see Figure 4.7). Cells expanded 1.85-fold ( $\pm 0.19$ ) under normoxic conditions and 2.23-fold ( $\pm 0.27$ ) under hypoxic conditions displaying a viability of  $78.5 \pm 9.8\%$  and  $86 \pm 3.1\%$  respectively (see Figure 4.8). Human MSCs of different origin displayed an approximately 1.3-fold increased growth rate when cultivated under hypoxic conditions [175]. Although not statistically significant, experimental data indicate a similar behavior when ASCs are cultivated in a STR. Furthermore, glucose consumption ( $0.85 \pm 0.1$  mmol) and lactate production ( $1.69 \pm 0.11$  mmol) were significantly lower in normoxic conditions compared to hypoxic conditions where glucose consumption was  $1.09 \pm 0.02$  mmol and lactate production  $2.05 \pm 0.09$  mmol. In the absence of oxygen glycolytic activity increases since glucose is metabolized rather by lactate acid fermentation than by oxidative phosphorylation in the mitochondria which reduces the efficiency of ATP production. However, under hypoxic cultivation cell numbers were slightly increased together with a higher viability.

**Stem cell properties** Surface markers of MSCs before and after cultivation in the STR were comparable (see Figure 4.9). Also, surface markers of cells cultivated under normoxic and hypoxic conditions were comparable and met the minimal criteria of MSCs. Furthermore, differentiation into adipogenic, chondrogenic and osteogenic lineage was performed (see Figure 4.10 and

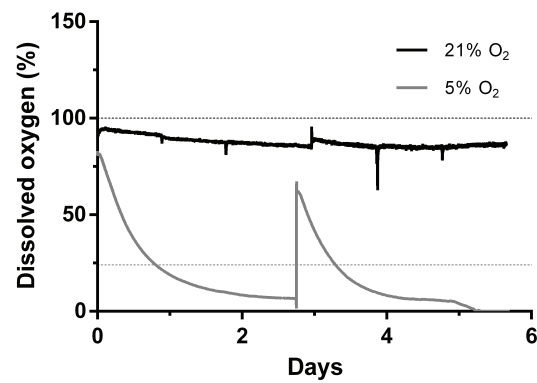


**Figure 4.7:** Dissolved oxygen during cultivation of MSCs in stirred tank reactor at 21 or 5 % O<sub>2</sub> ambient oxygen. Dashed lines indicate the respective DO concentration at respective equilibrium.

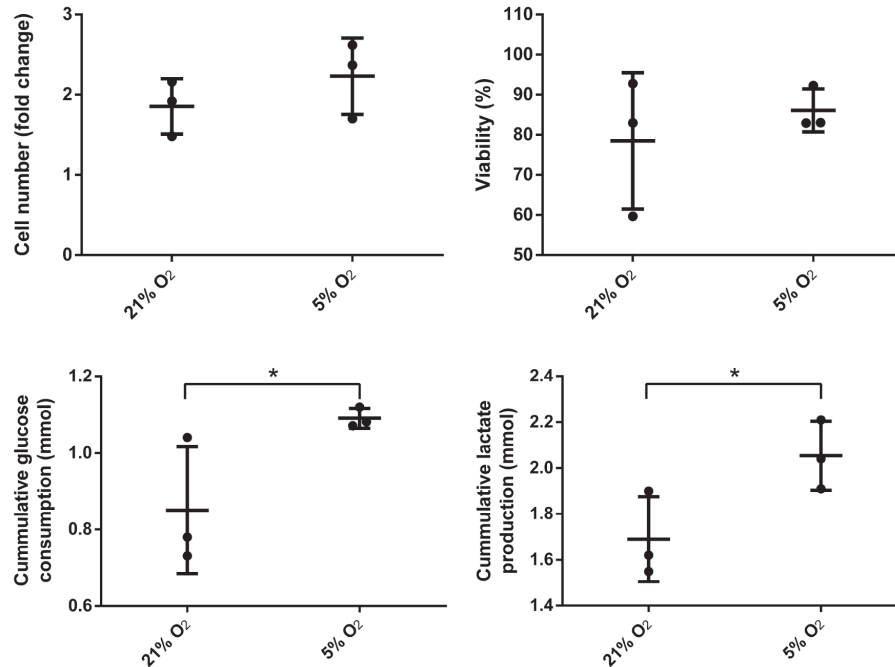


**Figure 4.8:** Yield of viable cells, overall viability and glycolytic activity of MSCs after 6 days cultivation under 21 and 5 % O<sub>2</sub> in a stirred tank reactor. Data represented as mean ± SD (n=3), asterisks indicate statistically significant difference ( $p < 0.1$ , confidence interval of 90 %).



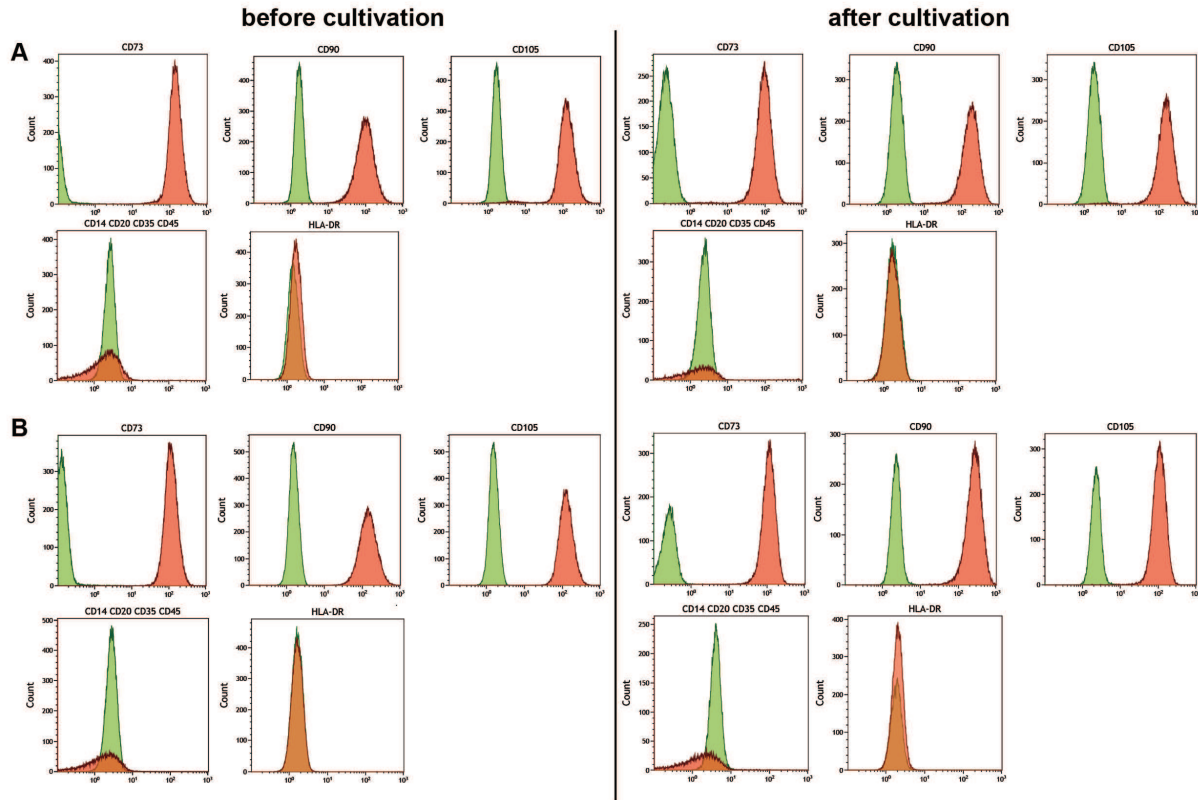


**Figure 4.9:** Phenotyping of MSCs before and after 6 days cultivation under A) 21 and B) 5 %  $O_2$  in a stirred tank reactor. Light gray areas indicate the isotype control, dark grey areas indicate phenotype.

Table 4.2). However, slightly elevated adipogenic and chondrogenic but a reduced osteogenic differentiation was observed in hypoxic compared to normoxic conditions. The majority of studies reported attenuated osteogenic [176] and adipogenic [177] but elevated chondrogenic [175] differentiation under hypoxic conditions although also elevated adipogenic differentiation was observed [238].

**Table 4.2:** Qualitative assessment of trilineage differentiation of human MSCs after aggregate cultivation in a STR. Adipogenesis was assessed by Oil Red O staining, chondrogenesis by alcian blue staining and osteogenesis by calcein and von Kossa (VK) staining.

Oxygen concentration	Osteogenesis	Chondrogenesis	Adipogenesis
21 %	+	~	~
5 %	~	+	+

~ little staining, + clear staining.

**Discussion** Cultivation of MSCs aggregates or spheroids is well established at the scale of hanging drops [246], microtiter plates [252] or shaking flasks [109, 253]. The maintenance of stem cell properties after cultivation on an orbital shaker was already demonstrated in a study with murine MSC aggregates [110]. Another study reports the cultivation of human MSCs in shaking flasks [109].

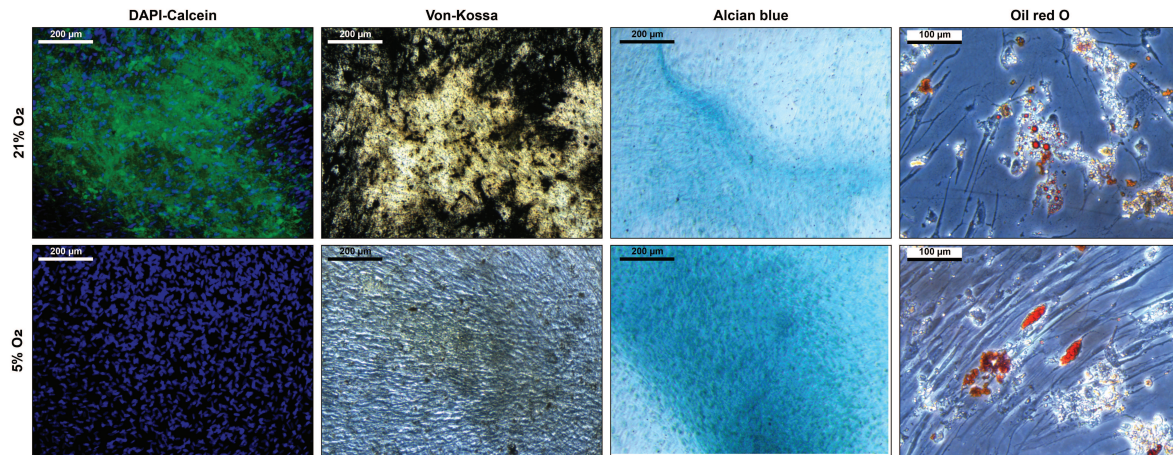


**Figure 4.10:** Differentiation of MSCs after 6 days cultivation under 21 and 5 %  $O_2$  in a stirred tank reactor. Osteogenic differentiation is indicated by DAPI-calcein staining for nuclei and extracellular calcium and Von-Kossa stain for extracellular phosphates. Chondrogenic differentiation is indicated by alcian blue staining which stains for glycosaminoglycans. Adipogenic differentiation is indicated by Oil Red O staining which stains the intracellular fatty vacuoles.

However, to the best of the author's knowledge cultivation of MSC aggregate in a STR has not been reported until now. Therefore, in this study the cultivation of MSC aggregates in a STR under normoxic (21 %  $O_2$ ) and hypoxic (5 %  $O_2$ ) conditions was demonstrated. Cells cultivated under hypoxic conditions displayed increased proliferation, viability (not significant) and glycolytic activity (significant) compared to normoxic conditions. Furthermore, MSCs maintained their stem cell properties as indicated by their immunophenotype (positive for CD73, CD90, CD105 and negative for CD14, CD20, CD35, CD45 and HLA-DR) and multilineage differentiation capacity. To avoid cell adhesion on the glass wall and impeller of the bioreactor the impeller speed was set to 600 RPM which resulted in an average shear stress of 0.02 – 2.5 Pa as indicated by CFD analysis [247]. MSCs are known to react to mechanical cues such as fluid shear forces and several studies reported differentiation when cells were exposed to shear stress as low as  $7.6 \cdot 10^{-5}$  [137] or 0.01 Pa [254]. However, flow cytometry analysis of surface marker expression revealed exclusively undifferentiated stem cells. Furthermore, cells maintained their trilineage differentiation potential. Cellular aggregates were shown to be temporally and spatially heterogeneous with regards to cellular architecture and expression of matrix proteins [103, 110, 253]. Therefore, cells on the aggregate surface might shield the inner cell mass from shear stress.

The traditional approach for the expansion of MSCs is the cultivation on two dimensional plastic surfaces. Although this approach is simple and reproducible it is time and material consuming to achieve high cell numbers. Also, a rather huge surface is required which often results in numerous cell culture vessels and extensive passaging of cells. Due to the comparably high number of opening events the risk of contamination is increased. Therefore, other approaches like the cultivation in hollow-fiber bioreactors with a high surface-to-volume ratio or microcarrier based systems were developed. For example the quantum system by Terumo expanded  $6.6 \cdot 10^8$  MSCs from a 25 ml bone marrow aspirate [200]. Also, expansion of MSCs on microcarrier was performed successfully in spinner flasks [255] and STRs [256]. However, the quantum system was mainly developed for use at clinical scale and thus might be oversized for research scale while cell

harvest is challenging in microcarrier based systems [257, 258]. Also, both approaches are limited by their surface capacity. Though the yield of the presented scaffold free aggregate cultivation of MSCs is comparably low this system offers a straight forward approach to cultivation of MSCs. Potentially, advantages of traditional suspension culture, such as simplicity, standardizability, rapid development of cultivation protocols and upscale are translatable to aggregate cultivation. Nevertheless, since homogeneity of aggregates is not given until now, the system may be of interest rather for the production of secreted compounds than expansion of cells. Especially, aggregate cultivation under hypoxic conditions might be of benefit in this context since the hypoxic environment in the core of aggregates was reported to increase expression of trophic factors such as VEGF, FGF-2, HGF and CXCR4 [108, 259] as well as ECM proteins such as fibronectin, collagen I, vitronectin and collagen IV [150]. However, the expression profile of MSC aggregates cultivated in an extensively stirred environment needs further investigation.

In order to improve the cultivation process with regards to yield, viability and reproducibility further work should focus on optimization of the bioreactor and impeller geometry. Furthermore, coating agents like silicon should be considered to prevent cell loss due to glass adherence. This might also reduce the required impeller speed and thus contribute to proliferation and viability of cells. Cultivation under hypoxic conditions seems to improve cell yield and viability. However, an oxygen concentration of  $\leq 12\%$  DO ( $\approx 2.5\%$  ambient  $O_2$ ) should be avoided as it was shown to decrease proliferation of MSCs [36]. Also, serum-free medium was optimized for MSC aggregate cultivation and shown to increase proliferation and similar or enhanced differentiation capacity compared to cultivation in serum-containing medium [110].

## 4.5 Conclusion

In conclusion, the implementation of dynamic conditions such as horizontal shaking supported growth and viability of 3D MSC aggregates. However, for large scale cultivation of aggregates, the format of microtiter plates is not suitable due to medium evaporation effects that cause impaired proliferation and viability. In order to maintain reproducibility the cultivation of previously formed spheroid-shaped aggregates in larger volumes was evaluated. Still, proliferation was decreased compared to aggregates spontaneously formed in cell suspension. Also, at the scale of 1 – 10 ml, medium change and sampling procedures remained challenging. However, proliferation and comparably high viability of MSC aggregates was observed in a STR. Although comparatively high shear forces in the range of 0.02 – 2.5 Pa are present in the stirred system MSCs maintained their surface marker expression profile and differentiation capacity. Hypoxic conditions slightly enhanced proliferation and viability of aggregates cultivated in the STR.

In fact, these are encouraging results since cell expansion was carried out in a simple process while stem cell properties were maintained. Yet, further studies need to focus on optimization of bioreactor and impeller geometry, dissolved oxygen concentration, coating agents and medium composition to improve expansion, viability and reproducibility of aggregates. Also secretion of trophic factors that are crucial for the regenerative capacity of MSCs needs to be evaluated during and after cultivation in a STR. The large scale production of MSC aggregates is an important step towards their application in cell-based therapies or tissue-engineering approaches.

# 5 Physiologic Differentiation Towards Osteogenic Lineage

## 5.1 Setting a physiologic environment for osteogenic differentiation

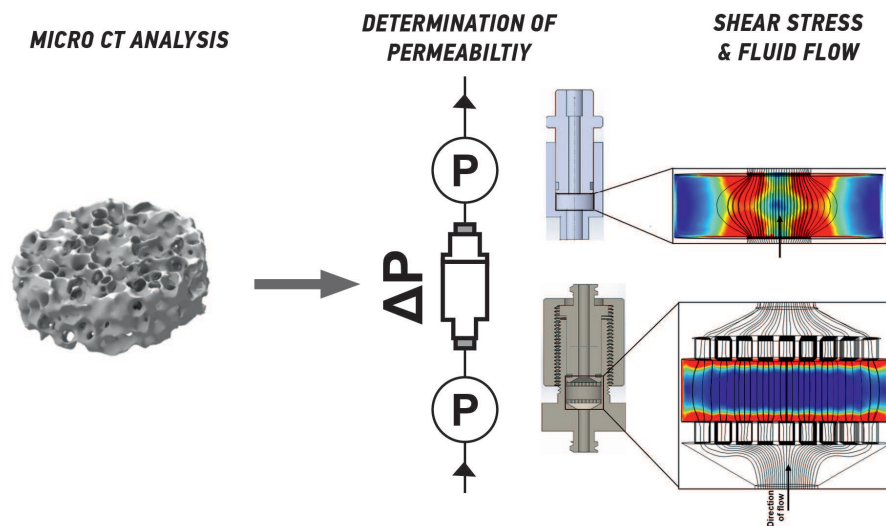
In the field of regenerative medicine and tissue engineering 3D cell culture processes are of growing importance. Especially, for the development of functional 3D tissue for *in vitro* models or tissue repair it is inevitable to study cell-cell or cell-scaffold interactions. Besides a suitable biomaterial and functional cells, proper culture conditions need to be established and optimized for each process. To generate physiologic conditions not only standard cell culture parameters but also extrinsic mechanical cues have to be applied during cultivation (see subsection 2.3.2). Although it is practically impossible to apply one single force while avoiding the others it is commonly accepted to distinguish between tension, compression, HP and fluid flow [94].

Flow perfusion systems are beneficial when mass transfer into the 3D construct becomes a limiting factor since oxygen and nutrition supply as well as waste removal are improved in perfused systems [180]. Furthermore, it is possible to apply fluid shear stress which is known to be present in *in vivo* bone tissue [131] and to have mechanotransductive effects on the differentiation of stem cells. Especially osteogenic differentiation was observed to be enhanced by fluid shear stress in numerous studies [6, 132, 134, 136]. To predict the fluid shear forces cells experience on a 3D scaffold different mathematical models were developed [132, 260, 261]. Moreover, based on x-ray computed tomography data and CAD models of bioreactors, computational fluid dynamics analysis were carried out to calculate shear forces [6, 207, 209, 262]. Therefore, if inherent biomaterial characteristics are known fluid shear stress can be calculated and applied via the respective flow velocity.

Also, HP is a physiologic mechanical force that was shown to have several effects on stem cell behavior [263]. It is commonly accepted that the *in vivo* HP in mammalian bone lies within the range of 10.7 – 120 mmHg [264]. Although HP has been mainly used to improve chondrogenesis of MSCs the effect of osteogenic differentiation was also investigated. Studies on chondrogenesis and osteogenesis found diverse effects of HP which is probably due to differing experimental setups [94]. However, HP was shown to enhance cellular viability and osteogenic differentiation [151, 263, 265]. Still, most bioreactors are limited with regards to sample size, number of samples, control of the process, automation and monitoring which is why 3D cell culture processes are difficult to be reproduced and standardized (see section 2.4). Several perfusion systems have been developed and proved to be beneficial for various 3D cell culture purposes [136, 266–268]. However, currently available systems often have limitations and drawbacks. Most of the systems

## STEM CELL DIFFERENTIATION

### BIOMATERIAL AND BIOREACTOR CHARACTERIZATION



### OPTIMIZATION OF THE MECHANICAL ENVIRONMENT

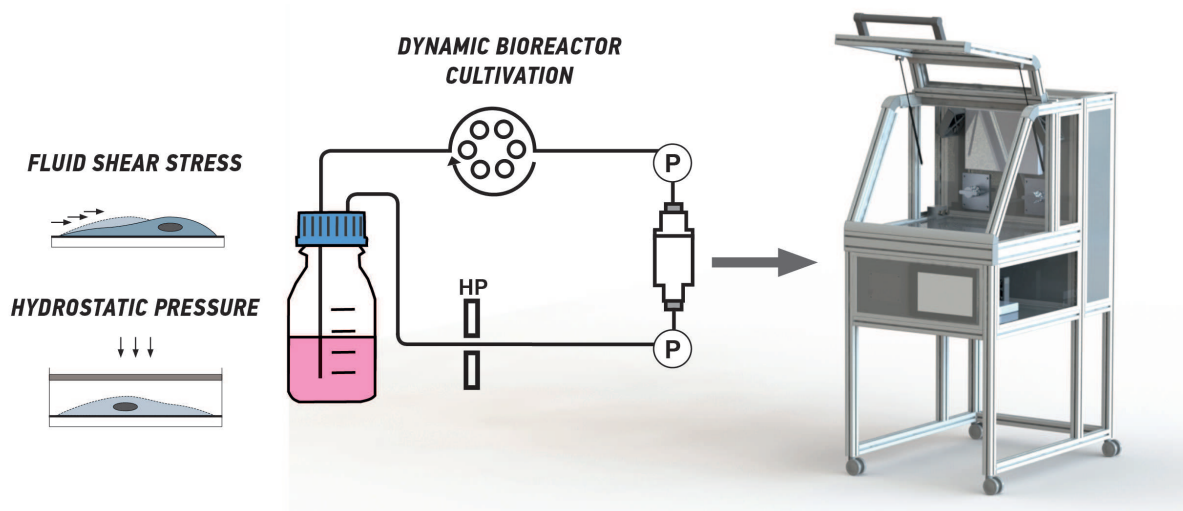


**Figure 5.1:** Graphical abstract describing the experimental work of chapter 5: a 3D biomaterial is characterized and the permeability determined with the use of non-invasive pressure sensors of a specialized incubator system. The permeability was then used to characterize shear stress conditions and fluid flow in two different mini perfusion bioreactor chambers with the help of CFD studies. Subsequently, optimization of the mechanical environment with regards to shear stress and hydrostatic pressure was carried out in the incubator system.

lack the possibility to cultivate multiple independent samples at once under different conditions. Therefore, optimization of cell culture conditions is time consuming, costly and the results may not be reproducible. Also, sensors that allow for comprehensive control of fluid shear forces or HP in perfusion bioreactors are desirable.

Therefore, this chapter describes how a mechanical environment can be set up that is likely to represent *in vivo* shear stress and pressure conditions. In an initial experiment with a biaxial rotating bioreactor the effect of fluid shear stress on osteogenic differentiation of ASCs was evaluated. Afterwards, a tailor-made incubator/bioreactor system was utilized to build a controllable environment with regards to fluid shear stress and hydrostatic pressure. Subsequently, extensive characterization and application with regards to osteogenic differentiation of ASCs is described (Figure 5.1).

## 5.2 Biaxial Bioreactor

The biaxial bioreactor by Quinxell was developed to enable for a broad range of tissue engineering processes. The system consists of a spherical glass chamber connected to a medium circuit that features an oxygenator column and is driven by a peristaltic pump. Further, the cultivation chamber is mounted to an arm that features rotation between 1 – 12 RPM while the chamber itself features rotation between 1 – 35 RPM. Thus, the bioreactor enables for independent rotation along two axis while the chamber itself is continually perfused (see Figure 5.2). The biaxial rotation utilizes moment of inertia to passive perfuse the mounted scaffold in the center of the chamber which enables not only for enhanced mass transfer but mechanical stimulation by fluid shear forces. Therefore, the system may enhance proliferation and differentiation of cells in 3D scaffolds. To evaluate the effect of shear stress generated with the biaxial bioreactor on osteogenic differentiation of human ASCs, cells were seeded on a Sponceram and cultivated for 21 days in either CCM or ODM and 21 % or 5 % O<sub>2</sub> (see section B.3). ASCs on Sponceram cultivated under static conditions in 6 well plates served as control.

Viability of cells on the scaffold was assessed via Calcein-AM and PI viability staining. The staining was found to be strongest in cells cultivated in the bioreactor. Under static conditions only few stained cells were observed (see Figure 5.3). DAPI staining of the nuclei revealed a homogeneous distribution of cells on scaffolds cultivated in the bioreactor but also in cells cultivated in CCM under static conditions and 5 % O<sub>2</sub> (see Figure 5.4). Since perfusion enhances mass transfer it is likely that cells under perfusion conditions display increased metabolic activity and thus viability. Regarding osteogenic differentiation of ASCs, the matrix mineralization in the form of extracellular calcein was most of all observed in samples cultivated in the bioreactor (see Figure 5.5). In contrast, only very few stained spots were observed in static cultivated samples. Interestingly, calcium deposition was also observed in bioreactor samples cultivated in CCM (as indicated by white arrows in Figure 5.5).

**Discussion** The results of the 3D cultivation of ASCs in the biaxial bioreactor system indicate an increased proliferation and viability of cells compared to cultivation under static conditions.

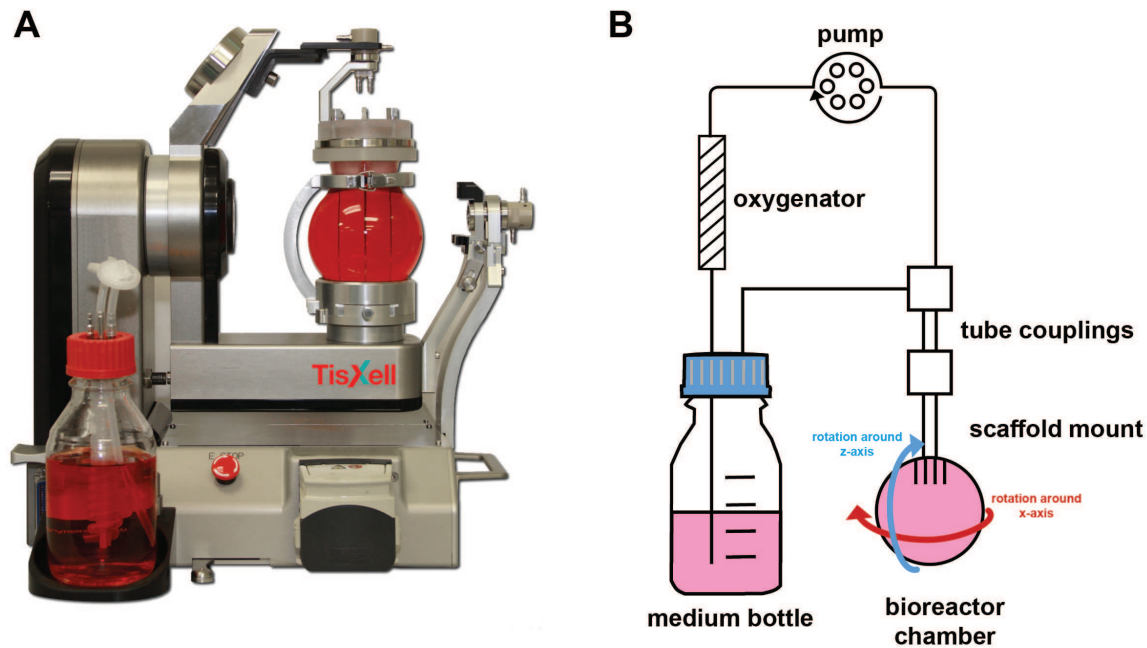


**Figure 5.2:** A) Picture and B) scheme of the biaxial bioreactor by Quinxell. The bioreactor features independent rotation around the x- and z-axis of a continuously perfused cultivation chamber.

Also, matrix mineralization was found to be elevated in dynamic conditions. Biaxial rotating systems were shown to increase the fluid flow velocity inside 3D scaffolds as well as shear stress on the scaffold surface compared to uniaxial rotation [206]. Furthermore, a previous study reported increased cell number, viability and matrix mineralization compared to perfusion bioreactors, spinner flasks and RWVs when cultivated at a rotational speed of 5 RPM on both axis [192, 269]. Also elevated expression of osteocalcin (OCN) and osteopontin (OPN) were reported [270] (rotational speed not specified). The trend of these studies was confirmed by the present results. However, in the present study rotation was set to 10 RPM for the X-axis and 20 RPM for the Z-axis of the bioreactor which might have resulted in higher shear forces compared to the study by Zhang et al. Nevertheless, the exact prediction of shear forces at a given rotation speed remains unknown. CFD analysis of the process could calculate the fluid velocity inside the scaffold and exerted shear forces [206]. However, these must be carried out for each specific process with regards to scaffold characteristics and rotation speed.

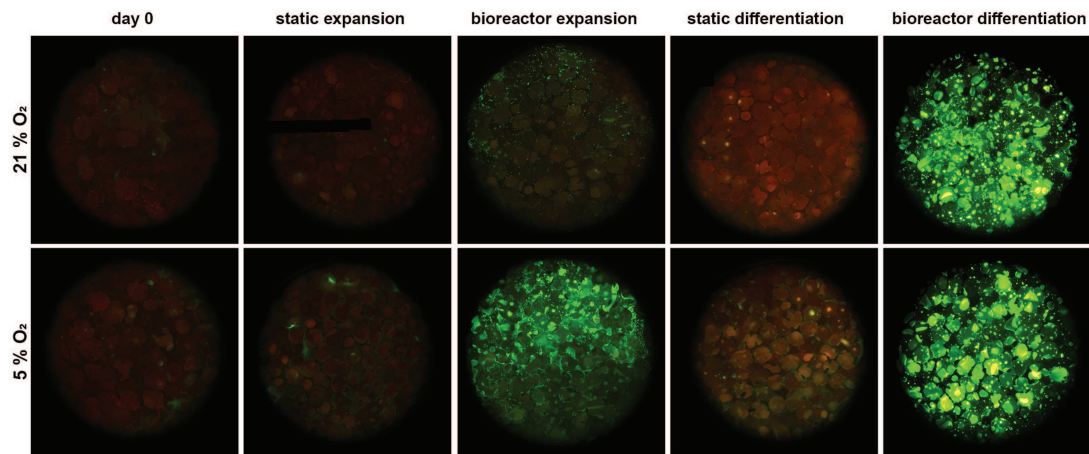


**Figure 5.3:** Calcein-AM and PI viability staining of MSCs cultivated for 21 days in either expansion (CCM) or osteogenic medium (ODM) under 21 or 5 %  $O_2$ . Each image represents the entire scaffold ( $d = 10$  mm).

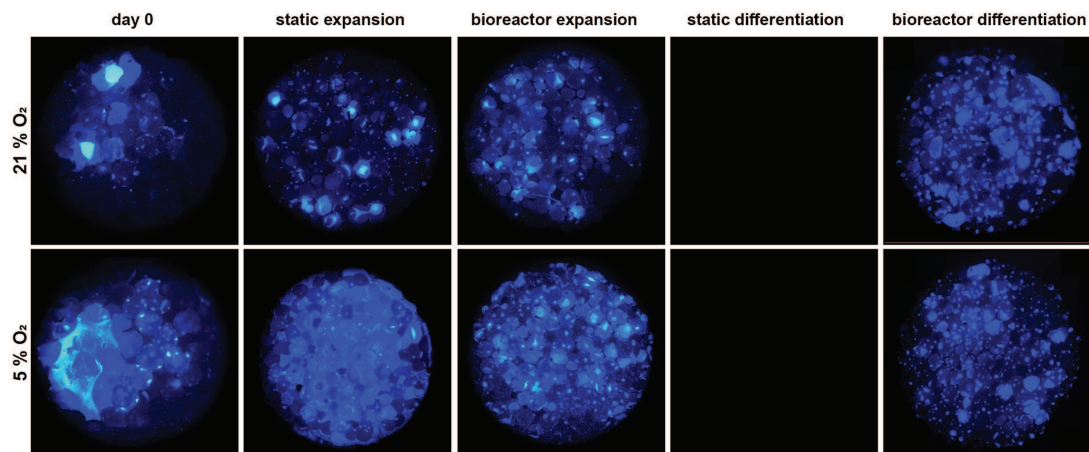


**Figure 5.4:** DAPI staining of MSCs cultivated for 21 days in either expansion (CCM) or osteogenic medium (ODM) under 21 or 5 %  $O_2$ . Each image represents the entire scaffold ( $d = 10$  mm).

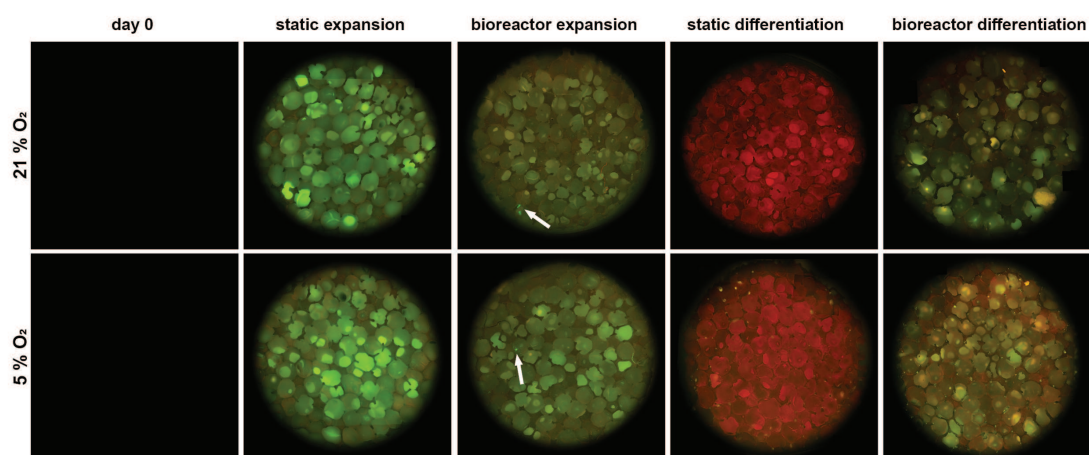


**Figure 5.5:** Calcein staining for extracellular calcium deposition of MSCs cultivated for 21 days in either expansion (CCM) or osteogenic medium (ODM) under 21 or 5 %  $O_2$ . Each image represents the entire scaffold ( $d = 10$  mm).



### 5.3 Mini Perfusion Bioreactor

In order to develop a versatile bioreactor system for reproducible small scale cultivation and differentiation of stem cells on 3D matrices a mini perfusion bioreactor was engineered. It was conceptually designed to host scaffolds of different shapes and sizes. The first model of the mini perfusion bioreactor (BR1) was described before [271]. Basically, it consists of a piston, a housing with an inner diameter of 10 mm and two Luer lock screws, all made of stainless steel. The inner flow channel of the piston is 3 mm and scaffolds with a thickness up to 12 mm (inner height of housing) can be inserted (s. Figure 5.6). O-rings made of ethylene propylene diene monomer (EPDM) 70 seal the chamber and connectors. Based on this, a second bioreactor chamber (BR2) was designed with the help of computer aided design (CAD) in order to improve BR1 with regards to handling, flexibility as well as flow and shear stress conditions. Therefore, Luer lock connectors were directly implemented into housing and piston to avoid unnecessary screws and thus possible leakage sites. A screw cap was introduced to adjust the housing to the scaffold thickness more precisely and sieve like medium distribution units (MDU) were implemented in order to generate a more homogeneous flow. To force the liquid to flow through the MDUs they are 10 mm in diameter and sealed with an EPDM 70 ring. Furthermore, 46 pores with a diameter of 650  $\mu\text{m}$  are arranged in a rectangular grid. Compared to BR1 the flow channel itself opens up upstream of the first MDU to the full diameter of the chamber (and thus the scaffold) and narrows again downstream of the second MDU (s. detailed view of Figure 5.6). In contrast to BR1, BR2 and the MDUs were manufactured from polyoxymethylene (POM). Materials for both bioreactors were chosen to be compatible with steam sterilization. For detailed information on the bioreactor components see Table A.7.

In this chapter the characterization of both bioreactor chambers with regards to flow profile, shear stress conditions and mixing behavior is covered. Furthermore, the bioreactor chambers were compared towards their improvement of osteogenic differentiation of MSCs on the 3D scaffold Sponceram and a proof of concept study with the decellularized bone matrix Tutoplast was conducted. Finally, multiple cultivation conditions with regards to flow rate (fluid shear stress) and HP were screened. Extracts of the presented work have been published in [272] and [254].

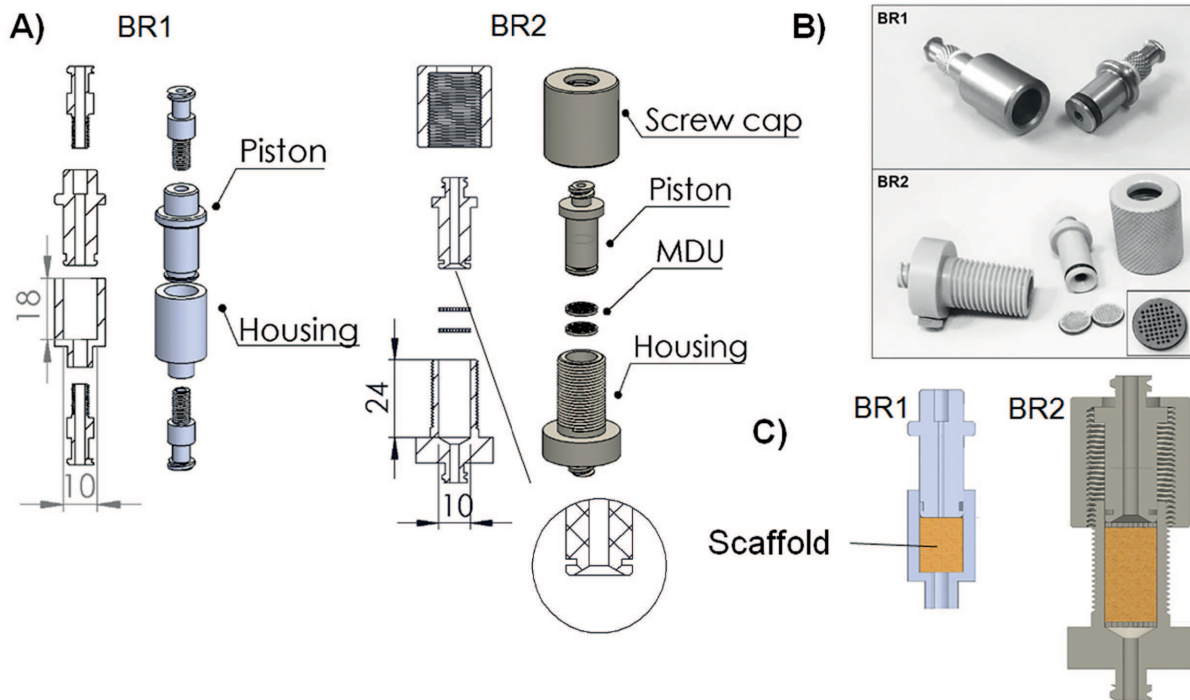


**Figure 5.6:** A) Explosion view, B) cross section with inserted biomaterial and C) pictures of the bioreactor chamber prototypes. The first prototype (BR1) was made of stainless steel whereas the second prototype (BR2) made of POM features two sieve-like medium distribution units (MDU). The flow channel of BR2 opens up to the full diameter of the chamber (detailed view) and the chamber is adjustable in height to allow scaffolds of different thickness to be inserted. The placement of the scaffold in both bioreactors is represented with a yellow box in panel B.

### 5.3.1 Incubator System

The mini perfusion bioreactor system was constructed to be operated in a specialized incubator system (s. Figure 5.7 A). Two peristaltic four-channel pumps are implemented in the back plate of the incubator. Also, the incubator is equipped with two pressure sensors that are usually used for *ex vivo* measurement of blood pressure and two pinch valves that enable for the application of HP. Both, flow rate and pinch valves are programmable via the integrated Siemens control which also allows for data acquisition of temperature, O<sub>2</sub>, CO<sub>2</sub> and pressure during cultivation.

In general, the mini perfusion system can be either placed as single reactor or multi reactor setup in the incubator (s. Figure 5.7 B, C). In both setups the bioreactor chamber is connected to a medium reservoir via fluorelastomer tubing with an inner diameter of 1.6 mm and Luer lock connectors in a circular manner. The single reactor setup enables for the application of HP and measurement of the pressure up- and downstream of the bioreactor chamber. In order to apply HP the tubing downstream of the chamber was mounted to the pinch valve. When the pinch valve closes it blocks the medium flow and due to the operating pump the pressure increases up to a defined threshold which causes the pinch valve to open again. To attenuate the increase of pressure a second, half filled flask was inserted in the medium circuit upstream of the chamber. Consequently, after the pinch valve closes and the pump keeps operating the medium level inside the flask increases and causing compression of air which in return causes an increase of HP. This setup was used to screen hydrostatic pressure conditions (see *Optimization of Hydrostatic*

*Pressure Conditions* in subsection 5.3.3). In the multi reactor setup up to four bioreactors per pump (eight per incubator) are installed without additional pressure sensors which allows for the parallel cultivation of multiple samples under the same flow conditions. This setup was used to screen different flow rates (see *Optimization of Shear Stress Conditions* in subsection 5.3.3).

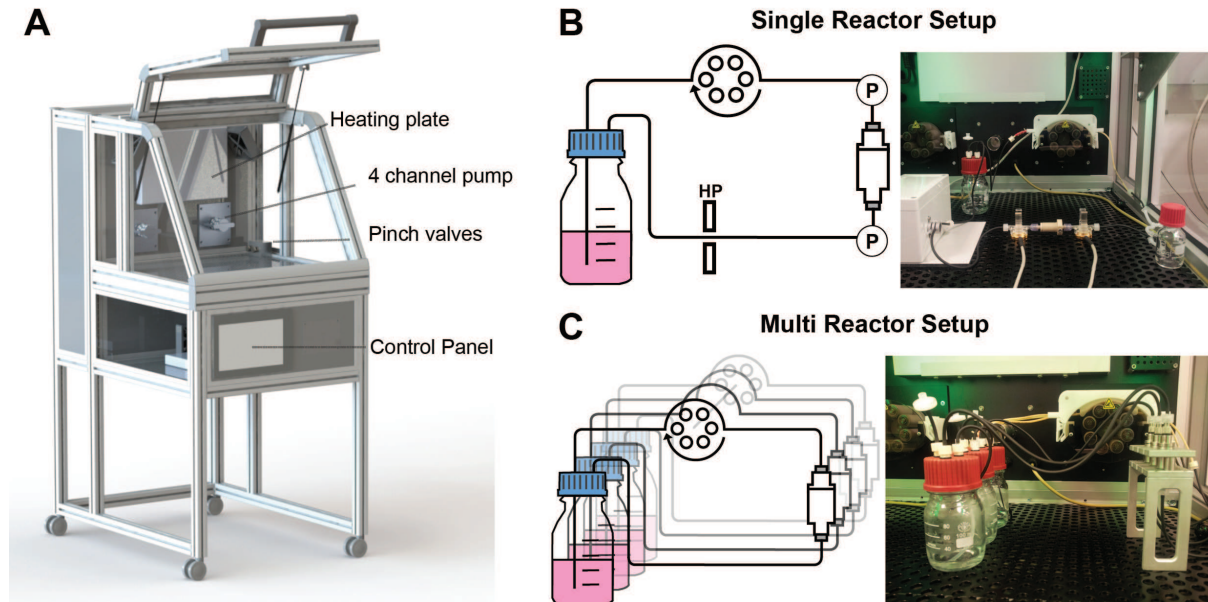


**Figure 5.7:** (A) Specialized incubator system with peristaltic four-channel pumps, pinch valves for the application of hydrostatic pressure (HP) and a touch screen control panel. The mini perfusion system was operated either in a single reactor setup (B) with an additional flask for attenuation of hydrostatic pressure increase and two pressure sensors (P) or in multi reactor setup (C) to enable cultivation of multiple samples under the same flow conditions.

### 5.3.2 Characterization

In order to evaluate the fluid flow and shear stress profile of both bioreactor chambers the incubator and bioreactor system was characterized. First, the pressure sensors were characterized and the permeability  $k$  of the 3D ceramic scaffold was determined. Afterwards, the permeability was applied to mathematical models and CFD simulations to estimate the shear stress cells would experience on the scaffold surface. Also, RTDs of both bioreactor chambers were determined to characterize the mixing and the fluid flow profile was simulated with the help of CFD.

**Pressure sensors and permeability** In order to determine the permeability of Sponceram the pressure sensors were characterized for flow rates ranging from 1.5 to 15 ml/min as described in section B.5. A circular bioreactor setup filled with ddH<sub>2</sub>O at 37°C was used during sensor characterization (see Figure 5.8). For each flow rate 4423 ± 4 data points were recorded with the data storage system of the incubator. Subsequently, the permeability was determined with the help of Darcy's law as described in section B.5. Measurement of the pressure differential  $\Delta P$  ( $P_1 - P_2$ ) was carried out for three randomly picked Sponceram discs (each n=3) which resulted in 4484 ± 71 recorded data points per flow rate and Sponceram disc.

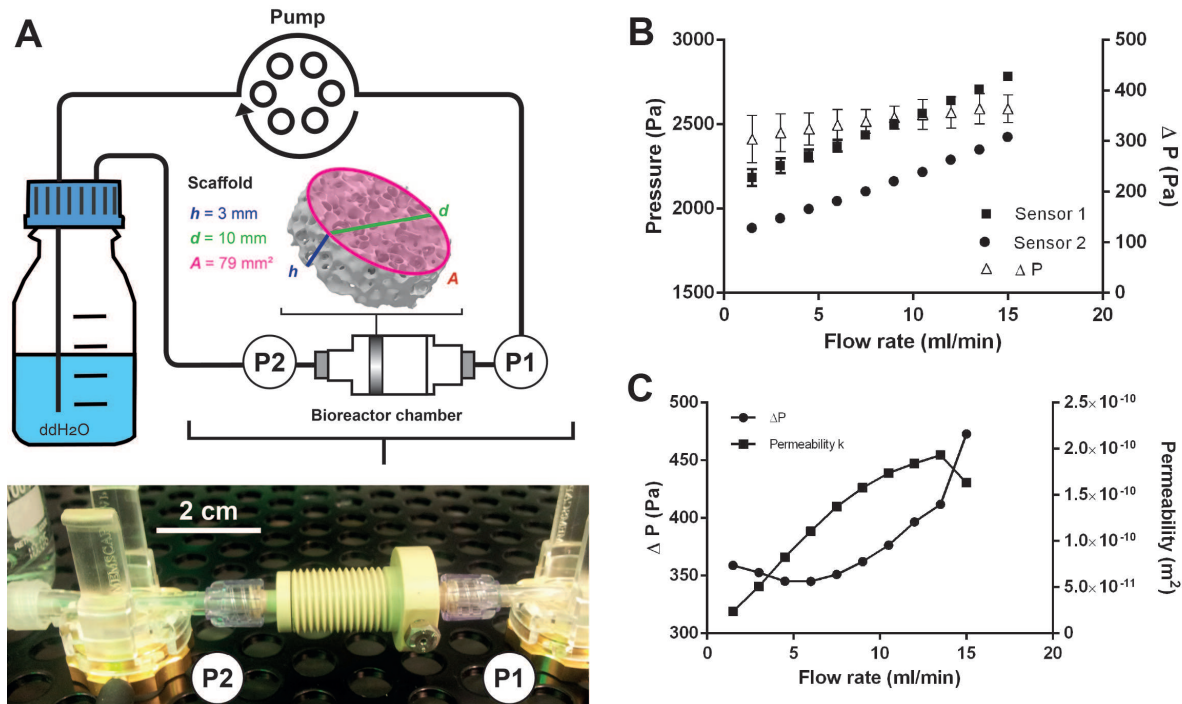


**Figure 5.8:** A) Scheme and picture of the bioreactor setup used for characterization of pressure sensors and determination of permeability  $k$ . Water at 37 °C was pumped through the bioreactor chamber without the porous scaffold Sponceram (for pressure sensor characterization) or with Sponceram (for determination of  $k$ ). Pressure sensors measured the pressure differential  $\Delta P$  via two sensors upstream ( $P_1$ ) and downstream ( $P_2$ ) of the bioreactor chamber non-invasively. Sponceram is depicted as volume rendering of a microCT scan and scaffold dimensions are given as  $h$  = height,  $d$  = diameter and  $A$  = area. B) Correlation of pressure and flow rate of both pressure sensors ( $n = 4423 \pm 4$  for each displayed data point). C) Pressure differential  $\Delta P$  with inserted scaffold and the resulting permeability  $k$  at different flow rates ( $4484 \pm 71$  for each displayed data point). All data displayed as mean  $\pm$  SD.

The built-in pressure sensors of the incubator are usually used for medical purposes to monitor blood pressure of patients in intensive care units by piezoresistive transducers. According to the manufacturer's specifications the sensors together with the amplifier have a pressure range of -20 – 300 mmHG (-2.6 – 40 kPa). Indeed, flow rates used in 3D perfusion cell culture are often as low as 0.3 – 3 ml/min [94] resulting in flow induced pressure of approximately < 3 kPa (depending on the tubing diameter). Hence, probably these implemented sensors do not measure as accurately as in their original setting. Still, characterization of the sensors displayed a strong linear correlation of pressure and flow rate ( $R^2 > 0.997$ ,  $p < 0.0001$ ; Figure 5.8). Interestingly the standard deviation of the measurements decreased with increasing flow rate indicating a more accurate measurement at higher flow rates. This is probably caused by the peristaltic pump that produces a more homogeneous flow when operated at higher speed. However, the pressure differential of both sensors was found to be very constant at  $338 \pm 20$  Pa ( $2.5 \pm 0.5$  mmHG). To determine the permeability  $k$  of Sponceram the pressure differential upstream and downstream of the bioreactor was recorded at different flow rates. Since  $k$  is an inherent material constant,  $\Delta P$  should increase proportionately with the flow rate. Although the pressure sensors appear to be sufficiently accurate the calculated permeability changed with the flow rate (Figure 5.8).  $\Delta P$  increased linearly for flow rates > 7.5 ml/min while  $k$  remained almost stable. Therefore,

the average of calculated  $k$ -values from 9 – 15 ml/min ( $k = 1.7 \pm 0.9 \cdot 10^{-10} \text{ m}^2$ ) was inserted in the mathematical models and CFD simulations. Indeed, these results match up with a previous study by Sanz-Herrera et al. where the permeability of more porous ( $\varepsilon = 80\%$ ) Sponceram was found to be  $k = 1.88 \cdot 10^{-8} \text{ m}^2$  [273]. Furthermore, permeability of cancellous bone was found to be approximately  $k = 2.1 \cdot 10^{-9} \text{ m}^2$  in the same study. The lower permeability measured in the present study is probably caused by the lower porosity ( $\varepsilon = 67\%$ ).

**Shear stress distribution** To assess the shear stress profile in both bioreactor chambers a CFD study was conducted as described in section B.5. Furthermore, the shear stress was calculated with a mathematical models based on the characteristics of the scaffold [261] as described in section B.5.

The interstitial Reynolds number  $Re_i$  was calculated first to ensure that Darcy's law is applicable ( $Re_i < 8$ ). It was found to be between 0.28 – 7 for flow rates between 1.5 – 15 ml/min which indicates laminar flow in this range. Depending on the flow rate and bioreactor geometry the average shear stress calculated by the simulation was between  $0.1 - 1 \cdot 10^{-2} \text{ Pa}$ , and maximum shear stress between  $8.8 - 85.2 \cdot 10^{-2} \text{ Pa}$  (see Table 5.1). Although average shear stress is similar in both bioreactor models the maximum shear stress is about 2-fold higher in BR1 indicating higher stress peaks due to the bioreactor geometry. Generally, the results of the simulation indicate higher shear forces at the surfaces of the scaffold where the fluid enters. In BR1 higher shear forces occur at the entrance, core and exit of the scaffold whereas the outer areas display very low shear forces. In contrast BR2 displays a much more homogeneous shear stress distribution throughout the scaffold (see Figure 5.9).

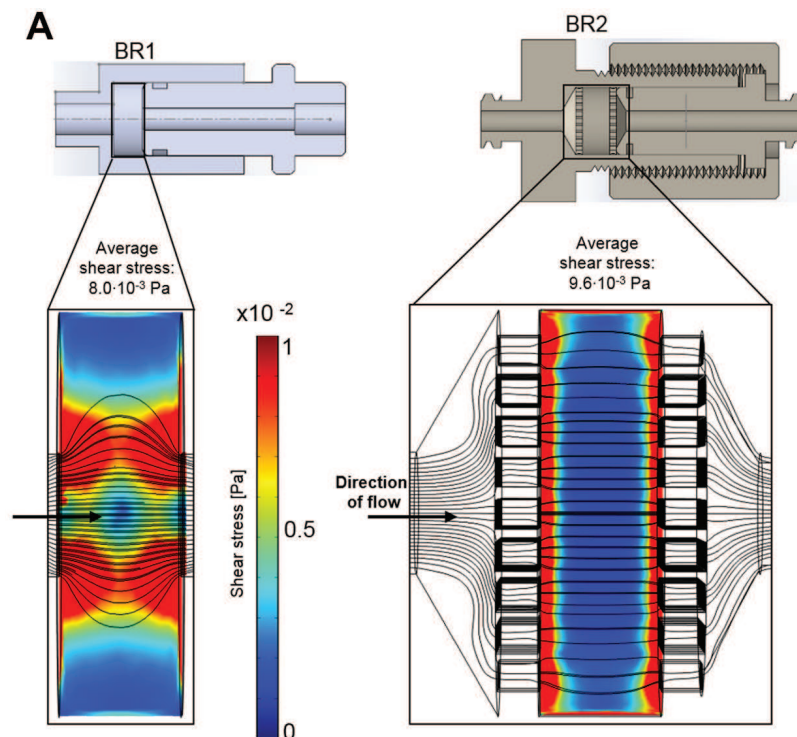


**Figure 5.9:** Graphical representation of results from CFD simulations of both bioreactor chambers. A) Shear stress distribution inside the bioreactor chambers with inserted scaffold (porosity: 66.7%, specific permeability  $k = 1.74 \cdot 10^{-10} \text{ m}^2$ ) at a volumetric flow rate of 1.5 ml/min.

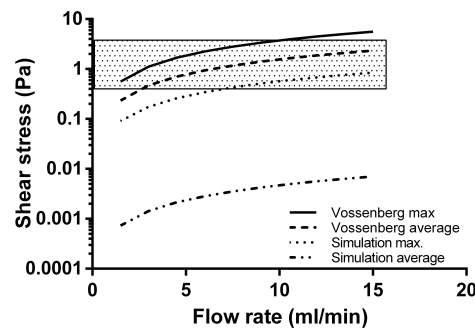


**Figure 5.10:** Shear stress prediction based on the determination of the permeability  $k$  of Sponceram and further calculation with the Vossenbergs model or CFD data. Depending on the flow rate the analytical model predicts shear forces in the physiologic *in vivo* range of 0.3 – 3 Pa (shaded area) whereas the computational modeling predicts shear forces approximately 3 orders of magnitude lower.

Furthermore, an analytical model that uses the permeability  $k$  as an indicator for wall shear stress was used to estimate shear stress and compared to the CFD derived calculation. The Vossenbergs model predicts average shear stress between 0.23 – 2.34 Pa which is approximately 3 orders of magnitude higher than predicted by CFD simulation. Maximum shear forces were calculated to be between 0.56 – 5.6 Pa which is approximately 6-fold higher than estimated by CFD simulation (see Figure 5.10 and Table 5.1). Probably simplification of the scaffold in the computational model lowers the prediction of shear forces. Also, in a study of Jungreuthmayer, et al. [207] where  $\mu$ CT data of a scaffold was used for CFD analysis the computational model underestimated shear forces compared to analytical models. Although estimations from computational and analytical model differ from each other the shear forces calculated from the analytical models were in the range of *in vivo* shear stress of bone, which is expected to be between 0.3 – 3 Pa [274].

**Table 5.1:** Data from CFD simulation and mathematical models describing average and maximum shear stress inside the scaffold. Shear stress is given in  $[\text{Pa} \cdot 10^{-2}]$

Bioreactor	Inlet velocity [mm/s]	CFD simulation		Vossenbergs model	
		$\tau_{\omega avg}$	$\tau_{\omega max}$	$\tau_{\omega avg}$	$\tau_{\omega max}$
BR1	3.5	0.1	8.8	23.4	56.0
	17.7	0.4	43.4	117.2	280.0
	35.4	0.8	85.3	234.4	560.0
BR2	3.5	0.1	4.6		
	17.7	0.5	22.9		
	35.4	1.0	45.4		

$\tau_{\omega avg}$  = average wall shear stress,  $\tau_{\omega max}$  = maximum wall shear stress

**Flow velocity and residence time distribution** A homogeneous flow profile throughout the bioreactor chamber is preferable since nutrition supply and waste removal is crucial in every 3D cultivation. Thus, a computational study was conducted to simulate the distribution of flow

**Table 5.2:** CFD derived data of the average and maximum velocities of fluid passing the scaffold inside bioreactor chambers BR1 and BR2. All velocities are given in [mm/s].

	Inlet velocity	Average velocity	Max. velocity	Ratio max. / average
BR1	3.5	0.4	6.2	16.0
	17.7	1.9	30.0	15.4
	35.4	3.9	56.5	14.5
BR2	3.5	0.3	1.7	5.3
	17.7	1.6	8.6	5.3
	35.4	3.2	17.3	5.4

**Table 5.3:** Differences of mean residence time  $T_m$  to ideal hydrodynamic residence time  $T$  in percent (at least n=3).

Flow rate [ml/min]	difference to $T$ in %		
	0.6	1.5	3.0
BR1 empty	16 ± 0.1	12 ± 0.4	30 ± 0.3
BR2 empty	37 ± 1.1	27 ± 0.8	23 ± 1.7
BR1 loaded	18 ± 0.1	31 ± 1.7	23 ± 1.7
BR2 loaded	127 ± 0.6	16 ± 0.5	15 ± 0.7

velocity and streamlines in the bioreactor with and without a scaffold inserted. The flow profile of the empty BR1 indicates a higher flow velocity exclusively in the center of the chamber (see Figure 5.11 A). In contrast, outer areas display velocities close to zero while circular streamlines indicate dead spaces. After introducing the scaffold into the model higher flow velocities were especially observed in the center region. In contrast, the MDUs of BR2 seem to support a homogeneous flow profile. The average and maximum velocity of the fluid that passed through the scaffold was derived from the CFD data (Table 5.2). In BR1 the maximum flow velocity is 16-fold higher than the average velocity whereas it is only 5-fold higher in BR2. Therefore, the MDUs seem to support a homogeneous flow velocity profile and reduce flow velocity peaks.

The RTD of a bioreactor characterizes the mixing behavior, and consequently is an important parameter in bioprocess engineering. Therefore, the RTDs of both bioreactor chambers at different flow rates were measured without and with the scaffold inserted as described in section B.5. Ratios of the ideal hydrodynamic residence time  $T$  and the real mean residence time  $T_m$  at different flow rates were compared (see Figure 5.11, Table 5.3).

$T$  is a theoretical value that describes the time a fluid volume needs to pass through the bioreactor when no back mixing occurs (like in an ideal plug flow reactor (PFR)). As expected both bioreactors did not behave like an ideal PFR and  $T_m$  was higher than  $T$  (12 – 37%) indicating back mixing. Moreover,  $T_m/T$  does not appear to be affected by flow rate or bioreactor geometry significantly. However, in BR2 the ratio of  $T_m/T$  seems to decrease with higher flow rates and is lower at 3 ml/min than in BR1 showing a more PFR like behavior. The curve fit of the RTDs of the empty bioreactor indicate a correlation between increasing flow rate and stronger mixing, resulting in a more continuous stirred tank reactor (CSTR) like mixing behavior (see Figure 5.11 B). At lower flow rates the fluid behaves more like in a PFR. Besides, inserting a

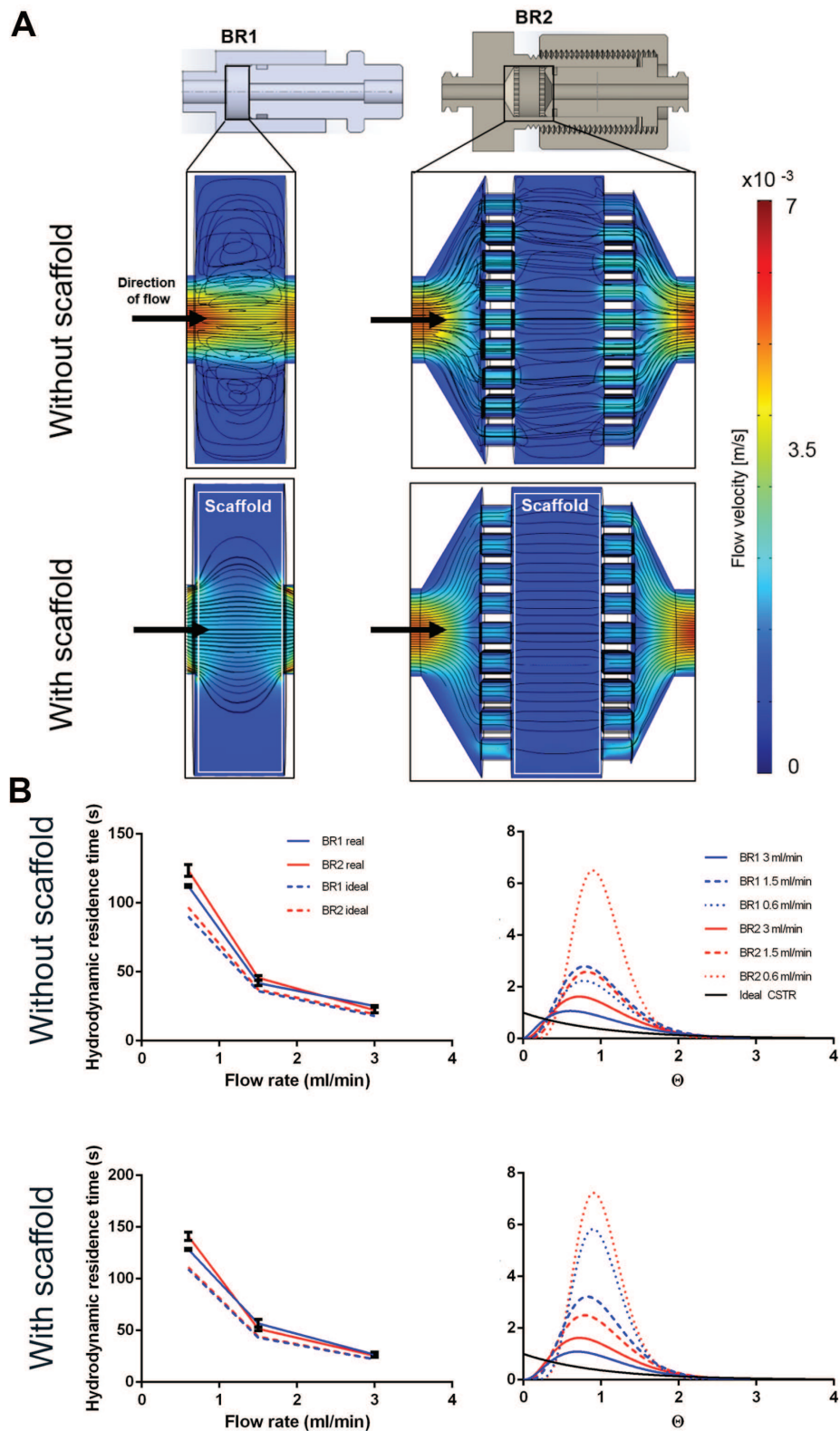


**Figure 5.11:** A) Graphical representation of the flow velocity profile and streamlines derived from computational analysis. B) Hydrodynamic residence time and residence time distributions of both bioreactor chambers with and without a scaffold inserted. Graphs of RTDs display global curve fits of at least  $n=3$  RTD measurements.



**Table 5.4:** Tanks in series and Bodenstein number of both bioreactors with and without scaffold. Tanks in series are derived from a global curve fit ( $n=3$ ). The Bodenstein number was calculated from raw data set.

Flow rate [ml/min]	Tanks in series			Bodenstein number		
	0.6	1.5	3.0	0.6	1.5	3.0
BR1 empty	4.6	4.8	2.5	6.1	6.3	7.0
BR2 empty	9.7	4.8	2.5	7.4	6.7	5.9
BR1 loaded	9.7	5.7	3.3	8.0	7.3	7.7
BR2 loaded	10.7	4.7	3.4	9.1	7.2	7.6

scaffold seems to inhibit back mixing and instead promotes a more uniform flow. The number of tanks in series  $N$  and the Bodenstein number  $Bo$  were both derived from the RTDs and are compared in Table 5.4. Generally, more tanks in series were observed at lower flow rates indicating a more plug flow like behavior. The chamber geometry of BR2 seems to support a more laminar flow with less back mixing whereas the chamber of BR1 seems to improve back mixing. Again, the insertion of a scaffold into the fluid pathway supports a plug flow behavior. For the flow rates of 1.5 – 3.0 ml/min  $N$  is between 2.5 – 5.7. When  $N \rightarrow 1$  the system is considered to be mixed completely. Thus, a flow rate of 1.5 ml/min and higher can be considered as optimal mixing. The Bodenstein number was derived from the raw data (not from the global curve fit) and should behave similar to the number of tanks-in-series (TIS) model. It was found to be highest at the lowest flow rate indicating low axial dispersion (except for BR1 empty). Though,  $Bo$  does not decrease with the flow rate considerably like the number of tanks in series. Data from the computational model together with the RTDs indicate almost optimal mixing in BR1 with a heterogeneous flow profile. In contrast, BR2 demonstrated less mixing but a homogeneous flow velocity profile.

**Comparison of bioreactor chambers** To evaluate the influence of the different flow profiles and shear stress distributions of BR1 and BR2 on osteogenic differentiation human ASCs ( $n=3$  donors) were cultivated for 21 days on Sponceram. Cells seeded on a 12 well plate ( $4000 \text{ c/cm}^2$ ) served as 2D static control. The seeded matrices were transferred to the bioreactor chamber (3D dynamic) after 3 days or kept in the well of a 6 well plate (3D static) and cultivated on CCM or ODM respectively. The cell number of each sample was determined via DNA quantification and was highest in the 3D and 2D control group. However, twice as much cells were found in BR2 compared to BR1 where the cell number did not change significantly to day 0 (see Figure 5.12). These findings were also confirmed by DAPI staining (Figure 5.13).

Glucose consumption and lactate production were steady throughout the entire cultivation period although lactate production decreased slightly after 12 days in dynamic conditions (see Figure 5.14). The overall glucose consumption and lactate production was found to be highest in 3D static (see Table 5.5). However, consumption and production per cell between day 19 and 21 indicates a higher glycolytic activity in cells cultivated in dynamic conditions. ALP activity, a marker for osteogenic differentiation, increased approximately after 12 – 14 days in 2D and 3D static conditions. In contrast, under dynamic conditions it was elevated from day 3 on but did

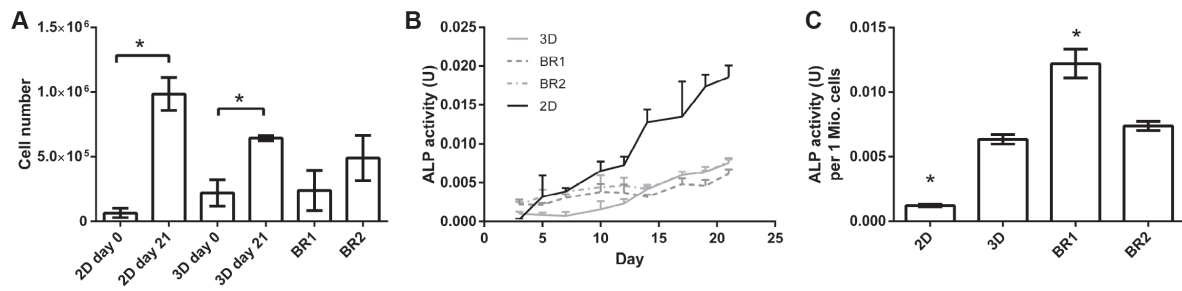


**Figure 5.12:** (A) Cell numbers, (B) course of ALP activity and (C) ALP activity per cell of ASCs cultivated on Sponceram in a perfusion bioreactor or under 3D and 2D static conditions. Data represented as mean  $\pm$  SD ( $n = 3$ ); \* indicates significant difference of the indicated conditions (A) or to 3D static (C) with a confidence interval of 99% and  $p < 0.001$ .

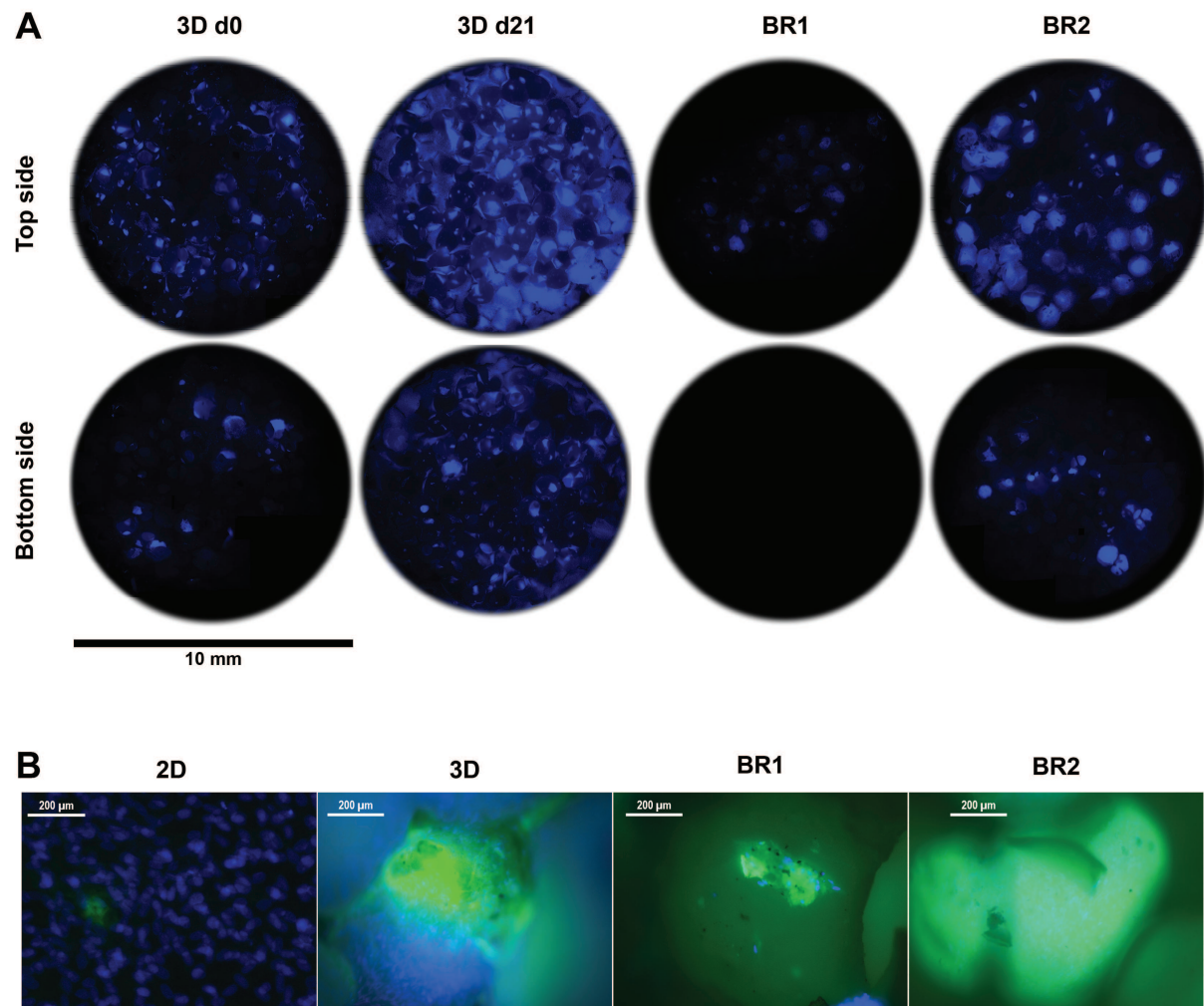


**Figure 5.13:** (A) DAPI stain and (B) DAPI-calcein double stain of Sponceram after 21 days cultivation with ASCs in two different perfusion bioreactor chambers (BR1 and BR2) or under static conditions (2D and 3D).

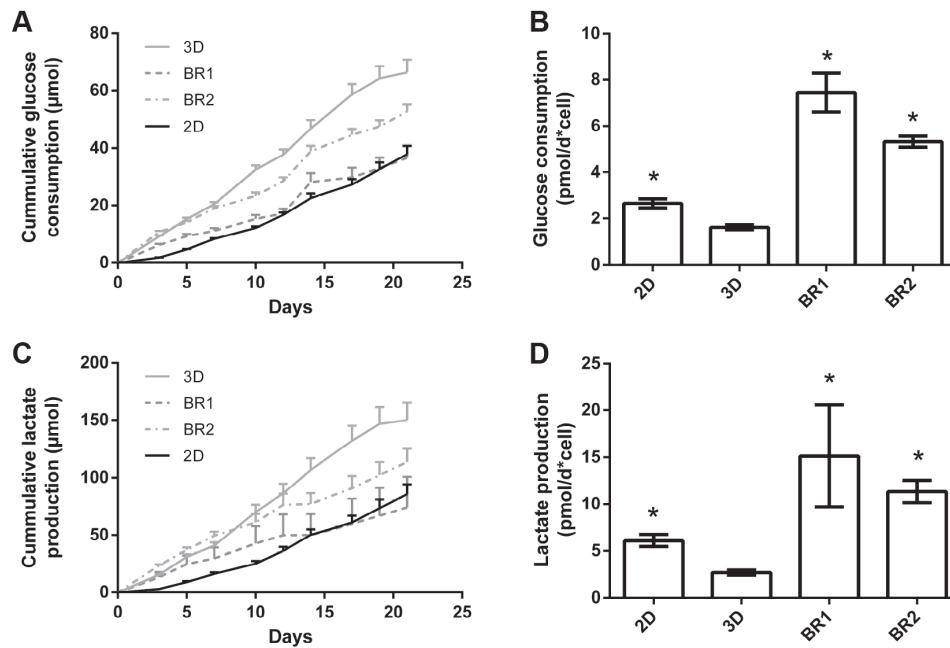


**Figure 5.14:** Course of (A) glucose consumption and (C) lactate production and (B) glucose consumption, (D) lactate production per cell between day 19 and 21 of ASCs cultivated on Sponceram in a perfusion bioreactor or under 3D and 2D static conditions. Data represented as mean  $\pm$  SD ( $n = 3$ ); \* indicates significant difference to 3D static with a confidence interval of 99 % and  $p < 0.001$ .

**Table 5.5:** Glucose consumption and lactate production of ASCs under different cultivation conditions ( $n=3$ ).

Condition	Cumulative glucose consumption ( $\mu\text{mol}$ )	Cumulative lactate production ( $\mu\text{mol}$ )	Ratio
2D	$37.9 \pm 2.9$	$85.5 \pm 8.7$	2.26
3D	$66.3 \pm 4.5$	$150.1 \pm 15.0$	2.26
BR1	$36.6 \pm 4.1$	$74.2 \pm 26.7$	2.15
BR2	$52.77 \pm 2.4$	$113.6 \pm 11.7$	2.02

not increase as much as under static conditions after 14 days. However, ALP activity per cell revealed an increased activity in all 3D conditions compared to 2D while the activity per cell in BR1 was found to be higher compared to BR2 (see Figure 5.12).

Matrix mineralization was determined by calcein and von Kossa stain. Calcium depositions were found in all conditions (Figure 5.13, Figure 5.15). However, only few stained areas were observed. Furthermore, phosphate depositions were found to be increased in BR1 but only slightly in BR2 and 3D static.

**Discussion** In order to build a physiologic environment for the osteogenic differentiation of ASCs a miniaturized perfusion bioreactor system together with a specialized incubator system was developed. Since the incubator system with the built-in pressure sensors can serve as a flexible platform for different cell culture applications and bioprocesses, the mini perfusion bioreactor

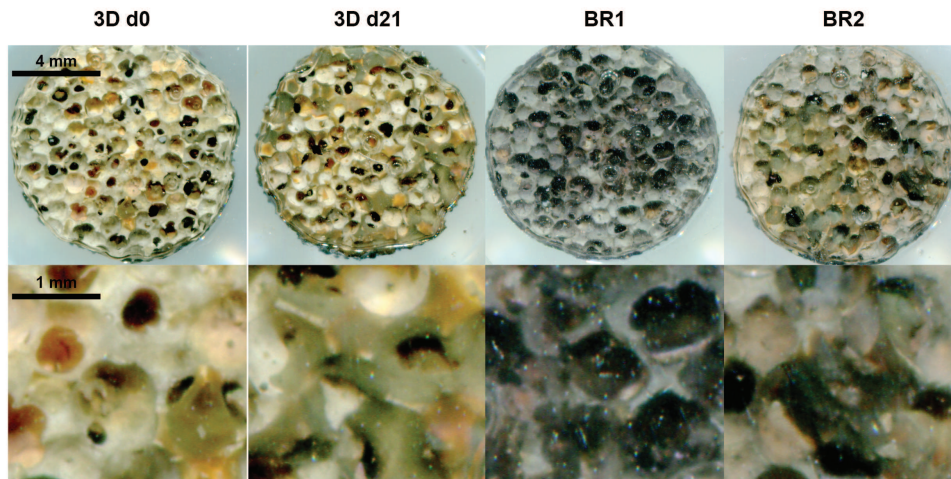


**Figure 5.15:** Von Kossa stain for extracellular phosphates on Sponceram after 21 days cultivation with ASCs in two different perfusion bioreactor chambers (BR1 and BR2) or under static conditions (3D).

system was consequently operated in it. Based on a first model of the mini perfusion bioreactor, a second model with additional features was designed and manufactured. Subsequently, both chambers were extensively characterized with regards to shear stress, flow velocity profile, streamlines and mixing behavior (assessed by RTDs). After characterization the effect of flow profiles and shear stress of both bioreactor chambers on osteogenic differentiation of ASCs was investigated. The general advantages of both chambers are depicted in Table 5.6.

With regards to mixing behavior BR2 displayed a more PFR like mixing behavior compared to BR1, flow rates of 1.5 ml/min and higher were considered to provide sufficient mixing. Although the RTDs from both bioreactors did not differ considerably the flow field experienced by cells might be different [275]. Recirculation areas found in the CFD simulation of BR1 indicate a different flow field than in BR2 where MDUs prevent those recirculation areas. The TIS model also revealed less axial dispersion in BR2. Indeed, MDUs in BR2 seem to promote a uniform flow velocity profile and plug flow like behavior throughout the scaffold while preserving proper mixing.

Furthermore, to estimate fluid shear stress inside a porous scaffold implemented pressure sensors were characterized. Although the mathematical model and the CFD simulation lack accuracy it is likely that physiologic fluid shear stress (e.g. for bone tissue engineering) occurs during cultivation at the evaluated flow rates. MDUs of BR2 proved to be beneficial in promoting a uniform flow velocity and shear stress distribution throughout the scaffold. A homogeneous flow and shear stress profile is highly preferable since it ensures maximum control and reproducible results during experiments.

To investigate effects of the different flow and shear stress profiles both bioreactor chambers were compared with regards to osteogenic differentiation of ASCs. For this, the flow rate was chosen according to the calculations of the simulation and mathematical model as follows. The average shear stress at a flow rate of 1.5 ml/min was between 0.001 (CFD) and 0.23 Pa (Vossen-berg) and the maximum shear stress was between 0.08 and 0.56 Pa which only partially lies in

the physiologic *in vivo* shear stress of 0.3 – 3 Pa. However, osteogenic differentiation performed in 3D conditions was found to be increased with shear stress about one order of magnitude lower than the *in vivo* shear stress [188]. Seemingly, lower shear forces are sufficient to induce osteogenic differentiation. Also, maximum shear stress was shown to increase dramatically compared to the average shear stress with increasing flow rate if the permeability constant  $k$  is below  $1 \cdot 10^{-10} \text{ m}^2$  [261]. In the present work, the permeability constant  $k$  of the scaffold was found to be  $1.7 \pm 0.9 \cdot 10^{-10} \text{ m}^2$ . Furthermore, the Vossenbergh model was developed for scaffolds with perpendicular fibers and thus the permeability might not be as predictive for shear stress as in a porous scaffold. Also, the CFD simulation lacks accuracy since it is based on a simplified geometry of the scaffold. Taken all together, the flow rate of the proof of concept study was set to 1.5 ml/min to generate shear forces at the lower end of the physiologic range in order to avoid excessive washout of cells.

After 21 days of cultivation the cell number was found to be increased in BR2 compared to BR1 while the cell distribution was more homogeneous as indicated by DAPI staining. However, cell number and glucose consumption indicate lower proliferation in dynamic conditions compared to static. Thus, cells in dynamic conditions might have been subject to washout by perfusion. The ratio of lactate production per mole consumed glucose is commonly used as an index for anaerobic metabolism which occurs mainly in proliferating mesenchymal stem cells. These cells display a higher ratio since they generate energy rather by anaerobic glycolysis than by oxidative phosphorylation [276]. Indeed, cells cultivated under dynamic conditions displayed a lower ratio (2.02 – 2.15) than under static conditions (2.26) which might indicate a shift to oxidative phosphorylation and therefore to differentiation. Also, ALP activity per cell was found to be higher in dynamic conditions and phosphate deposition was only visible in BR1. These findings suggest increased differentiation in dynamic conditions. However, the glucose consumption and lactated production per cell was found to be significantly higher in dynamic conditions compared to static. Controversially, a previous study by Pattappa et al. [277] reported reduced glycolytic activity during osteogenic differentiation. However, this study was carried out in conventional 2D static conditions. In contrast, 3D dynamic conditions increases mass transfer of nutrients, oxygen and waste products which together with mechanical stimulation may alter metabolic activity in comparison to 2D static cultivation conditions.

Regarding the influence of the flow and shear stress profile of BR1 and BR2 on the osteogenic differentiation, cells of BR1 showed increased ALP activity per cell and matrix mineralization compared to BR2. Interestingly, phosphate depositions were present only in the center of BR1 where flow velocity and shear stress is highest as indicated by CFD simulations. Furthermore, the maximum flow velocity at 1.5 ml was found to be 3.6-fold higher in BR1. Although it did not affect the average shear stress it caused a 1.9-fold increase in maximum shear stress. Also, maximum shear stress in BR1 was 88-fold higher than the average shear stress while it was only 46-fold higher in BR2. The findings of the CFD simulation together with the data from bioreactor cultivation suggest that in order to generate shear stress as high as in BR1, the volumetric flow rate needs to be increased in BR2.

In this comparative study, where both bioreactor chambers were operated at the same flow

**Table 5.6:** Conclusive overview on characteristics of BR1 and BR2.

Aspect	BR1	BR2
Advantages	<ul style="list-style-type: none"> <li>– sufficient mixing</li> <li>– increased matrix mineralization</li> <li>– increased ALP activity per cell</li> </ul>	<ul style="list-style-type: none"> <li>– sufficient mixing</li> <li>– homogeneous flow profile and shear stress distribution throughout the scaffold</li> <li>– increased proliferation</li> <li>– more homogeneous growth on the scaffold</li> </ul>
Disadvantages	<ul style="list-style-type: none"> <li>– inhomogeneous flow profile and shear stress distribution</li> </ul>	<ul style="list-style-type: none"> <li>– comparatively low matrix mineralization</li> </ul>

rate, BR1 supported an increased osteogenic differentiation of ASCs while BR2 rather maintained homogeneous cell growth than differentiation. Since it is likely that differentiation was induced by higher shear stress in the center of BR1, a higher flow rate resulting in similar shear stress conditions might foster comparable differentiation in BR2 as well. In conclusion, depending on the mathematical model, shear stress calculations derived from characterization of the matrix and CFD simulation suggested physiologic shear stress conditions for a broad flow rate spectrum of 1.5 – 15 ml/min. Perfusion systems have been proven to be beneficial for tissue engineering purposes such as bone or cartilage engineering [278, 279]. For instance, numerous studies show a higher matrix deposition or upregulation of relevant genes in comparison to static culture conditions when bone precursor cells are exposed to fluid shear stress [135, 280–284]. Although several tailor-made [188, 189, 285] and commercially available [286–288] perfusion systems were developed and successfully used, there is a lack of automated sensor-controlled systems that allow cultivation of multiple independent replicates under different conditions. In contrast, the presented incubator/bioreactor system enables for determination of permeability and thus estimation of shear stress at different flow rates.

### 5.3.3 Application

After extensive characterization of the incubator and bioreactor system a proof of concept study was carried out. For this, the decellularized cancellous bone matrix Tutoplast was characterized and tested towards its suitability for the osteogenic differentiation of ASCs. The material characteristics were assessed via microCT following routine procedures for the structural characterization of trabecular bone [289].

Subsequently biomaterial testing was carried out in the mini perfusion bioreactor BR1. Pieces of different size (4 – 10 mm) and weight (42 – 93 mg) were seeded with ASCs as described in section B.2 and cultivated for 21 days in the bioreactor at 0.6 ml perfusion with CCM or ODM respectively. Modified 15 ml polystyrene tubes with an inserted mesh and the same amount of medium (10 ml) used in the bioreactor system served as static control. For each condition  $n = 2$  bioreactor chambers each with  $n = 3$  independently seeded Tutoplast samples were operated.

To monitor osteogenic differentiation ALP activity was assessed from medium samples and viability of cells was determined. Samples from static conditions were processed for microCT and histological staining.

Furthermore, in order to optimize fluid shear stress conditions seeded Tutoplast scaffolds were cultivated for 6 days at four different flow rates (1.5, 3, 4.5 and 6 ml,  $n = 3$ ) in ODM. To calculate the corresponding shear stress equations B.6 and B.7 were used as described in section B.5.

Also, the effect of different HP regimes on viability and osteogenic differentiation was evaluated. For this, seeded Tutoplast scaffolds were cultivated at a flow rate of 1.5 ml in ODM while three different pressure regimes were applied (100, 250 and 500 mmHg). The cultivation was carried out in the "single-reactor setup" as depicted in Figure 5.7. Valves were programmed to different open/close regimes to build up different amounts of pressure respectively (for detailed valve programming see Table B.2). A defined pressure pattern of 3 h pressure / 3 h pause was applied throughout the entire cultivation period of 6 days.

**Characterization and initial testing of Tutoplast** The biomaterial Tutoplast was used for the osteogenic differentiation of human ASCs. First, the biomaterial was characterized towards important material parameters (s. Table 5.7) which were later used to estimate fluid shear stress. Pore size and porosity were found to result in a range of shear stress commonly used for 3D bioreactor cultivation (see next section **Bioreactor cultivation with Tutoplast**).

**Table 5.7:** Characteristic parameters of Tutoplast matrix. HA = hydroxyapatite

Parameter	Value
Porosity	66.9 %
Pore size	384 $\mu\text{m}$ ( $\pm 113 \mu\text{m}$ )
Mineral density	0.969 mgHA/ $\text{mm}^3$
Trabecular number	2.5755 /mm
Trabecular thickness	167.6 $\mu\text{m}$ ( $\pm 50.2 \mu\text{m}$ )

Furthermore, to initially test Tutoplast for its suitability for 3D cell culture, ASCs were cultivated for 21 days under static conditions. The material surface exhibits a complex, structured texture down to nano-scale level. Histological sections stained with hematoxylin and eosin (HE) revealed a loose network of proteins throughout the whole scaffold as well as remnants of bone marrow components (e.g. basal membrane of fat cells). After 21 days of static cultivation cells covered the entire scaffold with a closed compact cell layer which was found to be between (50 – 200  $\mu\text{m}$ ) and composed of several layers of cells (see Figure 5.16 and 5.17). In contrast, inside the scaffold loose connective tissue was found where the protein network seems to promote cell ingrowth. Therefore, Tutoplast was considered to be a suitable matrix for 3D cell culture of ASCs.

**Bioreactor cultivation with Tutoplast** Subsequently to initial biomaterial testing Tutoplast was evaluated towards its suitability for osteogenic differentiation under static and dynamic conditions. For this, shear stress as calculated from the material characteristics with a simplified model suggested by Goldstein et al. [132] (see Table 5.8). After 21 days of dynamic or static

cultivation rapid growth of cells and high viability was indicated Calcein-AM and PI staining. Overview images of the Calcein-AM and PI stain also displayed homogeneous cellular ingrowth into inner areas of the scaffolds (see Figure 5.18). The course of ALP activity revealed highest activity under dynamic conditions with cells cultivated in ODM followed by the dynamic control group. Likewise, ALP activity per cell was highest for cells cultivated under dynamic conditions in ODM. Micrographs obtained with SEM show mineral depositions of cells cultivated under dynamic conditions whereas those depositions are absent on static cultivated cells (see Figure 5.18). Notably, results of the biomaterial testing underline the importance of setting up physiologic conditions, especially of mechanical cues, since dynamically cultivated cells in CCM exhibited higher ALP activity and mineralization than static cells in ODM.

**Table 5.8:** Fluid shear stress conditions applied in flow rate optimization (\*calculation according to Goldstein et al. [132]).

Flow rate (ml/min)	Flow velocity (mm/s)	Shear stress (mPa) *
1.5	0.48	6.8
3	0.96	13.7
4.5	1.45	20.5
6	1.93	27.4



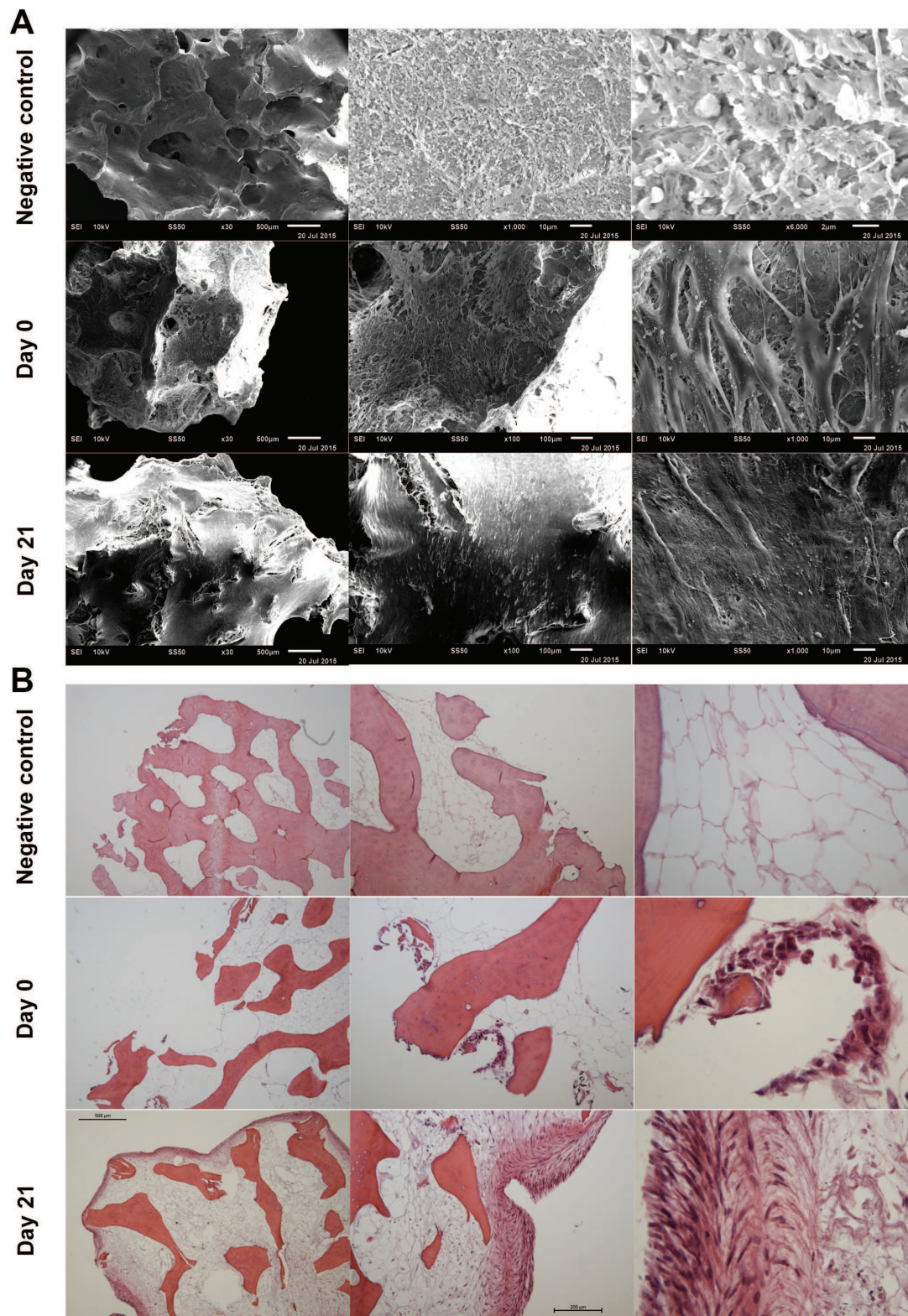


**Figure 5.16:** Characterization of Tutoplast: (A) scanning electron microscope (SEM) images (voltage: 10 kV; spot size: 50; magnification 100, 1000, 6000x respectively) and (B) Hematoxylin and eosin staining of the decellularized human bone matrix Tutoplast. Negative control without cells, after seeding with ASCs at day 0 and after 21 days static cultivation.

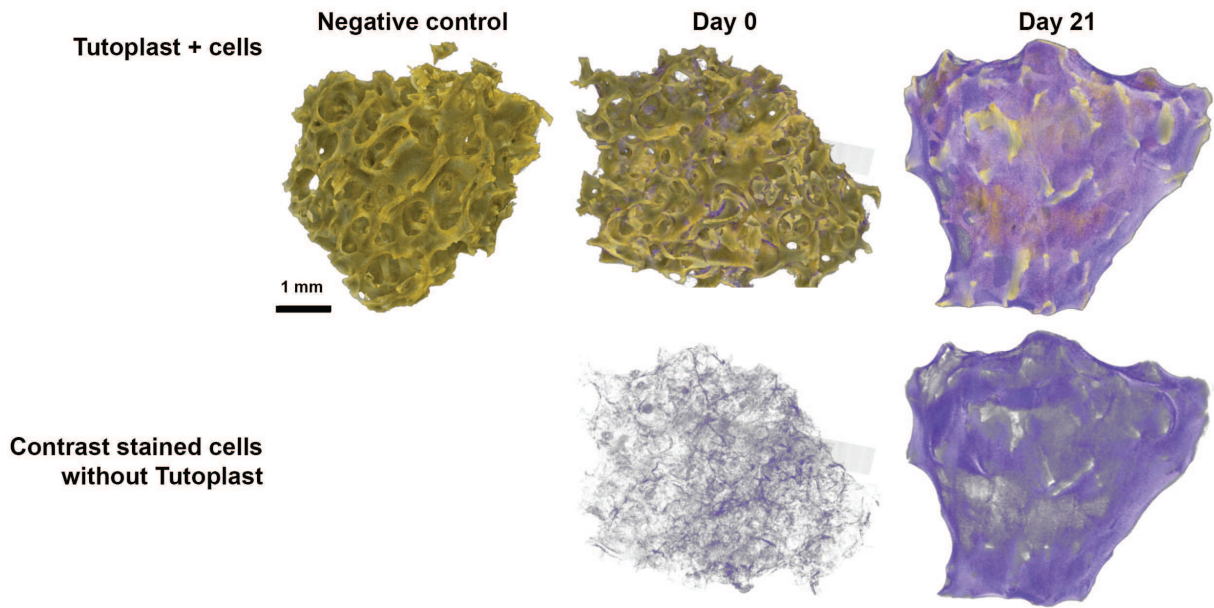


**Figure 5.17:** Characterization of Tutoplast: graphical representation of microCT scans of Tutoplast matrix with and without cells after seeding and 21 days of static cultivation.

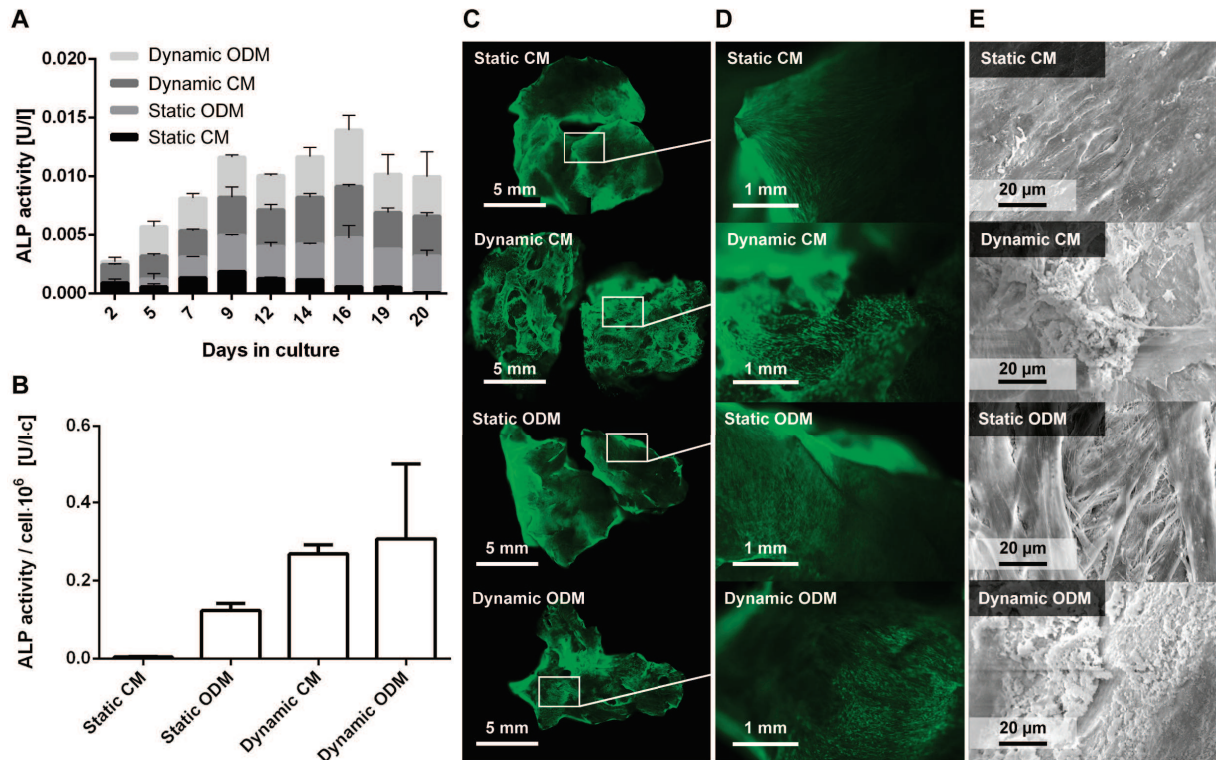


**Figure 5.18:** Biomaterial testing of Tutoplast: ASCs were cultivated for 21 days on Tutoplast in either CCM or ODM under static or dynamic conditions. A) ALP activity. B) ALP activity per cell on day 21. C) Stitched overview images and D) detail images of Calcein-AM and PI staining on day 21 (exposure: 60ms; gamma: 1.3; gain: 3.7x, magnification 4x). E) SEM micrographs on day 21 (voltage: 10 kV; spot size: 50; magnification 1000 x). Data represents mean  $\pm$  SD (n=2).

**Optimization of Shear Stress Conditions** It is well known that mechanical stimuli such as fluid shear stress influence cellular behavior and especially differentiation of stem cells. Shear forces experienced by ASCs on Tutoplast estimated in the perfusion bioreactor at flow rates of 1.5 to 6 ml/min were found to be between 10 – 40 mPa which is one magnitude lower than the commonly accepted in vivo range of 0.3 – 3 Pa [131] (Table 5.8). In order to optimize conditions for osteogenic differentiation the impact of different flow rates was investigated. ALP activity and viability was highest at a volumetric flow rate of 1.5 ml/min and decreased with increasing flow rate (Figure 5.19). Viability was also high under static conditions but did not result in high ALP activity. A flow rate of 1.5 ml/min was considered to promote osteogenic differentiation of ASCs on Tutoplast, and thus was used during optimization of hydrostatic pressure.

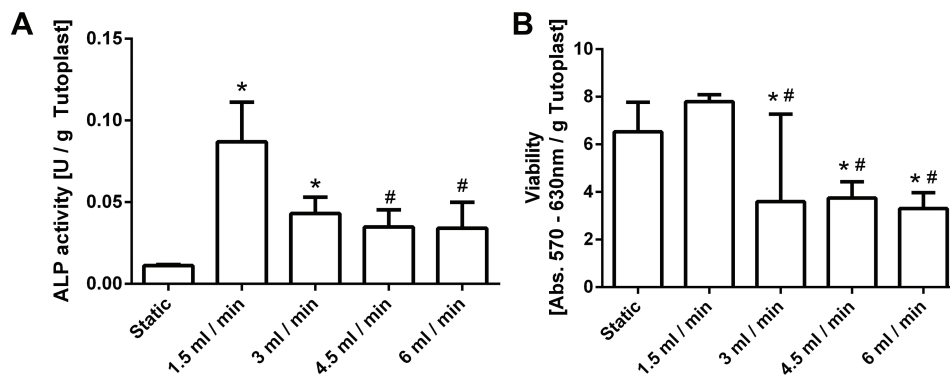


**Figure 5.19:** (A) ALP activity and (B) viability of ASCs seeded on Tutoplast and cultivated in osteogenic differentiation medium at different flow rates. Significantly lower to static (\*) or 1.5 ml/min (#). Data represents mean  $\pm$  SD (n=3).

**Optimization of Hydrostatic Pressure Conditions** The influence of HP on osteogenic differentiation was investigated in order to optimize differentiation of ASCs on Tutoplast. During cultivation cells were subjected to 3 h of HP pattern and 3 h rest for a period of 6 days (see Figure 5.20 A and B). A constant flow of 1.5 ml/min was applied throughout the entire period of cultivation. Since HP was applied by closing valves at constant flow, cells were not only subjected to different target pressures but also experienced different periods of increased pressure. Consequently, the lowest target pressure of 100 mmHg was reached about four times more frequently than the highest target pressure of 500 mmHg (detailed information about valve settings can be found in Table B.2). Therefore, to calculate the total amount of pressure cells experienced in different conditions data from pressure sensor was integrated (Figure 5.21).

Again, ALP activity was elevated in all dynamic conditions compared to static. Yet, no significant effect of HP compared to flow perfusion without HP was observed. However, viability seems to decrease with increasing HP. While a low viability does not necessarily indicate a low cell number fluorescent viability staining indicated a low density of cells with increasing HP. Nevertheless, it is mentionable that regardless of a low cell density and viability at 500 mmHg ALP activity was comparable to other dynamic conditions indicating an increased ALP activity per cell.

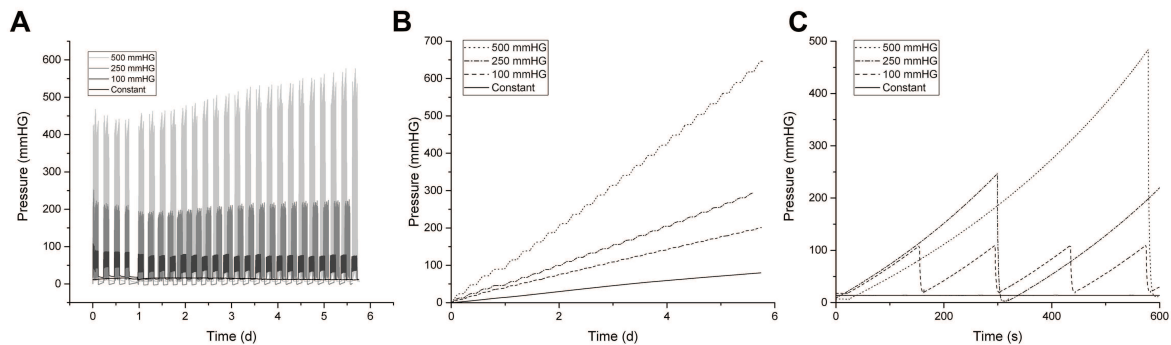


**Figure 5.20:** A) Hydrostatic pressure regime that was applied throughout the cultivation, B) magnification of pressure pattern that was applied during the 3 h of HP application, C) integrated total pressure that was applied on each condition.

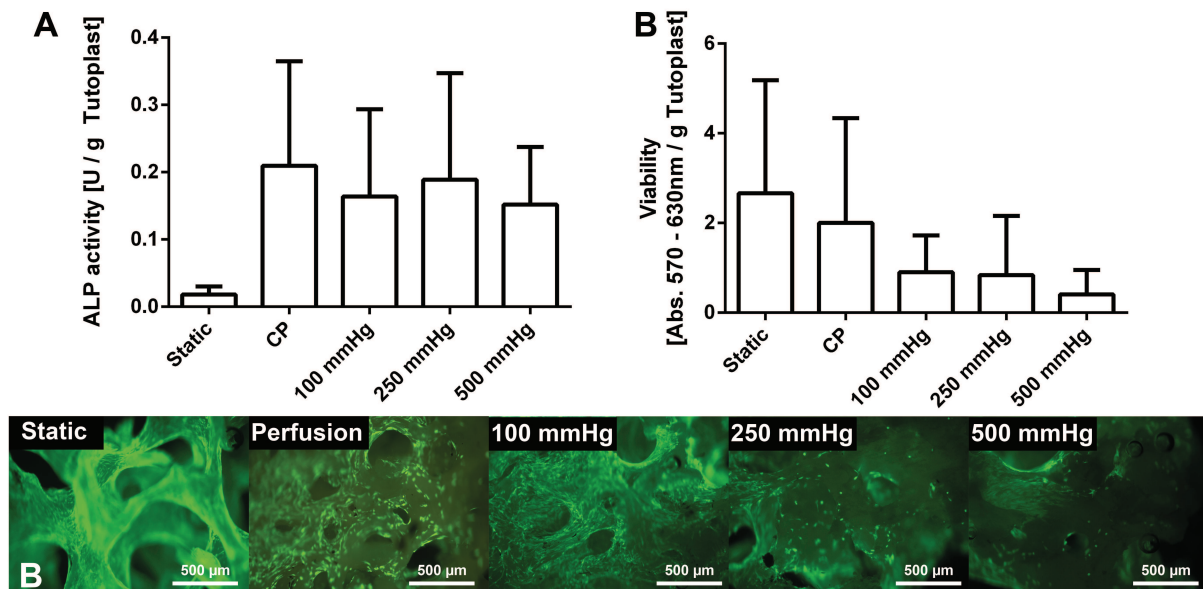


**Figure 5.21:** Optimization hydrostatic pressure: A) ALP activity, B) viability and C) Calcein-AM and PI viability staining of ASCs cultivated on Tutoplast for 6 days in ODM (exposure: 90 ms; gamma: 1; gain: 2.1x; magnification 4x). CP = continuous perfusion without application of hydrostatic pressure. Data represents mean  $\pm$  SD (n=3).

**Discussion** After extensive characterization of the mini perfusion bioreactor system in subsection 5.3.2, the functionality of the system was tested. Tutoplast, a human decellularized bone matrix was tested for its suitability for osteogenic differentiation of ASCs under dynamic conditions and several shear stress and hydrostatic pressure conditions were tested to optimize differentiation. HE staining as well as microCT scans confirmed a closed cell layer that covered the entire matrix while overview images of Calcein-AM and PI staining indicated homogeneous cellular ingrowth into the scaffold. Furthermore, ALP activity peaked at day 9 and 16 indicating osteogenic differentiation. Also, mineralization was observed in SEM micrographs. Therefore, Tutoplast was considered to be a suitable biomaterial for osteogenic differentiation.

When parameters like pore size, porosity and viscosity are constant, fluid shear forces depend exclusively on the flow velocity. Therefore, shear forces for different flow rates were calculated using the Goldstein model which assumes a uniform flow across the scaffold surface and parabolic flow through cylindrical pores. Since bone is a very inhomogeneous material with varying porosity, pore size and geometry and furthermore, the material did not fill the entire diameter of the bioreactor chamber these assumptions were not fulfilled. Consequently, the shear stress calculations can only be accepted as rough approximation. At a permeability constant  $k$  below  $1 \cdot 10^{-10} \text{ m}^2$  maximum shear stress increases dramatically with decreasing pore size and/or porosity compared to the average shear stress [261]. Also, stronger osteogenic differentiation was observed in 3D when experiments were performed under shear stress about one magnitude lower than in the commonly accepted physiologic range of  $0.3 - 3 \text{ Pa}$  [131, 188]. Because of the abovementioned reasons and to avoid possible wash out of cells flow rates for the optimization of osteogenic differentiation were chosen to be one order magnitude lower ( $0.01 - 0.04 \text{ Pa}$ ). However, viability and ALP activity were highest at a flow rate of  $1.5 \text{ ml/min}$  (approximately  $0.01 \text{ Pa}$ ) and ALP activity was significantly higher in all dynamic conditions compared to static. Other groups also reported increased ALP activity and viability when cells were subjected to shear stress of this magnitude [266, 283]. Subsequently, the effect of different HP regimes on the osteogenic differentiation was studied. ALP activity was elevated in all dynamic conditions compared to static conditions while viability was higher in static conditions. Though, no significant effect of ALP activity on HP compared to flow perfusion without HP was found. Still, results suggest an increased ALP activity per cell and thus indicate rather a positive effect of HP on osteogenic differentiation. In a study of Huang and Ogawa sinusoidal HP ( $0.5 \text{ Hz}$ ,  $0 - 3450 \text{ mmHg}$ ) was applied together with perfusion, osteogenic gene expression and viability of human MSCs was markedly improved [265]. Moreover, in a study where HP of  $1500 \text{ mmHg}$  ( $1 \text{ min HP}$ ,  $14 \text{ min pause}$ ) was applied together with fluid shear stress ( $0.79 \text{ Pa}$ ) in a spinner flask, ALP activity together with other osteogenic genes was elevated compared to fluid shear without HP [150]. However, this was not confirmed in the present experiments. These findings suggest to apply higher HP than in this study although *in vivo* pressure in mammalian bone marrow is expected to be  $10.7 - 120 \text{ mmHg}$  [264].

Former developed systems like the oscillating perfusion bioreactor [201, 267] or the TEB1000 by Ebers Medical [288] have demonstrated the importance of involving mechanical cues in 3D cell culture processes like differentiation of stem cells. Recently developed systems aim to overcome the weaknesses of previous systems. Hence, they are partially automated [290], allow for the

cultivation of more than one sample at once [190] or for cultivation of large-size constructs [285]. Still, there is no automated system that combines the benefits of perfusion and hydrostatic pressure while aiming for a higher throughput of independent samples. However, the incubator system together with the mini perfusion bioreactor system displays a comparably high degree of control on shear stress and hydrostatic pressure conditions if scaffold characteristics like porosity and pore size are known. Furthermore, comparably rapid screening of different conditions in parallel is possible.

## 5.4 Conclusion

In conclusion, osteogenic differentiation of ASCs was improved by adjusting process parameters. An incubator/bioreactor system was utilized to generate a more defined and controllable mechanical environment. Subsequent adjustment of fluid shear forces to a physiologic range resulted in increased matrix mineralization and higher viability of ASCs. Otherwise, employment of hydrostatic pressure did not result in elevated osteogenic differentiation. Furthermore, 3D cultivation of cells was found to improve viability compared to 2D cultivation.

However, characterization and control of the mechanical environment remains challenging. Even if material characteristics are assessed accurately, different mathematical models are applied and CFD studies are carried out, the actual shear stress cannot be measured directly and therefore remains unknown. Also, shear stress highly depends on the geometric features of a scaffold and is therefore far away from being homogeneously distributed over the entire surface. Indeed, in this work maximum shear stress was estimated to be up to 88-fold higher than the average shear stress.

CFD simulations are the most accurate tool available to estimate shear stress and flow profiles. Still, if CFD studies on each individual scaffold before cultivation were technically feasible, seeding of cells would alter geometric conditions again making prior analysis not totally predictable. Therefore, an approximation of shear stress together with rapid screening of different conditions as conducted in this work appears to be the most viable option to date. Thus, future work needs to focus on improvement of highly sensitive pressure sensors for low pressure conditions in order to determine the permeability accurately and online during cultivation. Furthermore, miniaturized pressure sensors that are directly implemented up- and downstream the scaffold would be of great benefit since it would enable for more accurate measurement of the pressure differential. Also, CFD studies should be carried out on original microCT data which was not feasible in this work since it requires a vast amount of computing capacity.

Hydrostatic pressure is inherently present in the human body. However, generation of HP in a defined controllable environment is challenging which is probably why studies on the effect of HP on osteogenic differentiation are still scarce and the experimental setups differ extremely. Therefore, it is important to develop systems that exert HP in a comparable manner. The incubator/bioreactor system evaluated in this work displays a first step to a controllable bioreactor for the application of HP. Nevertheless, a more advanced approach where pressure can be constantly exerted independently of the flow rate is highly desirable.

## 6 Conclusion and prospects

In the field of regenerative medicine MSCs are still considered as the primary candidate for cell-based therapies and tissue engineering approaches. Although scientific research and clinical trials prove numerous beneficial effects, the translation from "bench to bedside" has tremendous room for improvement. MSCs behave differently in an artificial environment and thus results of scientific studies are not always predictable for subsequent *in vivo* studies. Thus, the implementation of physiologic conditions in all steps of cultivation seems desirable in order to make *in vitro* results more predictable for *in vivo* studies. Therefore, the goal of this work was to describe concepts for implementation of physiologic conditions in isolation, expansion and differentiation of human MSCs.

The procedures for isolation of MSCs are getting more attention since the number of clinical studies increases and thus cells are frequently isolated. For therapeutic applications it is important to develop reproducible, high-yield, low-cost procedures that result in cell populations that fulfill the MSC minimal criteria. The isolation of stem cells by explant culture is currently the most promising approach since it is thought to generate a more physiologic environment during isolation. Therefore isolation by explant culture was investigated in this work. MSCs were derived from explant culture and traditional enzymatic treatment of adipose tissue and cultivated under normoxic or hypoxic conditions. The yield of explant culture derived cells was comparable to the traditional approach but cells needed more time for outgrowth and thus until harvest. However, the surface marker expression, differentiation capacity and growth capacity was comparable to cells from enzymatic treatment. Hypoxia caused increased proliferation but not an increased outgrowth of cells. However, proliferation until passage 10 and life span of MSCs was significantly increased under hypoxic conditions. Taken together this data indicates that isolation by explant culture provides MSCs with properties comparable to MSCs from enzymatic digestion. Furthermore, the procedure is simpler and therefore prone to automation and reproducibility. Still, improvement is required to reduce the time span until outgrowth and harvest of cells. Since the outgrowth from explant tissue is assumed to be a wound-healing response further chopping of the tissue might accelerate cellular outgrowth.

The generation of therapeutic relevant cell numbers of MSCs has been extensively investigated and discussed before. Since MSCs are adhesive growing cells current expansion technologies are based on the concept of a high surface-to-volume ratio which resulted in either cell factory- or microcarrier-based bioreactor systems. However, MSCs do not grow on 2D surfaces in their physiologic environment. In contrast, cellular aggregates were shown to trigger *in vivo*-like behavior of MSCs but were only investigated in small scale systems. Therefore, the upscale of the

generation and cultivation of MSC aggregates was demonstrated in this work and cellular aggregates were finally cultivated in a 130 ml CSTR under normoxic and hypoxic conditions. Cellular aggregates formed spontaneously from a single cell suspension and cells expanded up to 2.6-fold under hypoxic conditions. Although applied impeller speed was comparably high, cells expressed surface markers fulfilling minimal criteria of MSCs indicating maintenance of stem cell properties and not spontaneous differentiation. Furthermore, MSCs displayed trilineage differentiation after cultivation in the CSTR. Although the process needs further improvement it provides a new and interesting alternative to traditional expansion approaches. Indeed, bioreactor and impeller geometry, coating agents to prevent cellular adhesion on the glass wall or impeller and adjustment of oxygen concentration to avoid anoxic phases during cultivation would probably increase proliferation of cells.

Although the routine, clinical application of tissue engineered constructs seems to be in distant future, the generation of those constructs for the development of proper 3D *in vitro* models is required. Differentiation of MSCs is a complex process orchestrated by numerous factors and parameters making it challenging to mimic the natural environment in which it takes place. Mechanical forces are known to play a key role in differentiation processes. Therefore, this work conceptually describes how a mechanical environment can be estimated and finally generated to set up physiologic conditions for the differentiation of MSCs into the osteoblastic lineage. For this, an existing mini perfusion bioreactor was improved and both bioreactors were extensively characterized towards their mixing behavior, flow and shear stress profile via determination of residence time distributions, computational fluid dynamics and analytical models. Indeed, flow velocity and shear stress profile were more homogeneous in the improved chamber. Finally, the effects of the different mixing, flow and shear stress profiles were compared for osteogenic differentiation. The flow rate was set to result in a physiologic range of shear stress based on the aforementioned characterization which resulted in increased glycolytic activity, ALP-activity and matrix mineralization compared to static conditions. The first bioreactor displayed higher average and maximum shear forces which resulted in increased ALP-activity and matrix mineralization but inhomogeneous cell distribution and decreased proliferation. In contrast, in the improved bioreactor where the geometry caused distribution of the main fluid stream throughout the entire scaffold but at the same time reduced the average and maximum shear stress, MSCs did not display increased ALP-activity or matrix mineralization but a more homogeneous distribution of cells and increased proliferation. These data indicate that higher flow rates are necessary to cause comparable shear forces to induce osteogenic differentiation. Taken together, the previous characterization was predictable for a relative comparison of bioreactor geometries but not for calculating the optimal flow rate in advance.

Furthermore, the perfusion bioreactor system was harnessed together with an advanced incubator to serve as a platform for optimization of cultivation parameters. To improve osteogenic differentiation of MSCs several flow rates and hydrostatic pressure conditions were screened. Again, biomaterial characteristics were characterized in order to better estimate shear stress at certain flow rates. Screening of flow rates revealed an increase in ALP-activity matrix mineralization and viability compared to static conditions and was also successful to find the optimal



flow rate. Screening of hydrostatic pressure in combination with continuous perfusion conditions revealed that continuous perfusion without additional hydrostatic pressure displays higher ALP-activity and viability compared to all hydrostatic pressure conditions. These data indicate that shear forces but not hydrostatic pressure are crucial for the induction of osteogenic differentiation. Since the specialized incubator system together with the miniaturized bioreactor system allows for a parallel cultivation of multiple samples the system will possibly be beneficial in the development and optimization of a variety of 3D cell culture processes.

In general, these findings underline the importance of previous characterization of the used biomaterials and the bioreactor system in order to describe and quantify the mechanical environment that cells are exposed to during cultivation. Although it is encouraging that extensive characterization and the generation of a defined mechanical environment can actually result in improved differentiation, this is only a small step towards advanced dynamic 3D cell culture systems. Systems for the online monitoring of tissue growth or degree of differentiation in 3D dynamic processes are highly required to enable for comprehensive control and reproducible processes.

This work presents concepts for the implementation of physiologic conditions throughout major steps of stem cell cultivation - isolation, expansion and differentiation - in order to improve translation from scientific research to clinical applications. Also, keeping important stem cell properties is crucial for application in cell-based therapies. Therefore, extensive characterization of the crucial cultivation steps and subsequent generation of defined physiologic conditions is inevitable, yet remains challenging.

## References

- [1] Ed Field et al. “Projected growth of the world-wide stem cell market”. In: *Stem Cells in Regenerative Medicine: Science, Regulation and Business Strategies* (2015), p. 43.
- [2] Maria Isabella Gariboldi and Serena M Best. “Effect of ceramic scaffold architectural parameters on biological response”. In: *Frontiers in bioengineering and biotechnology* 3 (2015).
- [3] Jin Hao et al. “Mechanobiology of mesenchymal stem cells: perspective into mechanical induction of MSC fate”. In: *Acta Biomaterialia* 20 (2015), pp. 1–9.
- [4] Sébastien Sart et al. “Three-dimensional aggregates of mesenchymal stem cells: cellular mechanisms, biological properties, and applications”. In: *Tissue Engineering Part B: Reviews* 20.5 (2013), pp. 365–380.
- [5] Ivan Martin, David Wendt, and Michael Heberer. “The role of bioreactors in tissue engineering”. In: *TRENDS in Biotechnology* 22.2 (2004), pp. 80–86. ISSN: 0167-7799.
- [6] J. Hansmann et al. *Bioreactors in tissue engineering - principles, applications and commercial constraints*. Sp. Iss. SI 100OT Times Cited:1 Cited References Count:108. Mar. 2013. URL: %3CGo%20to%20ISI%3E://000315711300005.
- [7] Roman A Perez and Gemma Mestres. “Role of pore size and morphology in musculoskeletal tissue regeneration”. In: *Materials Science and Engineering: C* 61 (2016), pp. 922–939.
- [8] Axis Research Mind. *Regenerative Medicine - Global Trends, Estimates and Forecasts, 2013-2019*. Ed. by Radiant insights. accesses 2017-04-20. URL: <https://www.radiantinsights.com/research/regenerative-medicine-global-trends-estimates-and-forecasts-2013-2019>.
- [9] Robert R. Preti, Patricia Reilley, and Nancy Dvorin. *Annual Data Report 2016*. Ed. by Alliance for Regenerative Medicine. accessed 2017-04-20. URL: <https://alliancerm.org/page/arm-2016-annual-report>.
- [10] Vincent Ronfard et al. “Evaluating the Past, Present, and Future of Regenerative Medicine: A Global View”. In: *Tissue Engineering Part B: Reviews* (2016).
- [11] Deboki Chakravarti and Wilson W Wong. “Synthetic biology in cell-based cancer immunotherapy”. In: *Trends in biotechnology* 33.8 (2015), pp. 449–461.
- [12] Sara Reardon. “Leukaemia success heralds wave of gene-editing therapies”. In: *Nature* 527 (Nov. 5, 2015), pp. 146–147.
- [13] Joseph S Fernandez-Moure. “Lost in translation: the gap in scientific advancements and clinical application”. In: *Frontiers in Bioengineering and Biotechnology* 4 (2016).

- [14] Qasim A Rafiq et al. “The early career researcher’s toolkit: translating tissue engineering, regenerative medicine and cell therapy products”. In: *Regenerative medicine* 10.8 (2015), pp. 989–1003.
- [15] Joshua Hunsberger et al. “Manufacturing road map for tissue engineering and regenerative medicine technologies”. In: *Stem cells translational medicine* 4.2 (2015), pp. 130–135.
- [16] John Gardner et al. “Are there specific translational challenges in regenerative medicine? Lessons from other fields”. In: *Regenerative medicine* 10.7 (2015), pp. 885–895.
- [17] Matthias Renner et al. “Regulation of Clinical Trials with Advanced Therapy Medicinal Products in Germany”. In: *Regulatory Aspects of Gene Therapy and Cell Therapy Products*. Springer, 2015, pp. 87–101.
- [18] Paula Salmikangas et al. “Marketing regulatory oversight of advanced therapy medicinal products (ATMPs) in Europe: the EMA/CAT perspective”. In: *Regulatory Aspects of Gene Therapy and Cell Therapy Products*. Springer, 2015, pp. 103–130.
- [19] European Medicines Agency. *Reflection paper on classification of advanced therapy medicinal products*. May 15, 2015.
- [20] British Standards Institute (BSI). *Developing human cells for clinical applications in the European Union and the United States of America*. 2012. URL: <http://shop.bsigroup.com/forms/PASs/PAS-83/>.
- [21] Jeroen Pieper. *Regulatory: ATMPs and the EUTCD*. 2011. URL: <http://www.samedanltd.com/magazine/11/issue/149/article/2901>.
- [22] Paul-Ehrlich-Institut. *Arzneimittel für neuartige Therapien (ATMP)*. 2017. URL: <http://www.pei.de/DE/arzneimittel/atmp-arzneimittel-fuer-neuartige-therapien/atmp-arzneimittel-fuer-neuartige-therapien-node.html>.
- [23] Heidi Ledford. “4 Ways to fix the clinical trial: clinical trials are crumbling under modern economic and scientific pressures. Nature looks at ways they might be saved”. In: *Nature* 477.7366 (2011), pp. 526–529.
- [24] Dongeun Huh, Geraldine A Hamilton, and Donald E Ingber. “From 3D cell culture to organs-on-chips”. In: *Trends in cell biology* 21.12 (2011), pp. 745–754.
- [25] Bradley A Justice, Nadia A Badr, and Robin A Felder. “3D cell culture opens new dimensions in cell-based assays”. In: *Drug discovery today* 14.1 (2009), pp. 102–107.
- [26] Claudio R Thoma et al. “3D cell culture systems modeling tumor growth determinants in cancer target discovery”. In: *Advanced drug delivery reviews* 69 (2014), pp. 29–41.
- [27] Elizabeth Ratcliffe, Robert J Thomas, and David J Williams. “Current understanding and challenges in bioprocessing of stem cell-based therapies for regenerative medicine”. In: *British medical bulletin* 100.1 (2011), p. 137.
- [28] Julien Barthes et al. “Cell microenvironment engineering and monitoring for tissue engineering and regenerative medicine: the recent advances”. In: *BioMed research international* 2014 (2014).

- [29] Larry A Couture. “Scalable pluripotent stem cell culture: large-scale production of human embryonic stem cells will require improved culture methods”. In: *Nature biotechnology* 28.6 (2010), pp. 562–564.
- [30] Insoo Hyun. “The bioethics of stem cell research and therapy”. In: *The Journal of clinical investigation* 120.1 (2010), pp. 71–75.
- [31] Kazutoshi Takahashi et al. “Induction of pluripotent stem cells from adult human fibroblasts by defined factors”. In: *cell* 131.5 (2007), pp. 861–872.
- [32] Louise C Laurent et al. “Dynamic changes in the copy number of pluripotency and cell proliferation genes in human ESCs and iPSCs during reprogramming and time in culture”. In: *Cell stem cell* 8.1 (2011), pp. 106–118.
- [33] P A Conget and J J Minguell. “Phenotypical and functional properties of human bone marrow mesenchymal progenitor cells.” In: *Journal of cellular physiology* 181 (1 Oct. 1999), pp. 67–73. ISSN: 0021-9541. DOI: 10.1002/(SICI)1097-4652(199910)181:1<67::AID-JCP7>3.0.CO;2-C.
- [34] Hidemi Hattori et al. “Osteogenic potential of human adipose tissue-derived stromal cells as an alternative stem cell source”. In: *Cells Tissues Organs* 178.1 (2004), pp. 2–12.
- [35] Pierre Moretti et al. “Mesenchymal stromal cells derived from human umbilical cord tissues: primitive cells with potential for clinical and tissue engineering applications”. In: *Bioreactor Systems for Tissue Engineering II*. Springer, 2009, pp. 29–54.
- [36] Antonina Lavrentieva et al. “Strategies in umbilical cord-derived mesenchymal stem cells expansion: influence of oxygen, culture medium and cell separation”. In: *BMC proceedings*. Vol. 5. BioMed Central, 2011, P88.
- [37] Marco Tatullo et al. “Dental pulp stem cells: function, isolation and applications in regenerative medicine”. In: *Journal of tissue engineering and regenerative medicine* 9.11 (2015), pp. 1205–1216.
- [38] Malgorzata Witkowska-Zimny and Edyta Wrobel. “Perinatal sources of mesenchymal stem cells: Wharton’s jelly, amnion and chorion.” In: *Cellular and molecular biology letters* 16 (3 Sept. 2011), pp. 493–514. ISSN: 1689-1392. DOI: 10.2478/s11658-011-0019-7.
- [39] Ruchanee Salingcarnboriboon et al. “Establishment of tendon-derived cell lines exhibiting pluripotent mesenchymal stem cell-like property”. In: *Experimental cell research* 287.2 (2003), pp. 289–300.
- [40] Byoung-Moo Seo et al. “Investigation of multipotent postnatal stem cells from human periodontal ligament”. In: *The Lancet* 364.9429 (2004), pp. 149–155.
- [41] Jean G Toma et al. “Isolation of multipotent adult stem cells from the dermis of mammalian skin”. In: *Nature cell biology* 3.9 (2001), pp. 778–784.
- [42] MLBK Dominici et al. “Minimal criteria for defining multipotent mesenchymal stromal cells. The International Society for Cellular Therapy position statement”. In: *Cytotherapy* 8.4 (2006), pp. 315–317. ISSN: 1465-3249.

- [43] Xiaoxiao Long et al. “Neural cell differentiation in vitro from adult human bone marrow mesenchymal stem cells”. In: *Stem cells and development* 14.1 (2005), pp. 65–69.
- [44] Wenrong Xu et al. “Mesenchymal stem cells from adult human bone marrow differentiate into a cardiomyocyte phenotype in vitro”. In: *Experimental Biology and Medicine* 229.7 (2004), pp. 623–631.
- [45] Yanling Ma et al. “Reconstruction of chemically burned rat corneal surface by bone marrow–derived human mesenchymal stem cells”. In: *Stem cells* 24.2 (2006), pp. 315–321.
- [46] Joo Youn Oh et al. “The anti-inflammatory and anti-angiogenic role of mesenchymal stem cells in corneal wound healing following chemical injury.” In: *Stem cells (Dayton, Ohio)* 26 (4 Apr. 2008), pp. 1047–1055. ISSN: 1549-4918. DOI: 10.1634/stemcells.2007-0737.
- [47] Matthew B Murphy, Kathryn Moncivais, and Arnold I Caplan. “Mesenchymal stem cells: environmentally responsive therapeutics for regenerative medicine.” In: *Experimental & molecular medicine* 45 (Nov. 2013), e54. ISSN: 2092-6413. DOI: 10.1038/emm.2013.94.
- [48] J Michael Sorrell, Marilyn A Baber, and Arnold I Caplan. “Influence of adult mesenchymal stem cells on in vitro vascular formation.” In: *Tissue engineering. Part A* 15 (7 July 2009), pp. 1751–1761. ISSN: 1937-335X. DOI: 10.1089/ten.tea.2008.0254.
- [49] Lindolfo da Silva Meirelles and Nance Beyer Nardi. “Methodology, biology and clinical applications of mesenchymal stem cells.” In: *Frontiers in bioscience (Landmark edition)* 14 (Jan. 2009), pp. 4281–4298. ISSN: 1093-4715.
- [50] Ramakrishnaiah Siddappa et al. “Donor variation and loss of multipotency during in vitro expansion of human mesenchymal stem cells for bone tissue engineering.” In: *Journal of orthopaedic research : official publication of the Orthopaedic Research Society* 25 (8 Aug. 2007), pp. 1029–1041. ISSN: 0736-0266. DOI: 10.1002/jor.20402.
- [51] A Ardeshiryajimi et al. “Comparison of osteogenic differentiation potential of human adult stem cells loaded on bioceramic-coated electrospun poly (L-lactide) nanofibres”. In: *Cell proliferation* 48.1 (2015), pp. 47–58.
- [52] Jeffrey M Gimble, Adam J Katz, and Bruce A Bunnell. “Adipose-derived stem cells for regenerative medicine.” In: *Circulation research* 100 (9 May 2007), pp. 1249–1260. ISSN: 1524-4571. DOI: 10.1161/01.RES.0000265074.83288.09.
- [53] Kevin McIntosh et al. “The immunogenicity of human adipose-derived cells: temporal changes in vitro.” In: *Stem cells (Dayton, Ohio)* 24 (5 May 2006), pp. 1246–1253. ISSN: 1066-5099. DOI: 10.1634/stemcells.2005-0235.
- [54] James B Mitchell et al. “Immunophenotype of human adipose-derived cells: temporal changes in stromal-associated and stem cell–associated markers”. In: *Stem cells* 24.2 (2006), pp. 376–385.
- [55] Kavan S Johal, Vivien C Lees, and Adam J Reid. “Adipose-derived stem cells: selecting for translational success”. In: *Regenerative medicine* 10.1 (2015), pp. 79–96.

- [56] Hirotaka Suga et al. “Functional implications of CD34 expression in human adipose-derived stem/progenitor cells.” In: *Stem cells and development* 18 (8 Oct. 2009), pp. 1201–1210. ISSN: 1557-8534. DOI: 10.1089/scd.2009.0003.
- [57] Francesco De Francesco et al. “Human CD34/CD90 ASCs are capable of growing as sphere clusters, producing high levels of VEGF and forming capillaries.” In: *PloS one* 4 (8 Aug. 2009), e6537. ISSN: 1932-6203. DOI: 10.1371/journal.pone.0006537.
- [58] Naoki Yamamoto et al. “Isolation of multipotent stem cells from mouse adipose tissue.” In: *Journal of dermatological science* 48 (1 Oct. 2007), pp. 43–52. ISSN: 0923-1811. DOI: 10.1016/j.jdermsci.2007.05.015.
- [59] Ting Jiang et al. “Potent in vitro chondrogenesis of CD105 enriched human adipose-derived stem cells.” In: *Biomaterials* 31 (13 May 2010), pp. 3564–3571. ISSN: 1878-5905. DOI: 10.1016/j.biomaterials.2010.01.050.
- [60] Brian J Philips et al. “Prevalence of endogenous CD34+ adipose stem cells predicts human fat graft retention in a xenograft model.” In: *Plastic and reconstructive surgery* 132.4 (2013), pp. 845–858.
- [61] Benjamin Levi et al. “CD105 protein depletion enhances human adipose-derived stromal cell osteogenesis through reduction of transforming growth factor  $\beta$ 1 (TGF- $\beta$ 1) signaling”. In: *Journal of Biological Chemistry* 286.45 (2011), pp. 39497–39509.
- [62] Agnieszka Banas et al. “Adipose tissue-derived mesenchymal stem cells as a source of human hepatocytes.” In: *Hepatology (Baltimore, Md.)* 46 (1 July 2007), pp. 219–228. ISSN: 0270-9139. DOI: 10.1002/hep.21704.
- [63] Yunsong Liu et al. “Flow cytometric cell sorting and in vitro pre-osteoiduction are not requirements for in vivo bone formation by human adipose-derived stromal cells.” In: *PLoS ONE* 8.2 (2013), e56002. ISSN: 1932-6203.
- [64] Kotaro Yoshimura et al. “Progenitor-Enriched Adipose Tissue Transplantation as Rescue for Breast Implant Complications”. In: *The breast journal* 16.2 (2010), pp. 169–175.
- [65] R Pérez-Cano et al. “Prospective trial of adipose-derived regenerative cell (ADRC)-enriched fat grafting for partial mastectomy defects: the RESTORE-2 trial”. In: *European Journal of Surgical Oncology (EJSO)* 38.5 (2012), pp. 382–389.
- [66] Jaewoo Pak et al. “Current use of autologous adipose tissue-derived stromal vascular fraction cells for orthopedic applications”. In: *Journal of Biomedical Science* 24.1 (2017), p. 9.
- [67] Fergal J O’Brien. “Biomaterials & scaffolds for tissue engineering”. In: *Materials today* 14.3 (2011), pp. 88–95.
- [68] Susan Breslin and Lorraine O’Driscoll. “Three-dimensional cell culture: the missing link in drug discovery”. In: *Drug discovery today* 18.5 (2013), pp. 240–249.
- [69] Brendon M Baker and Christopher S Chen. “Deconstructing the third dimension—how 3D culture microenvironments alter cellular cues”. In: *J Cell Sci* 125.13 (2012), pp. 3015–3024.

- [70] Johan Malmström et al. “Bone Response Inside Free-Form Fabricated Macroporous Hydroxyapatite Scaffolds with and without an Open Microporosity”. In: *Clinical implant dentistry and related research* 9.2 (2007), pp. 79–88.
- [71] Adalberto L Rosa, Márcio M Beloti, and Richard van Noort. “Osteoblastic differentiation of cultured rat bone marrow cells on hydroxyapatite with different surface topography”. In: *Dental materials* 19.8 (2003), pp. 768–772.
- [72] Despina D Deligianni et al. “Effect of surface roughness of hydroxyapatite on human bone marrow cell adhesion, proliferation, differentiation and detachment strength”. In: *Biomaterials* 22.1 (2000), pp. 87–96.
- [73] Monika Rumpler et al. “The effect of geometry on three-dimensional tissue growth”. In: *Journal of the Royal Society Interface* 5.27 (2008), pp. 1173–1180.
- [74] J Knychala et al. “Pore geometry regulates early stage human bone marrow cell tissue formation and organisation”. In: *Annals of biomedical engineering* 41.5 (2013), pp. 917–930.
- [75] CKM Ng and KN Yu. “Proliferation of epithelial cells on PDMS substrates with micropillars fabricated with different curvature characteristics”. In: *Biointerphases* 7.1-4 (2012), p. 21.
- [76] Mengchi Xu et al. “In vitro assessment of three-dimensionally plotted nagelschmidtite bioceramic scaffolds with varied macropore morphologies”. In: *Acta biomaterialia* 10.1 (2014), pp. 463–476.
- [77] Cécile M Bidan et al. “Geometry as a factor for tissue growth: towards shape optimization of tissue engineering scaffolds”. In: *Advanced healthcare materials* 2.1 (2013), pp. 186–194.
- [78] Cécile M Bidan, Frances M Wang, and John WC Dunlop. “A three-dimensional model for tissue deposition on complex surfaces”. In: *Computer methods in biomechanics and biomedical engineering* 16.10 (2013), pp. 1056–1070.
- [79] E Gamsjäger et al. “Modelling the role of surface stress on the kinetics of tissue growth in confined geometries”. In: *Acta biomaterialia* 9.3 (2013), pp. 5531–5543.
- [80] Se Heang Oh et al. “Investigation of pore size effect on chondrogenic differentiation of adipose stem cells using a pore size gradient scaffold”. In: *Biomacromolecules* 11.8 (2010), pp. 1948–1955.
- [81] Dominique J Griffon et al. “Chitosan scaffolds: interconnective pore size and cartilage engineering”. In: *Acta biomaterialia* 2.3 (2006), pp. 313–320.
- [82] JX Lu et al. “Role of interconnections in porous bioceramics on bone recolonization in vitro and in vivo”. In: *Journal of Materials Science: Materials in Medicine* 10.2 (1999), pp. 111–120.
- [83] Jessica M Kemppainen and Scott J Hollister. “Differential effects of designed scaffold permeability on chondrogenesis by chondrocytes and bone marrow stromal cells”. In: *Biomaterials* 31.2 (2010), pp. 279–287.

- [84] JC Ashworth, SM Best, and RE Cameron. “Quantitative architectural description of tissue engineering scaffolds”. In: *Materials Technology* 29.5 (2014), pp. 281–295.
- [85] Jennifer C Ashworth et al. “Cell invasion in collagen scaffold architectures characterized by percolation theory”. In: *Advanced healthcare materials* 4.9 (2015), pp. 1317–1321.
- [86] Eric LW De Mulder, Pieter Buma, and Gerjon Hannink. “Anisotropic porous biodegradable scaffolds for musculoskeletal tissue engineering”. In: *Materials* 2.4 (2009), pp. 1674–1696.
- [87] F Despang et al. “Synthesis and physicochemical, in vitro and in vivo evaluation of an anisotropic, nanocrystalline hydroxyapatite bisque scaffold with parallel-aligned pores mimicking the microstructure of cortical bone”. In: *Journal of tissue engineering and regenerative medicine* 9.12 (2015), E152–E166.
- [88] Xigeng Miao and Dan Sun. “Graded/gradient porous biomaterials”. In: *Materials* 3.1 (2009), pp. 26–47.
- [89] Chengtie Wu et al. “Three-dimensional printing of hierarchical and tough mesoporous bioactive glass scaffolds with a controllable pore architecture, excellent mechanical strength and mineralization ability”. In: *Acta biomaterialia* 7.6 (2011), pp. 2644–2650.
- [90] Sonia Fiorilli et al. “Electrophoretic deposition of mesoporous bioactive glass on glass–ceramic foam scaffolds for bone tissue engineering”. In: *Journal of Materials Science: Materials in Medicine* 26.1 (2015), pp. 1–12.
- [91] Jennifer S Park et al. “The effect of matrix stiffness on the differentiation of mesenchymal stem cells in response to TGF- $\beta$ ”. In: *Biomaterials* 32.16 (2011), pp. 3921–3930.
- [92] Adam J Engler et al. “Matrix elasticity directs stem cell lineage specification”. In: *Cell* 126.4 (2006), pp. 677–689.
- [93] Nathaniel Huebsch et al. “Harnessing traction-mediated manipulation of the cell/matrix interface to control stem-cell fate”. In: *Nature materials* 9.6 (2010), pp. 518–526.
- [94] Andrew J Steward and Daniel J Kelly. “Mechanical regulation of mesenchymal stem cell differentiation”. In: *Journal of anatomy* 227.6 (2015), pp. 717–731. ISSN: 1469-7580.
- [95] Rowena McBeath et al. “Cell shape, cytoskeletal tension, and RhoA regulate stem cell lineage commitment”. In: *Developmental cell* 6.4 (2004), pp. 483–495.
- [96] R Tse Justin and Adam J Engler. “Stiffness gradients mimicking in vivo tissue variation regulate mesenchymal stem cell fate”. In: *PloS one* 6.1 (2011), e15978.
- [97] Adam Papadimitropoulos et al. “Engineered decellularized matrices to instruct bone regeneration processes”. In: *Bone* 70 (2015), pp. 66–72.
- [98] Hongxu Lu et al. “Autologous extracellular matrix scaffolds for tissue engineering”. In: *Biomaterials* 32.10 (2011), pp. 2489–2499.
- [99] Kim EM Benders et al. “Extracellular matrix scaffolds for cartilage and bone regeneration”. In: *Trends in biotechnology* 31.3 (2013), pp. 169–176.



- [100] Hans Clevers. “Modeling development and disease with organoids”. In: *Cell* 165.7 (2016), pp. 1586–1597.
- [101] Thomas J Bartosh et al. “Aggregation of human mesenchymal stromal cells (MSCs) into 3D spheroids enhances their antiinflammatory properties”. In: *Proceedings of the National Academy of Sciences* 107.31 (2010), pp. 13724–13729.
- [102] Nai-Chen Cheng et al. “Short-Term Spheroid Formation Enhances the Regenerative Capacity of Adipose-Derived Stem Cells by Promoting Stemness, Angiogenesis, and Chemotaxis”. In: *Stem cells translational medicine* 2.8 (2013), pp. 584–594.
- [103] Jessica E Frith, Brian Thomson, and Paul G Genever. “Dynamic three-dimensional culture methods enhance mesenchymal stem cell properties and increase therapeutic potential”. In: *Tissue Engineering Part C: Methods* 16.4 (2009), pp. 735–749.
- [104] Zoe Cesarz and Kenichi Tamama. “Spheroid culture of mesenchymal stem cells”. In: *Stem cells international* 2016 (2015).
- [105] Isotta Chimenti et al. “Stem Cell Spheroids and Ex Vivo Niche Modeling: Rationalization and Scaling-Up”. In: *Journal of Cardiovascular Translational Research* (2017), pp. 1–17.
- [106] Ruei-Zhen Lin and Hwan-You Chang. “Recent advances in three-dimensional multicellular spheroid culture for biomedical research”. In: *Biotechnology journal* 3.9-10 (2008), pp. 1172–1184.
- [107] Jose Alvarez-Pérez, Paloma Ballesteros, and Sebastián Cerdán. “Microscopic images of intraspheroidal pH by 1H magnetic resonance chemical shift imaging of pH sensitive indicators”. In: *Magnetic Resonance Materials in Physics, Biology and Medicine* 18.6 (2005), pp. 293–301.
- [108] Suk Ho Bhang. “Angiogenesis in ischemic tissue produced by spheroid grafting of human adipose-derived stromal cells”. In: *Biomaterials* 32.11 (2011), pp. 2734–2747.
- [109] Stella Alimperti et al. “Serum-free spheroid suspension culture maintains mesenchymal stem cell proliferation and differentiation potential”. In: *Biotechnology progress* 30.4 (2014), pp. 974–983.
- [110] Priya R Baraniak and Todd C McDevitt. “Scaffold-free culture of mesenchymal stem cell spheroids in suspension preserves multilineage potential”. In: *Cell and tissue research* 347.3 (2012), pp. 701–711.
- [111] WA Hodge et al. “Contact pressures in the human hip joint measured in vivo”. In: *Proceedings of the National Academy of Sciences* 83.9 (1986), pp. 2879–2883.
- [112] C Huang et al. “Effects of cyclic compressive loading on chondrogenesis of rabbit bone-marrow derived mesenchymal stem cells”. In: *Stem cells* 22.3 (2004), pp. 313–323.
- [113] Zhen Li et al. “Mechanical load modulates chondrogenesis of human mesenchymal stem cells through the TGF- $\beta$  pathway”. In: *Journal of cellular and molecular medicine* 14.6a (2010), pp. 1338–1346.

- [114] Laszlo Kupcsik et al. “Improving chondrogenesis: potential and limitations of SOX9 gene transfer and mechanical stimulation for cartilage tissue engineering”. In: *Tissue Engineering Part A* 16.6 (2010), pp. 1845–1855.
- [115] Daniel Pelaez, Chun-Yuh Charles Huang, and Herman S Cheung. “Cyclic compression maintains viability and induces chondrogenesis of human mesenchymal stem cells in fibrin gel scaffolds”. In: *Stem cells and development* 18.1 (2009), pp. 93–102.
- [116] Stephen Thorpe, Conor Buckley, and Andrew Steward. “The external mechanical environment can override the influence of local substrate in determining stem cell fate”. In: *Journal of Biomechanics* 45 (2012), S441.
- [117] Christopher B Horner et al. “Magnitude-Dependent and Inversely-related Osteogenic/Chondrogenic Differentiation of Human Mesenchymal Stem Cells Under Dynamic Compressive Strain”. In: *Journal of Tissue Engineering and Regenerative Medicine* (2016).
- [118] H Schechtman and DL Bader. “In vitro fatigue of human tendons”. In: *Journal of biomechanics* 30.8 (1997), pp. 829–835.
- [119] Greg A Johnson et al. “Tensile and viscoelastic properties of human patellar tendon”. In: *Journal of Orthopaedic Research* 12.6 (1994), pp. 796–803.
- [120] L Duchemin et al. “Prediction of mechanical properties of cortical bone by quantitative computed tomography”. In: *Medical engineering & physics* 30.3 (2008), pp. 321–328.
- [121] Siddarth D Subramony et al. “The guidance of stem cell differentiation by substrate alignment and mechanical stimulation”. In: *Biomaterials* 34.8 (2013), pp. 1942–1953.
- [122] Yun Feng Rui et al. “Mechanical loading increased BMP-2 expression which promoted osteogenic differentiation of tendon-derived stem cells”. In: *Journal of Orthopaedic Research* 29.3 (2011), pp. 390–396.
- [123] Louise A McMahon et al. “Regulatory effects of mechanical strain on the chondrogenic differentiation of MSCs in a collagen-GAG scaffold: experimental and computational analysis”. In: *Annals of biomedical engineering* 36.2 (2008), pp. 185–194.
- [124] Ruwan D Sumanasinghe, Susan H Bernacki, and Elizabeth G Loba. “Osteogenic differentiation of human mesenchymal stem cells in collagen matrices: effect of uniaxial cyclic tensile strain on bone morphogenetic protein (BMP-2) mRNA expression”. In: *Tissue engineering* 12.12 (2006), pp. 3459–3465.
- [125] Elaine M Byrne et al. “Gene expression by marrow stromal cells in a porous collagen-glycosaminoglycan scaffold is affected by pore size and mechanical stimulation”. In: *Journal of Materials Science: Materials in Medicine* 19.11 (2008), pp. 3455–3463.
- [126] Ariel D Hanson et al. “Osteogenic effects of rest inserted and continuous cyclic tensile strain on hASC lines with disparate osteodifferentiation capabilities”. In: *Annals of biomedical engineering* 37.5 (2009), pp. 955–965.
- [127] EM Kearney et al. “Tensile strain as a regulator of mesenchymal stem cell osteogenesis”. In: *Annals of biomedical engineering* 38.5 (2010), pp. 1767–1779.

- [128] Chien-Hsun Huang et al. “Interactive effects of mechanical stretching and extracellular matrix proteins on initiating osteogenic differentiation of human mesenchymal stem cells”. In: *Journal of cellular biochemistry* 108.6 (2009), pp. 1263–1273.
- [129] Anne K Haudenschild et al. “Pressure and distortion regulate human mesenchymal stem cell gene expression”. In: *Annals of biomedical engineering* 37.3 (2009), pp. 492–502.
- [130] M. A. Swartz and M. E. Fleury. “Interstitial flow and its effects in soft tissues”. In: *Annu Rev Biomed Eng* 9 (2007). 208RN Times Cited:130 Cited References Count:133 Annual Review of Biomedical Engineering, pp. 229–256. ISSN: 1523-9829. URL: <http://www.ncbi.nlm.nih.gov/pubmed/20151333>.
- [131] S. Weinbaum, S. C. Cowin, and Y. Zeng. “A model for the excitation of osteocytes by mechanical loading-induced bone fluid shear stresses”. In: *J Biomech* 27.3 (Mar. 1994). Weinbaum, S Cowin, S C Zeng, Y J Biomech. 1994 Mar;27(3):339-60., pp. 339–60. ISSN: 0021-9290 (Print) 0021-9290 (Linking). URL: <http://www.ncbi.nlm.nih.gov/pubmed/8051194>.
- [132] Aaron S Goldstein et al. “Effect of convection on osteoblastic cell growth and function in biodegradable polymer foam scaffolds”. In: *Biomaterials* 22.11 (2001), pp. 1279–1288. ISSN: 0142-9612.
- [133] F. Zhao, R. Chella, and T. Ma. “Effects of shear stress on 3-D human mesenchymal stem cell construct development in a perfusion bioreactor system: Experiments and hydrodynamic modeling”. In: *Biotechnology and Bioengineering* 96.3 (Feb. 2007). Zhao, Feng Chella, Ravindran Ma, Teng P40RR017447/RR/NCRR NIH HHS/ Biotechnol Bioeng. 2007 Feb 15;96(3):584-95., pp. 584–95. ISSN: 0006-3592 (Print) 0006-3592 (Linking). URL: <http://www.ncbi.nlm.nih.gov/pubmed/16948169>.
- [134] L. A. Sharp, Y. W. Lee, and A. S. Goldstein. “Effect of low-frequency pulsatile flow on expression of osteoblastic genes by bone marrow stromal cells”. In: *Ann Biomed Eng* 37.3 (Mar. 2009). Sharp, Lindsay A Lee, Yong W Goldstein, Aaron S R21AR051945/AR/NIAMS NIH HHS/ R21AR055200/AR/NIAMS NIH HHS/ Ann Biomed Eng. 2009 Mar;37(3):445-53. doi: 10.1007/s10439-008-9632-7. Epub 2009 Jan 8., pp. 445–53. ISSN: 1573-9686 (Electronic) 0090-6964 (Linking). URL: <http://www.ncbi.nlm.nih.gov/pubmed/19130228>.
- [135] Michael J Jaasma and Fergal J O’Brien. “Mechanical stimulation of osteoblasts using steady and dynamic fluid flow”. In: *Tissue Engineering Part A* 14.7 (2008), pp. 1213–1223. ISSN: 1937-3341.
- [136] Mirjam Fröhlich et al. “Bone grafts engineered from human adipose-derived stem cells in perfusion bioreactor culture”. In: *Tissue Engineering Part A* 16.1 (2009), pp. 179–189. ISSN: 1937-3341.
- [137] Claudia Kleinhan et al. “A perfusion bioreactor system efficiently generates cell-loaded bone substitute materials for addressing critical size bone defects”. In: *Biotechnology journal* 10.11 (2015), pp. 1727–1738.

- [138] Ryan J McCoy and Fergal J O'Brien. "Influence of shear stress in perfusion bioreactor cultures for the development of three-dimensional bone tissue constructs: a review". In: *Tissue Engineering Part B: Reviews* 16.6 (2010), pp. 587–601.
- [139] Sonia Partap et al. "Stimulation of osteoblasts using rest periods during bioreactor culture on collagen-glycosaminoglycan scaffolds". In: *Journal of Materials Science: Materials in Medicine* 21.8 (2010), pp. 2325–2330.
- [140] Michelle R Kreke, William R Huckle, and Aaron S Goldstein. "Fluid flow stimulates expression of osteopontin and bone sialoprotein by bone marrow stromal cells in a temporally dependent manner". In: *Bone* 36.6 (2005), pp. 1047–1055.
- [141] Michelle R Kreke et al. "Effect of intermittent shear stress on mechanotransductive signaling and osteoblastic differentiation of bone marrow stromal cells". In: *Tissue Engineering Part A* 14.4 (2008), pp. 529–537.
- [142] Niamh A Plunkett, Sonia Partap, and Fergal J O'Brien. "Osteoblast response to rest periods during bioreactor culture of collagen-glycosaminoglycan scaffolds". In: *Tissue Engineering Part A* 16.3 (2009), pp. 943–951.
- [143] Yan Huang et al. "Effect of fluid shear stress on cardiomyogenic differentiation of rat bone marrow mesenchymal stem cells". In: *Archives of medical research* 41.7 (2010), pp. 497–505.
- [144] Yan Huang and Yubo Fan. "Effect of intermittent fluid shear stress on cardiomyogenic differentiation of rat bone marrow mesenchymal stem cells". In: *World Congress on Medical Physics and Biomedical Engineering May 26-31, 2012, Beijing, China*. Springer. 2013, pp. 1953–1956.
- [145] Emile L Boulpaep et al. "Medical Physiology a Cellular and Molecular Approach". In: *Signal Transduct* 48 (2009), p. 27.
- [146] David N Irani. *Cerebrospinal fluid in clinical practice*. Elsevier Health Sciences, 2009.
- [147] Richard Klabunde. *Cardiovascular physiology concepts*. Lippincott Williams & Wilkins, 2011.
- [148] D Zhang, S Weinbaum, and SC Cowin. "Estimates of the peak pressures in bone pore water". In: *TRANSACTIONS-AMERICAN SOCIETY OF MECHANICAL ENGINEERS JOURNAL OF BIOMECHANICAL ENGINEERING* 120 (1998), pp. 697–703.
- [149] Kjirste C Morrell et al. "Corroboration of in vivo cartilage pressures with implications for synovial joint tribology and osteoarthritis causation". In: *Proceedings of the National Academy of Sciences of the United States of America* 102.41 (2005), pp. 14819–14824.
- [150] Su-Hyang Kim et al. "ERK 1/2 activation in enhanced osteogenesis of human mesenchymal stem cells in poly (lactic-glycolic acid) by cyclic hydrostatic pressure". In: *Journal of Biomedical Materials Research Part A* 80.4 (2007), pp. 826–836.
- [151] Brittany McGowan. "The Effects of Applied Hydrostatic Pressure on Osteogenic Differentiation of Mouse Mesenchymal Stem Cells in an In Vitro 3D Culture". In: (2014).

- [152] Benjamin D Elder and Kyriacos A Athanasiou. “Hydrostatic pressure in articular cartilage tissue engineering: from chondrocytes to tissue regeneration”. In: *Tissue Engineering Part B: Reviews* 15.1 (2009), pp. 43–53.
- [153] Jae Young Jeong et al. “Effects of intermittent hydrostatic pressure magnitude on the chondrogenesis of MSCs without biochemical agents under 3D co-culture”. In: *Journal of Materials Science: Materials in Medicine* 23.11 (2012), pp. 2773–2781. ISSN: 0957-4530.
- [154] FRANK R Noyes and EDWARD S Grood. “The strength of the anterior cruciate ligament in humans and Rhesus monkeys”. In: *J Bone Joint Surg Am* 58.8 (1976), pp. 1074–1082.
- [155] Daniel Tzu-Bi Shih and Thierry Burnouf. “Preparation, quality criteria, and properties of human blood platelet lysate supplements for ex vivo stem cell expansion”. In: *New biotechnology* 32.1 (2015), pp. 199–211.
- [156] Norbert Stute et al. “Autologous serum for isolation and expansion of human mesenchymal stem cells for clinical use”. In: *Experimental hematology* 32.12 (2004), pp. 1212–1225.
- [157] Price Blair and Robert Flaumenhaft. “Platelet  $\alpha$ -granules: basic biology and clinical correlates”. In: *Blood reviews* 23.4 (2009), pp. 177–189.
- [158] Janka Kisucka et al. “Platelets and platelet adhesion support angiogenesis while preventing excessive hemorrhage”. In: *Proceedings of the National Academy of Sciences of the United States of America* 103.4 (2006), pp. 855–860.
- [159] Chandana Tekkotte et al. ““Humanized” stem cell culture techniques: the animal serum controversy”. In: *Stem cells international* 2011 (2011).
- [160] Thierry Burnouf et al. “Blood-derived biomaterials and platelet growth factors in regenerative medicine”. In: *Blood reviews* 27.2 (2013), pp. 77–89.
- [161] Karen Bieback et al. “Human alternatives to fetal bovine serum for the expansion of mesenchymal stromal cells from bone marrow”. In: *Stem cells* 27.9 (2009), pp. 2331–2341.
- [162] O Kilian et al. “Effects of platelet growth factors on human mesenchymal stem cells and human endothelial cells in vitro”. In: *European journal of medical research* 9.7 (2004), pp. 337–344.
- [163] Panagiota A Sotiropoulou et al. “Characterization of the optimal culture conditions for clinical scale production of human mesenchymal stem cells”. In: *Stem cells* 24.2 (2006), pp. 462–471.
- [164] Ying Zhou, Dan Yu, and Huiyong Zhu. “Optimization of culture condition of human bone marrow stromal cells in terms of purification, proliferation, and pluripotency”. In: *In Vitro Cellular & Developmental Biology-Animal* 50.9 (2014), pp. 822–830.
- [165] Ting Lo et al. “Glucose reduction prevents replicative senescence and increases mitochondrial respiration in human mesenchymal stem cells”. In: *Cell transplantation* 20.6 (2011), pp. 813–825.
- [166] Alessandro Bizzarri et al. “Continuous oxygen monitoring in subcutaneous adipose tissue using microdialysis”. In: *Analytica chimica acta* 573 (2006), pp. 48–56.

- [167] Dominic C Chow et al. “Modeling pO<sub>2</sub> distributions in the bone marrow hematopoietic compartment. II. Modified Kroghian models”. In: *Biophysical journal* 81.2 (2001), pp. 685–696.
- [168] J. S. Harrison et al. “Oxygen saturation in the bone marrow of healthy volunteers”. In: *Blood* 99.1 (Jan. 2002). Harrison, Jonathan S Rameshwar, Pranela Chang, Vicotr Bandari, Persis Blood. 2002 Jan 1;99(1):394., p. 394. ISSN: 0006-4971 (Print) 0006-4971 (Linking). URL: <http://www.ncbi.nlm.nih.gov/pubmed/11783438>.
- [169] Helen Wiseman and Barry Halliwell. “Damage to DNA by reactive oxygen and nitrogen species: role in inflammatory disease and progression to cancer.” In: *Biochemical Journal* 313.Pt 1 (1996), p. 17.
- [170] L. B. Buravkova et al. “Mesenchymal stem cells and hypoxia: Where are we?” In: *Mitochondrion* 19 (Nov. 2014). A Sp. Iss. SI Ax0dy Times Cited:12 Cited References Count:89, pp. 105–112. ISSN: 1567-7249. URL: <http://dx.doi.org/10.1016/j.mito.2014.09.001>.
- [171] Kazuki Iida et al. “Hypoxia enhances colony formation and proliferation but inhibits differentiation of human dental pulp cells”. In: *archives of oral biology* 55.9 (2010), pp. 648–654.
- [172] Warren L Grayson et al. “Hypoxia enhances proliferation and tissue formation of human mesenchymal stem cells”. In: *Biochemical and biophysical research communications* 358.3 (2007), pp. 948–953.
- [173] A. Lavrentieva et al. “Effects of hypoxic culture conditions on umbilical cord-derived human mesenchymal stem cells”. In: *Cell Communication and Signaling* 8 (July 2010). 655QW Times Cited:59 Cited References Count:35. ISSN: 1478-811X. URL: <http://dx.doi.org/10.1186/1478-811X-8-655>.
- [174] Chih-Chien Tsai et al. “Hypoxia inhibits senescence and maintains mesenchymal stem cell properties through down-regulation of E2A-p21 by HIF-TWIST”. In: *Blood* 117.2 (2011), pp. 459–469.
- [175] JC Estrada et al. “Culture of human mesenchymal stem cells at low oxygen tension improves growth and genetic stability by activating glycolysis”. In: *Cell Death & Differentiation* 19.5 (2012), pp. 743–755. ISSN: 1350-9047.
- [176] Preeti Malladi et al. “Effect of reduced oxygen tension on chondrogenesis and osteogenesis in adipose-derived mesenchymal cells”. In: *American Journal of Physiology-Cell Physiology* 290.4 (2006), pp. C1139–C1146.
- [177] Francisco Dos Santos et al. “Ex vivo expansion of human mesenchymal stem cells: a more effective cell proliferation kinetics and metabolism under hypoxia”. In: *Journal of cellular physiology* 223.1 (2010), pp. 27–35.
- [178] T. Hatlapatka. “Entwicklung von Expansionsstrategien für Misch- und Subpopulationen mesenchymaler Stromazellen aus dem Nabelschnurgewebe unter xeno- freien Kultivierungsbedingungen.” PhD thesis. Leibniz University of Hanover, 2011.

- [179] Hatim Hemed, Bernd Giebel, and Wolfgang Wagner. "Evaluation of human platelet lysate versus fetal bovine serum for culture of mesenchymal stromal cells". In: *Cytotherapy* 16.2 (2014), pp. 170–180. ISSN: 1465-3249.
- [180] Elias Volkmer et al. "Hypoxia in static and dynamic 3D culture systems for tissue engineering of bone". In: *Tissue Engineering Part A* 14.8 (2008), pp. 1331–1340. ISSN: 1937-3341.
- [181] Maik Stiehler et al. "Effect of dynamic 3-D culture on proliferation, distribution, and osteogenic differentiation of human mesenchymal stem cells". In: *Journal of Biomedical Materials Research Part A* 89.1 (2009), pp. 96–107. ISSN: 1552-4965.
- [182] Tzu-Wei Wang et al. "Regulation of adult human mesenchymal stem cells into osteogenic and chondrogenic lineages by different bioreactor systems". In: *Journal of Biomedical Materials Research Part A* 88.4 (2009), pp. 935–946. ISSN: 1552-4965.
- [183] Keith J Gooch et al. "Effects of mixing intensity on tissue-engineered cartilage". In: *Biotechnology and Bioengineering* 72.4 (2001), pp. 402–407. ISSN: 1097-0290.
- [184] Vassilios I Sikavitsas, Gregory N Bancroft, and Antonios G Mikos. "Formation of three-dimensional cell/polymer constructs for bone tissue engineering in a spinner flask and a rotating wall vessel bioreactor". In: *Journal of biomedical materials research* 62.1 (2002), pp. 136–148. ISSN: 1097-4636.
- [185] Cynthia M Begley and Stanley J Kleis. "The fluid dynamic and shear environment in the NASA/JSC rotating-wall perfused-vessel bioreactor". In: *Biotechnology and Bioengineering* 70.1 (2000), pp. 32–40. ISSN: 1097-0290.
- [186] Solvig Diederichs et al. "Dynamic cultivation of human mesenchymal stem cells in a rotating bed bioreactor system based on the Z<sup>®</sup> RP platform". In: *Biotechnology progress* 25.6 (2009), pp. 1762–1771. ISSN: 1520-6033.
- [187] Anne Neumann et al. "Characterization and Application of a Disposable Rotating Bed Bioreactor for Mesenchymal Stem Cell Expansion". In: *Bioengineering* 1.4 (2014), pp. 231–245.
- [188] Gregory N Bancroft, Vassilios I Sikavitsas, and Antonios G Mikos. "Technical note: Design of a flow perfusion bioreactor system for bone tissue-engineering applications". In: *Tissue engineering* 9.3 (2003), pp. 549–554. ISSN: 1076-3279.
- [189] Alexander M Sailon et al. "A novel flow-perfusion bioreactor supports 3D dynamic cell culture". In: *BioMed Research International* 2009 (2009). ISSN: 1110-7243.
- [190] M. Piola et al. "Design and Functional Testing of a Multichamber Perfusion Platform for Three-Dimensional Scaffolds". In: *Scientific World Journal* (2013). 288TP Times Cited:0 Cited References Count:30. ISSN: 1537-744X. URL: %3CGo%20to%20ISI%3E://000329635100001.
- [191] Akhilandeshwari Ravichandran, Yuchun Liu, and Swee-Hin Teoh. "Review: bioreactor design towards generation of relevant engineered tissues: focus on clinical translation". In: *Journal of Tissue Engineering and Regenerative Medicine* (2017).
- [192] Zhi-Yong Zhang et al. "A biaxial rotating bioreactor for the culture of fetal mesenchymal stem cells for bone tissue engineering". In: *Biomaterials* 30.14 (2009), pp. 2694–2704.

- [193] Bao-Ngoc B Nguyen et al. “Dynamic bioreactor culture of high volume engineered bone tissue”. In: *Tissue Engineering Part A* 22.3-4 (2016), pp. 263–271.
- [194] EBERS Medical Technology. *TC-3 bioreactor*. Apr. 28, 2017. URL: [http://www.ebersmedical.com/files/brochures/Brochure\\_TC-3.pdf](http://www.ebersmedical.com/files/brochures/Brochure_TC-3.pdf).
- [195] K. Ulubayram et al. “Engineering a 3D cardiac patch through cardiomyogenic differentiation of rMSCs by synchronous mechanical and electrical stimulations”. In: *frontiers*. Mar. 30, 2016.
- [196] Vikesh V Chandaria, James McGinty, and Niamh C Nowlan. “Characterising the effects of in vitro mechanical stimulation on morphogenesis of developing limb explants”. In: *Journal of Biomechanics* 49.15 (2016), pp. 3635–3642.
- [197] Christopher J Hillary et al. “Developing repair materials for stress urinary incontinence to withstand dynamic distension”. In: *PloS one* 11.3 (2016), e0149971.
- [198] NE Timmins et al. “Closed system isolation and scalable expansion of human placental mesenchymal stem cells”. In: *Biotechnology and bioengineering* 109.7 (2012), pp. 1817–1826.
- [199] Sathish Kumar, Christoph Wittmann, and Elmar Heinzle. “Review: minibioreactors”. In: *Biotechnology Letters* 26.1 (2004), pp. 1–10.
- [200] Patrick J Hanley. “Efficient manufacturing of therapeutic mesenchymal stromal cells with the use of the Quantum Cell Expansion System (vol 16, pg 1048, 2014)”. In: *Cytotherapy* 16.10 (2014), pp. 1449–1449.
- [201] Alessandra Braccini et al. “Three-dimensional perfusion culture of human bone marrow cells and generation of osteoinductive grafts”. In: *Stem cells* 23.8 (2005), pp. 1066–1072.
- [202] Arnaud Scherberich et al. “Three-Dimensional Perfusion Culture of Human Adipose Tissue-Derived Endothelial and Osteoblastic Progenitors Generates Osteogenic Constructs with Intrinsic Vascularization Capacity”. In: *Stem cells* 25.7 (2007), pp. 1823–1829.
- [203] Francisco dos Santos et al. “Toward a clinical-grade expansion of mesenchymal stem cells from human sources: a microcarrier-based culture system under xeno-free conditions”. In: *Tissue Engineering Part C: Methods* 17.12 (2011), pp. 1201–1210.
- [204] Stephan Kaiser et al. “Fluid Flow and Cell Proliferation of Mesenchymal Adipose-Derived Stem Cells in Small-Scale, Stirred, Single-Use Bioreactors”. In: *Chemie Ingenieur Technik* 85.1-2 (2013), pp. 95–102.
- [205] Marco Cantini et al. “Numerical fluid-dynamic optimization of microchannel-provided porous scaffolds for the co-culture of adherent and non-adherent cells”. In: *Tissue Engineering Part A* 15.3 (2008), pp. 615–623.
- [206] Harmeet Singh et al. “Flow modelling within a scaffold under the influence of uni-axial and bi-axial bioreactor rotation”. In: *Journal of biotechnology* 119.2 (2005), pp. 181–196.
- [207] Christian Jungreuthmayer et al. “A comparative study of shear stresses in collagen-glycosaminoglycan and calcium phosphate scaffolds in bone tissue-engineering bioreactors”. In: *Tissue Engineering Part A* 15.5 (2008), pp. 1141–1149. ISSN: 1937-3341.



- [208] H Scott Fogler. “Elements of chemical reaction engineering”. In: (1999).
- [209] Frédéric Maes et al. “Computational models for wall shear stress estimation in scaffolds: A comparative study of two complete geometries”. In: *Journal of biomechanics* 45.9 (2012), pp. 1586–1592.
- [210] Efrem Curcio et al. “Kinetics of oxygen uptake by cells potentially used in a tissue engineered trachea”. In: *Biomaterials* 35.25 (2014), pp. 6829–6837.
- [211] Martin Rodbell. “The metabolism of isolated fat cells IV. Regulation of release of protein by lipolytic hormones and insulin”. In: *Journal of Biological Chemistry* 241.17 (1966), pp. 3909–3917.
- [212] Patricia A Zuk et al. “Human adipose tissue is a source of multipotent stem cells”. In: *Molecular biology of the cell* 13.12 (2002), pp. 4279–4295.
- [213] H Jahr et al. “Endotoxin-mediated activation of cytokine production in human PBMCs by collagenase and Ficoll”. In: *Journal of molecular medicine* 77.1 (1999), pp. 118–120.
- [214] Francesca Vargas et al. “Endotoxin activity of collagenase and human islet transplantation”. In: *The Lancet* 350.9078 (1997), p. 641.
- [215] TJ Cavanagh et al. “Crude collagenase loses islet-isolating efficacy regardless of storage conditions”. In: *Transplantation proceedings*. Vol. 29. 4. Elsevier. 1997, pp. 1942–1944.
- [216] Matthew J Barnett et al. “Quantitative assessment of collagenase blends for human islet isolation”. In: *Transplantation* 80.6 (2005), pp. 723–728.
- [217] Toshiyuki Yamamoto et al. “Deterioration and variability of highly purified collagenase blends used in clinical islet isolation”. In: *Transplantation* 84.8 (2007), pp. 997–1002.
- [218] Ludovic Zimmerlin et al. “Stromal vascular progenitors in adult human adipose tissue”. In: *Cytometry Part A* 77.1 (2010), pp. 22–30.
- [219] Tommaso Rada, Rui L Reis, and Manuela E Gomes. “Distinct stem cells subpopulations isolated from human adipose tissue exhibit different chondrogenic and osteogenic differentiation potential”. In: *Stem Cell Reviews and Reports* 7.1 (2011), pp. 64–76.
- [220] Beatriz Paredes et al. “Phenotypic differences during the osteogenic differentiation of single cell-derived clones isolated from human lipoaspirates”. In: *Journal of tissue engineering and regenerative medicine* 5.8 (2011), pp. 589–599.
- [221] Giuseppe Astori et al. “In vitro and multicolor phenotypic characterization of cell subpopulations identified in fresh human adipose tissue stromal vascular fraction and in the derived mesenchymal stem cells”. In: *Journal of Translational Medicine* 5.1 (2007), p. 55.
- [222] Ikuo Ishige et al. “Comparison of mesenchymal stem cells derived from arterial, venous, and Wharton’s jelly explants of human umbilical cord”. In: *International journal of hematology* 90.2 (2009), pp. 261–269.
- [223] Leandra S Baptista et al. *An alternative method for the isolation of mesenchymal stromal cells derived from lipoaspirate samples*. 2009.

- [224] Katsumi Ebisawa et al. "Ultrasound enhances transforming growth factor  $\beta$ -mediated chondrocyte differentiation of human mesenchymal stem cells". In: *Tissue engineering* 10.5-6 (2004), pp. 921–929.
- [225] Keita Miyanishi et al. "Dose-and time-dependent effects of cyclic hydrostatic pressure on transforming growth factor- $\beta$ 3-induced chondrogenesis by adult human mesenchymal stem cells in vitro". In: *Tissue engineering* 12.8 (2006), pp. 2253–2262.
- [226] Craig A Simmons et al. "Cyclic strain enhances matrix mineralization by adult human mesenchymal stem cells via the extracellular signal-regulated kinase (ERK1/2) signaling pathway". In: *Journal of biomechanics* 36.8 (2003), pp. 1087–1096.
- [227] Marlene Knippenberg et al. "Adipose tissue-derived mesenchymal stem cells acquire bone cell-like responsiveness to fluid shear stress on osteogenic stimulation". In: *Tissue engineering* 11.11-12 (2005), pp. 1780–1788.
- [228] MJ Oedayrajsingh-Varma et al. "Adipose tissue-derived mesenchymal stem cell yield and growth characteristics are affected by the tissue-harvesting procedure". In: *Cytotherapy* 8.2 (2006), pp. 166–177.
- [229] Dmitry Bulgin, Erik Vrabic, and Enes Hodzic. "Autologous bone-marrow-derived-mononuclear-cells-enriched fat transplantation in breast augmentation: evaluation of clinical outcomes and aesthetic results in a 30-year-old female". In: *Case reports in surgery* 2013 (2013).
- [230] Forum S Shah et al. "A non-enzymatic method for isolating human adipose tissue-derived stromal stem cells". In: *Cytotherapy* 15.8 (2013), pp. 979–985.
- [231] Nancy Priya et al. "Explant culture: a simple, reproducible, efficient and economic technique for isolation of mesenchymal stromal cells from human adipose tissue and lipoaspirate". In: *Journal of tissue engineering and regenerative medicine* 8.9 (2014), pp. 706–716.
- [232] Fatemeh Hendijani. "Explant culture: An advantageous method for isolation of mesenchymal stem cells from human tissues". In: *Cell Proliferation* (2017).
- [233] Hoon-Ki Sung et al. "Adipose vascular endothelial growth factor regulates metabolic homeostasis through angiogenesis". In: *Cell metabolism* 17.1 (2013), pp. 61–72.
- [234] Britt G Gabrielsson et al. "Depot-Specific Expression of Fibroblast Growth Factors in Human Adipose Tissue". In: *Obesity* 10.7 (2002), pp. 608–616.
- [235] Felicia Ng et al. "PDGF, TGF- $\beta$ , and FGF signaling is important for differentiation and growth of mesenchymal stem cells (MSCs): transcriptional profiling can identify markers and signaling pathways important in differentiation of MSCs into adipogenic, chondrogenic, and osteogenic lineages". In: *Blood* 112.2 (2008), pp. 295–307.
- [236] Anna Otte et al. "Mesenchymal stem cells maintain long-term in vitro stemness during explant culture". In: *Tissue Engineering Part C: Methods* 19.12 (2013), pp. 937–948.
- [237] Ahmad Ghorbani, Seyed Amir Jalali, and Masoumeh Varedi. "Isolation of adipose tissue mesenchymal stem cells without tissue destruction: a non-enzymatic method". In: *Tissue and Cell* 46.1 (2014), pp. 54–58.

- [238] MG Valorani et al. “Pre-culturing human adipose tissue mesenchymal stem cells under hypoxia increases their adipogenic and osteogenic differentiation potentials”. In: *Cell proliferation* 45.3 (2012), pp. 225–238.
- [239] Michael P Francis et al. “Isolating adipose-derived mesenchymal stem cells from lipoaspirate blood and saline fraction”. In: *Organogenesis* 6.1 (2010), pp. 11–14.
- [240] Jonathan Rodriguez et al. “Evaluation of three devices for the isolation of the stromal vascular fraction from adipose tissue and for ASC culture: a comparative study”. In: ().
- [241] Owen G Davies et al. “Isolation of adipose and bone marrow mesenchymal stem cells using CD29 and CD90 modifies their capacity for osteogenic and adipogenic differentiation”. In: *Journal of tissue engineering* 6 (2015), p. 2041731415592356.
- [242] Anna M Knapinska et al. “Matrix metalloproteinases as reagents for cell isolation”. In: *Enzyme and Microbial Technology* 93 (2016), pp. 29–43.
- [243] Wei-Wei Xu et al. “Differentiation potential of human adipose tissue derived stem cells into photoreceptors through explants culture and enzyme methods”. In: *International Journal of Ophthalmology* 10.1 (2017), p. 23.
- [244] Wenjie Wang et al. “3D spheroid culture system on micropatterned substrates for improved differentiation efficiency of multipotent mesenchymal stem cells”. In: *Biomaterials* 30.14 (2009), pp. 2705–2715.
- [245] Wen-Yu Lee et al. “The use of injectable spherically symmetric cell aggregates self-assembled in a thermo-responsive hydrogel for enhanced cell transplantation”. In: *Biomaterials* 30.29 (2009), pp. 5505–5513.
- [246] Cornelia Hildebrandt, Heiko Büth, and Hagen Thielecke. “A scaffold-free in vitro model for osteogenesis of human mesenchymal stem cells”. In: *Tissue and Cell* 43.2 (2011), pp. 91–100.
- [247] Dominik Egger et al. “Hypoxic Three-Dimensional Scaffold-Free Aggregate Cultivation of Mesenchymal Stem Cells in a Stirred Tank Reactor”. In: *Bioengineering* 4.2 (2017), p. 47.
- [248] SK Kapur et al. “Human adipose stem cells maintain proliferative, synthetic and multipotential properties when suspension cultured as self-assembling spheroids”. In: *Biofabrication* 4.2 (2012), p. 025004.
- [249] Guo-Shiang Huang et al. “Spheroid formation of mesenchymal stem cells on chitosan and chitosan-hyaluronan membranes”. In: *Biomaterials* 32.29 (2011), pp. 6929–6945.
- [250] Ruei-Zeng Lin et al. “Dynamic analysis of hepatoma spheroid formation: roles of E-cadherin and  $\beta$ 1-integrin”. In: *Cell and tissue research* 324.3 (2006), pp. 411–422.
- [251] Yubing Sun, Christopher S Chen, and Jianping Fu. “Forcing stem cells to behave: a biophysical perspective of the cellular microenvironment”. In: *Annual review of biophysics* 41 (2012), pp. 519–542.
- [252] Fabian Langenbach et al. “Generation and differentiation of microtissues from multipotent precursor cells for use in tissue engineering”. In: *Nature protocols* 6.11 (2011), pp. 1726–1735.

- [253] S. Sart, S. N. Agathos, and Y. Li. “Process engineering of stem cell metabolism for large scale expansion and differentiation in bioreactors”. In: *Biochemical Engineering Journal* 84 (Mar. 2014). Ad8au Times Cited:1 Cited References Count:111, pp. 74–82. ISSN: 1369-703X. URL: %3CGo%20to%20ISI%3E://000333489700010.
- [254] Dominik Egger et al. “Application of a Parallelizable Perfusion Bioreactor for Physiologic 3D Cell Culture”. In: *Cells Tissues Organs* (2017).
- [255] Gemma Eibes et al. “Maximizing the ex vivo expansion of human mesenchymal stem cells using a microcarrier-based stirred culture system”. In: *Journal of biotechnology* 146.4 (2010), pp. 194–197.
- [256] Francisco dos Santos et al. “A xenogeneic-free bioreactor system for the clinical-scale expansion of human mesenchymal stem/stromal cells”. In: *Biotechnology and Bioengineering* 111.6 (2014), pp. 1116–1127.
- [257] Ning Liu et al. “Stem cell engineering in bioreactors for large-scale bioprocessing”. In: *Engineering in Life Sciences* 14.1 (2014), pp. 4–15.
- [258] Alvin W Nienow et al. “A potentially scalable method for the harvesting of hMSCs from microcarriers”. In: *Biochemical Engineering Journal* 85 (2014), pp. 79–88.
- [259] Qunzhou Zhang et al. “Three-dimensional spheroid culture of human gingiva-derived mesenchymal stem cells enhances mitigation of chemotherapy-induced oral mucositis”. In: *Stem cells and development* 21.6 (2011), pp. 937–947.
- [260] Su Wang and John M Tarbell. “Effect of fluid flow on smooth muscle cells in a 3-dimensional collagen gel model”. In: *Arteriosclerosis, thrombosis, and vascular biology* 20.10 (2000), pp. 2220–2225. ISSN: 1079-5642.
- [261] P. Vossenberget et al. “Darcian permeability constant as indicator for shear stresses in regular scaffold systems for tissue engineering”. In: *Biomechanics and Modeling in Mechanobiology* 8.6 (Dec. 2009). 523KM Times Cited:9 Cited References Count:14, pp. 499–507. ISSN: 1617-7959. URL: %3CGo%20to%20ISI%3E://000272072100006.
- [262] Yann Guyot et al. “A three-dimensional computational fluid dynamics model of shear stress distribution during neotissue growth in a perfusion bioreactor”. In: *Biotechnology and bioengineering* 112.12 (2015), pp. 2591–2600.
- [263] P Becquart et al. “Human mesenchymal stem cell responses to hydrostatic pressure and shear stress”. In: *Eur Cell Mater* 31 (2016), pp. 160–73.
- [264] Umut Atakan Gurkan and Ozan Akkus. “The mechanical environment of bone marrow: a review”. In: *Annals of biomedical engineering* 36.12 (2008), pp. 1978–1991.
- [265] Chenyu Huang and Reimc Ogawa. “Effect of hydrostatic pressure on bone regeneration using human mesenchymal stem cells”. In: *Tissue Engineering Part A* 18.19-20 (2012), pp. 2106–2113. ISSN: 1937-3341.
- [266] Warren L Grayson et al. “Effects of initial seeding density and fluid perfusion rate on formation of tissue-engineered bone”. In: *Tissue Engineering Part A* 14.11 (2008), pp. 1809–1820. ISSN: 1937-3341.

- [267] D Wendt et al. "Oscillating perfusion of cell suspensions through three-dimensional scaffolds enhances cell seeding efficiency and uniformity". In: *Biotechnology and Bioengineering* 84.2 (2003), pp. 205–214. ISSN: 1097-0290.
- [268] Feng Zhao and Teng Ma. "Perfusion bioreactor system for human mesenchymal stem cell tissue engineering: dynamic cell seeding and construct development". In: *Biotechnology and Bioengineering* 91.4 (2005), pp. 482–493. ISSN: 1097-0290.
- [269] Zhi-Yong Zhang et al. "Neo-vascularization and bone formation mediated by fetal mesenchymal stem cell tissue-engineered bone grafts in critical-size femoral defects". In: *Biomaterials* 31.4 (2010), pp. 608–620.
- [270] Patrina SP Poh et al. "In vitro and in vivo bone formation potential of surface calcium phosphate-coated polycaprolactone and polycaprolactone/bioactive glass composite scaffolds". In: *Acta biomaterialia* 30 (2016), pp. 319–333.
- [271] Alfred Gugerell et al. "Adipose-derived stem cells cultivated on electrospun l-lactide/glycolide copolymer fleece and gelatin hydrogels under flow conditions—aiming physiological reality in hypodermis tissue engineering". In: *Burns* 41.1 (2015), pp. 163–171. ISSN: 0305-4179.
- [272] Dominik Egger et al. "Development and Characterization of a Parallelizable Perfusion Bioreactor for 3D Cell Culture". In: *Bioengineering* 4.2 (2 May 25, 2017). Ed. by Christoph Herwig, p. 51. DOI: 10.3390/bioengineering4020051. URL: <http://www.mdpi.com/2306-5354/4/2/51/htm>.
- [273] J. A. Sanz-Herrera et al. "Mechanical and flow characterization of Sponceram carriers: Evaluation by homogenization theory and experimental validation". In: *J Biomed Mater Res B Appl Biomater* 87.1 (Oct. 2008). Sanz-Herrera, Jose A Kasper, Cornelia van Griensven, Martijn Garcia-Aznar, Jose M Ochoa, Ignacio Doblare, Manuel J Biomed Mater Res B Appl Biomater. 2008 Oct;87(1):42-8. doi: 10.1002/jbm.b.31065., pp. 42–8. ISSN: 1552-4981 (Electronic) 1552-4973 (Linking). URL: <http://www.ncbi.nlm.nih.gov/pubmed/18395821>.
- [274] S. P. Fritton and S. Weinbaum. "Fluid and Solute Transport in Bone: Flow-Induced Mechanotransduction". In: *Annual Review of Fluid Mechanics* 41 (2009). 401WI Times Cited:69 Cited References Count:145 Annual Review of Fluid Mechanics, pp. 347–374. ISSN: 0066-4189. URL: <http://000262972800017>.
- [275] Bahar Bilgen, I Midey Chang-Mateu, and Gilda A Barabino. "Characterization of mixing in a novel wavy-walled bioreactor for tissue engineering". In: *Biotechnology and Bioengineering* 92.7 (2005), pp. 907–919. ISSN: 1097-0290.
- [276] Chien-Tsun Chen et al. "Coordinated changes of mitochondrial biogenesis and antioxidant enzymes during osteogenic differentiation of human mesenchymal stem cells". In: *Stem Cells* 26.4 (2008), pp. 960–968.
- [277] Girish Pattappa et al. "The metabolism of human mesenchymal stem cells during proliferation and differentiation". In: *Journal of cellular physiology* 226.10 (2011), pp. 2562–2570.

- [278] Lea Bjerre et al. “Flow perfusion culture of human mesenchymal stem cells on silicate-substituted tricalcium phosphate scaffolds”. In: *Biomaterials* 29.17 (2008), pp. 2616–2627. ISSN: 0142-9612.
- [279] Frank W Janssen et al. “A perfusion bioreactor system capable of producing clinically relevant volumes of tissue-engineered bone: in vivo bone formation showing proof of concept”. In: *Biomaterials* 27.3 (2006), pp. 315–323. ISSN: 0142-9612.
- [280] M. Grellier et al. “Responsiveness of human bone marrow stromal cells to shear stress”. In: *J Tissue Eng Regen Med* 3.4 (June 2009). Grellier, Maritie Bareille, Reine Bourget, Chantal Amedee, Joelle England *J Tissue Eng Regen Med*. 2009 Jun;3(4):302-9. doi: 10.1002/term.166., pp. 302–9. ISSN: 1932-7005 (Electronic) 1932-6254 (Linking). URL: <http://www.ncbi.nlm.nih.gov/pubmed/19283726>.
- [281] Y. J. Li et al. “Oscillatory fluid flow affects human marrow stromal cell proliferation and differentiation”. In: *Journal of Orthopaedic Research* 22.6 (Nov. 2004). 866GM Times Cited:124 Cited References Count:46, pp. 1283–1289. ISSN: 0736-0266. URL: <http://www.ncbi.nlm.nih.gov/pubmed/15524762>.
- [282] Seyed Mohammad Jafar Haeri et al. “Osteogenic differentiation of human adipose-derived mesenchymal stem cells on gum tragacanth hydrogel”. In: *Biologicals* 44.3 (2016), pp. 123–128. ISSN: 1045-1056.
- [283] Gregory N Bancroft et al. “Fluid flow increases mineralized matrix deposition in 3D perfusion culture of marrow stromal osteoblasts in a dose-dependent manner”. In: *Proceedings of the National Academy of Sciences* 99.20 (2002), pp. 12600–12605. ISSN: 0027-8424.
- [284] S Scaglione et al. “Effects of fluid flow and calcium phosphate coating on human bone marrow stromal cells cultured in a defined 2D model system”. In: *Journal of Biomedical Materials Research Part A* 86.2 (2008), pp. 411–419. ISSN: 1552-4965.
- [285] Leandro S Gardel et al. “A novel bidirectional continuous perfusion bioreactor for the culture of large-sized bone tissue-engineered constructs”. In: *Journal of Biomedical Materials Research Part B: Applied Biomaterials* 101.8 (2013), pp. 1377–1386. ISSN: 1552-4981.
- [286] R Hernández-Córdova et al. “Indirect three-dimensional printing: A method for fabricating polyurethane-urea based cardiac scaffolds”. In: *Journal of Biomedical Materials Research Part A* (2016). ISSN: 1552-4965.
- [287] Blaise D Porter et al. “Noninvasive image analysis of 3D construct mineralization in a perfusion bioreactor”. In: *Biomaterials* 28.15 (2007), pp. 2525–2533. ISSN: 0142-9612.
- [288] Joanna Filipowska, Gwendolen C Reilly, and Anna M Osyczka. “A single short session of media perfusion induces osteogenesis in hBMSCs cultured in porous scaffolds, dependent on cell differentiation stage”. In: *Biotechnology and Bioengineering* (2016). ISSN: 1097-0290.
- [289] Mary L Bouxsein et al. “Guidelines for assessment of bone microstructure in rodents using micro-computed tomography”. In: *Journal of bone and mineral research* 25.7 (2010), pp. 1468–1486.

- 
- [290] Ming Ding et al. “An automated perfusion bioreactor for the streamlined production of engineered osteogenic grafts”. In: *Journal of Biomedical Materials Research Part B: Applied Biomaterials* 104.3 (2016), pp. 532–537.
- [291] Maxwell V Chor and Wei Li. “A permeability measurement system for tissue engineering scaffolds”. In: *Measurement Science and Technology* 18.1 (2006), p. 208. ISSN: 0957-0233.

# List of Figures

1.1	Graphical abstract . . . . .	3
2.1	Worldwide Regenerative Medicine Companies . . . . .	4
2.2	Overlap and interplay of EU directives . . . . .	6
2.3	Translational research . . . . .	9
2.4	Hierarchical structure of 3D matrices . . . . .	13
2.5	The percolation diameter . . . . .	14
2.6	Aggregate formation . . . . .	15
2.7	Effects of hypoxia . . . . .	21
2.8	Bioreactors in RM . . . . .	23
3.1	Graphical abstract: mesenchymal stem cell isolation . . . . .	31
3.2	Isolation procedures . . . . .	33
3.3	Cellular outgrowth of different isolation procedures . . . . .	34
3.4	Comparison of yields of different isolation procedures . . . . .	34
3.5	Phenotype analysis of cells from different isolation procedures . . . . .	36
3.6	Population doublings of cells from different isolation procedures . . . . .	37
3.7	Population doublings of cells from different isolation procedures until P10 . . . . .	38
3.8	PDL of cells from different isolation procedures until P10 . . . . .	38
3.9	$\beta$ -galactosidase assay . . . . .	39
3.10	Differentiation of cells from different isolation procedures I . . . . .	40
3.11	Differentiation of cells from different isolation procedures II . . . . .	41
3.12	– . . . . .	44
4.1	Graphical abstract: Scaffold-free stem cell cultivation . . . . .	47
4.2	Aggregate Cultivation in Microtiter Plates . . . . .	49
4.3	Upscale of Aggregate Cultivation I . . . . .	50
4.4	Upscale of Aggregate Cultivation II . . . . .	51
4.5	Upscale of Aggregate Cultivation III . . . . .	51
4.7	Dissolved oxygen during cultivation of MSCs in STR . . . . .	54
4.8	Yield, viability and glycolytic activity of MSCs cultivated in a STR . . . . .	54
4.9	Phenotype analysis of MSCs after cultivation in a STR . . . . .	55
4.10	Differentiation of MSCs after cultivation in a STR . . . . .	56
5.1	Graphical abstract: physiologic differentiation . . . . .	59
5.2	The biaxial bioreactor by Quinxell . . . . .	61



---

5.3	Viability after cultivation in the biaxial bioreactor . . . . .	62
5.4	DAPI stain after cultivation in the biaxial bioreactor . . . . .	62
5.5	Calcein stain after cultivation in the biaxial bioreactor . . . . .	62
5.6	The mini perfusion bioreactor . . . . .	64
5.7	The incubator system . . . . .	65
5.8	Pressure sensors and permeability . . . . .	66
5.9	CFD simulation of shear stress in two bioreactor chambers . . . . .	67
5.10	Comparison of shear stress calculations . . . . .	68
5.11	CFD simulation of fluid flow in two bioreactors . . . . .	70
5.12	Comparison of bioreactor chambers: cell number and ALP activity . . . . .	72
5.13	Comparison of bioreactor chambers: DAPI-calcein doublestain . . . . .	72
5.14	Comparison of bioreactor chambers: glycolytic activity . . . . .	73
5.15	Comparison of bioreactor chambers: matrix mineralization . . . . .	74
5.16	Characterization of Tutoplast: SEM and HE stain . . . . .	79
5.17	Characterization of Tutoplast: microCT scans . . . . .	80
5.18	Biomaterial testing of Tutoplast . . . . .	80
5.19	Optimization of shear stress conditions: ALP activity and viability . . . . .	81
5.20	Hydrostatic pressure regimes . . . . .	82
5.21	Optimization of hydrostatic pressure conditions: ALP activity and viability . . . . .	82

# List of Tables

2.1	Definitions of medicinal products . . . . .	7
2.2	Approved ATMPs . . . . .	8
2.3	Mechanical forces in the human body . . . . .	19
2.4	Growth factors in blood-derived products . . . . .	20
2.5	Crucial factors for cultivation of MSCs . . . . .	22
2.6	Commercially available bioreactors . . . . .	27
2.7	Design and development of bioreactors . . . . .	28
3.1	Cellular outgrowth and harvest of different isolation procedures . . . . .	32
3.2	Comparative overview of isolation procedures. . . . .	43
4.1	Comparison of upscale approaches . . . . .	52
4.2	Differentiation of MSCs from aggregate cultivation . . . . .	55
5.1	Comparison of shear stress calculations . . . . .	68
5.2	Characteristics of fluid flow in two bioreactors . . . . .	69
5.3	Residence time distribution and hydrodynamic residence time . . . . .	69
5.4	Comparison of Tanks in series and Bodenstein number in two bioreactors . . . . .	71
5.5	Comparison of bioreactor chambers: glycolytic activity . . . . .	73
5.6	Overview of BR1 and BR2 . . . . .	76
5.7	Characteristic parameters of Tutoplast . . . . .	77
5.8	Fluid shear stress conditions in flow rate optimization . . . . .	78
A.1	This table contains all used devices. . . . .	113
A.2	This table contains all used disposables. . . . .	114
A.3	This table contains all used chemicals. . . . .	114
A.4	This table contains all used buffers and solutions. . . . .	116
A.5	This table contains all used kits. . . . .	116
A.6	This table contains all used media. . . . .	117
A.7	This table contains all components from which the custom bioreactors were set up. . . . .	117
A.8	This table contains all used software. . . . .	118
B.1	Detailed list of cells used in experimental procedures. . . . .	119
B.2	Valve settings for the application of different pressure regimes. . . . .	122

# A Material

## A.1 Instruments and laboratory equipment

**Table A.1:** This table contains all used devices.

Product	Manufacturer
Autoclave, Varioklav 500E	Thermo Scientific
Balance, AW-9202 and AW-224	Sartorius
BD FACS Canto II	
Cell counting chamber, Neubauer improved	Brand
Centrifuge, 5702 and 5415 R	Eppendorf
Centrifuge, HERAEUS AC017	Thermo Scientific
Scanner Epson V33	Epson
Fluorescence microscope DMIL LED	Leica
Fluorescence microscope camera DFC42C	Leica
Fluorescence microscope light EL6000	Leica
Fluorescence filter system I3 S DMIL	Leica
Incubator, HERACELL 150i	Thermo Scientific
Incubator, HERACELL 240i	Thermo Scientific
Incubator with integrated pumps	IncuReTERM GmbH
Liquid nitrogen tank, Cryotherm 55121	BiosafeMD
Magnetic stirrer	IKA Labortechnik
Micro-CT, $\mu$ CT35	Scanco Medical AG
Microscope (transmitted light), DMIL LED	Leica
Microscope camera, ICC50HD	Leica
Nano-CT, VersaXRM-500	Xradia, Inc.
Nitrogen generator	Parker
Oxygen sensor transmitter, OXY4Mini	Presens
Pipettes Research <sup>®</sup> Plus	Eppendorf
Pipetting aid Pipetboy acu	IBS Integra Biosciences
Platereader, Infinite <sup>®</sup> M1000 PRO	Tecan
Platereader, MultiSkan FC	Thermo Fisher Scientific
Scanning electron microscope JSM-6510	JEOL
Shake flask reader (SFR)	Presens
Shaker, Skyline Orbital Shaker	ELMI
Shandon Tissue Excelsior	Thermo Fisher Scientific

Sterile workbench, HERASAFE KS	Thermo Scientific
Sterile workbench, MSC Advantage	Thermo Scientific
Vortexer, Vortexgenie 2	Scientific Industries
Water bath	GFL

## A.2 Disposables

**Table A.2:** This table contains all used disposables.

Product	Manufacturer	Order number
6, 24, 96 well plates	Sarstedt	83.3920, 83.3922, 83.3924
12 well plate	TPP	92012
12 well fibrin coated well plate	BD Bioscience	354501
96 well, black, transparent bottom	greiner bio-one	655906
Cell culture flask 25, 75, 175 cm <sup>2</sup>	Sarstedt	83.3910, 83.3911, 83.3912
Cell strainer	Falcon <sup>®</sup>	352340
Centrifuge tube 15, 50 ml	greiner bio-one	188271, 227261
Cryo tube, CRYO.S, 2 ml	greiner bio-one	122278
Parafilm <sup>®</sup> M	Brand	291-1213
Pasteur pipettes	Brand	747720
/Pipette tip 0.5 – 50 $\mu$ l	Roth	9260.1
Pipette tip 10 – 200 $\mu$ l, 50 – 1000 $\mu$ l	Brand	732008, 732012
Reaction tube, safe seal 1.5 ml	Sarstedt	72.706
Sterile filter, Filtropur S 0.2 $\mu$ l	Sarstedt	83.1827
Syringe 5 ml	Braun	4617053V
Syringe 10 ml	Terumo <sup>®</sup>	SS-10L
Serological pipettes (2 – 50 ml)	greiner bio-one	710180, 606180, 607180, 760180, 768180
Sponceram <sup>®</sup>	Zellwerk	1011052
Tutoplast, 4 – 10 mm cancellous chips	RTI Biologics <sup>™</sup> -Tutogen	68123

## A.3 Chemicals

**Table A.3:** This table contains all used chemicals.

Product	Manufacturer	Order number
$\alpha$ MEM basal medium	Thermo Fisher Scientific	12000
Accutase <sup>®</sup> solution	Sigma Aldrich	A6964

Accumax <sup>TM</sup> solution	Sigma Aldrich	A7089
Alcian Blue 8GX	Sigma Aldrich	A3157
Alicarin Red S	Carl Roth	0348.2
Calcein	Sigma Aldrich	C0875
Calcein AM	Sigma Aldrich	C1350
Calcium chloride	Sigma Aldrich	C1016
Collagenase	Sigma Aldrich	C2673
DAPI	Sigma Aldrich	D8417
Dexamethasone	Sigma Aldrich	D4902
DMSO	Sigma Aldrich	D8418
Dulbeccos MEM (DMEM)	Sigma Aldrich	D7777
Eosin Y solution	Carl Roth	3137.1
Ethanol 96 %	AustrAlco	Ps-025-14
Ethanol Rotipuran 99,8 %	Carl Roth	
Fibronectin from human plasma	Biochrom GmbH	L7117
Formaldehyde solution 36.5 –38 %	Sigma Aldrich	F8775
Gentamycin (10 mg/ml)	Lonza	LZBE02-012E
Glutaraldehyde (50 %)	Carl Roth	203856
$\beta$ -glycerolphosphate	Sigma Aldrich	50020
Hank's Buffer	Sigma Aldrich	H2387
Heparin	Ratiopharm	3029820
Hematoxylin	Richard Allan Scientific	
Human platelet lysate	PL Bioscience	PL-S-100-01
L-ascorbat-2-phosphat	Sigma Aldrich	A4544
Magnesium chloride	Sigma Aldrich	M8266
NH AdipoDiff Medium	Miltenyi Biotec GmbH	130-091-677
NH ChondroDiff Medium	Miltenyi Biotec GmbH	130-091-679
NH OsteoDiff Medium	Miltenyi Biotec GmbH	130-091-678
Nonident P40	Sigma Aldrich	74385
Oil Red O solution (0.5 %)	Sigma Aldrich	O1516
Phosphate buffered saline	Thermo Fisher Scientific	21600044
PL <sub>MATRIX</sub>	PL Bioscience	PLM-005.01
pNPP tablet	Sigma Aldrich	N2270
Propidium iodide	Sigma Aldrich	202398
Protein kinase K	Sigma Aldrich	P6556
SDS-solution	Sigma Aldrich	71736
Silver nitrate solution (5 %)	Carl Roth	N053.1
Sodium carbonate	Sigma Aldrich	S7795
Sodium chloride	Sigma Aldrich	S5888
Sodium hydrogen carbonate	Sigma Aldrich	401676
Tetrazolium bromide (MTT)	Sigma Aldrich	M5655
Tris	Applichem	A2264

Tris buffered saline	Sigma Aldrich	T5030
Tris tablet	Sigma Aldrich	N2270
Trypan blue	Sigma Aldrich	T8154

## A.4 Buffers and solutions

**Table A.4:** This table contains all used buffers and solutions.

Solution	Composition
Alcian blue solution	1 % (w/v) alcian blue in 3 % acidic acid
Alicarin red solution	0.5 % (w/v) alicarin red in ddH <sub>2</sub> O
Calcein-AM stock solution	1 mM calcein-AM in DMSO
DAPI buffer	100 mM Tris pH 7, 150 mM NaCl, 1 mM CaCl <sub>2</sub> , 0.5 mM, MgCl <sub>2</sub> , 0.1 % Nonident-P40
DAPI stock solution	20 mg/ml DAPI in ddH <sub>2</sub> O
Flow cytometry buffer	0.5 % FBS, 2 mM EDTA in PBS
Hank's buffer I	9.5 g/l in ddH <sub>2</sub> O
Hank's buffer II	2.5 % human platelet lysate in Hank's buffer I
Lysis buffer	10 mM Tris HCl pH 8.5, 5 mM EDTA, 0.2 % SDS, 0.2 M NaCl, 0.1 mg/ml protein kinase K
MTT stock solution	5 mg/ml in PBS
pNPP stock solution	1 Tris buffer tablet, 1 pNPP tablet in 4 ml ddH <sub>2</sub> O and 2 ml PBS
PI stock solution	151.1 $\mu$ M PI in ddH <sub>2</sub> O
SDS solubilization solution	5 % (w/v) in 0.01 M HCl
TE buffer	Tris HCl pH 7.5, EDTA 0.1 mM
Von Kossa decolorization solution	5 % Na <sub>2</sub> CO <sub>3</sub> , 0.2 % formaldehyde in ddH <sub>2</sub> O

## A.5 Kits

**Table A.5:** This table contains all used kits.

Product	Manufacturer	Order number
In vitro toxicology assay kit (TOX8)	Sigma Aldrich	TOX8-1KT
MSC Phenotyping kit, human	Miltenyi Biotec GmbH	130-095-198
Quant-iT <sup>TM</sup> PicoGreen <sup>®</sup> dsDNA Assay Kit	Thermo Fisher Scientific	P7589
Senescence $\beta$ -galactosidase staining kit	Cell Signalling Technology	9860S

## A.6 Media

**Table A.6:** This table contains all used media.

Media	Composition
Cryo-medium	Culture medim, 10 % (v/v) human platelet lysate, 10 % (v/v) DMSO
Culture medium	2.5 % (v/v) human platelet lysate, 0.5 % (v/v) gentamycin, 1 U/ml heparin in $\alpha$ MEM
Osteogenic medium	2.5 % human platelet lysate, 5 mM $\beta$ -glycerolphosphate, 0.1 $\mu$ M dexamethasone, 0.2 mM L-ascorbate-2-phosphate, 0.5 % gentamycin, 1 U/ml heparin in $\alpha$ MEM
Chondrogenic medium	NH ChondroDiff, 0.5 % gentamycin
Adipogenic medium	NH AdipoDiff, 0.5 % gentamycin

## A.7 Bioreactor components

**Table A.7:** This table contains all components from which the custom bioreactors were set up.

Component	Manufacturer	Order number
Continuously stirred tank reactor	TERM, University Hospital Würzburg	
Fluran <sup>®</sup> fluorelastomer tubing	VWR	63014
Luer Lock connector female	Pieper-Filter	NM-LF S16
Luer Lock connector male	Pieper-Filer	PP-LM S16
Mini-Perfusion bioreactor BR1	Workshop of the Institute of Technical Chemistry, Leibniz University Hannover	
Mini-Perfusion bioreactor BR2	Workshop of the Institute of Chemistry, University Graz	
O-Ring EPDM 70, 6 x 1 mm	Carl-Otto-Gherkens	A4N2035748
Pressure sensor SP-844	MEMSCAP	
Pressure transducer SP-844-28 for SP-844	MEMSCAP	
Pump Hose BPT 1.52 mm	PharMed	070539-19
Silicon tubing (1.5 x 3 mm)	VWR	VWRI 228-0702

## A.8 Software

**Table A.8:** This table contains all used software.

Product	Company	Version
Adobe InDesign	Adobe Systems	CC 2015/2017
BD FACS DIVA™	BD Bioscience	
COMSOL Multiphysics	COMSOL AB	5.0
Drishti	ANU Vizlab	2.0
Excel	Microsoft	2013/2016
MATLAB	The MathWorks, Inc.	R2014a
Motion Manager	FAULHABER	5
Fiji ( <i>Fiji is just ImageJ</i> )	Open source	
GraphPad PRISM	GraphPad Software	6
Image Composite Editor	Microsoft	2.0
Kaluza Flow Cytometry	Beckman Coulter, Inc.	1.3
OriginPro	OriginLab	2015
SolidWorks	Dassault Systèmes	2015



## B Methods

### B.1 Cell culture

**General notes on cell culture** All sterile work was performed in a class II workbench while all used equipment was sterilized with 70 % ethanol before use. All flasks were autoclaved for 30 min at 120 °C and liquid solutions sterile filtered or autoclaved as well. If not stated otherwise all liquids were pre-warmed to 37 °C in a water bath.

**General notes on isolation of stem cells** Mesenchymal stem cells used in the experiments of this work were isolated from human adipose tissue of different donors and origins as listed in table B.1. Cells of different donors were used as declared in the description of each experimental procedure respectively. Adipose tissue was received from the department of plastic and reconstructive surgery Wilhelminenspital, Vienna, Austria. All patients gave written informed consent. The tissue was processed within 4 h after surgery.

**Table B.1:** Detailed list of cells used in experimental procedures.

Sex	Age	Origin	Date	Used in section
Female	42	Abdominoplasty	20.01.16	Mesenchymal Stem Cell Isolation (3)
Female	52	Abdominoplasty	02.03.16	Mesenchymal Stem Cell Isolation (3)
Female	48	Breast reconstruction	17.08.16	Mesenchymal Stem Cell Isolation (3); Aggregate Cultivation in a Stirred Tank Reactor (4.4); Characterization (5.3.2)
Male	40	Abdominoplasty	11.11.15	Mesenchymal Stem Cell Isolation (3); Approaches for Upscale of Aggregate Cultivation (4.3)
Female	50	Abdominoplasty	03.02.15	Aggregate Cultivation in Microtiter Plates (4.2); Application (5.3.3)
Female	55	Abdominoplasty	12.07.13	Aggregate Cultivation in Microtiter Plates (4.2); Approaches for Upscale of Aggregate Cultivation (4.3); Biaxial Bioreactor (5.2); Application (5.3.3)

**Isolation via enzymatic treatment** For the isolation of MSCs from adipose tissue via enzymatic digestion the tissue was cut into portions of approximately 20 g (the exact amount was noted for determination of the yield) avoiding blood vessels and connective tissue and transferred to a 50 ml centrifugation tube. Subsequently, the portions were minced to a homogeneous pulp, 10 ml collagenase solution (2 mg/ml in Hank's buffer I) were added and incubated for 1 h at 37 °C after vortexing. Following, the digested pulp was vortexed again, half of the volume transferred

to a new centrifuge tube, topped up to 40 ml with Hank's buffer I and centrifuged for 5 min at 200 x g. The fatty supernatant was transferred to a new centrifuge tube, the middle layer (collagenase solution) was discarded and the flicked pellet (stromal vascular fraction) transferred to the fatty supernatant. Afterwards, the tube was topped up to 40 ml with Hank's buffer I and centrifuged for 10 min at 400 x g. The supernatant was removed, the pellet resuspended in 40 ml Hank's buffer II and centrifuged for 10 min at 400 x g. Afterwards, the supernatant was discarded, the pellet resuspended in 30 ml culture medium and transferred to a T-175 flask. The flasks were incubated at 21 or 5 % O<sub>2</sub> for 3 – 7 days until adherent cells were observed. Subsequently, the medium and remaining tissue pieces were removed and fresh medium added. After cells grew about 80 – 90 % confluent they were subcultivated or cryopreserved.

**Isolation via explant culture** For the isolation of MSCs from adipose tissue via explant culture the tissue was cut into portions of approximately 10 g (exact weight was noted for determination of yield). The tissue portion was rinsed with PBS to remove remaining blood and cut into pieces of approximately 5 mm<sup>3</sup> which were placed on cell culture dishes (100 mm diameter). Each dish was carefully covered with 2.5 ml culture medium to avoid floating of the fat tissue and incubated at 21 or 5 % O<sub>2</sub> for 7 – 9 days until adherent cells were observed. Following, tissue pieces were removed and dishes rinsed with PBS to remove fatty droplets. Fresh medium was added (2.5 ml) and cells were cultivated for another 2 – 3 days until approximately 80 % confluency was reached. Afterwards, cells were subcultivated or cryopreserved.

**Cell thawing** In order to thaw cryopreserved cells the cryo vial was transferred to a 37°C water bath and thawed only just until the cell suspension became liquid. Subsequently, 1 ml room temperate  $\alpha$ MEM was added, the cell suspension transferred to a centrifugation tube and the vial rinsed with 2 ml  $\alpha$ MEM. After 2 min the cell suspension was filled up to 10 ml with  $\alpha$ MEM and centrifuged 5 min at 300 x g. The supernatant was removed, cells resuspended in 15 ml culture medium, the cell suspension transferred to a T-75 flask and incubated at 37°C.

**Subcultivation** If not stated otherwise cells were cultivated in T-flasks and microtiter plates of different sizes in a standard incubator at 37°C, 5 % CO<sub>2</sub> and 21 % O<sub>2</sub>. For subcultivation cells were seeded at 3000 or 4000 cells/cm<sup>2</sup> and allowed to grow approximately 80 % confluent. To detach cells for further cultivation they were rinsed with PBS and incubated in Accutase at 37°C (10 – 15 min). Accutase treatment was stopped with 1.5-fold volume of culture medium and the cell suspension transferred into a centrifuge tube for centrifugation at 300 x g for 5 min. After removal of supernatant the pellet was dissolved in culture medium, the cell number was determined with a counting chamber and cells seeded again.

**Cryopreservation** In order to cryopreserve cells they were centrifuged at 300 x g for 5 min and resuspended in cryo-medium at a density of 1·10<sup>6</sup> cells/ml. Subsequently, 1 ml of the cell suspension was transferred to a cryo vial and cooled down to -80°C over night. Within 1 – 3 days cryo vials were transferred to a liquid nitrogen tank (-196°C) for long term storage.

## B.2 Three dimensional cell culture

Since cell culture on three dimensional matrices differs from standard two dimensional cell culture approaches the following sections will cover the basic principles of the different three dimensional cell culture approaches.

**Scaffold-free aggregate cultivation in a microtiter plate** For scaffold-free cultivation mesenchymal stem cells (MSCs) were seeded at different densities in a 96 well round bottom plate with cell repellent surface. The plate was either cultivated static (no agitation) or placed on an horizontal shaker at 100 RPM in a standard incubator. Cultivation was carried out for 4 days while medium was not changed. For cultivation in continuously stirred tank reactor please refer to B.3.

**Sponceram** For cultivation of MSC on Sponceram the discs were autoclaved prior to seeding. MSC in passage 2 were centrifuged at 300 x g for 5 min and resuspended in culture medium to a density of  $6 \cdot 10^6$  cells/ml. The Sponceram discs were placed into a 24 well plate, evenly covered with 50  $\mu$ l of the cell suspension ( $3 \cdot 10^5$  cells) and incubated without additional medium for 2 h in a standard incubator. Afterwards, the scaffolds were covered with 2 ml medium and incubated for 3 – 4 days before further static cultivation or dynamic cultivation in a bioreactor system.

**Tutoplast** Tutoplast is provided freeze-dried by the manufacturer. To ensure the entire scaffold is accessible for cells it needed to be rehydrated and degassed. For this, Tutoplast chips were placed into a syringe with culture medium. The syringe was closed with a female Luer lock and the piston was pulled in order to generate a vacuum. Consequently, the trapped air was released by unscrewing the Luer lock and the procedure repeated until no air bubbles left the scaffold anymore. Rehydrated chips were stored at 4 °C for up to one week. Prior to seeding the scaffolds were room tempered and placed into a 24 well plate. MSC in passage 2 were centrifuged at 300 x g for 5 min and resuspended in culture medium to a density of  $2 \cdot 10^6$  cells/ml. Subsequently, each sample was covered with 50  $\mu$ l of the cell suspension ( $1 \cdot 10^5$  cells) and incubated without additional medium for 2 h in a standard incubator. After that, the scaffolds were covered with 2 ml medium and incubated for 3 – 4 days prior to further static cultivation or dynamic cultivation in a bioreactor system.

## B.3 Bioreactor cultivation

**Biaxial rotating bioreactor** Prior to cultivation the biaxial rotating bioreactor was steam sterilized and MSC in passage 2 were seeded on Sponceram according to B.2. The seeded scaffolds were incubated for 1 day in a standard incubator before they were transferred to the bioreactor chamber and attached to the scaffold mount. The medium bottle was filled with 120 ml medium and the entire system was located to a standard incubator at 37 °C and 21 or 5 % O<sub>2</sub> respectively. Subsequently, the medium pump was set to 12 RPM ( $\cong$  12 ml/min) and the rotation speed was set to 10 RPM for the L-arm and 20 RPM for the bioreactor chamber. Samples were cultivated for 21 days and medium changes were performed on day 7 and 14 (50 ml).

**Mini-perfusion bioreactor** Prior to cultivation the mini-perfusion bioreactor system was steam sterilized and MSC in passage 2 were seeded on Sponceram or Tutoplast according to B.2. Sponceram was placed into the bioreactor chambers BR1 or BR2 upside down with the seeded side facing the bottom of the chamber. Because of its irregular shape Tutoplast was placed randomly into the chamber (three seeded samples per chamber). The medium reservoir was filled with 10 ml culture medium or osteogenic medium, respectively. The bioreactors were placed into the IncuReTERM incubator, flow rate was set according to the respective experiment (s. 5.3) and the system was then perfused with medium continuously for 21 or 6 days. For analyses 1 ml medium was changed every 2 – 3 days whereas 7 ml were replaced on day 7 and 14. For medium changes perfusion was stopped, bioreactors disconnected from peristaltic pumps and transferred to a sterile workbench. At the end of each experiment the samples were carefully removed from the chambers by either pressing them carefully out with a pipette tip (Sponceram) or by transferring them with forceps (Tutoplast) into a well plate for further analyses.

For the application of hydrostatic pressure the bioreactors were setup up in a "single-reactor setup" as depicted in Figure 5.7. To apply defined hydrostatic pressure (HP) rgmies pinch valves of the incubator were programmed to different open/close regimes (see Table B.2)

**Table B.2:** Valve settings for the application of different pressure regimes.

Target pressure (mmHg)	Valve closed (s)	Valve open (s)	Time closed during 3 h
100	148	8	80
250	301	20	32
500	498	40	20

**Continuously stirred tank reactor** After steam sterilization the CSTR was filled with PBS at 37 °C in order to calibrate the PreSens oxygen sensor. The tank was filled and emptied through one of the ports in the lid while the lid itself was kept closed at all time.

**Seeding:** After calibration PBS was removed with a suction pump and the tank was filled with 130 ml of a  $1 \cdot 10^5$  cells/ml single cell suspension of MSCs in passage 2 ( $13 \cdot 10^6$  cells total). Cell culture medium with 10 instead of 2.5 % human platelet lysate (HPL) was used. Cells for cultivation at 5 % O<sub>2</sub> have been also isolated and subcultivated at 5 % O<sub>2</sub> until seeding. After seeding the port was closed and the bioreactor transferred to the IncuReTERM incubator. The motor was mounted at the top of the lid and connected to the drive shaft of the impeller. Also, the fiberglass cable was placed on the oxygen sensor spot. Afterwards, the impeller speed was set to 600 revolutions per minute (RPM) in the "FAULHABER Motion Manager" software. Atmospheric oxygen was set to 21 or 5 %, respectively.

**Medium change:** After 3 days 100 ml of the medium was replaced. For this, motor and sensor cable were disconnected and the bioreactor transferred to a sterile workbench. Aggregates and cells were allowed to sediment for 15 min before medium was removed from the bioreactor to 4 50 ml centrifugation tubes (each 25 ml). Subsequently, the tubes were centrifuged for 5 min at 500 x g, the supernatant removed and the pellets flicked. 25 ml fresh medium was added to

the first tube in order to resuspend the pellet and after that used to resuspend the pellet of the other tubes. Finally, the medium was transferred back into the bioreactor. Again, 25 ml fresh medium was added to the first tube in order to rinse the tube, and after that used to rinse the other tubes. After these 25 ml were transferred to the bioreactor the remaining 50 ml were added directly to the bioreactor. The bioreactor was again connected to the motor and sensor cable and the impeller started.

**Cell counting:** After 6 days the impeller was stopped and the medium containing cells and aggregates was transferred to 4 50 ml centrifugation tubes, the tank was rinsed with 40 ml PBS, the PBS added to the tubes (10 ml per tube) and the tubes centrifuged for 5 min at 500 x g. The bioreactor tank was filled with 25 ml of a 37°C pre-warmed Accumax solution and incubated 15 min at 37°C in order to remove adherent cells from the glass wall. In parallel, the supernatant was removed, the pellets resuspended in 40 ml PBS, unified in one tube and again centrifuged for 5 min at 500 x g. The supernatant was removed and the pellet resuspended in the Accumax solution from the bioreactor tank. After this, the solution was incubated 15 min in a 37°C water bath. Then, cells were counted by trypan blue staining in a cell counting chamber, and the solution was set on a horizontal shaker at 300 RPM and 37°C in order to dissociate the aggregates completely. Cells were counted by trypan blue staining after 15, 30 min of incubation determine cell number and viability (overall 45 min incubation). Then, the cell suspension was passed through a cell strainer to separate single cells from remaining aggregates and the cell strainer was placed in a 6 well plate. After centrifugation (5 min at 300 x g) 6 ml of the Accumax solution was transferred to the cell strainer in the 6 well plate to dissociate remaining aggregates. The remaining Accumax solution was removed from the cell pellet and the pellet was resuspended in 25 ml fresh culture medium for further subcultivation or cryopreservation. The 6 well plate with the cell strainer was placed on a horizontal shaker, incubated for 1 h at 37°C and 100 RPM. Afterwards, cells were counted again.

## B.4 Biomaterial characterization

**Permeability** To measure the permeability of a porous scaffold the pressure inside the bioreactor system was measured simultaneously upstream ( $P_1$ ) and downstream of the bioreactor chamber ( $P_2$ ) at different flow rates (see Figure 5.8). The differential pressure  $\Delta P$  ( $P_1 - P_2$ ) can be used together with characteristics of the biomaterial to calculate the permeability  $k$  with Darcy's law:

$$k = \frac{(Q \cdot \mu \cdot h)}{(A \cdot \Delta P)} \quad (\text{B.1})$$

where  $Q$  refers to the volumetric flow rate,  $\mu$  is the dynamic viscosity of water at 37°C,  $h$  is the height and  $A$  the area of the biomaterial. Permeability was determined for the ceramic zirconium dioxide matrix Sponceram which has been characterized extensively before and was shown to have bone-like properties [273]. It has a porosity of 66.7%, an average pore size of 510  $\mu\text{m}$ , a diameter of 10 mm and a thickness of 3 mm. The differential pressure was measured at different flow rates ranging from 1.5 to 15 ml/min (increment of 0.5 ml/min) with the same setup

used during sensor characterization. The data was recorded with the incubator's data acquisition. Each flow rate was measured for 10 min resulting in  $4484 \pm 71$  data points for each flow rate and measurement. Three randomly picked Sponceram discs were used for the measurements (each  $n = 3$ ).

## B.5 Bioreactor characterization

**Pressure sensors** The pressure in the bioreactor tubing system was studied for each sensor separately at flow rates ranging from 1.5 to 15 ml/min. For this, the pump was programmed to increase the flow rate stepwise by 0.5,ml/min every 10,min ( $n=3$ ). As the data acquisition system recorded each change in pressure these measurements resulted in  $4423 \pm 4$  data points for each flow rate. A circular bioreactor setup filled with ddH<sub>2</sub>O at 37°C was used during sensor characterization (see Figure 5.8).

**Shear stress calculation** After determination of permeability the fluid shear stress that cells on the scaffold surface are exposed to was estimated with a mathematical model.

For laminar flow systems, the wall shear stress  $\tau_\omega$  is defined by the normal velocity gradient at the wall:

$$\tau_\omega = \mu \frac{\partial u}{\partial n} \quad (\text{B.2})$$

where  $\mu$  is the dynamic viscosity,  $u$  the flow velocity and  $n$  the  $x$ -,  $y$ - and  $z$ -direction. Based on Equation B.2 the average ( $\tau_{\omega avg}$ ) and maximum shear stress ( $\tau_{\omega max}$ ) was calculated from the entire scaffold domain which was introduced in the COMSOL model as described in section B.5 *Computational fluid dynamics analyses*. Furthermore, the computational fluid dynamics (CFD) derived shear stress was compared with a model proposed by Vossenberget al. [261] which uses the permeability constant  $k$  as an indicator for shear stress. It also uses the permeability constant  $k$  to calculate the average ( $\tau_{\omega avg}$ ) and maximum shear stress ( $\tau_{\omega max}$ ) at a flow velocity of 100  $\mu\text{m/s}$ :

$$\tau_{\omega avg} = 9.82 \cdot 10^{-12} k^{-0.914} \quad (\text{B.3})$$

$$\tau_{\omega max} = 3.36 \cdot 10^{-10} k^{-0.807} \quad (\text{B.4})$$

In fact, equations B.3 and B.4 are only valid in systems with laminar flow assuming Darcy's law is applicable. This is the case as long as the interstitial Reynolds number  $Re_i < 8$  [291]. Consequently,  $Re_i$  was calculated from the bioreactor and scaffold parameters:

$$Re_i = \frac{(\rho \cdot \psi \cdot D_P)}{(\mu (1 - \varepsilon))} \quad (\text{B.5})$$

where  $\rho$  is the density of water at 37°C,  $D_P$  the average pore diameter,  $\psi$  the sphericity (for simplicity assumed to be 1) and  $\varepsilon$  the porosity.

If permeability  $k$  of a biomaterial is not known, shear stress can also be estimated with a more simple approach suggested by Goldstein [132]. It assumes as uniform flow across the (scaffold) surface and a parabolic flow through cylindrical pores. The mean velocity  $u_m$  is then given by

$$u_m = \frac{Q}{\varepsilon \pi \left(\frac{D}{2}\right)^2} \quad (\text{B.6})$$

where  $Q$  is the volumetric flow rate,  $\varepsilon$  is the porosity and  $D$  is the bioreactor (and scaffold) diameter.  $\tau_\omega$  is then given by

$$\tau_\omega = 8\mu \frac{u_m}{D_P} \quad (\text{B.7})$$

**Computational fluid dynamics analyses** To estimate the flow profile and streamlines in the perfusion bioreactor, 3D models were generated with CAD in Solidworks 2015 and imported to COMSOL Multiphysics. The porous media flow model was used where the steady-state Navier-Stokes equations were solved. The material was set to *water* at 37°C, the inlet boundary condition to *velocity* with *normal inflow velocity* and the outlet boundary condition was set to *pressure*. For all solid walls *no slip* boundary conditions were set. The mesh was created by COMSOL with a *normal* element size. The shear stress distribution in a porous scaffold was simulated with same model. To simplify the scaffold a cylinder of the same dimensions with porous matrix conditions was introduced to the model. Porosity and permeability were set according to the characteristics of the scaffold (for Sponceram porosity is 66.7% and permeability is  $1.7 \pm 0.9 \cdot 10^{-10} \text{ m}^2$ ). A stationary study was conducted using 3.6, 17.8 and 35.6 mm/s as flow velocities at the bioreactor inlet which corresponds to the volumetric flow rates of 1.5, 7.5 and 15 ml/min. The velocity profile, streamlines and shear stress distribution of the bioreactor chambers were plotted from these results.

**Residence time distribution** To characterize the mixing behavior of a bioreactor system the residence time distribution (RTD) can be obtained from wash out experiments. For this a Dirac pulse with a tracer substance is injected at the entrance of the bioreactor chamber. Simultaneously the concentration of the tracer substance at the exit is measured. First the bioreactor volume  $V_R$  was measured by weighing the reactor chamber with and without water. The volumetric flow rate  $Q$  was measured by weighing the water that was pumped through the system within a certain time. The hydrodynamic residence time  $T$  was derived from  $V_R/Q$ . To obtain the RTD a Dirac pulse of 100  $\mu\text{l}$  methylene blue solution 1:18 in ddH<sub>2</sub>O was injected at the entrance of the bioreactor chamber during perfusion. Drops were collected 10 cm downstream in a 96 well plate and the absorbance at 688 nm of each well was measured with a plate reader. The measurement was carried out for  $t = 0 \dots 4 \cdot T$  at 0.6, 1.5 and 3 ml/min (at least n=3). The RTD was then derived from the data collected in the washout experiments as described before [187]. Briefly, the residence time function  $E(t)$  is calculated by dividing the concentration of the tracer at each time point by the integral of the tracer concentration from  $t = 0 \dots 4 \cdot T$ . To compare measurements of different bioreactors, the dimensionless residence time function  $E(\Theta)$  can be derived from  $E(t)$ .

The tanks-in-series (TIS) model describes real bioreactors as a cascade of perfectly mixed continuous stirred tank reactor (CSTR) with  $N$  tanks in series [208]. For  $N \rightarrow 1$  the bioreactor behaves like a CSTR, for  $N \rightarrow \infty$  it behaves like plug flow reactor (PFR) without any axial mixing. Data obtained in the washout experiments was fit to the TIS model with a global curve fit using the software OriginPro with  $N$  as the key parameter of the following equation:

$$E(\Theta) = \frac{N(N\Theta)^{(N-1)}}{(N-1)!} e^{-N\Theta} \quad (\text{B.8})$$

A real bioreactor can also be described with the dispersion model where the dimensionless Bodenstein number  $Bo$  describes the ratio between convective transport to axial diffusion. For a system with open-open boundary conditions it can be derived from the response curve of a Dirac pulse as follows:

$$Bo = \frac{1 + \sqrt{8 \cdot \sigma_{\Theta}^2 + 1}}{\sigma_{\Theta}^2} \quad (\text{B.9})$$

$$\sigma_{\Theta}^2 = \frac{\sigma^2}{T^2} \quad (\text{B.10})$$

with  $\sigma^2$  as the variance and  $\sigma_{\Theta}^2$  as the dimensionless variance. For  $Bo \rightarrow 1$  the axial dispersion is high indicating strong back mixing. For  $Bo \rightarrow \infty$  the axial dispersion is 0 indicating no back mixing.

## B.6 Assays

**Differentiation capacity** To determine the differentiation capacity MSC were seeded in passage 2 at 4000 cells/cm<sup>2</sup> in a fibronectin coated 12 well plate (either manually coated or pre-coated by manufacturer). Manually coated plates were coated with 2 μg/cm<sup>2</sup> fibronectin (152 μl of a 50 μg/ml fibronectin in ddH<sub>2</sub>O). The plates were air dried for 45 min at room temperature, sealed with parafilm and stored at 4 °C. Prior to use wells were rinsed once with PBS. After seeding cells were allowed to grow confluent (usually 2 – 3 days) and the medium was changed to adipogenic, chondrogenic or osteogenic differentiation medium respectively. Cells were cultivated in differentiation medium for 21 days and medium changed every 2 – 3 days. On day 21 the cells were fixated with ethanol or paraformaldehyde according to the respective staining.

**Proliferation capacity** For the determination of the proliferation capacity of MSC isolated by enzymatic or explant isolation cells were seeded in 6 well plates at a density of 4000 cells/cm<sup>2</sup> ( $n = 3$ ) and incubated at 21 or 5% O<sub>2</sub>. When cells were approximately 80% confluent the medium was removed, cells rinsed with PBS, 500 μl accutase were added and cells incubated at 37 °C (15 – 20 min). Afterwards, 800 μl medium was added and cells centrifuged at 300 x g for 5 min. Medium was removed, the pellet flicked and dissolved in a appropriate amount of medium. The cell number was determined by trypan blue staining, cells were pooled and seeded again at a density of 3000 or 4000 cells/cm<sup>2</sup>. Cells were subcultivated until the cumulative cell number plateaued.



The population doublings  $PD$  during a specific time span  $\Delta t = t_n - t_0$  were then calculated with

$$PD = \frac{\ln\left(\frac{x_n}{x_0}\right)}{\ln 2} \quad (\text{B.11})$$

where  $x_0$  refers to the cell number at time point  $t_0$  and  $x_n$  to the cell number at  $t_n$ . The population doubling time  $t_{PD}$  was then calculated by

$$t_{PD} = \frac{\Delta t}{PD} \quad (\text{B.12})$$

**Flow cytometric analysis** To determine MSC surface marker expression cells were detached by accutase treatment and stained with MSC phenotyping kit (Miltenyi Biotech GmbH) according to manufacturer's instructions. Stained cells ( $5 \cdot 10^5$  cells per aliquot) were resuspended in  $300 \mu\text{l}$  flow cytometry buffer and acquisition carried out on the BD FACS CantoII with the BD FACS DIVA<sup>TM</sup> software. At least  $1 \cdot 10^4$  gated events per sample were recorded. Finally, all data was analyzed with the Kaluza Flow Cytometry software.

**Senescence-associated  $\beta$ -galactosidase staining** Senescence of MSC was assessed by senescence-associated  $\beta$ -galactosidase staining kit (Cell Signalling Technology). For this, cells were seeded at  $4000 \text{ cells}/\text{cm}^2$  in a 6 well plate and incubated until cell growth plateaued (as estimated by phase contrast microscopy). Then, cells were rinsed with PBS, fixated, covered with staining solution and incubated over night in a  $\text{CO}_2$  free incubator at  $37^\circ\text{C}$  according to the manufacturer's instructions. The staining was documented by transmitted light microscopy.

**MTT viability assay** For the determination of viability of cells on a scaffold it was placed in a 24 well plate, rinsed with PBS and incubated for 4 h at  $37^\circ\text{C}$  in 1 ml of MTT working solution (10 % MTT stock solution in PBS). Afterwards, the sample was scanned (Epson V33) in order to document stained areas. To dissolve the precipitated formazan dye  $900 \mu\text{l}$  of SDS solubilization solution were added and the sample incubated over night at  $37^\circ\text{C}$ . Subsequently,  $8 \times 200 \mu\text{l}$  of the solution were transferred to a 96 well plate and absorption (570 - 630 nm) was acquired with a plate reader (MultiSkan).

**TOX8 viability assay** In order to determine the viability of 3D MSC aggregates  $100 \mu\text{l}$  of the aggregate suspension was transferred to a 96 well plate and  $10 \mu\text{l}$  TOX8 stock solution were added. Subsequently, the plate was incubated 2 h at  $37^\circ\text{C}$  on a horizontal shaker at 100 RPM. Increase of fluorescence (560/590 nm) was determined with a plate reader (Tecan).

**Alkaline phosphatase activity** For the determination of ALP activity from the liquid cell culture supernatant 1 ml sample per measurement point was collected during cultivation and stored at  $-20^\circ\text{C}$ . For measurement samples of one experiment were all thawed together at room temperature and after centrifugation for 5 min at  $14000 \times g$  and  $4^\circ\text{C}$  the supernatant was transferred to a new 1.5 ml tube. Subsequently,  $8 \times 80 \mu\text{l}$  were transferred to wells a 96 well plate,  $20 \mu\text{l}$  of pNPP stock solution were added to each well and the plate incubated for 60 min at

37°C. Immediately absorption (405 nm) was recorded with a plate reader (Tecan). The amount of p-nitrophenolate (product of the enzymatic reaction) was determined with a calibration line which was acquired before ( $y = 0.0317x$ ,  $R^2 = 0.99584$ ,  $n=3$ ). The ALP activity  $U$  ( $\mu\text{mol}/\text{min}$ ) which corresponds to the amount of enzyme that converts 1  $\mu\text{mol}$  of substrate per minute was then calculated by:

$$\text{ALP-activity } U = \left( \frac{c_{pNP}}{0.1391} \cdot t^{-1} \right) \quad (\text{B.13})$$

where  $c_{pNP}$  is the concentration of p-nitrophenolate ( $\mu\text{g}/\text{ml}$ ), 0.1391 the conversion factor from  $\mu\text{g}/\text{ml}$  to  $\mu\text{mol}/\text{l}$  and  $t$  the incubation time (min). Consequently,  $U \cdot V$  with  $V$  as the volume (l) gives the volumetric enzyme activity.

**DNA isolation and quantification** In order to isolate DNA from samples an adequate amount of lysis buffer was added and samples incubated for at least 3 h at 37°C at 100 RPM. 3D samples were incubated in a standard incubator on a horizontal shaker whereas 2D samples were detached by accutase treatment prior to addition of lysis buffer, transferred to 1.5 ml tubes and incubated in a heating block. In order to precipitate DNA 250  $\mu\text{l}$  of the lysate were transferred to a 1.5 ml tube and 500  $\mu\text{l}$  100 % Ethanol (4°C) were added. Tubes were inverted several times and incubated over night at -20°C to foster DNA precipitation. Subsequently, tubes were centrifuged 20 min at 14.000 x g (4°C), supernatant was removed and the pellet washed with 500  $\mu\text{l}$  70 % Ethanol (4°C). Again, tubes were centrifuged 5 min at 14.000 x g, supernatant was removed and pellets air dried. Finally, the pellet was dissolved in a appropriate amount of TE buffer. DNA was quantified with the Quant-iT™ PicoGreen® dsDNA Assay Kit following the manufacturer's protocol.

## B.7 Histology

After microscopic x-ray computed tomography Tutoplast samples were processed for histology. For this, samples were decalcified in either EDTA or a solution of sodium citrate and formic acid in ddH<sub>2</sub>O for 3 weeks. Subsequently, the samples were dehydrated in an ascending series of ethanol and xylene and embedded in paraffin wax using a Shandon Tissue Excelsior. Afterwards, samples were deparaffinized in xylene and sections were rehydrated in descending ethanol series (100, 96, 70 %). Subsequently, sections were stained with hematoxylin for 6 min and eosin for 5 min in ddH<sub>2</sub>O. Sections dehydrated again (96, 100 % ethanol and xylene) and covered with DPX mounting medium.

## B.8 Staining procedures

In this section fixation and staining procedures are described. However, for 3D samples (Sponceram or Tutoplast) rinsing was always performed for 5 min on a horizontal shaker at 100 RPM and incubation in the respective staining solution was as well performed on a horizontal shaker at 100 RPM (same duration as 2D samples).

**Ethanol fixation** For fixation with ethanol cells were rinsed three times with PBS, covered with  $-20^{\circ}\text{C}$  cold ethanol 96 % and incubated at  $4^{\circ}\text{C}$  for 1 h. Afterwards, samples were rinsed three times with PBS, covered with PBS and stored at  $4^{\circ}\text{C}$ .

**Paraformaldehyde fixation** For fixation with paraformaldehyde (PFA) cells were rinsed three times with PBS, covered with 4 % paraformaldehyde in PBS and incubated 10 min (30 min for 3D samples) at room temperature. Afterwards, samples were rinsed three times with PBS, covered with PBS and stored at  $4^{\circ}\text{C}$ .

**Glutaraldehyde fixation** For fixation with glutaraldehyde cells were rinsed with PBS, covered with 2.5 % glutaraldehyde in ddH<sub>2</sub>O and incubated for 2 h at  $4^{\circ}\text{C}$ . Afterwards, cells were rinsed thrice with ddH<sub>2</sub>O for 15 min.

**DAPI staining** Prior to staining the cell nuclei with 4',6-diamidin-2-phenylindol (DAPI) the samples were fixated in ethanol. Cells or scaffolds were rinsed with PBS, covered with DAPI staining solution (1  $\mu\text{l}$  DAPI stock in DAPI buffer) and incubated for 20 min at room temperature. Subsequently, cells were rinsed with PBS twice and documented by fluorescence microscopy (excitation/suppression filter: 360/470 nm).

**Calcein staining** Calcium deposition of the extracellular matrix was stained with calcein. Prior to staining with calcein samples were fixated in ethanol. Afterwards, samples were rinsed with ddH<sub>2</sub>O, covered with calcein staining solution (5  $\mu\text{g}/\text{ml}$  calcein in ddH<sub>2</sub>O) and incubated over night at room temperature. Subsequently, samples were rinsed three times with PBS and staining documented by fluorescence microscopy (excitation/suppression filter: 490/515 nm).

**Von Kossa staining** The von Kossa staining was used to stain phosphate deposition of the extracellular matrix. Prior to staining samples were fixated with ethanol. Samples were then rinsed three times with ddH<sub>2</sub>O, covered with 5 % silver nitrate solution and incubated for 30 min at room temperature in the dark. Subsequently, cells were washed thrice with ddH<sub>2</sub>O, exposed to UV light for 2 min and rinsed with decolorization solution for 2 min. Afterwards, samples were rinsed three times with ddH<sub>2</sub>O and staining was documented with scanner and microscope.

**Alicarin red staining** Alicarin red was used to stain calcium deposition of the extracellular matrix. Prior to staining cells were fixated with ethanol. Samples were then rinsed with PBS, covered with alicarin red solution and incubated for 15 min at room temperature. Subsequently, samples were rinsed several times with PBS until the supernatant remained clear and staining was documented with scanner and microscope.

**Alcian blue staining** Alcian blue staining was used to stain proteoglycan aggrecan of the extracellular matrix. Beforehand, cells were fixated with ethanol. Samples were then rinsed with washing solution (3 % acetic acid in ddH<sub>2</sub>O) for 3 min, covered with alcian blue staining solution and incubated for 30 min at room temperature. Afterwards, cells were rinsed with washing

solution until the supernatant remained clear and staining was documented by phase contrast microscopy.

**Oil Red O staining** Oil Red O staining was used to stain lipid vacuoles of cells. Prior to staining cells were fixated in PFA. Samples were then rinsed thrice with ddH<sub>2</sub>O, covered with Oil Red O solution and incubated for 20 min at room temperature. Afterwards, cells were rinsed with ddH<sub>2</sub>O until the supernatant remained clear and staining was documented by phase contrast microscopy.

**Calcein-AM and PI viability staining** To assess viability cells were stained with calcein acetoxymethyl ester (calcein-AM; stains for living cells) and propidium iodide (PI; dead cells). For this, samples were rinsed with PBS, covered with calcein-AM staining solution (4  $\mu$ l/ml calcein stock in PBS) and incubated 20 min at 37 °C. Afterwards, 33  $\mu$ l of PI stock solution were added and samples incubated for 1 min at room temperature. Subsequently, samples were rinsed two times with PBS, covered with PBS and staining immediately documented by fluorescence microscopy (excitation/suppression filter: 490/515 nm).

## B.9 Scanning electron microscopy

After glutaraldehyde fixation cells were dehydrated with increasing ethanol series. For this, samples were incubated successive in 50, 60, 70, 80, 90 and 100 % ethanol for 15 min at 100 RPM on a horizontal shaker. Subsequently, cells were incubated in 33, 66 and 100 % hexamethyldisilazane in ethanol for 5 min at 100 RPM, air dried and sputtered with 5 nm palladium-gold in argon plasma for observation in a scanning electron microscope.

## B.10 X-ray microtomography

After fixation with paraformaldehyde samples were covered with 70 % ethanol and stained with 1 % phosphotungstic acid in 70 % ethanol for 24 h in order to enhance contrast of cells. Subsequently, samples were rinsed with 70 % ethanol, transferred to a 1.5 ml tube and mounted in 1.5 % agarose. Samples were either scanned in the Scanco  $\mu$ CT35 or Xradia VersaXRM-500. Images were exported as Dicom sequences and visualized with the Drishti software.

## B.11 Image processing

In order to present comparative overview images of entire 3D samples after fluorescent staining procedures images of the entire scaffold were acquired with approximately 1/3 overlap at the right and left boarder and 1/5 overlap on the upper and lower boarder at 4x magnification (30 - 50 images per sample). Subsequently, images were automatically merged with Microsoft Image Composer to one image.

## B.12 Aggregate size analysis with ImageJ

The aggregate size of experiments from section 4.2 was carried out with ImageJ. For this, at least 6 pictures of each condition were processed. Pictures were converted to grayscale 8-bit and threshold was adjusted to generate a black and white image in which only the cellular aggregate remained black. The aggregate was then selected with the *Wand* tool and the selection was fitted to an ellipsoid shape. The circumference, perimeter and area of the fitted ellipse were then measured with the built-in measurement tool. The data was imported in Excel for further calculations.

# Curriculum Vitae

## *Personal details:*

*Name* Dominik Egger  
*Date of birth* 20.05.1987  
*Place of birth* Langenhagen, Germany

## *Education*

- 2014 – 17 **Graduation** (Dr. rer. nat.), Leibniz Universität Hannover and Universität für Bodenkultur Wien, Grade „*summa cum laude*“ (with highest honor)
- 2014 **Master Thesis:** “Evaluation of the influence of physiologic dynamic cultivation conditions on human mesenchymal stem cells from adipose tissue“
- 2011 – 14 **Master of Science** „Life Science“, Leibniz Universität Hannover, Grade “very good”
- 2012 **Research internship abroad**, research at the "Hebrew University of Jerusalem", Israel (three month)
- 2008 – 11 **Bachelor of Science** “Life Science”, Leibniz Universität Hannover, Grade “excellent”
- 2005 – 07 **Education Paramedic**, Medizinischen Bildungszentrum Nord Hannover
- 2005 **College**, Gymnasium Sophienschule Hannover

## *Professional Experience*

- 2014 – 17 **Research associate**, Universität für Bodenkultur Wien
- 2010 – 12 **Student research associate**, Leibniz Universität Hannover und Medizinische Hochschule Hannover
- 2006 **Volunteering**, medical services in India (three month)

## *Further Education*

- 2016 **Symposium** “Symposium for Young Investigators in Regenerative Medicine”, Krems, Austria
- 2016 **Conference** “3D Cell Culture”, Freiburg, Germany
- 2015 **Sponsorship for conference** “European Society for Animal Cell Technology, ESACT”, Barcelona, Spain
- 2015 **Award** “Karl-Schügerl-Preis” for Master Thesis (2<sup>nd</sup> price), Hannover, Germany

- 2015 **Conference** “Strategies in Tissue Engineering”, Würzburg, Germany
- 2015 **Conference** “ATMP 2015 - Issues and challenges from bench to bedside”, Tutzingen, Germany
- 2015 **Workshop** “3D Volume Rendering”, Vienna, Austria
- 2014 **Summer school** “Advances in Tissue Engineering”, Rice University, Houston, Texas, USA
- 2014 **Pre-conference Workshop**, Vienna, Austria
- 2014 **Workshop** “Cellulose in Cell Culture”, Vienna, Austria

## *Skills*

- Languages* German (mother tongue), English (C1), Spanish (A1)
- Software* MS Office (Word, Excel, PowerPoint), writing in Latex, COMSOL Multiphysics, Adobe Photoshop / InDesign, ImageJ, Drishti, OriginLab, GraphPad

## Publication record

### Article

**Egger, D.**, Schwedhelm, I., Hansmann, J., Kasper, C. (2017). Hypoxic Three-Dimensional Scaffold-Free Aggregate Cultivation of Mesenchymal Stem Cells in a Stirred Tank Reactor. *Bioengineering*, 4(2), 47.

**Author Contributions:** D.E. designed and performed cell culture experiments, data analysis and prepared the manuscript (40%); I.S. designed the CSTR, performed computational analysis and prepared the manuscript (30%); J.H. prepared the manuscript (10%); C.K. designed the study and prepared the manuscript (20%).

**Egger, D.**, Fischer, M., Clementi, A., Ribitsch, V., Hansmann, J., Kasper, C. (2017) Development and Characterization of a Parallelizable Perfusion Bioreactor for 3D Cell Culture. *Bioengineering*, 4(2), 51.

**Author contributions:** D. Egger designed and performed experiments, data analysis and prepared the manuscript (60%). M. Fischer performed experiments and data analysis (10%). A. Clementi performed experiments (10%). V. Ribitsch contributed to design and manufacturing of the bioreactor (10%). C. Kasper designed the study and contributed to preparation of the manuscript (10%).

**Egger, D.**, Spitz, S., Fischer, M., Handschuh, S., Glösmann, M., Friemert, B., Egerbacher M., Kasper, C. (2017). Application of a Parallelizable Perfusion Bioreactor for Physiologic 3D Cell Culture. *Cells Tissues Organs*, 203(5), 316-326.

**Author contributions:** D. Egger designed and performed experiments, data analysis and prepared the manuscript (50%). S. Spitz performed experiments and data analysis (10%). M. Fischer performed experiments and data analysis (10%). S. Handschuh performed CT analysis (5%). M. Glösmann performed CT analysis (5%). B. Friemert contributed to design of the study (5%). M. Egerbacher performed histologic analyses and contributed to design of the study (5%). C. Kasper designed the study and contributed to preparation of the manuscript (10%).



**Egger, D.**, Kasper, C. „Hypoxie – wenn weniger Sauerstoff mehr (Stammzellen) macht“, *BIOspektrum* 2017, 23(4), Springer-Verlag

**Author contributions:** D. Egger prepared figures and the manuscript (60%). C. Kasper designed and prepared the manuscript (40%).

**Egger, D.**, Krammer, M., Hansmann, J., Walles, H., Kasper, C. (2015, December). Dynamic cultivation of human stem cells under physiological conditions. In *BMC Proceedings* (Vol. 9, No. 9, p. P68). BioMed Central.

**Author contributions:** D. Egger designed and performed experiments, data analysis and prepared the manuscript (60%). M. Krammer performed experiments (10%). J. Hansmann contributed to the design of the study (10%). H. Walles contributed to the design of the study (10%). C. Kasper designed and prepared the manuscript (10%).

Neumann, A., Lavrentieva, A., **Egger, D.**, Hatlapatka, T., Kasper, C. (2013, December). Approaches for automatized expansion and differentiation of human MSC in specialized bioreactors. In *BMC Proceedings* (Vol. 7, No. 6, p. P47). BioMed Central.

**Author contributions:** A. Neumann designed and performed experiments, data analysis and prepared the manuscript (30%), A. Lavrentieva performed experiments and prepared the manuscript (30%). D. Egger performed experiments (10%). T. Hatlapatka contributed to the design of the study and preparation of the manuscript (15%). C. Kasper designed the study and prepared the manuscript (15%).

### **Book Chapter (not published yet)**

**Egger, D.**; Clementi, A.; Charwat, V.; Kasper, C. Cell Culture Conditions - Cultivation of Stem Cells under Dynamic Conditions. In *Tissue Engineering and Regeneration: Cell Engineering and Regeneration*; Redl, H., Ed.; Springer Nature, 2017.

**Author contributions:** D. Egger, A. Clementi, V. Charwat prepared the manuscript (each 25%). C. Kasper designed the chapter and prepared the manuscript (25%).

### Oral presentations

*Optimization of isolation and expansion of human mesenchymal stem cells under physiologic conditions*, SYIRM Symposium, 2016, Krems, Austria

*Monitoring osteogenic differentiation of MSC under dynamic culture conditions*, Conference on Advanced Medicinal Therapeutic Products, 2015, Tutzingen, Germany

*Dynamic 3D cultivation and differentiation of human stem cells under physiological conditions*, International Student Congress, Medical University Graz, 2015, Graz, Austria

### Poster presentation

**D. Egger**, S. Spitz, M. Fischer, S. Handschuh, M. Glösmann, B. Friemert, M. Egerbacher, C. Kasper, Optimization of flow and hydrostatic pressure conditions for 3D differentiation of stem cells, Stem Cell Network NRW, 2017, Muenster, Germany

**D. Egger**, S. Spitz, J. Hansmann, C. Kasper, Miniaturized perfusion bioreactor system for highly parallelized cultivation of stem cells, 3D Cell Culture Freiburg, 2016, Freiburg, Germany

**D. Egger**, M. Krammer, J. Hansmann, H. Walles, C. Kasper, Effects of physiological fluid shear stress in the osteogenic differentiation of human stem cells, Würzburger Initiative Tissue Engineering (WITE), 2015, Würzburg, Germany

**D. Egger**, M. Krammer, J. Hansmann, H. Walles, C. Kasper, Dynamic cultivation of human stem cells under physiological conditions, European Society of Animal Cell Culture Techniques (ESACT) Congress, June 2015, Barcelona, Spain.

**D. Egger**, M. Krammer, J. Hansmann, H. Walles, C. Kasper, Dynamic 3D cultivation and differentiation of human stem cells under physiological conditions, Third International Students Congress, June 2015, Graz, Austria.

M. Krammer, **D. Egger**, V. Charwat C. Kasper, Development of strategies for cultivating human mesenchymal stem cells MSC under dynamic culture conditions, Austrian Association of Molecular Life Sciences and Biotechnology (ÖGMBT), 2015, Salzburg, Austria

A. Neumann, **D. Egger**, A.Gugerell, J. Kober, M. Keck, C. Kasper, Optimizing Cultivation Conditions for adMSC Expansion and Differentiation by Combining Different Matrices in Tailor Made Mini Perfusion Bioreactors, World Conference of Regenerative Medicine, November 2013, Leipzig, Germany.

A. Neumann et al, A. Lavrentieva, **D. Egger**, T. Hatlapatka, C. Kasper, Approaches for Automatized Expansion and Differentiation of human MSC in Specialized Bioreactors, European Society of Animal Cell Culture Techniques (ESACT) Congress, June 2013, Lille, France.